ALFRED-WEGENER-INSTITUT
HELMHOLTZ-ZENTRUM FÜR POLAR-
UND MEERESFORSCHUNG

776
2023

Berichte
zur Polar- und Meeresforschung

Reports on Polar and Marine Research

The Expedition PS129 of the Research Vessel POLARSTERN to the Weddell Sea in 2022

Edited by

Mario Hoppema

with contributions of the participants

HELMHOLTZ

Die Berichte zur Polar- und Meeresforschung werden vom Alfred-Wegener-Institut, Helmholtz-Zentrum für Polar- und Meeresforschung (AWI) in Bremerhaven, Deutschland, in Fortsetzung der vormaligen Berichte zur Polarforschung herausgegeben. Sie erscheinen in unregelmäßiger Abfolge.

Die Berichte zur Polar- und Meeresforschung enthalten Darstellungen und Ergebnisse der vom AWI selbst oder mit seiner Unterstützung durchgeführten Forschungsarbeiten in den Polargebieten und in den Meeren.

Die Publikationen umfassen Expeditionsberichte der vom AWI betriebenen Schiffe, Flugzeuge und Stationen, Forschungsergebnisse (inkl. Dissertationen) des Instituts und des Archivs für deutsche Polarforschung, sowie Abstracts und Proceedings von nationalen und internationalen Tagungen und Workshops des AWI.

Die Beiträge geben nicht notwendigerweise die Auffassung des AWI wider.

Herausgeber
Dr. Horst Bornemann

Redaktionelle Bearbeitung und Layout
Susan Amir Sawadkuhi

Alfred-Wegener-Institut
Helmholtz-Zentrum für Polar- und Meeresforschung
Am Handelshafen 12
27570 Bremerhaven
Germany

www.awi.de
www.awi.de/reports

The Reports on Polar and Marine Research are issued by the Alfred Wegener Institute, Helmholtz Centre for Polar and Marine Research (AWI) in Bremerhaven, Germany, succeeding the former Reports on Polar Research. They are published at irregular intervals.

The Reports on Polar and Marine Research contain presentations and results of research activities in polar regions and in the seas either carried out by the AWI or with its support.

Publications comprise expedition reports of the ships, aircrafts, and stations operated by the AWI, research results (incl. dissertations) of the Institute and the Archiv für deutsche Polarforschung, as well as abstracts and proceedings of national and international conferences and workshops of the AWI.

The papers contained in the Reports do not necessarily reflect the opinion of the AWI.

Editor
Dr. Horst Bornemann

Editorial editing and layout
Susan Amir Sawadkuhi

Alfred-Wegener-Institut
Helmholtz-Zentrum für Polar- und Meeresforschung
Am Handelshafen 12
27570 Bremerhaven
Germany

www.awi.de
www.awi.de/en/reports

Titel: Kein Tag wie jeder andere – Polarstern durchquert das Eis der Weddel-See
(Foto: Timo Hecken)

Cover: What a day – Polarstern crosses the ice of the Weddel Sea
(Photo: Timo Hecken)

The Expedition PS129
of the Research Vessel POLARSTERN
to the Weddell Sea in 2022

Edited by

Mario Hoppema

with contributions of the participants

Please cite or link this publication using the identifiers

https://hdl.handle.net/10013/epic.ef53786c-4ddd-439e-a639-1739b799d696

https://doi.org/10.57738/BzPM_0776_2023

ISSN 1866-3192

PS129

03 March 2022 – 28 April 2022

Cape Town – Punta Arenas

Chief scientist
Mario Hoppema

Coordinator
Ingo Schewe

Contents

1. ÜBERBLICK UND FAHRTVERLAUF

Mario Hoppema DE.AWI

Die Expedition PS129 des deutschen Polarforschungsschiffes *Polarstern* führte von Kapstadt in südwestlicher Richtung zum Nullmeridian und dort entlang weiter in die Antarktis (Abb. 1.1). Die *Neumayer-Station* wurde zu logistischen Zwecken (Übergabe von Material) kurz angefahren. Danach wurde die Arbeit in einem von der EWOS-Gruppe definierten Gebiet ausgeführt. Anschließend wurde der Transekt quer durch das Weddellmeer zwischen Kapp Norvegia und der Spitze der Antarktischen Halbinsel mit zwischendurch zwei Exkursionen nach Süden abgefahren, vor allem um Schallquellen zu verankern (Abb. 1.1). Diese Expedition war Teil einer Fortsetzung der Langzeit-Zeitreihen im Rahmen des HAFOS Projekts (Hybrid Antarctic Float Observation System). HAFOS ist dem Klima, dem Ozean und der Ökosystem-Dynamik gewidmet. Die HAFOS-Zeitreihe geht zurück bis auf die 1980/1990-er Jahre, insbesondere bezüglich der Hydrografie, der Nährstoffe, des gelösten Sauerstoffs und des CO_2-Systems. Ein weiterer, substantieller Teil von PS129 betrifft EWOS (Eastern Weddell Sea Observation System); dies beinhaltet die koordinierten und systematischen Beobachtungen der sympagischen, pelagischen und benthischen Teile des Ökosystems des Weddellmeers. Nach der letzten Verankerung nahe Elephant Island und dem Überqueren der Drakestraße endete die Expedition am 28. April 2022 in Punta Arenas, Chile (Abb. 1.1).

Ein erheblicher Teil der Ziele der wissenschaftlichen Vorhaben wurden in bewährter Zusammenarbeit zwischen Schiff und Wissenschaft erreicht. Jedoch wurden nicht alle Ziele erreicht, erstens durch einige Tage stürmischen Wetters, die leider in der eng bemessenen Zeit der Fahrt nicht einkalkuliert waren und zweitens durch einen Schaden am Schiff, der eine schnellere Fahrt durch das anwesende Meereis verhinderte und das Brechen des Eises nicht zuließ. Insbesondere konnten verschiedene Schallquellen, die für HAFOS von großer Bedeutung sind, nicht auf der im Süden des Weddellmeers vorgesehenen Position verankert werden; außerdem konnte der Großteil der EWOS-Arbeiten im Weddellmeer außerhalb der EWOS-Box nicht stattfinden.

Während der Expedition PS129 wurden wissenschaftlichen Projekte aus den Bereichen physikalische Ozeanographie, Meeresbiologie und Meereschemie bearbeitet, die gemeinsam darauf abzielten, die Entwicklung der Wassermassen des Weddellmeers und seiner ökologischen und chemischen Kreisläufe zu verstehen. Die Projekte und die damit verbundenen Aktivitäten an Bord waren im einzelnen:

1. **HAFOS** (Hybrid Antarctic Float Observing System) untersucht mittels ozeanographischer Tiefseeverankerungen, hydrographischen Schnitten und autonomen Floats die Zirkulation und Entwicklung des Warmen Tiefenwassers (WDW) und Bodenwassers (WSBW) des Weddellmeers. Biologische Aspekte von HAFOS betreffen die akustische Ökologie des Weddellmeers und seiner Fauna, wofür Verankerungen mit autonomen Unterwasserrekordern ausgestattet wurden.

- Fahren von 55 CTD-Stationen mit Rosette und L-ADCP
- Aufnahme von 9 ozeanographischen Verankerungen sowie Auslage von 17 ozeanographischen Verankerungen

- (3 Verankerungen konnten nicht aufgenommen werden)
- Auslegung von 6 Argo Floats (für das Bundesamt für Seeschifffahrt und Hydrographie, Deutschland)
- Auslegung von 22 AWI Floats
- 21 Kalibrierungsvorgänge von 8 Schallquellen
- Kontinuierliche Erfassung von Temperatur, Salzgehalt (Thermosalinograph) und Strömungsprofilen (sADCP)

2. Als Ziel des Teilprojekt **HAFOS-nutrients** wurden die Nährstoffe Phosphat, Nitrat, Silikat, Nitrit und Ammonium in Wasserproben aus der ganzen Wassersäule bestimmt um auf dieser Weise Nährstoff-Schnitte durchs Weddellmeer zu bekommen; diese wiederum sollen mit früheren Schnitten verglichen werden. Zusätzlich wurden Proben für $\delta^{13}C$ und $\delta^{15}N$ Isotopen von partikulärem Material (POM) genommen.

- 954 Wasserproben genommen
- 4770 Datenpunkte für die verschiedenen Nährstoffe

3. **HAFOS-BGC** (Biogeochemie) befasst sich mit dem Kohlenstoff-Kreislauf des Weddellmeers. Die Daten werden mit früheren Daten aus demselben Gebiet verglichen um (anthropogene) Trends und Variabilität zu bestimmen. Anorganischer Kohlenstoff (und gelöster Sauerstoff) wurden beprobt in Wasser aus der ganzen Wassersäule. Analysiert wurden:

- 881 Proben auf Gesamt-CO_2 (= TCO_2 oder DIC oder C_T)
- 881 Proben auf Gesamt-Alkalinität (A_T)
- 430 Proben auf gelöstem Sauerstoff

4. **SOCCOM** (Southern Ocean Carbon and Climate Observations and Modelling) beobachtet und modelliert biogeochemische Kreisläufe des Südpolarmeers; die Beobachtungen werden mittels biogeochemischer, profilierender Treibbojen durchgeführt, die über das gesamte Südpolarmeer hinweg verteilt, ausgelegt wurden.

- Auslegung von 9 biogeochemischen Argo Floats

5. **COMA** (Chemical controls on Organic Matter Aggregation/ Chemische Regulierung von Aggregation organischen Materials) erforscht die Übergänge zwischen gelösten, kolloidalen und partikulären organischen Stoffen im Ozean. Es widmet sich der Frage, ob bestimmte chemische Klassen im Pool von organischen Molekülen im Südpolarmeer die Aggregation und die Metall-Komplexion bestimmen.

- Probennahme bei 48 CTD-Stationen
- Probennahme von 38 Stationen mit Wasser aus dem Snorchel im Brunnenschacht
- Die Gesamtmenge an verschiedenen Proben:

- Gelöster organischer Kohlenstoff (DOC): 994
- Partikulärer organischer Kohlenstoff (POC): 241
- Gesamtorganischer Kohlenstoff (TOC): 127
- Gelöstes organisches Material (DOM) Extraktion, großes Volumen: 44
- Fe^{2+}-Ionen: 25
- Fe^{3+}-Ionen: 23
- Liganden: 25
- Gelöstes organisches Material (DOM) Extraktion, kleines Volumen: 451
- Nährstoffe: 28
- Bakterien: 107
- Fluoreszenz: 808
- Community-Proben (TARA): 44

6. **DEFIANT** (Drivers and Effects of Fluctuations in sea Ice in the ANTarctic/Antrieb und Effekte von Fluktuationen im Meereis in der Antarktis) liefert mechanistische Kenntnisse des Antriebs und des Einflusses der Meereisvariabilität, wobei es die dramatische Meereisabnahme aus dem Jahr 2016 miteinschließt. Messungen an verschiedenen Eis-Stationen, sowohl vom Schiff aus als auch per Hubschrauber, wurden durchgeführt:

- Auslegung eines ITP (Ice Thetered platform)
- Auslegung einer WIMBO-Boje
- Radar-Messungen über Pfannkucheneis
- 4 mal Radar-Messungen am Eis auf Eisschollen
- 3 mal Licht-Messungen am Eis auf Eisschollen
- Wasserproben an CTD-Stationen für ^{18}O-Messungen

7. **EWOS** (Eastern Weddell Sea Observation System) fand vor allem auf dem Schelf und im Einstromgebiet vor Kapp Norvegia im östlichen Weddellmeer statt. Es hat zum Zweck eine quantitative Abschätzung zu geben hinsichtlich der biogeochemischen Flüsse zwischen Phytoplankton- und Zooplankton-Gemeinschaften, dem marinen Leben, wie Krill und Riesen-Antarktisdorsch, in Beziehung zu den treibenden Umweltkräften, und den dazugehörenden passiven und trophischen Kohlenstoff-Flüssen von der Oberfläche in den tiefen Ozean. EWOS-II erforscht die Schlüsselvariablen und treibenden Kräfte, die die Hauptkompartimente des Ökosystems strukturieren; obendrein werden die Zusammensetzung und die Biodiversität von eis-assoziierten pelagischen und benthischen Biota untersucht. EWOS-III hat die benthischen Biodiversitätsmuster, den Sauerstoffverbrauch und die Nährstoffflüsse untersucht und zwar durch optische und akustische Meeresboden-Abbildungen, Probennahme von Makrobenthos und *ex situ* Inkubationsexperimente von Sedimentkernen.

- 4 Einsätze vom Fisch-Lander
- 2 mal Long Lines ausgelegt und aufgenommen
- 4 Agassiz-Trawls wurden gezogen
- 5 SUITS (Surface and Under-Ice Trawl) gefahren
- 7 Multinetze eingesetzt
- 8 mal wurde das RMT (Rectangular Midwater Trawl) benutzt
- 6 Eis-Stationen wurden gemacht, entweder mit dem Hubschrauber oder vom Schiff
- 7 mal wurde das ROV (Remotely Operated Vehicle) eingesetzt, vom Schiff oder vom Hubschrauber
- TV-MUC (Multicorer) wurde 7 mal eingesetzt
- Der Multigrab wurde 9 mal benutzt
- Das OFOBS (Ocean Floor Observation and Bathymetry System) kam 9 mal zum Einsatz

Letztendlich dienten die Hubschrauber als Transportmittel, um vom Schiff abgesetzte Arbeiten, logistische Aufgaben und Beobachtungsflüge durchzuführen. Insgesamt ergaben sich 57 Flüge von 66:39 Stunden kumulativer Dauer wie folgt:

- 3 Flüge für Technik (1:32 h)
- 2 Flüge zur Eiserkundung (2:20 h)
- 5 Trainingsflüge (4:30 h)
- 4 logistische Flüge (Transporte, 1:38 h)
- 1 Passagierflug (0:50 h)
- 25 Flüge für wissenschaftliche Arbeiten (u.a. zu Eisschollen für Eisarbeiten und ROV-Einsätze (27:43 h))
- 17 Flüge zur Vögel- und Säugetierbeobachtung (28:06 h).

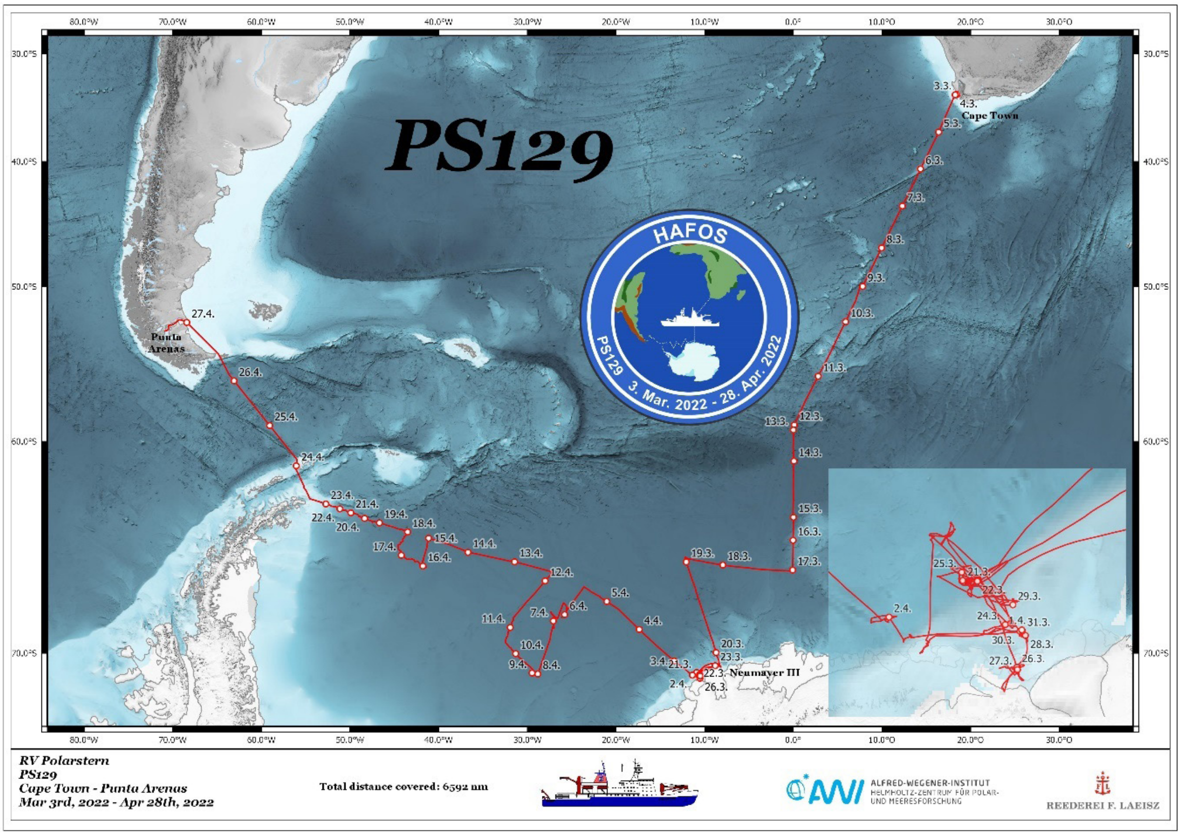

Abb. 1.1: Fahrtverlauf der Expedition PS129 mit Beginn in Kapstadt, Südafrika und Ende in Punta Arenas, Chile. Der Ausschnitt rechts unten zeigt das Gebiet bei Kapp Norvegia, wo hauptsächlich die EWOS-Arbeiten stattfanden ('EWOS-Box'). Für die Daten dieser Fahrt siehe auch: https://doi.pangaea.de/10.1594/PANGAEA.947251

Fig. 1.1: Cruise track of the expedition PS129 starting in Cape Town, South Africa, and ending in Punta Arenas, Chile. The detail of the map at bottom right shows the area off Kapp Norvegia where mainly the work of the EWOS group occurred (the 'EWOS box') For data of this expedition, see also: https://doi.pangaea.de/10.1594/PANGAEA.947251

SUMMARY AND ITINERARY

The expedition PS129 of the German polar research vessel *Polarstern* headed south-west from Cape Town to the Prime Meridian and from there further south to the Antarctic (Fig. 1.1). *Neumayer Station III* was briefly visited for logistical purposes (transfer of material). After that, the work was carried out in a region defined by the EWOS group. Still further, the transect was occupied across the Weddell Sea between Kapp Norvegia and the tip of the Antarctic Peninsula, with two excursions to the south in between, mainly to deploy sound sources (Fig. 1.1). This expedition was part of a continuation of the long-term time series within the framework of the HAFOS project (Hybrid Antarctic Float Observation System). HAFOS is dedicated to climate, ocean and ecosystem dynamics. The HAFOS time series started in the 1980s/1990s, particularly with respect to the hydrography, nutrients, dissolved oxygen and the CO_2 system. Another substantial part of PS129 concerns the EWOS programme (Eastern Weddell Sea Observation System); this includes the coordinated and systematic observations of the sympagic, pelagic and benthic parts of the Weddell Sea ecosystem. After the last mooring work near Elephant Island and crossing the Drake Passage, the expedition ended on 28 April 2022 in Punta Arenas, Chile (Fig. 1.1).

A significant number of goals of the scientific projects were achieved in successful cooperation between ship and science. However, not all objectives were met, firstly, due to a number of days of stormy weather, which unfortunately were not taken into account in the tight planning of the expedition, and secondly, due to damage to the ship, which prevented faster steaming through the sea ice and which did not allow the breaking of the ice. In particular, various sound sources, which are of great importance for HAFOS, could not be moored at the positions planned further south in the Weddell Sea; moreover, most of the EWOS work in the Weddell Sea outside the EWOS box could not be conducted.

During expedition PS129, scientific projects in the fields of physical oceanography, marine biology and marine chemistry were executed, which together aim to shed light on the evolution of the water masses of the Weddell Sea and its ecological and chemical cycles. The projects and related activities on board were in detail:

1. **HAFOS** (Hybrid Antarctic Float Observing System) investigates the circulation and evolution of the Warm Deep Water (WDW) and the bottom water (WSBW) of the Weddell Sea using oceanographic deep-sea moorings, hydrographic sections and autonomous floats. Biological aspects of HAFOS concern the acoustic ecology of the Weddell Sea and its fauna, for which moorings were equipped with autonomous underwater recorders.

- Casting 55 CTD stations with rosette sampler and L-ADCP
- Recovery of 9 oceanographic moorings and deployment of 17 oceanographic moorings
- (3 moorings could not be recovered)
- Deployment of 6 Argo Floats (for the Federal Maritime and Hydrographic Agency, Germany)

- Deployment of 22 Argo floats of AWI
- 21 calibrations of 8 sound sources
- Continuous acquisition of temperature, salinity (i.e., thermosalinograph) and current profiles (sADCP)

2. The aim of the sub-project **HAFOS-nutrients** was to determine the nutrients phosphate, nitrate, silicate, nitrite and ammonium in water samples from the entire water column in order to obtain nutrient sections through the Weddell Sea; these in turn will be compared with earlier realizations of these sections. In addition, $\delta^{13}C$ und $\delta^{15}N$ isotopes were sampled from particulate matter (POM).

- 954 water samples taken
- 4770 data points for all the different nutrients

3. **HAFOS-BGC** (Biogeochemistry) deals with the carbon cycle of the Weddell Sea. The data will be compared to previous data from the same area to determine (anthropogenic) trends and variability. Inorganic carbon (and dissolved oxygen) were determined in water from the entire water column. Number of samples analysed:

- 881 samples for total CO_2 (= TCO_2 or DIC or C_T)
- 881 samples for total alkalinity (A_T)
- 430 samples for dissolved oxygen

4. **SOCCOM** (Southern Ocean Carbon and Climate Observations and Modelling) observes and models biogeochemical cycles of the Southern Ocean; observations are made by means of biogeochemical profiling floats deployed throughout the Southern Ocean.

- Deplyoment of 9 biogeochemical Argo Floats

5. **COMA** (Chemical controls on Organic Matter Aggregation) investigates the transitions between dissolved, colloidal and particulate organic matter in the ocean. It addresses the question of whether certain chemical classes in the pool of organic molecules in the Southern Ocean determine aggregation and metal complexation.

- Sampling at 48 CTD stations
- Sampling of 38 stations with water from the snorkel in the moon pool

  - The total amount of different samples:Dissolved organic carbon (DOC): 994

  - Particulate organic carbon (POC): 241

  - Total organic carbon (TOC): 127

  - Dissolved organic matter (DOM) extraction, large volume: 44

  - Fe^{2+} ions: 25

  - Fe^{3+} ions: 23

  - Ligands: 25

- Dissolved organic matter (DOM) extraction, small volume: 451

- Nutrients: 28

- Bacteria: 107

- Fluorescence: 808

- Community samples (TARA): 44

6. **DEFIANT** (Drivers and Effects of Fluctuations in sea Ice in the ANTarctic) delivers a mechanistic understanding of the drivers and inpact of sea ice variability, including the dramatic sea ice decline of 2016. Measurements at various ice stations, both from the ship and by helicopter, were carried out:

- Deployment of an ITP (Ice Thetered platform)
- Deploymant of a WIMBO buoy
- Radar measurements over pancake ice
- 4 times radar measurements on ice at ice floes
- 3 times light measurements on ice at ice floes
- Water sampling at CTD stations for ^{18}O measurements

7. **EWOS** (Eastern Weddell Sea Observation System) took place mainly on the shelf and in the inflow area off Kapp Norvegia in the eastern Weddell Sea. It aims to quantitatively estimate the biogeochemical fluxes between phytoplankton and zooplankton communities, marine life, such as krill and giant Antarctic toothfish, in relation to environmental drivers, and the associated passive and trophic carbon fluxes from the surface to the deep ocean. EWOS-II explores the key variables and drivers that structure the main ecosystem compartments; in addition, the composition and biodiversity of ice-associated pelagic and benthic biota are studied. EWOS-III studied benthic biodiversity patterns, oxygen consumption and nutrient fluxes by means of optical and acoustic seabed imaging, sampling of macrobenthos and *ex situ* sediment core incubation experiments.

- 4 deployments of the Fish Lander
- 2 long lines laid out and recorded
- 4 Agassiz trawls were drawn
- 5 SUITS (Surface and Under-Ice Trawl) were deployed
- 7 multinets deployed
- RMT (Rectangular Midwater Trawl) was used 8 times
- 6 ice stations were occupied, either by helicopter or from the ship
- ROV (Remotely Operated Vehicle) was deployed 7 times, from the ship or from helicopter
- TV-MUC (multicorer) was used 7 times

- Multigrab was used 9 times
- OFOBS (Ocean Floor Observation and Bathymetry System) was deployed 9 times

Finally, the helicopters served as a means of transport to carry out work away from the ship, including logistical tasks and observation flights. A total of 57 flights of 66:39 hours cumulative duration was flown as follows:

- 3 flights for technology (1:32 h)
- 2 sea-ice reconaissance flights (2:20 h)
- 5 training flights (4:30 h)
- 4 logistic flights (transports, 1:38 h)
- 1 passenger flight (0:50 h)
- 25 flights for scientific work (including to ice floes for ice work and ROV missions (27:43 h))
- 17 flights for bird and mammal observation (28:06 h).

WEATHER CONDITIONS DURING PS129

Patrick Suter DE.DWD

Expedition PS129 was conceived to contribute to scientific projects with the aim of understanding the evolution of the water masses of the Weddell Sea and neighbouring regions, as well as their ecological and chemical cycles; in particular, by continuing the long-term time series of the HAFOS and the EWOS projects. The first individual samplings, as well as the recovery and deployment of deep-water moorings were done on the transit from Cape Town to the *Neumayer Station III*. Close to *Neumayer Station*, *Polarstern* attempted to dock at the edge of the ice shelf, but unfortunately the sea state was too rough. The helicopter was then able to supply *Neumayer*. After that, the main part of the projects was conducted to the west in Weddell Sea. The HAFOS project served oceanographic deep-sea moorings, hydrographic sections with measurements of chemical variables and measurements of autonomous floats.

On the shelf and in the area off Kapp Norvegia in the eastern Weddell Sea, i.e., the main EWOS area, the aim was to quantitatively assess the biogeochemical fluxes between phytoplankton and zooplankton communities, and the marine resources living there, such as krill and the Antarctic toothfish. After leaving the Weddell Sea near Elephant Island, further floats were released on the transit to Punta Arenas. The aim was to collect hydrographic data with which the measurements of the deep-water moorings can be calibrated.

Transit Cape Town - Neumayer Station III

After the crew and science change had taken place the previous day, the expedition began with the departure from Cape Town on 4 March 2022. It started under calm weather conditions. Between a subtropical high over the South Atlantic Ocean and a low southeast of South Africa, moderate southeasterly winds occurred in the harbour of Cape Town. It was mostly sunny and pleasantly warm with temperatures up to 23°C. On the open sea, the wind increased to 6-7 Bft and the waves reached 1.5 to 2 m for a time. On the following day, *Polarstern*, sailing south-southwest, crossed a broad subtropical high-pressure zone which extended eastwards from the South Atlantic to south of the Cape of Good Hope. As a result, the southeast wind weakened to around 2 Bft by the evening.

On 6 March, *Polarstern* crossed 40°S and reached the northern flank of a low-pressure complex with its main centre near the Antarctic coast. This marked the transition from the warm subtropics to the colder mid latitudes. Triggered by a large north-south pressure gradient, a strong and repeatedly wet westerly flow set in. Winds from the northwest reached 6-7 Bft with the passage of a shallow cold front with weak precipitation. Behind the front, changeable conditions with a mix of sun and cumulus clouds set in. The wind shifted to the west with a temporary slight decrease. In the following night, 7 March, another cold front followed, bringing in much cooler air and causing the temperature to drop below 10° C. The westerly wind reached an average of 7 Bft with gale-force gusts at times. The waves from the west also increased gradually from an initial 2.5-3 m to 4 m by the evening and to around 5 m at night. In the course of the day, a high-pressure ridge from the west provided temporary calmer conditions. Afterwards, the low-pressure complex near 60°S and 0°E took over again. On 8 March, a strong to partly stormy northwesterly flow was established, in which a next cold front crossed the area. The associated frontal nimbostratus clouds led to a cloudy and at times wet day. In the afternoon, the overcast clouds temporarily turned into fog. Unstable polar air flowed in behind the cold front. Thus, on 9 March, changeable showery weather set in in the area near 50°S, with additional forcing from an upper-level trough, as well as upper-level cold air. Temperatures ranged from 2 to 4°C and precipitation turned to snow, including small hail. The westerly wind increased to 7-8 Bft on average. In combination with showers, the gusts repeatedly reached gale force and in isolated cases even slightly over 50 kt. With swells from the southwest with 2.5-3 m and strong wind sea, the significant wave height rose to around 4.5 m; some waves were even higher.

On 10 March, *Polarstern* was situated between two low-pressure zones; one in the south near the Antarctic coast and another one northwest of the cruising area. Between the low-pressure formations, the pressure contrasts decreased and the westerly current weakened. The air mass also stabilised somewhat after a final morning shower of small hail. The waves, with mainly swell from the southwest, still reached 3-3.5 m at first, slowly decreasing to 2-2.5 m. However, the wave length was about the same as the length of the ship, which led to a pronounced stamping motion and made the planned helicopter training flights impossible for this day. Subsequently, a high-pressure ridge approached from the west, extending southeastwards from a high near 40°S 15°W. With temperatures around freezing level and winds from the southwest to northwest with 4-6 Bft, snow showers occurred from time to time during the day. On 13 March, the ridge moved eastwards over the area.

In the evening of 13 March, a low-pressure system approached from the west. On its front, the current turned to the north, later to the northeast, and reached near-gale force from the night onwards. At the same time, the working area near 60°S 0°E was hit from the north by a frontal system, which brought in a lot of moisture. Thus, 14 March was in the middle of the warm front, cloudy all day with low cloud ceilings. With the inflow of milder sea air and thus temperatures just above freezing, the snow that started in the second half of the day changed from sleet to drizzle. With the stormy winds, the waves temporarily increased to 3.5-4 m. During the day, the gale with a core near 57°S 15°W slowly began to weaken and shifted southeastward. This resulted in the formation of a two-core low-pressure complex, which moved over the working area until 15 March. The northeast wind weakened to 3-4 Bft. The sea state also flattened out again to 2 m. On 16 March, *Polarstern* was still under the influence of a low-pressure zone and was flanked by a low-pressure core in the west and east. The weather was characterised by low stratus clouds, which occasionally turned into fog. At the same time, 16 March marked the last day with temperatures above freezing, until 24 April. While *Polarstern* was moving further south, the pressure contrasts at the southern edge of the low-pressure zone increased and a strong easterly flow developed by the evening. At the same time, somewhat drier air flowed in again near the ground. The conditions on 17 March were comparable, while still being located at the southern edge of the low-pressure zone near 66°30'S 0°E. However, the cloud base of the stratocumulus clouds was rising, as cooler and drier air slowly flowed in. As a result of this also the visibility improved. On 18 March, a gale moved southeastwards from the north with slight strengthening to east of the cruising area near 63°S 20°E. *Polarstern* moved west at the same time. This turned the wind to the south at 4-5 Bft. This dry southerly current of continental origin caused a large hole in the stratocumulus cloud cover and the sun shone repeatedly during the day. On 19 March, station work near 66°S 12°W was completed by noon, after which the expedition continued to the ice shelf edge near the *Neumayer Station III* research station. On the way to the ice shield, *Polarstern* was accompanied by southwesterly winds of 6-7 Bft and an often very cloudy sky.

Neumayer Station III – EWOS Box

In the afternoon of 20 March, *Polarstern* reached the ice shelf edge near Atka Bay. Shortly before that, the sea ice cover also increased. The ship was caught between a high-pressure ridge, which extended from a high north of the Falkland Islands into the northern Weddell Sea, and a low-pressure zone in the east. Dry and very cold polar air flowed in with the strong to near-gale southwesterly current. The temperature dropped to -16°C by the evening, and due to the so-called wind chill effect, the felt temperature was -30°C. The helicopter flights for the *Neumayer* supply could be carried out in the afternoon with only little cloud cover. These were supported by meteorological observations and forecasts from the meteorologist at *Neumayer*.

On 21 March, *Polarstern* continued southwest into the so-called EWOS box. There, the aforementioned ridge moved eastwards over the working area and caused the wind to decrease. Behind the ridge, the current turned south to southeast. At the same time, a low over the Weddell Sea steered a gale from the Antarctic Peninsula eastwards. By Tuesday morning, the gale was just west of the ship. As a result, winds increased strongly from east to northeast during the night to 22 March. During the day the wind reached gale force for more than seven hours, with severe storm gusts of up to 56 kt. In addition, a frontal system with massive warm air advection passed over the working area. With repeated heavy snowfall, a veritable blizzard prevailed at times. The research work had to be interrupted due to these weather conditions. The initially existing loose sea ice was broken up by the storm and the wind sea rose to 2.5-3 m within a very short time. The gale moved east along the coast over *Polarstern*. As a result, the wind decreased somewhat in the afternoon and station work could be resumed in the sea ice.

On 23 March, a high-pressure ridge from the west temporarily provided calmer conditions. This fair-weather window was used for further necessary helicopter flights to *Neumayer Station III*: The ship set off again to *Neumayer Station III*. On the way thereto, the clouds dissipated and, in the afternoon with southwesterly winds of 5-6 Bft, flight conditions were excellent. In the evening, the high-pressure ridge moved eastwards over *Polarstern*. As a result, the wind decreased further and the return to the EWOS box was characterised by very calm conditions. However, this calm was only short-lived and only the calm before the (next) storm.

In the night to 24 March, a rapidly intensifying low followed from the Weddell Sea and lay just west of *Polarstern* until the morning. As a result, the northeasterly wind increased quickly and reached gale force in the second half of the night, when the associated frontal system was reached. During the course of the day, the strong gale shifted slightly north of the research area towards the east. After a temporary slight decrease to 8 Bft, the wind increased again in the afternoon and reached 51 kt on a 10-minute average, as well as severe gale-force gusts up to 61 kt. Because most of the ship was in the sea ice, there were only little waves. At times, swell coming in from the north reached up to 1.5 m.

In the night to 25 March, the gale moved off to the east. On its rear side, drier air flowed in and the current had turned to the south with a significant decrease. A high-pressure ridge approached from the northern Weddell Sea, starting from a high-pressure zone in the South Atlantic Ocean. Until 27 March, this provided quite calmer conditions in the EWOS box and moderate to occasionally strong winds from the southwest. Dry and increasingly cold polar air sneeked in from the southern Weddell Sea. At the same time, the sun was shining repeatedly on 25 and 26 March. In the course of 27 March, the ridge began to retreat to the north and a shallow low-pressure zone, coming from the Weddell Sea, slowly gained influence. As a result, the flow slowly strengthened and turned to east, and a weak frontal system brought a little snow at times. On 28 March, the low-pressure zone decayed slowly and the easterly wind decreased to around 4 Bft.

29 March was the prelude to another series of storms. A severe gale was located at the northern edge of the Weddell Sea near 65°S 38°W and slowly extended its large storm field towards *Polarstern* until the night to 30 March. As a result, the easterly wind increased steadily and reached 9-10 Bft on average in the first half of the day on 30 March, some hurricane-force gusts were also recorded. In addition, a warm front and strong warm air advection caused cloudy conditions with intermittent snowfall. The research work had to be stopped because of the strong wind and *Polarstern* moved to a somewhat sheltered position in the lee of a large iceberg. In addition, the water there was only relatively shallow and covered extensively by sea ice, which should prevent the build-up of high waves. The chosen location in the lee of the iceberg caused the wind to drop temporarily to 6-7 Bft on 31 March, but it was very gusty and gale-force gusts were recorded repeatedly. Subsequently, the gale moved eastward and was followed from the north by another rapidly intensifying low. This secondary low was caught by the gale directly north of the working area by 1 April and a hurricane-force low developed. Accordingly, the wind increased again to 8-9 Bft on average by early morning and hurricane-force winds of 12 Bft were already measured. As the hurricane-force low deepened further and reached 947 hPa at its core, the pressure gradient over the working area also increased further. As a result, the easterly wind further increased and for 9 hours heavy hurricane-force winds swept over the ship. The maximum recorded 3-second gust reached 81 kt, and over 90 kt were observed in the 1-second gusts! At the 10-minute average wind speed force 11 Bft was measured. It must be assumed that without the direct protection in the lee of the iceberg a few hundred metres away, wind speed would even have been somewhat higher. Because of the extreme winds, the thin sea ice was broken up and pushed away. However, due to the favourable location with only a small area of water, no high waves could build up.

In the night to 2 April, the hurricane-force low had shifted to the west, weakening, as well as its frontal system. At the same time, a second low-pressure core formed east of *Polarstern*. As a result, the easterly wind decreased to 7-8 Bft by morning and to 6-7 Bft by noon. This allowed station work to start near the Weddell Sea transect 70°45'S 11°45'W. In the evening, as the ship headed northwest out of the sea ice, the sea increased to 2.5 m.

Transect across the Weddell Sea

On 3 April, *Polarstern* stayed under the two-core low-pressure zone from the former hurricane-force low. The low-pressure core, which initially lay in the west, was crossed by mid-afternoon and the fresh to strong northeasterly current turned to the southwest after a short phase of light winds and then quickly increased to 7-8 Bft. With the increase in wind, the sea also rose from 1.5-2 m at the beginning to around 3 m. At the same time, with some uplifting und the moist unstable air mass, snow showers occurred. In the night to 4 April, a high-pressure ridge started its influence from the west, which pushed the low-pressure zone eastwards. This caused a tightening of the gradient, which led to a gale-force southwesterly wind. Sea with swell from the west to northwest also temporarily increased to 3.5-4 m, with a significantly much higher single wave hitting the ship shortly after midnight. In the course of the day, the ridge moved eastwards over the research area and the wind weakened to 4-5 Bft. On 5 April, *Polarstern* arrived at the front of an extensive low-pressure zone which extended northwards from the Weddell Sea. Within a warm front, the northeast wind briefly increased to 7 Bft during the night. Behind the front, the wind shifted temporarily to the west and decreased to 4-5 Bft. At the same time, on 5 April embedded in the low-pressure zone, a developing gale moved from the Falkland Islands to the northern edge of the Weddell Sea by the evening. This caused a strong pressure drop on board: Within 24 hours (2022-04-05 12:00 UTC to 2022-04-06 12:00 UTC), the air pressure on board dropped from 992 to 947.7 hPa. The northeast wind increased again 7 to 8 Bft by the evening within a next warm front. With the inflow of moist, mild sea air, the snow temporarily changed to rain and the temperature scraped at the 0° C mark with a maximum of -0.1° C.

Until the morning of 6 April, the severe gale lay with its core (945 hPa) just east of *Polarstern*. As a result, the northeasterly wind once again reached full gale force in the morning, causing severe gale-force winds of up to 61 kt. In the early morning, the sea reached 3.5-4 m with swell from northerly directions. In the course of the morning, the stormy wind led to a significant increase in wind sea within a very short time. The waves reached up to 6 m and at times almost 10 m. Single waves were even higher and, logically, the research work was stopped. In the afternoon, the severe gale shifted slightly to the southwest, which led to a brief decrease in wind to 6-7 Bft. By the evening, *Polarstern* had moved to the northeastern flank of the storm, which led to a renewed tightening of the gradient and an increase in wind to around 8 Bft from the northwest. At the same time, however, the waves had decreased considerably, so the ship headed south along the Weddell Sea transect and the research work was resumed on 7 April. As the ship headed south, the sea ice became thicker and more extensive. Due to the approach to the low core, the northwesterly wind decreased to 5 Bft by the afternoon. In the night to 8 April, the ship crossed the core of the former gale and was during the day in the southern part of the low, located at the southernmost station point in the thick sea ice of the central Weddell Sea near 70°50'S 29°05'W.

On 9 and 10 April, *Polarstern* was located in the southwest of a large-scale low-pressure zone with a former gale-force low to the north of the ship and another low to the south in the Weddell Sea. This resulted in fresh to occasionally strong winds from south to south-west. These directed very cold polar air into the working area. The temperature dropped to -21.9° C in the night to 10 April. With the temporary wind shift to the west, the temperature rose again to -12° C, before even colder air flowed in with the renewed south-westerly wind in the night to 11 April. This led to a minimum of -23.5° C, which was also the lowest temperature recorded on this expedition. With wind speeds of 5-6 Bft, the wind-chill temperature was below -35° C at times. The weather situation changed only little on 11 April. Only towards the northwest another low-pressure system appeared which subsequently moved east of the working area towards the southeast. Due to favourable weather conditions, helicopter flights were done daily from 8 to 11 April in order to create additional stations on the ice. On 12 April, a high-pressure ridge approached from the west. A strong westerly flow was established downstream of it. Near the ground, the air mass remained quite dry and the temperature rose to -5° C by evening. *Polarstern* temporarily left the ice on its way north. The sea with swell from northwest to west increased to 2-2.5 m during the day. During the following night, the ridge moved over the working area. On 13 April, another gale approached from the north with an associated frontal system. As a result, the wind shifted from initially west to northwest over north to east by the evening and increased to 8-9 Bft. With the inflow of milder and moister air, low stratus clouds developed, which also changed to fog at times. Temperatures around -1° C led to wet snowfall in the afternoon. *Polarstern* then continued west along the transect. The gale nestled over the Weddell Sea, with its core just southwest of the ship. The barograph on board reported a minimum air pressure of 949.6 hPa, which was almost equal to the low-core pressure of 949 hPa calculated by the weather model. With the proximity to the core, the wind already decreased again in the night to 14 April and then jumped between 5 and 7 Bft, but temporarily also at 3 Bft. In the afternoon, fog again occurred within the low core, before a bent-back occlusion again provided light snowfall in the evening.

Continuing westwards, *Polarstern* entered the northwestern part of the gale. This led to gale-force southwesterly winds from the night to 15 April. After another station near 65°S 41°W, another trip south-southwestwards into the thicker sea ice of the Weddell Sea followed in the course of 15 April. The working area was once again flooded by very cold polar air, so that temperatures around -20° C were recorded again until the morning of 16 April. In the meantime, the low-pressure zone had shifted somewhat towards the east and a high-pressure ridge approached from the Antarctic Peninsula. As a result, the southwesterly wind dropped to around 6 Bft during the day. The very cold air mass remained. The dry and very cold air led to the dissipation of stratocumulus and stratus clouds by the morning of 16 April. This provided optimal conditions for helicopter flights to support ice stations away from the ship. Over the few open water spots, the formation of shallow sea smoke was observed due to the large temperature differences between water and air.

By 17 April, the aforementioned high-pressure ridge strengthened into an independent high-pressure system and continued to approach from the west. Starting from another high northeast of the Falkland Islands, a high-pressure bridge extended southward to the Weddell Sea. The wind weakened to 3 Bft from noon onwards and there was pure sunshine from early morning until late in the evening. The formation of sea smoke was also suppressed compared to the previous day, as most open water areas were frozen over due to the persistent cold. In the afternoon of 18 April, the high-pressure connection was temporarily interrupted by a low-pressure system moving northeastwards from the northern tip of the Antarctic Peninsula. The still cold air mass was slightly moistened from the west, which resulted in low-lying stratus during the first half of the day. On 19 April, the high moved northwards from the central Weddell Sea and moved over the working area near 64°45'S 43°30'W. As the high centre was slightly east of *Polarstern*, a slowly increasing northerly flow started in the afternoon. Apart from mid- and upper-level clouds, it was quite sunny, which led to very favourable flying conditions. By 20 April, the high-pressure system had moved further northeast. At the same time, a low-pressure zone formed in the west. Less cold and more humid air sneeked in between the pressure formations with a strong northerly flow. As this milder air moved in, low stratus or fog prevailed throughout the day. In the afternoon, wet snow began to fall at temperatures of around -1° C. By 21 April, the low-pressure zone had moved from the west directly over the working area in the northwest of the Weddell Sea. With the resulting wind shift to the west, later south, and its decrease, wetter and colder air was brought in. Between two embedded lows, one southeast of the ship and the second northeast of Elephant Island, the converging air in between led to a frontal system that approached from the north from afternoon onwards and eventually caused snow fall.

On 22 April, a new high-pressure ridge approached from the west and pushed the low-pressure zone eastwards. As a result, the south to southwest wind reached 4-5 Bft on average. The colder air that was brought in caused the temperature to drop down to -14° C. Because the air was very dry at the same time, the initial clouds dissipated and it was mostly sunny. Towards evening, the wind temporarily dropped almost completely as the ridge approached. In the night of 23 April, the ridge moved east over the area. On the back side of the ridge, the northeast to north wind increased to 4-5 Bft. With the approach of a low-pressure zone in the northwest and west, the pressure gradient and consequently the north wind increased to 6 Bft by the evening. With intermittent snow showers, helicopter operations had to be cancelled early that day. The work on the Weddell Sea transect ended in the evening of 23 April near Joinville Island.

Transit Elephant Island - Punta Arenas

The last CTD and mooring work of this expedition took place on 24 April during the transit from Joinville Island to Elephant Island, as well as west of Elephant Island. On the transit during the night to 24 April, a strong and humid north to northwest current continued to prevail. At the same time, *Polarstern* left the sea ice. The milder sea air flowing in caused the temperature to rise above 0° C and the precipitation changed from sleet to rain. During the day, *Polarstern* slowly moved to the southern flank of a low-pressure complex over Patagonia and the Falkland Islands. This caused the northeasterly flow to turn to the east by the evening, and drier air was able to prevail temporarily from the morning hours onwards. However, from the afternoon onwards, pre-frontal clouds again appeared from the north. At first high, later also medium-level clouds spread across the sky. In addition, shallow fog banks persisted at times near Elephant Island, but never really formed into fog. After the successful completion of the station work near

Elephant Island, *Polarstern* began its return transit through the notorious Drake Passage to Punta Arenas in the late afternoon of 24 April.

At the beginning of the Drake Passage, *Polarstern* sailed along the southern edge of the low-pressure zone over Patagonia and the Falkland Islands. This set up a strong easterly current in which a frontal system on 25 April provided a lot of moisture, a high-reaching nimbostratus cloud cover and repeated precipitation. The sea with swell from the northeast increased to about 2.5 m during the night of 25 April. During the day, the low-pressure zone led by a gale near the Falkland Islands moved slowly eastwards. As a result, the current weakened and turned southeast to south. The waves also decreased slightly to around 2 m. On 26 April, the ship was on the southwestern edge of the low-pressure zone in the area of only small pressure contrasts. This resulted in moderate southwesterly winds at the beginning and weak winds from the afternoon onwards. Due to the unstable stratification in the lower part of the troposphere, there were rain showers in the vicinity of the ship, otherwise the sun was able to assert itself a little at times through the broken cloud cover. The sea with swell from the northeast and also southwest decreased from an initial 2 m to 1-1.5 m in the course of the day. From the night to 27 April, the ship reached the southwestern flank of a low-pressure system that was simultaneously moving from Argentina to the Falkland Islands. This established a southerly current of 7 Bft, rarely 8 Bft, which turned southwesterly in the night to 28 April. The increase in wind caused the sea with swell from the southeast to rise again to 2-2.5 m. The sky showed a various and constantly changing cloud pattern with intermittent sunshine and rain showers. When *Polarstern* reached the Strait of Magellan in the evening, the swell subsided again; at the same time, a much drier air mass flowed in. Due to local jet effects, the wind strengthened locally in the Strait of Magellan, reaching 7-8 Bft at times, before the wind dropped to 5-6 Bft by Thursday morning and turned to the west. On the morning of 28 April, *Polarstern* eventually reached the port of Punta Arenas, bringing expedition PS129 to an end.

2. HAFOS: MAINTAINING THE AWI'S LONG TERM OCEAN OBSERVATORY IN THE WEDDELL SEA

2.1 Physical Oceanography

Olaf Boebel[1], Jacob Allerholt[1], Carina Engicht[1], Mario Hoppema[1], Pedro Llanillo[1], Clea Parcerisas[2], Ole Pinner[1], Irene Torrecilla Roca[1], Stefanie Spiesecke[1], Sandra Tippenhauer[1]

[1]DE.AWI
[2]BE.VLIZ

Grant-No. AWI_PS129_01

Outline and Objectives

Due to its potential to internally store and transport vast amounts of heat and CO_2, the ocean is a key element of the global climate system. Its response to changes in the forcing is expressed and controlled by its stratification, which is governed by the vertical distribution of temperature and salinity. Until the turn of the 21 century, shipborne observations were the only means of obtaining sufficiently accurate vertical profiles of water mass properties, but progress in sensor technology now allows using autonumous systems. The current backbone of the Global Ocean Observing System (GOOS) is the Argo system, which consists of an array of more than 3,000 profiling floats, distributed throughout the world oceans. Provided by an international group of oceanographic institutions, it aims at establishing a real-time data stream of mid- and upper (< 2,000 m) ocean temperature and salinity profiles augmented by a mid-depth oceanic circulation pattern due to the floats' intrinsic drift between profiles.

However, core Argo instrumentation is restricted to oceanic regions that are ice free year-round, as the floats need to surface to be localized and to transmit their profile data via satellite link. HAFOS (Hybrid Antarctic Float Observing System) constitutes an extension of core Argo into seasonally ice-covered waters of the Weddell Gyre, overcoming these limitations through a combination of well tested technologies to close the observational gaps in the Antarctic Ocean (Boebel, 2013, 2017, 2019). To this end, AWI pushed technological developments to extend the operational range of Argo floats into seasonally ice-covered regions by initiating the development of ice-resilient floats featuring an ice-sensing algorithm (ISA; Klatt et al., 2007) which aborts a floats' ascent to the sea surface when the presence of sea ice is likely, as determined from the existence of a layer of near-surface winter water. To be able to (retrospectively) track the floats that continued their mission under sea ice, RAFOS (Ranging And Fixing Of Sound) technology (Rossby et al., 1986) is used, based on an array of RAFOS sound sources.

To determine trends and fluctuations in the characteristics of the main Antarctic water masses (i.e., Warm Deep Water, WDW, and Antarctic Bottom Water, AABW), a set of about a dozen hydrographic moorings has been maintained by AWI and expanded throughout the past 30 years. HAFOS builds on this backbone by having added RAFOS sound sources for under-ice tracking of Argo floats since 2002. Near-bottom recorders continue truly climatological time series as sentinels for climate change in the formation areas of bottom waters, whereas the profiling floats record the water mass properties in the upper ocean layers. Passive acoustic monitoring allows linking marine mammal distribution in the open ocean to ongoing ecosystem changes, thereby complementing the physical measurements with biosphere observations at its highest trophic level. These efforts focus on a region where year-round oceanographic and marine mammal observations are notoriously sparse and difficult to obtain.

HAFOS complements international efforts to establish an ocean observing system in the Antarctic as a legacy of the International Polar Year 2007/2008 (IPY) and as a contribution to the Southern Ocean Observing System (SOOS), which is under development under the auspices of the Scientific Committee of Antarctic Research (SCAR) and the Scientific Committee on Oceanic Research (SCOR).

Work at sea

Most moored oceanographic instruments are, by and large, designed for deployment periods of maximum 3 years before they need to be recovered for maintenance and battery replacement. Hence, one major goal of expedition PS129 was to recover and redeploy moorings deployed during PS117 in 2018/19, to secure the collected data and to continue these observations for another 2-3 years.

The oceanographic studies during PS129 focused on two major areas, the Prime Meridian and the Weddell Sea, continuing more than 30 years of *in situ*-observations in the Atlantic sector of the Southern Ocean. Recovering moored instruments, we obtained time series of water mass properties throughout the oceanic deep and surface layers. For this purpose, moorings featuring current meters, temperature and salinity sensors, sound sources and passive acoustic recorders were recovered (Tab. 2.2 and Fig. 2.1) and (re-)deployed (Tab. 2.3 and Fig. 2.2). Provisioning against any failure of the ultra-short baseline hydroacoustic positioning and recovery system (POSIDONIA), we kept the mini-ROV Fiona (ROV = remotely operated vehicle) ready for ROV-assisted mooring recovery, if need would arise. Mooring work was conducted by a team of 5 crew (first mate, boatswain, crane operator and 2 capstan operators) and 4-5 scientists (2 for instrument handling, 1 or 2 at the winder and a reporter).

To enhance the vertical resolution and to calibrate moored sensors, CTD (Conductivity Temperature Depth) stations were occupied at and in-between the mooring locations. The CTD/water sampler consisted of a SBE911plus CTD system in combination with a rosette water sampler SBE32 with 24 12-litre bottles (Tab. 2.4). To determine the distance to the bottom, an altimeter from Benthos was mounted. A transmissometer from Wetlabs, a SBE43 oxygen sensor from Seabird Electronics and a fluorometer were incorporated in the sensor package. Additionally, two RDI-150 kHz ADCPs (Acoustic Doppler Current Profiler), one pointing upward, one pointing downward were attached to the rosette sampler to measure the current velocity profile. A CTD/L-ADCP section was conducted between Kapp Norvegia and the Antarctic Peninsula, towards which the stations' resolution was enhanced between mooring 257-5 (near 45°W) and the tip of the Antarctic Peninsula (Fig. 2.3) aiming at delineating the export plume of Antarctic Bottom Water. The CTD was operated by a crew of two (winch operator and deck hand) and a scientific CTD watch of two. Data management was done under the auspices of the CTD team leader.

Redeployed moorings host sound sources (Tab. 2.3 and Fig. 2.4), providing RAFOS (Ranging and Fixing of Sound) signals for retrospective under-ice tracking of the ISA-Argo floats deployed during PS129 and passive acoustic recorders to record ambient (biotic and abiotic) sounds. ISA (ice sensing algorithm) and RAFOS receiver equipped Argo floats were launched to capture temperature-salinity profiles in the Weddell Sea proper. Numbering 22 floats (Tab. 2.10 and Fig. 2.5), these receive hydroacoustic RAFOS signals from a total of 9 RAFOS sound sources hosted by the aforementioned moorings, allowing retrospective tracking of their drift under the sea ice and hence localization of the profiles they collected.

Additionally, in support of the international Argo programme, 6 core Argo floats were deployed *en route* for the Bundesamt für Seeschifffahrt und Hydrographie (BSH; Tab. 2.11 and Fig. 2.5) between Cape Town and 60°S. A total of 9 biogeochemical Argo floats (Tab. 2.12 and Fig 2.5) were deployed in support of the American SOCCOM project (Southern Ocean Carbon and Climate Observations and Modeling, https://soccom.princeton.edu).

2.1.1 Oceanographic moorings

Our moorings serve three purposes:

- to host oceanographic instruments that take local measurements at typically hourly intervals, like temperature, salinity or current velocity at the very location of the instrument (Tab. 2.1),
- to host passive acoustic recorders which monitor for marine mammal presence at 10s of km ranges, and
- to host RAFOS sound sources which facilitate the tracking of RAFOS receiver equipped Argo floats roaming freely throughout the Weddell Sea.

Standard mooring design includes Aquadopp velocity profilers and CTD loggers at 800 m (the floats' park depth) and CT loggers near the sea floor (Tab. 2.1). Moorings along the continental shelf break near Kapp Norvegia (EWS001-01 and EWS002-01) and the Antarctic Peninsula (AWI207-12 and AWI261-02) are augmented with additional temperature sensors, ADCPs and bottom pressure sensors to delineate the coastal current's structure.

Tab. 2.1: Moored instrument types, recorded parameters and sampling scheme

Instrument Type	Type	Parameter	typical sample period
SBE 37 SMP	CTD recorder	p, T, S	1800 s
SBE 37 SM	CT recorder	T	1800 s
SBE 39	T (+ p) recorder	p, T	600 s
SBE 53	Bottom pressure logger	p	900 s
SBE 56	Temperature logger	T	60 s
Aquadopp	Current profiler	u, v, w	1800 s

Moorings AWI251-03/04, close to Elephant Island, feature an AZFP (Acoustic Zooplankton and Fish Profiler, ASL), which record the backscatter of acoustic pings emitted at four different frequencies (38 kHz, 125 kHz, 455 kHz, 769 kHz) to detect zooplankton. Furthermore, a 75 kHz ADCP (Acoustic Doppler Current Profiler) is included in that mooring for information on the oceanic currents at the mooring position.

Generally, near each mooring location, a CTD was cast to be able to reference the moored temperature and salinity recorder's accuracy. Due to temporal limitations resulting from the ship-speed constraints imposed on this expedition, calling at the south-westernmost mooring AWI250-3 was not attempted.

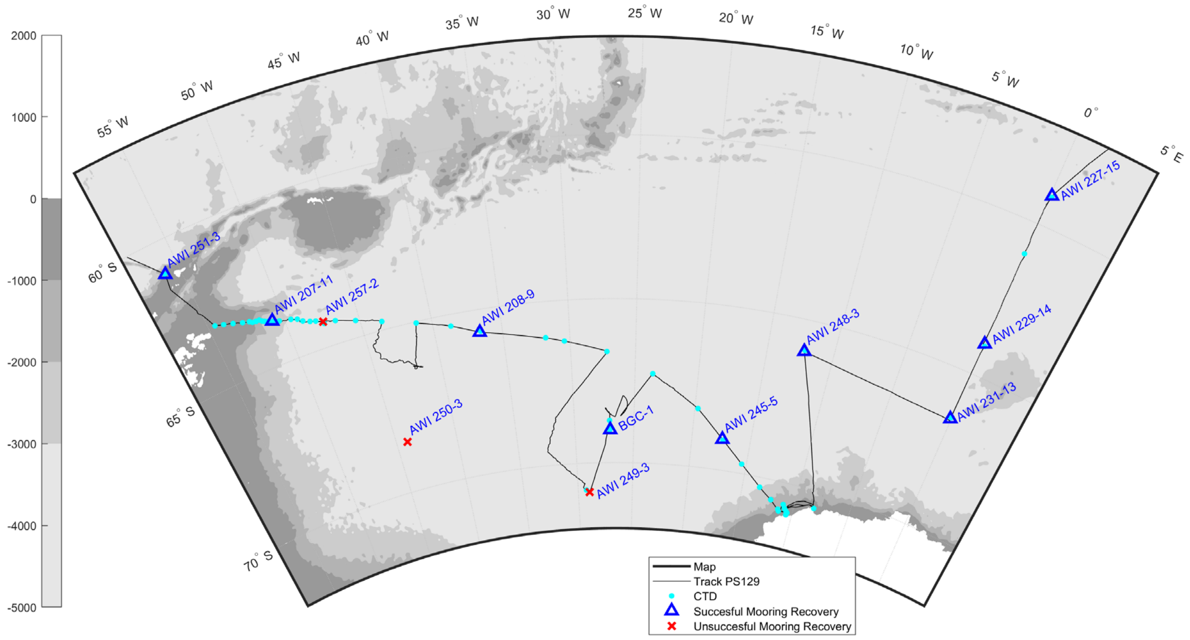

Fig. 2.1: Map of the Weddell Sea depicting the locations of successful (blue triangles) and unsuccessful (red crosses) mooring recoveries during PS129. Moorings are labelled "AWIxxx-nn", with xxx indicating Mooring ID and nn the number of consecutive deployments.

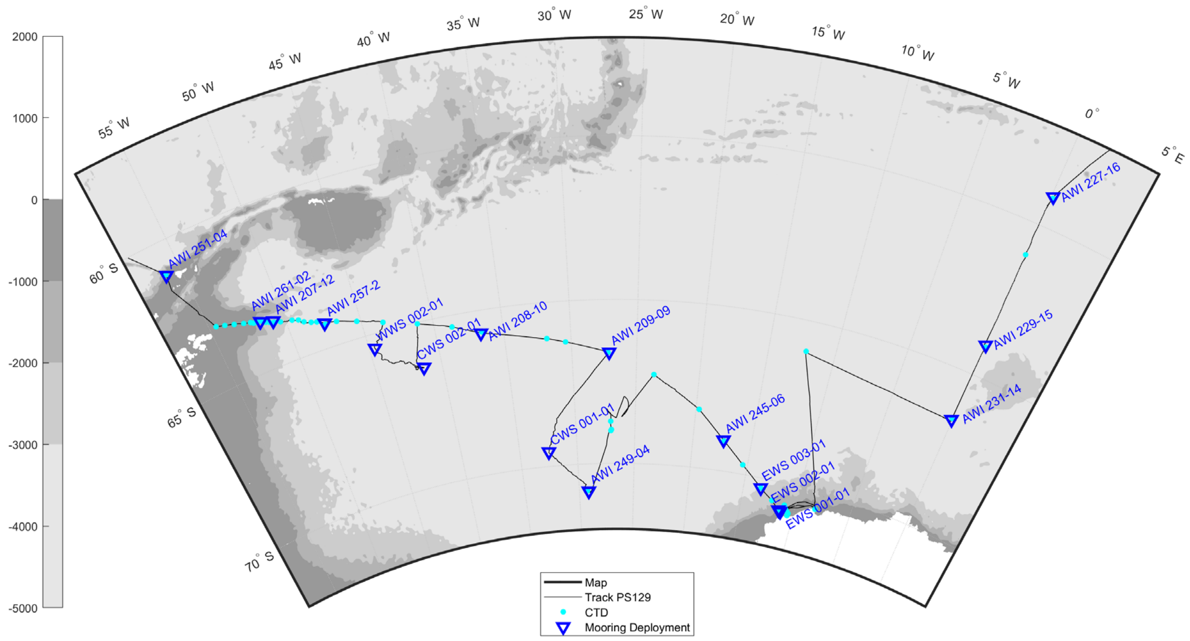

Fig. 2.2: Map of the Weddell Sea depicting the locations of mooring deployments during PS129. Moorings are labelled "ZZZxxx-nn", with ZZZxxx indicating the Mooring ID and nn the number of consecutive deployments.

Tab. 2.2: Instrumentation of moorings recovered during PS129. The column "CTD" gives the station number of the CTD casts carried out near the mooring location at deployment and recovery

For further information see the end of the Chapter.

Tab. 2.3: Instrumentation of mooring deployments during PS129

For further information see the end of the Chapter.

2.1.2 CTD observations

Ship borne CTD/rosette deployments

CTD casts were conducted pursuing three independent objectives:

- to revisit the CTD/CO_2/O_2 section across the Weddell Sea from Kapp Norvegia to the tip of the Anarctic Peninsula (WOCE repeat section SR4) across its entire length after nine years (last occupancy 2010/11),
- to collect temperature and salinity profiles at the mooring positions to tie the moored sensors single point time series to the full depth density profile,
- to revisit the spatially highly resolved repeat CTD section at the tip of the Antarctic Peninsula three years after its last occupation,
- to obtain pre- and post calibrations of the moored sensors.

The CTD/rosette was operated using the standard SeaBird SBE911plus setup, equipped with double sensors for temperature, salinity and oxygen, and one sensor each for pressure, substance fluorescence chlorophyll *a* and beam transmission. In addition, 24 12-litre OTE bottles for water sampling were attached. An altimeter was mounted to monitor the distance to the seafloor. Additionally, a high precision thermometer (SBE35, sn77/sw6345), as well as up and downward looking L-ADCPs were mounted to the rosette; ADCP SN 23293 (sw1309) as master, looking down, and ADCP SN 23292 (sw1258) as slave, looking up. Serial numbers as well as sensor web IDs are given in Table 2.4.

Tab. 2.4: CTD configurations for PS129

Sensor	Serial numbers	Sensor web ID
SBE9/Druck	321	3214
SBE3plus (primary)	1374	5844
SBE4c (primary)	3590	5870
SBE5 pump (primary)	5843	8544
SBE3plus (secondary)	1338	5842
SBE4c (secondary)	3173	4121
SBE5 pump (secondary)	5840	5865
SBE43 (primary)	4070	8542

Sensor	Serial numbers	Sensor web ID
SBE43(secondary)	4062	8543
Transmissometer, CStar	1220	4126
Fluorometer, EcoFLR	1346	5906
Altimeter	51533	4122
SBE35	0077	6345
ADCP down, master	23293	1309
ADCP up, slave	23292	1258

CTD Configuration 2 for PS129, only sensor changes are given here

Sensor	Serial numbers	Sensor web ID
Transmissometer, CStar	814	5913
Altimeter	1229	5904

CTD Configuration 3 for PS129, only sensor changes are given here

Sensor	Serial numbers	Sensor web ID
SBE43 (secondary)	1605	8546

CTD Configuration 4 for PS129, only sensor changes are given here

Sensor	Serial numbers	Sensor web ID
SBE43 (secondary)	0743	5881 or 6182
Altimeter	51533	4122

CTD Configuration 5 for PS129, only sensor changes are given here

Sensor	Serial numbers	Sensor web ID
SBE43 (secondary)	1834	5883

During this expedition, data from 54 full ocean depth CTD profiles were collected (Tab. 2.5). A map of the locations of the CTD stations is provided by Figure 2.3.

Tab. 2.5: CTD casts of PS129

For further information see the end of the Chapter.

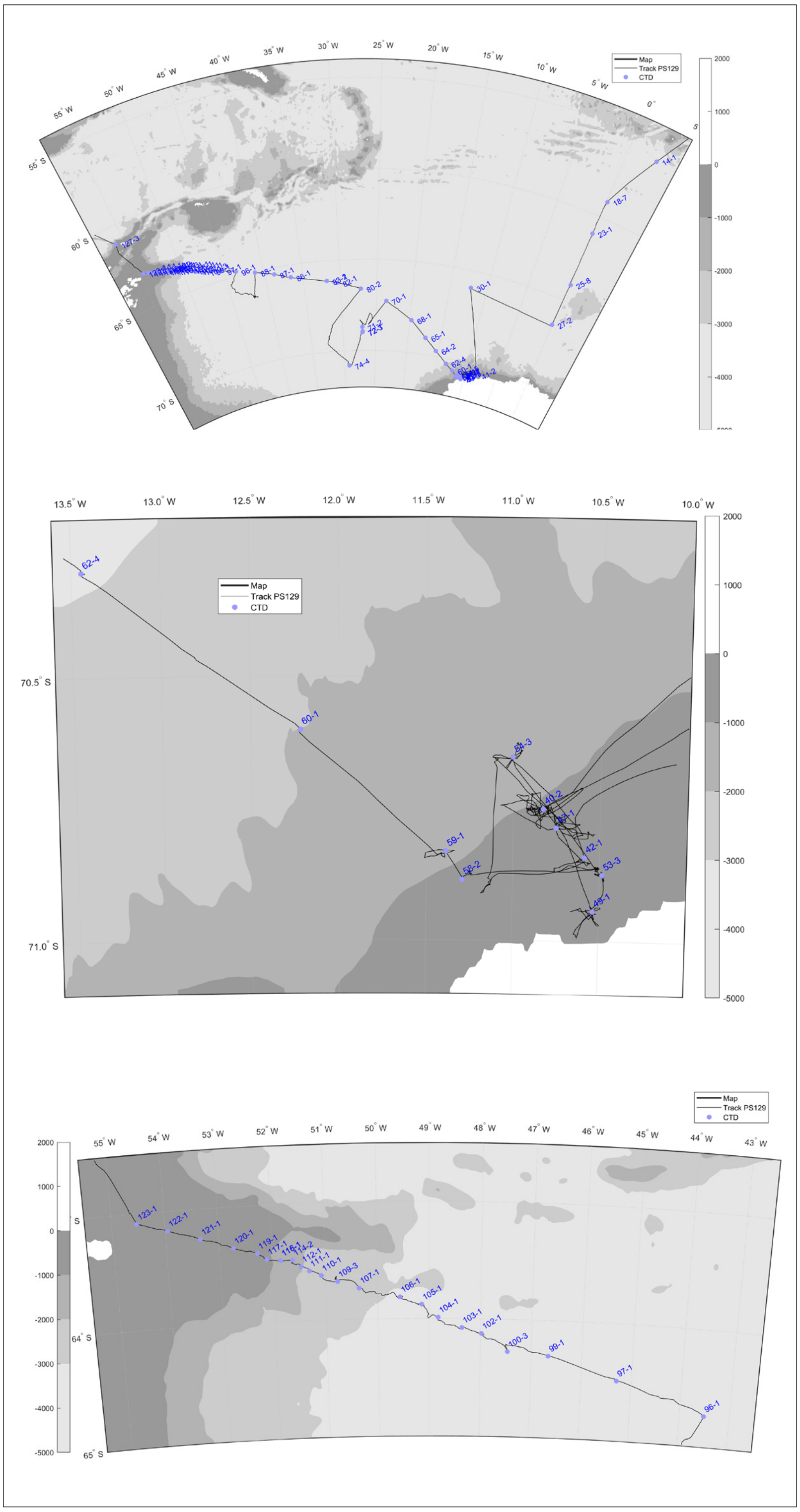

Fig. 2.3: Map of locations of CTD stations (top). Enlarged map of the CTD section near Kaap Norvegia (middle). Enlarged map of the CTD section towards the tip of the Antarctic Peninsula (bottom)

Labels indicate station and cast numbers as given in the station list.

Ocean Floor Observation and Bathymetry System borne CTD measurements

The Ocean Floor Observation and Bathymetry System (OFOBS) is used to assess distribution patterns of larger epibenthic organisms and other objects (see Section 7.3). It carries a still image camera, a forward-facing acoustic camera, a 2-band sidescan sonar system, an Ultra-Short BaseLine system transponder (USBL) and an HD-Video camera. It is lowered to the seafloor and then towed with typically 0.5 kt with an altitude between 1.5 and 10 m above ground. To access the basic physical conditions the observed organisms are living in, a CTD probe was mounted to the OFOBS frame. The CTD was a battery powered, pre-programmed, internally recording SBE-37. A list with station names, positions and file names is given in Table 2.6.

Tab. 2.6: OFOBS CTD deployments

For further information see the end of the Chapter.

2.1.3. CTD-mounted ADCP (L-ADCP)

Set-up

Two 300 kHz RDI Workhorse ADCPs were mounted on the CTD/rosette to act as lowered ADCPs (L-ADCP). The L-ADCP assembly consists of the two 300 kHz ADCPs (SN 23292 – slave, SN23293 – master) and a battery container. When on deck, communication was established to a computer in the winch control room via two cables (for master and slave), which were attached before and after each cast to the ADCPs to start and stop the ADCPs and to download the data. The ADCPs were operated using the GUI of the LADCP tool V1.7 from GEOMAR.

Data collection

L-ADCP measurements were conducted at all CTD stations. The data were downloaded after each cast, time between casts permitting. The master (downward looking device) and slave (upward looking device) data file names consist of the station number (three digits), an abbreviation indicating the viewing direction (UP for upward and DN for downward) and a running number with three digits beginning with 000, representing the file number, in case there are multiple files. For example, at station 4, data is saved in the files “004DN000.000” and “004UP000.000”. These files are stored in a folder named alike the station number. In these folders, log files documenting all actions conducted as starting (with configurations), stopping and downloading are kept as well.

When starting a new cast, the ADCP software automatically counts upwards to define the new cast number. This results in the fact that cast numbers are not counting up continuously but have some gaps, in case where the ADCP was started and stopped in between casts. L-ADCP and CTD cast numbers are given inTable 2.5. A battery change was done after L-ADCP cast number 23 and again after cast 31.

Configurations

The settings documented in Table 2.7 were used during the entire expedition. Specifically, we used 20 bins with a bin size of 10 m (i.e., a maximum range of 200 m), beam coordinates, no blanking after transmission, narrow band processing, one ping per ensemble and 1.2 seconds per ensemble.

Tab. 2.7: Configuration file of the Master L-ADCP

```
[LADCP]
last_profile_number=1
base_path=C:\ladcp\scripts\..\
network_path=L:\scientists\ladcp\raw\
cruise_id=PS129
up_installed=1
down_installed=1
total_pings=213259
total_ping_time=37.0
erase_button=enabled
download_files=all
last_action=stop
ntp_server=192.168.20.3
[Master-Commands]
mode_15=1
ambiguity_velocity=250
bin_number=20
bin_length=1000
blank_after_transmit=0
broadband=1
sensor_source=0111101
coordinate_transformation=00111
flow_control=11101
pings_per_ensemble=1
time_between_pings=0
time_per_ensemble=1.2
master_slave=1
wait_ensembles_before_sync=0
master_slave_when_to_sync=011
wait_time_before_sync=5500
power_output=255
[Slave-Commands]
mode_15=1
ambiguity_velocity=250
bin_number=20
bin_length=1000
blank_after_transmit=0
broadband=1
sensor_source=0111101
coordinate_transformation=00111
flow_control=11101
pings_per_ensemble=1
time_between_pings=0
time_per_ensemble=1.2
master_slave=2
master_slave_when_to_sync=011
wait_time_before_start_without_sync=200
power_output=255
```

Data processing

On board, data processing was carried out with the GEOMAR L-ADCP software version 10, which is executed in Matlab. The software combines, if available, data from the L-ADCP, CTD, navigational data, and a vessel mounted ADCP to conduct the velocity inversion method.

The CTD data were provided in two files, one containing data averaged onto 1 dbar and another one averaged onto 1 second. Both files where prepared unsing the programme Manage CTD. For the sADCP data, the output from the GEOMAR sADCP software (OSSI19) was used.

The software package executed in Matlab produces significant amounts of diagnostic output stored in a log file in the log folder and displayed in 16 figures saved in the folder plots. The output not only displays the calculated velocities in zonal (u) and meridional (v) directions, but also additional figures that help to identify error sources and problems of the acquisition process.

2.1.4. HAFOS sound source array

A major goal of this expedition was to reinstall the RAFOS sound source array which is used to retrospectively track the ISA-Apex floats while under ice. All previously moored HAFOS sources had been removed already during *Polarstern* expedition PS117 as, at that time, no ISA floats were present in the Weddell Gyre.

During PS129, a total of 7 sound sources were deployed. We used the opportunity of a complete reinstallation of the array to reduce the temporal spread of signals emitted by the sources from 12:00–14:10 UTC to 12:40–13:20 UTC. This allowed float-side a reduction of listening windows from 11:30–14:30 UTC (180 min duration) to 12:30–13:30 (60 min duration), resulting is significant savings in energy. A summary of sound source activities is given in Table 2.8 as well as in Figure 2.4.

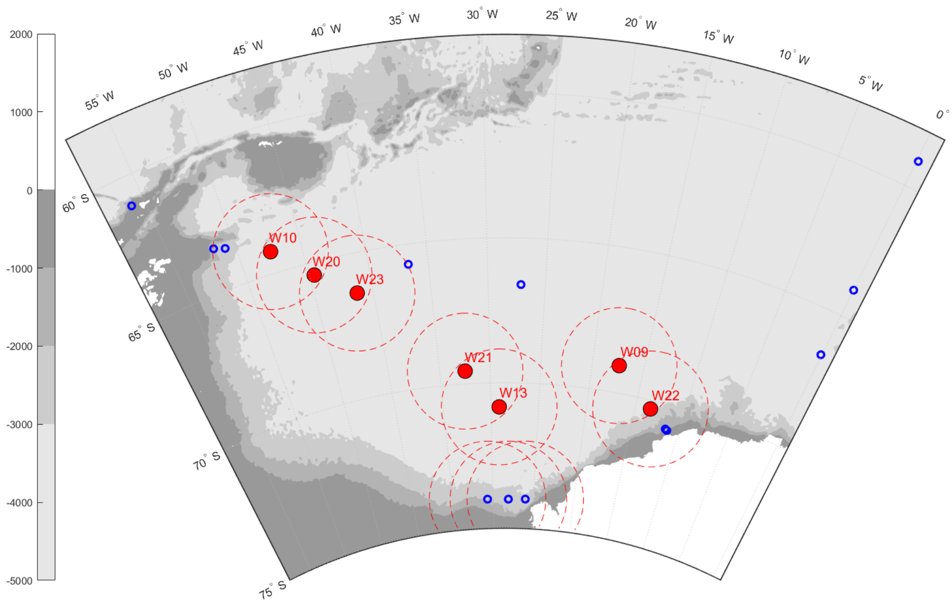

Fig. 2.4: HAFOS sound source array as deployed during PS129 (red dots with red dotted circles at 200 km radius). Presumably active sources deployed near 74°S during PS124 a year earlier are marked by small blue circles with red dotted circles. Moorings deployed during PS129 without sound sources are marked by small blue circles. Top-right to the marked position: sound source array ID

Tab. 2.8: Metadata of RAFOS sound sources deployed during PS129

For further information see the end of the Chapter.

2.1.5 Argo float deployments

During PS129, a total of 22 ice resilient APEX floats, produced by Teledyne Webb Research, U.S.A., were deployed. All floats had been appropriated by AWI and are equipped with identical sensor suits. They feature an adjustable Ice Sensing Algorithm (ISA-2), set to -1.70°C (parameter IceCriticalT) between 40 and 15 dbar (parameters IceDetectionP and Ice EvasionP), with a surfacing response retarded by 11 days (parameter IceBreakupDays, equivalent of one profile). Interim data storage internally saves all profiles that could not be transmitted in real-time due to ISA-triggered aborts of surfacing attempts and transmits these profiles during ice-free conditions. RAFOS technology is used for under ice tracking. For data transmission Iridium SBD is used. The floats were ballasted to drift at a depth of 800 m and acquire profiles from 2,000 m depth upwards every 10 days, for the first 4 profiles every 3 days. The first profile is taken directly after deployment after having sagged to 2,000 m. Floats were launched using the pressure activated autostart option, with and wake-up period of 120 m. The float's boot was filled with seawater prior to deployment, to ensure floats would sink right away after launch and not interfere with any potentially present sea ice (in fact, most floats were launched at or near 100% sea-ice coverage into the ship's swath from the ship's stern. Attempts to enlarge the spot of open water by steering hard starboard proved little helpful, as this introduced an undercurrent which carried the floats to the portside edge of the open water wake and upwards into the sea ice present there.

All floats were subjected to a self-test aboard *Polarstern* a few days prior to deployment. To this end, floats were placed outside the meteorologist's office in good view of open skies. Nevertheless, satellite communication repeatedly did not work on the first try (see Tab. 2.9). To prevent freezing of residual water in the CTD during the around 30 min long satellite communication tests, foot and hand warmers were draped around the CTD, with variable success as indicated by the temperatures reported during the self-test. One float failed to communicate by SailLoop during the test phase and will be returned to the manufacturer. Float deployment information is presented in Table 2.10 and Figure 2.5.

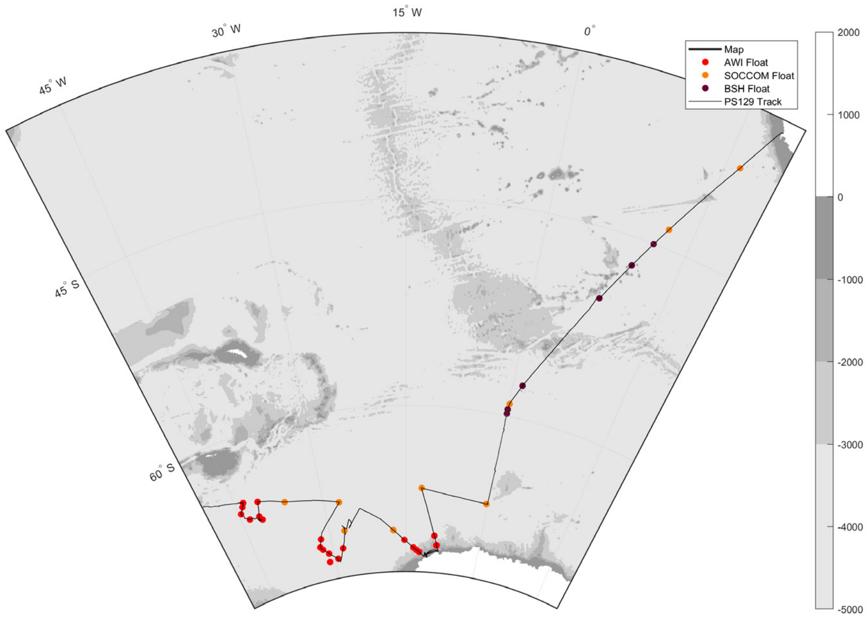

Fig. 2.5: Locations of deployments of floats provided by AWI, BSH and SOCCOM

Tab. 2.9: Ice resilient APEX float tests and clock readings

For further information see the end of the Chapter.

Tab. 2.10: Ice resilient APEX float deployments, all featuring Ice Sensing Algorithm (ISA) and RAFOS receivers

For further information see the end of the Chapter.

2.1.6. Argo float deployments on behalf of BSH / Argo Germany

During PS129, a total of 6 ARVOR-I floats were deployed on behalf of Argo Germany. Four of them are equipped with an adjustable Ice Sensing Algorithm (ISA), set to -1.79°C between 50 and 20 dbar, with a surfacing response retarded by 1 profile. Profiles that could not be transmitted in real-time due to ISA-triggered aborts of surfacing attempts are stored into the float internal memory and transmitted next time the float surfaces. For data transmission Iridium SBD is used. The floats were ballasted to drift at a depth of 1,000 m and acquire profiles from 2,000 m depth upwards 1 day after deployment for the first profile and every 10 days for the next profiles. The first profile is taken 2 hours after activation and after having sagged to 2,000 m. Float identification information given in float profiles can be downloaded on https://www.jcommops.org/board/wa/Platform?ref=xxxxxxx with xxxxxxx standing for the WMO number. Float deployment information is presented in Table 2.11 and plotted in Figure 2.5 (dark red dots).

Tab. 2.11: ARVOR float deployments *Ice Sensing Algorithm (ISA)

For further information see the end of the Chapter.

2.1.7. BGC float deployments on behalf of SOCCOM

During PS129, a total of 9 BGC (biogeochemical) SOCCOM floats were deployed – SOCCOM, Southern Ocean Carbon and Climate Observations and Modeling, is a multi-institutional U.S. programme. Floats were lowered by rope to the sea surface. Float deployment information can be found in Table 2.12 and is plotted in Figure 2.5 (orange dots).

Tab. 2.12: SOCCOM float deployments

For further information see the end of the Chapter.

2.1.8. Salinity calibrations by salinometer

To calibrate the conductivity sensors, water samples for salinity were taken regularly and measured with the Optimare Precision Salinometer (OPS). Prior to measurement, samples where degassed by heating them to 30°C for 1 hour, venting the overpressure and let them adjust to room temperature. In total, 220 salinity samples were measured using the OPS-006 or OPS-007 instruments. As a standard, the OPS-006 is the one to be used by scientists, while OPS-007 is used by the ship’s crew. As OPS-006 exhibited a discontinuity in the salinity readings on 3 April 2022, the OPS-007 was used for the subsequent measurements while the OPS-006 was cleaned. Once the OPS-006 showed stable readings again it was reemployed. On 25 April 2022, however, the OPS-006 became unusable as the pre-bath stirrer broke.

Table 2.13 lists all salinity measurements. Out of the 220 salinity measurements, 5 were unusable due to unstable readings of the OPS. For 2 out of these 5 instances, the reason is unknown. To examine the impact of the degassing procedure on the salinity measurements, outgassing was skipped for 3 samples. For those 3 samples, the OPS measurement did not stabilize, indicating that the OPS cannot obtain stable measurements if samples are not degassed properly. In addition to the samples measured on board, 68 samples were shipped to AWI, for later analyses and comparisons between an Optimare Precision Salinometer and an Autosal instrument, the latter of which was used on *Polarstern* cruises earlier in time. Final calibration of the CTD data will be performed using the salinometer measurements together with the post-cruise manufacturer calibration of the sensors.

Tab. 2.13: Salinity measurements by salinometer. Numbers printed red indicate values that exhibited a discontinuity in the OPS reading, resulting in their exclusion from the calibration process.

For further information see the end of the Chapter.

2.1.9. Vessel mounted ADCP (sADCP)

Polarstern is equipped with an Ocean Surveyor 150 kHz (RD-Instruments) Acoustic Doppler Current Profiler (sADCP) to monitor ocean currents. The sADCP was operated using the settings given in Table 2.14. During most of the expedition the sADCP was operated in slave mode, triggered by the K-Synch unit. Pinging was synchronized between the sADCP and the EK-80, which uses four different frequencies (38 kHz, 70 kHz, 120 kHz, 200 kHz) in FM-mode (broadband) and a single 18 kHz ping for echosounding (depth). Zero waiting time was set for the sADCP and EK-80. For the 18 kHz depth sounder, a depth dependent waiting time was set. Before those settings where found, the sADCP was stopped and restarted several times for changing the configuration of the synch-unit as well as EK-80 calibrations.

For protection against ice, the Ocean Surveyor is mounted in a water filled cavity behind a window, in the ship's hull. When steaming through ice, air accumulates inside the window over time, which negatively affects the data quality. During PS129 the air was regularly released by the laboratory electrician.

The data from the sADCP were merged online with the corresponding navigation data (i.e., the vessel's GPS system) and stored on the hard disk using the program VMDAS. Pitch, roll and heading data are converted from NMEA. Current velocity data were collected in beam coordinates to apply corrections during post processing. Processing during the cruise was conducted using GEOMAR s-ADCP software (OSSI19). Final data processing and quality control will be performed at AWI.

Tab. 2.14: Configuration file of the sADCP

```
; Restore factory default settings in the ADCP
cr1h

; set the data collection baud rate to 9600 bps,
; no parity, one stop bit, 8 data bits
; NOTE:  VmDas sends baud rate change command after all other commands in
; this file, so that it is not made permanent by a CK command.
cb411

; Set for narrowband single-ping profile mode (NP), 80 (NN), 4-meter bins (NS),
; 4-meter blanking distance (NF)
WP000
NP001
NN080
NS0400
NF0400
;WV390 (default)

; Disable single-ping bottom track (BP),
BP000

; output velocity, correlation, echo intensity, percent good
ND111100000

; Ping as fast as possible
TP000000

; Since VmDas uses manual pinging, TE is ignored by the ADCP
; and should not be set.
;TE0000000

; Set to calculate speed-of-sound, no depth sensor, external synchro heading
; sensor, pitch or roll being used, no salinity sensor, use internal transducer
; temperature sensor
EZ1011101

; Output beam data (rotations are done in software)
EX00000
; Set transducer misalignment (hundredths of degrees).
; Ignored here but set in VmDAS options.
;EA00000

; Set transducer depth (decimeters)
ED00110

; Set Salinity (ppt)
ES35

;set external triggering and output trigger; no trigger
CX0,0 (either on or off)

;set external triggering and output trigger
;CX1,3 (either on or off)

; save this setup to non-volatile memory in the ADCP
CK
```

2.1.10. Thermosalinograph

There are two SBE21 SeaCAT thermosalinographs with additional external thermometers SBE38 for minimum thermal contamination from the ship. The two systems are operated in parallel on the same seawater intake. The pumped system is equipped with a flow meter and set to pump 60 L min^{-1}. Position and time information is added via NMEA telegram. The system is located in the ships keel with the water intake at about 11 m depth, depending on the ships draft.

During PS129, the system was running continuously and switched off only for short maintenance and cleaning. For calibration, salinity samples are taken irregularly, depending on the ice conditions. On average, samples are taken every other week and measured with an Optimare Precision Salinometer on board by the ship's laboratory electrician. The sensors are usually operated for one full expedition season (about half a year, depending on expedition schedule) and changed during port calls in Bremerhaven. Once post-cruise calibration of sensors has been performed, the data is processed and calibrated by Fielax GmbH and stored in the PANGAEA data repository.

2.1.11. RAFOS source tuning

A detailed description of the objectives and approach of tuning the RAFOS sources *in situ* is given in the expedition report of ANT-XXIX/2 (Boebel, 2015). During PS129, the frequency response of 7 sound sources was determined using 19 tuning runs: all systems, except one, featured new anodized aluminum resonance tubes and had a total length of 2220-2230 mm. One system had already been tuned on a previous expedition (D0046, end length: 1,900 mm). Due to a refurbishment of this source by the manufacturer, its tuning required checking.

Tuning, i.e., shortening the length of a resonator tube until it resonates at the RAFOS center frequency of 260 Hz, of the new resonator tubes was performed in up to four tuning runs per resonator. Before each shortening, the frequency response of resonators was determined by using up to four consecutive 80-sec long frequency sweeps per run. Start times of sweeps were spaced by 10 minutes to allow the electronics to cool down before starting a new sweep. As the tuning procedure was adapted a number of times during the cruise, the frequency range of each sweep within a run varied.

Before shortening the tubes, the frequency response of the source was determined by using consecutive 80-sec sweeps over a total frequency range from 230-265 Hz. In the first and second tuning step, 3 sweeps were configured to cover the current expected resonance frequency +/- 8 Hz, and the RAFOS frequency. In the third and last tuning step, one sweep from 256-264 Hz and the RAFOS sweep were performed to obtain the final resonance frequency and source level. Details of the steps were adapted during the expedition according to new findings in the resonance frequency behavior (Tab. 2.15).

The sound source's configuration for the tuning was stored on an SD card and set to start on a fictional future date. Prior to the lowering of the sound source, a time approximately 45 minutes before this fictional date/time was set to give the system enough time to be lowered to the measurement depth of 800 m before starting the first sweep.

Sound sources were lowered horizontally to 800 m depth in waters of at least 2,000 m depth using winch #32. A 10-m-long rope with a Sound Velocity Profiler (Valeport) was hanging below the sound source for sound velocity measurements. An additional 25 kg weight was attached below the Sound Velocity Profiler and two 25 kg weights were attached directly underneath the sound source. During the first measurements, the sound sources were directly attached to the winch cable using a sling around the middle part and the electronics of the source.

Starting 18 March 2022, a metal bar was attached to the empty brackets on the opposite side to the electronics with the intention to prevent the sound source from swinging during the tuning measurements. For redundancy of the acoustic recordings, 3 icListen (SN 1413, 1414 and 1415) were attached 40 m above the sound source at 1/8 wavelength spacing directly to the winch cable. Results, however, showed inconsistent sound pressure levels. To minimize potential near-field effects, the distances between the source and the recorders was changed to around 84 m.

Tab. 2.15: Sound source tunings with sweep parameters by step

Event Time	Reso-nator	Electro-nics	Run	sweep 1 [Hz]	sweep 2 [Hz]	sweep 3 [Hz]	sweep 4 [Hz]
12.03.2022 18:55	D0047	EI0043	Run 1	230 - 240	240 - 250	250 - 260	
12.03.2022 20:35	D0048	EI0061	Run 1	230 - 240	240 - 250	250 - 260	
13.03.2022 10:48	D0046	EI0066	Run 1	255 - 265	RAFOS		
15.03.2022 19:58	D0046	EI0066	Run 2	257 - 263	RAFOS		
17.03.2022 03:52	D0048	EI0061	Run 2	249 - 255	255 - 261	RAFOS	
18.03.2022 14:11	D0046	EI0043	Run 3	257 - 263	RAFOS		
18.03.2022 15:58	D0048	EI0061	Run 3	257 - 263	RAFOS		
18.03.2022 17:29	D0017	EI0067	Run 1	230 - 238	238 - 246	246 - 254	
03.04.2022 01:07	D0017	EI0058	Run 2	240 - 248	248 - 256	256 - 264	RAFOS
03.04.2022 03:19	D0043	EI0047	Run 1	230 - 238	238 - 246	246 - 254	RAFOS
03.04.2022 05:04	D0018	EI0050	Run 1	230 - 238	238 - 246	246 - 254	RAFOS
04.04.2022 16:46	D0043	EI0047	Run 2	246 - 254	254 - 262	RAFOS	
04.04.2022 18:31	D0017	EI0058	Run 3	246 - 254	254 - 262	RAFOS	
04.04.2022 20:11	D0018	EI0050	Run 2	246 - 254	254 - 262	RAFOS	
08.04.2022 13:06	D0043	EI0047	Run 3	256 - 264	RAFOS		
08.04.2022 21:40	D0018	EI0050	Run 3	256 - 264	RAFOS		
08.04.2022 23:15	D0017	EI0058	Run 4	256 - 264	RAFOS		
15.04.2022 17:00	D0030	EI0066	Run 1	235-243	239.38- 240.90		
17.04.2022 08:08	D0030	EI0066	Run 2	256 - 264	RAFOS		

After completion of each run, recordings from the acoustic recorders were saved from the icListen's internal storage to hard disk. Using Audacity, sweeps belonging to a given sound source were manually cut at their boundaries from the displayed spectrogram and saved as single files.

A python script was used to determine the (current) resonance frequency of the highest root-mean-square amplitude SLmax sweep [dB] (Tab. 2.16). A MATLAB™ script used the current resonance frequency, current tube length and environmental parameters (e.g., sound velocity at tuning depth, water density) to derive the target resonance length and the excess length to be cut. During the first cut, a length of only about two third of the calculated difference was cut, while on the second cut, the remaining calculated length difference was cut. Additionally, 3 boreholes were drilled on each side with a diameter of 12 mm and the center 30 cm from the edge. Isolators were glued into the borehole. After this the last remaining tuning measurement was performed.

Tab. 2.16: Sound source tunings. A block of three lines each represents a single tuning run with the three lines distinguishing the measurements from the three icListen hydrophones. Dist. [m] gives the distance from the source to the hydrophone. Length [mm] gives the overall tube length for both tubes end to end. fpk sweep = frequency of spectral peak, SLmax sweep = maximum band-passed filtered source level during sweep, SL RAFOS = source level during RAFOS sweep re 1 µPa

Sound Source	electr. ID	icListen ID	Run	f_{pk}. sweep [Hz]	SL_{max} sweep [dB]	SL RAFOS [dB]	Coil	Amp.	Dist. [m]	Length [mm]	DateTime
D0017	EI0067	1413	1	242.5	186.4	NA	off	100	82	2220	202203181802
D0017	EI0067	1414	1	242.5	188.48	NA	off	100	82	2220	202203181802
D0017	EI0067	1415	1	241.0	187.46	NA	off	100	82	2220	202203181802
D0017	EI0058	1413	2	241.0	177.63	168.21	off	95	84.2	2220	202204030147
D0017	EI0058	1414	2	249.0	170.49	167.44	off	95	81.4	2220	202204030147
D0017	EI0058	1415	2	240.5	178.35	167.74	off	95	82.8	2220	202204030147
D0018	EI0050	1413	1	240.0	173.2	168.64	off	95	84.2	2230	202204030545
D0018	EI0050	1414	1	241.5	168.68	167.45	off	95	81.4	2230	202204030545
D0018	EI0050	1415	1	240.0	177.44	170.03	off	95	82.8	2230	202204030545
D0043	EI0047	1413	1	239.0	175	156.92	off	95	82.2	2230	202204030350
D0043	EI0047	1414	1	239.0	172.31	155.82	off	95	81.4	2230	202204030350
D0043	EI0047	1415	1	237.5	174.21	155.46	off	95	82.8	2230	202204030350
D0046	EI0066	1413	1	NA	NA	162.23	off	100	42.8	1900	202203131123
D0046	EI0066	1414	1	NA	NA	161.35	off	100	41.4	1900	202203131123
D0046	EI0066	1415	1	NA	NA	165.44	off	100	40.0	1900	202203131123
D0046	EI0066	1413	2	NA	NA	180.09	on	100	40.0	1900	202203152034
D0046	EI0066	1414	2	NA	NA	176.91	on	100	41.4	1900	202203152034
D0046	EI0066	1415	2	NA	NA	188.46	on	100	42.8	1900	202203152034
D0046	EI0043	1413	3	NA	NA	173.98	on	90	82.0	1900	202203181445
D0046	EI0043	1414	3	NA	NA	168.66	on	90	82.0	1900	202203181445
D0046	EI0043	1415	3	NA	NA	177.11	on	90	82.0	1900	202203181445
D0047	EI0043	1413	1	232.5	170.23	NA	off	100	42.8	2240	202203122106
D0047	EI0043	1414	1	243.0	163.6	NA	off	100	41.4	2240	202203122106
D0047	EI0043	1415	1	238.5	176	NA	off	100	40.0	2240	202203122106
D0048	EI0061	1413	1	241.5	178.26	NA	off	100	42.8	2220	202203121930
D0048	EI0061	1414	1	241.5	175.04	NA	off	100	41.4	2220	202203121930
D0048	EI0061	1415	1	241.5	178.28	NA	off	100	40.0	2220	202203121930
D0048	EI0061	1413	2	259.0	161.15	160.63	off	100	40.0	1964	202203170430
D0048	EI0061	1414	2	256.5	164.88	162.89	off	100	41.4	1964	202203170430
D0048	EI0061	1415	2	256.0	171.24	168.39	off	100	42.8	1964	202203170430
D0048	EI0061	1413	3	NA	NA	168.47	on	90	82.0	1965	202203181634
D0048	EI0061	1414	3	NA	NA	170.04	on	90	82.0	1965	202203181634
D0048	EI0061	1415	3	NA	NA	171.91	on	90	82.0	1965	202203181634
D0017	EI0058	1413	3	246.0	172.36	158.45	off	95	84.2	2006	202204041909
D0017	EI0058	1414	3	249.69	170.07	156.4	off	95	81.4	2006	202204041909
D0017	EI0058	1415	3	245.0	169.66	161.82	off	95	82.8	2006	202204041909
D0018	EI0050	1413	2	248.0	178.39	163.88	off	95	84.2	2010	202204042050
D0018	EI0050	1414	2	250.0	176.13	162.91	off	95	81.4	2010	202204042050
D0018	EI0050	1415	2	250.0	176.52	169.54	off	95	82.8	2010	202204042050

Sound Source	electr. ID	icListen ID	Run	f_{pk}. sweep [Hz]	SL_{max} sweep [dB]	SL RAFOS [dB]	Coil	Amp.	Dist. [m]	Length [mm]	DateTime
D0043	EI0047	1413	2	250.99	175.43	160.38	off	95	84.2	2006	202204041725
D0043	EI0047	1414	2	251.03	173.87	159.44	off	95	81.4	2006	202204041725
D0043	EI0047	1415	2	248.36	172.09	161.74	off	95	82.8	2006	202204041725
D0017	EI0058	1413	4	NA	NA	187.79	on	95	84.2	1845	202204082354
D0017	EI0058	1414	4	NA	NA	186.58	on	95	81.4	1845	202204082354
D0017	EI0058	1415	4	NA	NA	189.81	on	95	82.8	1845	202204082354
D0018	EI0050	1413	3	256.5	181.97	176.41	on	95	84.2	1865	202204082220
D0018	EI0050	1414	3	256.5	179.77	174.78	on	95	81.4	1865	202204082220
D0018	EI0050	1415	3	256.5	183.23	181.62	on	95	82.8	1865	202204082220
D0043	EI0047	1413	3	NA	NA	172.71	on	95	84.2	1890	202204081345
D0043	EI0047	1414	3	NA	NA	171.19	on	95	81.4	1890	202204081345
D0043	EI0047	1415	3	NA	NA	169.89	on	95	82.8	1890	202204081345
D0030	EI0066	1413	1	241.5	178	NA	on	95	84.2	2230	202204151630
D0030	EI0066	1414	1	242.0	174.51	NA	on	95	81.4	2230	202204151630
D0030	EI0066	1415	1	240.5	178.76	NA	on	95	82.8	2230	202204151630
D0030	EI0066	1413	2	NA	NA	163.44	off	95	84.2	1900	202204170650
D0030	EI0066	1414	2	NA	NA	162.95	off	95	81.4	1900	202204170650
D0030	EI0066	1415	2	NA	NA	168.94	off	95	82.8	1900	202204170650

Operational results

2.1.12. Oceanographic moorings

Details of the recovered hydrographic instrumentation and the length of each data record retrieved are listed in Table 2.17. In general, the instruments performed well, providing, with few exceptions, data for the full deployment period.

Tab. 2.17: Recovered hydrographic instruments (34 in total), their condition and data record length

Mooring	Instrument Type	SN	Data record length [days]	Recorded Full period (Y/N)	Type of failure	Physical condition from visual inspection at recovery
227-15	SBE37	12479	1166	Y	-	Good
229-14	SBE37	2098	1168	Y	-	Good
229-14	SBE37	2385	1168	Y	-	Good
229-14	SBE37	2382	1168	Y	-	Good
229-14	SBE37	2396	1168	Y	-	Good
229-14	SBE37	9492	1168	Y	-	Good
229-14	SBE37	9494	1168	Y	-	Good
229-14	SBE37	9495	1168	Y	-	Good
229-14	SBE37	9496	1168	Y	-	Good
229-14	SBE37	9497	1168	Y	-	Good
229-14	SBE37	12481	1168	Y	-	Good

Mooring	Instrument Type	SN	Data record length [days]	Recorded Full period (Y/N)	Type of failure	Physical condition from visual inspection at recovery
229-14	Aquadopp	12654	1168	Y	-	Good
229-14	Aquadopp	12658	1168	Y	-	Good
231-13	SBE37	10944	1175	Y	-	Good
245-5	SBE37	8124	590	N	Recording interrupted	Good
248-3	SBE37	8123	151	N	Recording interrupted	Good
BGC-1	SBE37	449	379	Y	-	Good
BGC-1	SBE37	2100	379	Y	-	Good
BGC-1	SBE56	6513	379	Y	-	Good
BGC-1	SBE56	7824	379	Y	-	Good
BGC-1	SBE56	7825	379	Y	-	Good
208-9	SBE37	9841	1176	Y	-	Good
208-9	SBE37	3812	0	N	No data recorded	Good
208-9	Aquadopp	12685	1177	Y	-	Good
207-11	Aquadopp	12745	1178	Y	-	Good
207-11	SBE37	6928	1177	Y	-	Good
207-11	SBE37	9847	1177	Y	-	Good
207-11	SBE37	10934	1177	Y	-	Good
207-11	SBE37	10937	1177	Y	-	Good
207-11	SBE37	10943	1177	Y	-	Good
207-11	SBE39	8641	1177	Y	-	Good
207-11	SBE39	8642	1177	Y	-	Good
207-11	SBE39	8643	1177	Y	-	Good
251-3	SBE37	2096	1177	Y	-	Good

2.1.13. *In-situ* calibration of moored instruments

All Seabird® instruments (SBE37ct, SBE37ctp, SBE39plus, and SBE56) were compared *in situ* with the 911plus CTD system prior to mooring deployment or after recovery. Up to 15 units were attached at a time to the frame of the rosette water sampler. For the *in situ* calibration, the sampling interval was set to 10 seconds and programmed to begin sampling prior to the CTD reaching its maximum depth. The CTD/rosette was stopped at two different depths exhibiting low stratification for 5 minutes to obtain approximately 30 records for comparison with the CTD reading.

During PS129, the following modifications have been applied to the standard calibration process of moored instruments:

1. For the instruments without pressure sensor (SBE56, old SBE37):
    a. Interpolation of CTD pressure by using timestamps as the reference between CTD and instruments.

b. Correction of the actual pressure effect on the conductivity, c, according to equation below as suggested by Povl Abrahamsen, BAS[1].

$$c_{corr} = c_{instr} \cdot \frac{1+(\kappa_T \cdot T_{inst}) + (\kappa_p \cdot p_{ref})}{1+(\kappa_T \cdot T_{inst}) + (\kappa_p \cdot p_{interp})} \text{, with}$$

c_{corr}	*the corrected conductivity;*
c_{instr}	*the instrument's conductivity reading;*
κ_T	*the correction coefficient for temperature effects on conductivity,* $3.25 \cdot 10^{-6}\ °C^{-1}$;
κ_p	*the correction coefficient for pressure effects on conductivity,* $-9.57 \cdot 10^{-8}\ dbar^{-1}$;
T_{inst}	*the intruments temperature reading during the calibration period* [°C];
p_{ref}	*for SBE37ct (without pressure sensor), the reference perssure , eqalling 0 dbar (zero);*
p_{interp}	*for SBE37ct (without pressure sensor), the interpolated pressure during the measument period [dbar].*

This correction reduces the conductivity offsets between instrument and CTD by up to one order of magnitude (for example the offset of SN238 was reduced from 0.0819 to 0.0047, and for SN239 from 0.0212 to 0.0090).

2. The CTD file bin-averaged every 1 second is now preferred over the CTD file bin-averaged every 1 dbar to compute the offsets of the moored instruments as this allows reconstructing the pressures of moored instruments without pressure and also to obtain a more accurate (time) mean of the CTD values during the calibration stop. In contrast, the standard calibration process computed the offsets to the value of a selected CTD pressure level (bin-averaged by 1 dbar and thus time independent) instead. This was less accurate than using the mean of the actual CTD values measured during the 5 mins calibration stop. Both the CTD and the attached instruments are oscillating in depth during the calibration stop and thus, using the actual time dependent sampling points to compute their offsets is more advisable.

3. Correct for the cropping issue limited to 8 instruments. As several calibration casts were done with more than 8 instruments, this meant that the truncation of the values selected from the calibration stop would not be exactly the same for all the instruments (the cropping needed to be done more than once). This is solved by a modification in the main routine (guiSBEvsCTD.m) that allows for truncating the time series of up to 18 instruments at the same time.

   Further modifications: Addition of the SBE56 instrument type, inclusion of the times of the CTD and attached instruments, calibration plots with time in the X-axis instead of sampling counts and including the actual CTD values and mean along the calibration stop.

[1]More details in SeaBird's Application Note nº 10 (May 2013, "Compensation of Sea-Bird Conductivity sensors").

Tab. 2.18: Comparison for Seabird sensors SBE37 moored during PS117. Columns CTD and PRES indicate the corresponding station number and the CTD pressure during the 5-minute stop. Xcorr = Xreading + ΔX, with X = temperature (t), conductivity(c) or pressure (p)

Mooring	Type	SN	CTD	Δp [dbar}	ΔT [ºC]	Δc [mS cm^{-1}]	ΔS [psu]	pres [dbar]
227-16	SBE37	1232	none					
227-16	SBE37	10933	none					
229-15	SBE37	238	018-07	R	-0.0059	0.0047	0.0124	4680
229-15	SBE37	10929	018-07	-8.5	0.0017	0.0069	0.0105	4680
229-15	SBE37	10930	018-07	-7.4	0.0025	0.0063	0.0085	4680
229-15	SBE37	10931	018-07	-7.7	0.0012	0.0086	0.0129	4680
229-15	SBE37	10932	018-07	-7.3	0.0013	0.0039	0.0066	4680
231-14	SBE37	239	018-07	R	-0.0006	0.0090	0.0121	4680
231-14	SBE37	9848	018-07	-8.2	0.0020	0.0056	0.0084	4680
229-15	SBE37	225	023-01	R	0.0013	0.0110	0.0125	5465
229-15	SBE37	230	023-01	R	-0.0041	0.0102	0.0174	5465
EWS01-01	SBE37	10928	023-01	-9.1	0.0016	0.0055	0.0089	5465
EWS01-01	SBE37	10940	023-01	-9.1	0.0021	0.0066	0.0096	5465
EWS01-01	SBE37	10941	023-01	-9.1	0.0011	0.0065	0.0106	5465
EWS01-01	SBE37	10942	023-01	-10.3	0.0015	0.0053	0.0091	5465
EWS01-01	SBE56	7826	040-02	R	0.0010	-	-	918
EWS01-01	SBE56	7827	040-02	R	0.0005	-	-	918
EWS01-01	SBE56	7828	040-02	R	0.0005	-	-	918
EWS01-01	SBE56	7829	040-02	R	0.0010	-	-	918
EWS02-01	SBE37	2088	023-01	-9.3	0.0022	0.0018	0.0036	5465
EWS02-01	SBE37	9490	023-01	-4.4	0.0011	0.0047	0.0065	5465
EWS02-01	SBE37	10946	023-01	-9.0	0.0009	0.0042	0.0078	5465
EWS02-01	SBE37	10947	023-01	-7.6	0.0012	0.0056	0.0087	5465
EWS02-01	SBE37	11420	023-01	1.0	0.0006	0.0066	0.0073	5465
EWS02-01	SBE56	7830	040-02	R	0.0008	-	-	918
EWS02-01	SBE56	7831	040-02	R	0.0013	-	-	918
EWS02-01	SBE56	7833	040-02	R	0.0009	-	-	918
EWS02-01	SBE56	6368	040-02	R	-0.0002	-	-	918
EWS02-01	SBE56	6986	040-02	R	-0.0048	-	-	918
EWS02-01	SBE56	6988	040-02	R	0.0106	-	-	918
EWS02-01	SBE56	6989	040-02	R	-0.0048	-	-	918
EWS03-01	SBE37	224	023-01	R	-0.0001	0.0118	0.0152	5465
EWS03-01	SBE37	3814	060-01	1.5	0.0008	0.0045	0.0041	1907
245-6	SBE37	218	023-01	R	-0.0014	0.0140	0.0193	5465
245-6	SBE37	9838	023-01	-6.2	0.0007	0.0133	0.0185	5465
249-4	SBE37	9832	023-01	-9.3	0.0005	0.0069	0.0119	5465
249-4	SBE37	235	030-01	R	-0.0008	0.0107	0.0145	5107
208-10	SBE37	442	030-01	R	0.0037	0.0108	0.0098	5107
208-10	SBE37	9487	030-01	-5.1	0.0013	0.0068	0.0093	5107
209-09	SBE37	440	030-01	R	-0.0004	0.0096	0.0127	5107
209-09	SBE37	9491	030-01	-5.8	0.0018	0.0055	0.0074	5107

Mooring	Type	SN	CTD	Δp [dbar}	ΔT [ºC]	Δc [mS cm^{-1}]	ΔS [psu]	pres [dbar]
208-10	SBE37	442	030-01	R	0.0037	0.0108	0.0098	5107
208-10	SBE37	9487	030-01	-5.1019	0.0013	0.0068	0.0093	5107
CWS01-01	SBE37	233	064-02	R	0.0005	0.0124	0.0154	4819
CWS01-01	SBE37	2090	064-02	-4.7	0.0006	0.0066	0.0097	4819
CWS01-01	SBE37	2090	064-02	-4.7	0.0006	0.0066	0.0097	4819
CWS02-01	SBE37	444	064-02	-0.2	-0.0041	0.0107	0.0181	4819
CWS02-01	SBE37	2101	064-02	-5.1	0.0009	0.0059	0.0086	4819
WWS02-01	SBE37	9488	064-02	-5.8	0.0013	0.0058	0.0085	4819
WWS02-01	SBE37	232	064-02	-0.2453	-0.0011	0.0112	0.0157	4819
257-3	SBE37	435	080-02	0.0	-0.0090	0.0106	0.0232	4924
257-3	SBE37	7690	080-02	0.8	0.0018	0.0080	0.0079	4924
207-12	SBE37	2089	064-02	1.3	0.0012	0.0046	0.0040	4819
207-12	SBE37	11421	064-02	0.4	0.0018	0.0066	0.0064	4819
207-12	SBE37	2094	064-02	-8.7	0.0016	0.0095	0.0140	4819
207-12	SBE37	2234	064-02	-1.5	0.0015	0.0089	0.0103	4819
207-12	SBE37	2099	064-02	-4.2	0.0000	0.0033	0.0059	4819
207-12	SBE39	7860	080-02	-6.4	0.0014	-	-	4924
207-12	SBE39	7861	080-02	2.7	0.0012	-	-	4924
207-12	SBE39	7862	080-02	-6.0	0.0014	-	-	4924
261-02	SBE37	9840	080-02	-6.2	0.0009	0.0057	0.0089	4924
261-02	SBE37	2092	080-02	-4.8	0.0021	0.0052	0.0064	4924
261-02	SBE37	2093	080-02	-5.8	0.0016	0.0062	0.0086	4924
261-02	SBE37	9834	080-02	-6.7	0.0016	0.0051	0.0076	4924
261-02	SBE37	12478	080-02	-8.3	0.0011	0.0011	0.0036	4924
261-02	SBE56	6990	040-02	-	0.0012	-	-	918
261-02	SBE56	6991	040-02	-	0.0011	-	-	918
261-02	SBE56	7068	040-02	-	0.0039	-	-	918
261-02	SBE56	7069	040-02	-	0.0008	-	-	918
251-04	SBE37	2395	060-01	1.6	0.0018	0.0038	0.0022	1907

R: Pressure reconstructed from the CTD pressure

Tab. 2.19: Offsets for Seabird sensors SBE37 and SBE39 recovered during PS129. Their temperature and conductivity data were adjusted based on a linear interpolation between pre- (dt1, dc1) and post recovery (dt2, dc2 dp2) offsets. For pressure the post recovery offset was applied as a constant offset. Xcorr = Xreading + ΔX, with X representing temperature (T), conductivity(c) or pressure (p)

MOORING	Type	SN	ΔT1 (ºC)	Δc1 (mS/cm)	Δp1 (dbar)	Δt2 (ºC)	Δc2 (mS/cm)	Δp2 (dbar)
227-15	SBE37	12479	0.0012	0.0079	-4.5	0.0012	0.0060	-4.4
229-14	SBE37	2098	0.0011	0.0034	-4.4	0.0006	-0.0002	-7.5
229-14	SBE37	2396	0.0016	0.0109	-	0.0019	0.0059	-0.02
229-14	SBE37	9492	-0.0001	0.0017	-3.4	0.0001	0.0071	-7.0
229-14	SBE37	9494	0.0006	0.0010	-3.3	0.0011	0.0039	-7.4

MOORING	Type	SN	ΔT1 (ºC)	Δc1 (mS/cm)	Δp1 (dbar)	Δt2 (ºC)	Δc2 (mS/cm)	Δp2 (dbar)
229-14	SBE37	9495	0.0009	0.0038	-1.0	0.0011	0.0057	-6.0
229-14	SBE37	9496	0.0008	0.0038	-3.7	0.0010	0.0126	-8.1
229-14	SBE37	9497	0.0008	0.0044	-4.4	0.0012	0.0048	-9.1
229-14	SBE37	12481	0.0012	0.0044	-3.4	0.0012	-0.0035	-7.9
229-14	SBE37	2385	0.0003	0.0208	-	0.0005	0.0044	-
229-14	SBE37	2382	0.0022	0.0220	-	0.0019	0.0046	-
231-13	SBE37	10944	0.0003	0.0009	-5.7	0.0003	-0.0001	-10.8
245-5	SBE37	8124	0.0011	0.0048	-1.6	0.0014	0.0038	-5.2
248-3	SBE37	8123	0.0014	0.0029	0.6	0.0019	0.0031	-2.8
BGC-1	SBE37	449	-	-	-	-0.0050	0.0081	R
BGC-1	SBE37	2100	-	-	-	0.0013	0.0072	-8.4
BGC-1	SBE56	6513	-	-	-	0.0750	-	R
BGC-1	SBE56	7824	-	-	-	2.3101	-	R
BGC-1	SBE56	7825	-	-	-	0.4178	-	R
208-9	SBE37	9841	0.0014	0.0010	-4.7	0.0020	-0.0014	-5.1
208-9	SBE37	3812	0.0013	0.0060	3.3	no data	no data	no data
207-11	SBE37	6928	0.0011	0.0110	-	0.0036	0.0075	-
207-11	SBE37	9847	0.0017	0.0041	-1.3	0.0032	-0.0755	-0.7
207-11	SBE37	10934	0.0007	0.0054	-4.3	0.0031	0.0039	-1.5
207-11	SBE37	10937	0.0012	0.0096	-2.6	0.0027	0.0040	-2.4
207-11	SBE37	10943	0.0018	0.0035	-6.1	0.0025	0.0008	-3.0
207-11	SBE39	8641	0.0016	-	-5.4	-0.0018	-	-2.1
207-11	SBE39	8642	0.0012	-	-7.4	-0.0051	-	-2.3
207-11	SBE39	8643	0.0008	-	-7.2	-0.0045	-	-2.8
251-3	SBE37	2096	0.0008	0.0057	-4.3	-0.0036	0.0168	0.4

2.1.14. Salinity calibrations by salinometer

On board comparisons between salinometer-based salinity measurements of water samples and concurrent *in situ* CTD data exhibited conspicuously large deviations for both conductivity sensors for some measurements between 10 and 17 April 2022, both with regard to time as well as pressure (Fig. 2.6).

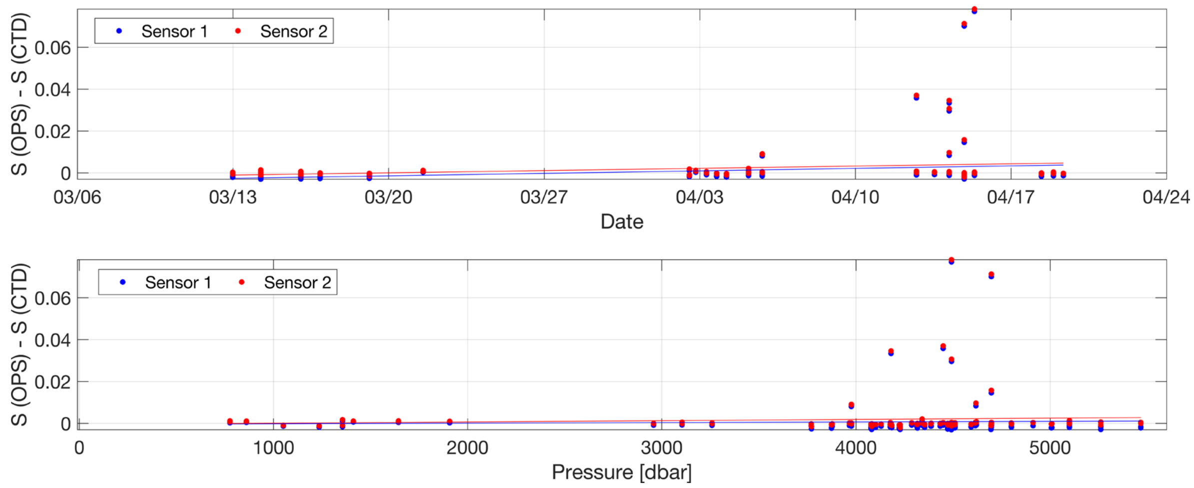

Fig. 2.6: Deviation in salinity between OPS measurements and in situ CTD measurements versus date (top) and pressure (bottom) for the primary (blue) and secondary (red) sensors (all samples). Conductivity sensor #1 = SBE4c #3590; Conductivity sensor 2 = SBE4c #3173

Concurrent spreads like these point towards issues with the sampled water rather than the sensors, which is why we excluded theses measurements from the preliminary onboard evaluation.

After the failure of the OPS-006 on 3 April 2022, measurements continued and 5 further samples were measured. Those 5 samples show a systematic offset with regard to all other samples and are thus excluded from the calculation of offsets applied of the CTD data. Furthermore, 9 samples showed exceedingly large deviations >0.008, whereas the average deviation was 0.001. The reason for the larger deviation is unknow but contamination during sampling is the most likely cause. Those 9 samples were also not taken into account for correcting the CTD sensor data.

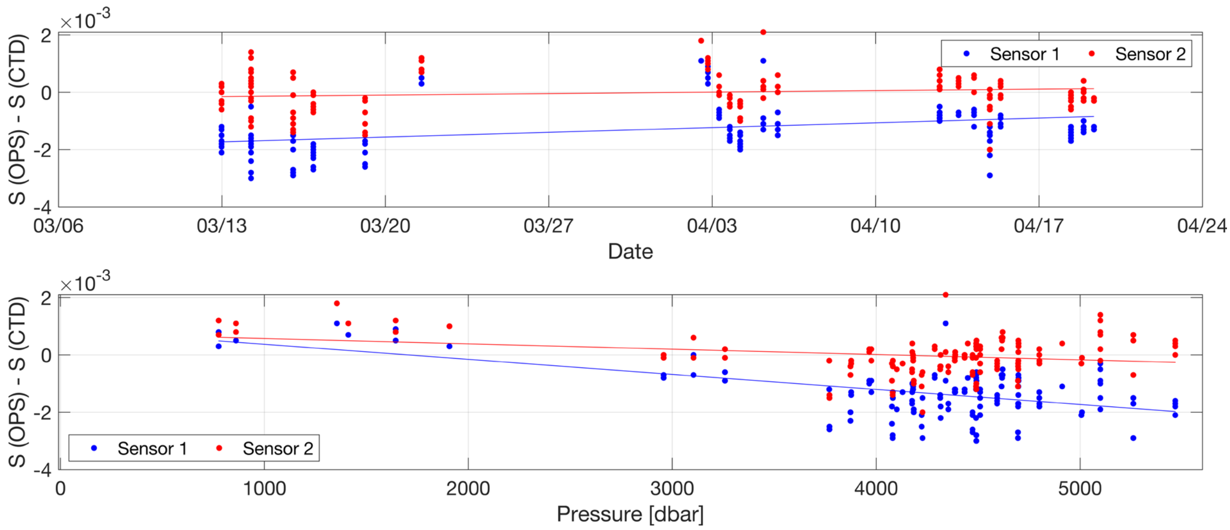

Fig. 2.7: Deviation in salinity between OPS measurements and in-situ CTD measurements versus date (top) and versus pressure (bottom) for primary and secondary sensor after a first quality check and removal of erroneous OPS measurements

Analysis of the prevailing data (Fig. 2.7) reveals that sensor #1 (blue) exhibits a slightly larger temporal drift as well as a larger pressure dependency compared to sensor #2 (red). Thus, sensor #2 will likely be chosen as the better performing one and the data of channel 2 will likely be used for the final data set. After further control for suspicious OPS measurements the final calibration of the CTD data will be performed on the basis of the remaining salinometer measurements together with the post-cruise manufacturer calibration of the sensors. Sensors will be sent to SeaBird for post-expedition calibration, which will be applied to data prior to publication of the final data in PANGAEA.

2.1.15. CTD-mounted ADCP (L-ADCP)

Overall, the obtained information resembled the scientific assumptions and agreed well with vessel mounted ADCP data. Most of the time, the error of the velocities was on the order of 5 to 10 cm s^{-1}. Thus, data should be handled with care and post-processing is required. Table 2.20 summarizes which casts suffered from one or more warnings:

- large compass differences (> 15°), due to the high latitude of the study area
- the routine does not only perform the velocity inversion, but calculates a solution based on the shear method as well. If both disagree substantially, the error estimate is larger.

Reprocessing the data with a different setting may change these problems.

Tab. 2.20: List of common problems of L-ADCP casts by station number

For further information see the end of the Chapter.

2.1.16. RAFOS source tuning

Figure 2.8 gives an overview of each source's frequency response curve for runs 1 through 4, (unconventionally) from right to left. Each row represents a specific RAFOS sound source. The graphs plot source levels (estimated using a $20 \cdot \log_{10}(r)$ propagation loss from the received levels, with r the distance source to hydrophone, given in colored labels at the top right of each plot) versus the tone's momentary frequency. Using about 40 m hydrophone source distance ($7 \cdot \lambda$) resulted, with one exception (D0048, first run), in rather inconsistent measurements between hydrophones (spaced by 1.4 m, i.e., about $\lambda/4$ of the 260 Hz wave (λ = 5.8m). Changing the distance about 80 m, and mechanically fixing the source's axis at a right angle towards the hydrophones provided more consistent results. Final source level measurements, when transmitting a true RAFOS sweep and resonance coil on, varied between 170 and 180 dB re. 1µPa with one noteworthy outlier just below 190 dB re 1µPa.

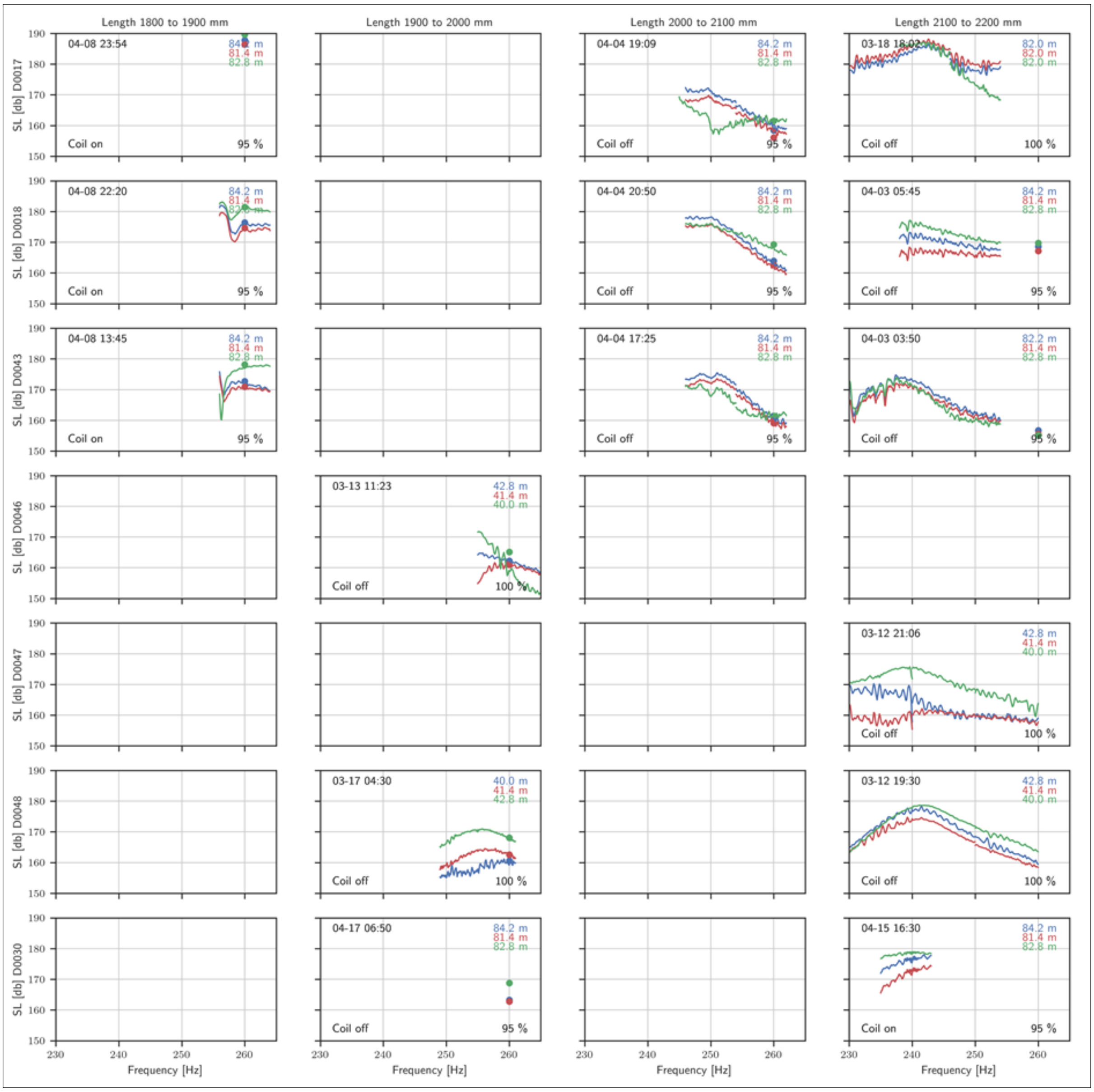

Fig. 2.8: Resonance curves of develogic RAFOS sources sorted by sound source (rows) and tube length (columns), becoming progressively shorter from right to left. Colored curves indicate the sound pressure level as received by the three hydrophones; 1413 = blue, 1414 = red, 1415 = green. Distances between hydrophones and source are listed in each plots' legend.

2.1.17. Use of MiniROV vLBV300 (Fiona) for mooring recovery

Experience showed, that, on occasion, acoustic releases fail to open the clutch to the anchor chain when acoustically commanded to do so. The reasons for this are manifold, including, e.g., electronic failure of the releases' electronics, low batteries or a mechanical jamming of the clutch by biofouling or anode residues. The risk of such failures increases with time. To nevertheless be able to recover such moorings, the Seabotix vLBV300 (vectorized Little Benthic Vehicle) ROV "Fiona" had been acquired and successfully deployed on *Polarstern* expeditions PS103 and PS117.

Learning from the experiences made during these expeditions, we moved the spool holding the recovery rope from underneath the ROV (which caused excessive pitching during high ROV speeds during PS117) to behind where it creates less drag when moving forward at increased speeds while beating a current. Additionally, moorings now feature acoustic Posidonia transponders in the 200 to 300 m depth range, such that the mooring location is more precisely known during the search phase with the ROV's sonar and video.

During PS129, two occasions offered themselves for deployment of Fiona when moorings were positioned underneath a sea-ice cover of nearly 100%. However, temporal constraints resulting from the speed constraints imposed on this expedition, in the end prohibited the use of Fiona. Fiona had nevertheless been set up proactively, resulting in some additional experience with the IT network setup, which is described below.

Amendment to notes in expedition report of PS117 regarding communication setup

Please refer to the PS117 expedition report for a detailed starter on how to set up communication between the navigational computer (the Integrated Navigation Control Console, INC or an external laptop). This paragraph builds on that description and provides additional information only.

The navigational software SeaNetPro requires the following navigation data to be provided as serial input:

- the ship's position
- Fiona's position via GAPS
- the mooring position via Posidonia, possibly 2 units (release and transponder).

The ship's georeferenced position is continuously being tracked by the ship's navigational system. The ship's server continuously sends NMEA datagrams:

$GPGGA,155901,**5837.290,S,05946.345,W**,2,9,1,48.6,M,19.8,M,,,,*55

$GPHDT,**319.8,T***36

$PSRPS,**-1.149,-0.738**,8.03*6A

The $GPGGA telegram provides position.

The $PGHDT telegram provides the heading

The $PSRPS telegram provides roll and pitch, though it is unclear how SeaNetPro makes use of this information.

The UDP broadcast for ship position and heading is custom telegram set up by the sysman, containing the datagrams GPHDT and GPGGA.

Fiona's location relative to the GAPS head is continuously being tracked with the GAPS short baseline navigational system. Fiona bears an Applied Acoustic GAPS compatible Mini-beacon (transponder) which responds by sending a ping upon reception of an interrogation ping, while shipside the GAPS antenna is being deployed through the moonpool. GAPS sends HPR400 datagrams, like

$PSIMSSB,231407.73,B01,A,,**C,H**,M,**29.65,-65.86,1593.59**,1.83,T,1.055685,0.00*66

C indicates the use of cartesian coordinates, and H the Vessel being heads up (bow = north) with the first (bold) value the Starboard distance, and the second (bold) value the Forwards distance.

The mooring's absolute location is continuously being tracked with the POSIDONIA short baseline navigational system by sending pings to (both) acoustic release (near the bottom) and acoustic transponder (at 200-300 m depth). POSIDONIA sends $PTSAG datagrams, like

$PTSAG,#755615,230823.957,22,04,2022,**0,6328.66281,S,05136.85417,W**,F,0011.70,1,9999.00*12

$PTSAG,#755625,230823.424,22,04,2022,**1,6328.61924,S,05136.85302,W**,F,1750.71,1,9999.00*1B

with ID = 0 usually referring to the ship-borne Posidonia head (embedded in the hull) and ID = 1 or ID = 2 to the respective (moored) transponder. The ship's and Posidonia ID = 0 positions should move in parallel, separated by the offset between the Posidonia Window and the ships inertial navigation systems position.

This information is provided via datagrams sent by Ethernet to the navigational computer (INC or Laptop) with SeaNetPro ingesting datagrams sent to the respective ethernet port's IP-Address via virtual com ports. Because the Ethernet port is being recognized by the INC-PC as an Ethernet connection, software is required to feed the incoming datagrams to the SeaNetPro software. For this, the emulation (by the programme com0com2) of serial ports is required, as well as a programme (udp2serial) that redirects the input from the Network ports to the emulated serial ports (Fig. 2.9).

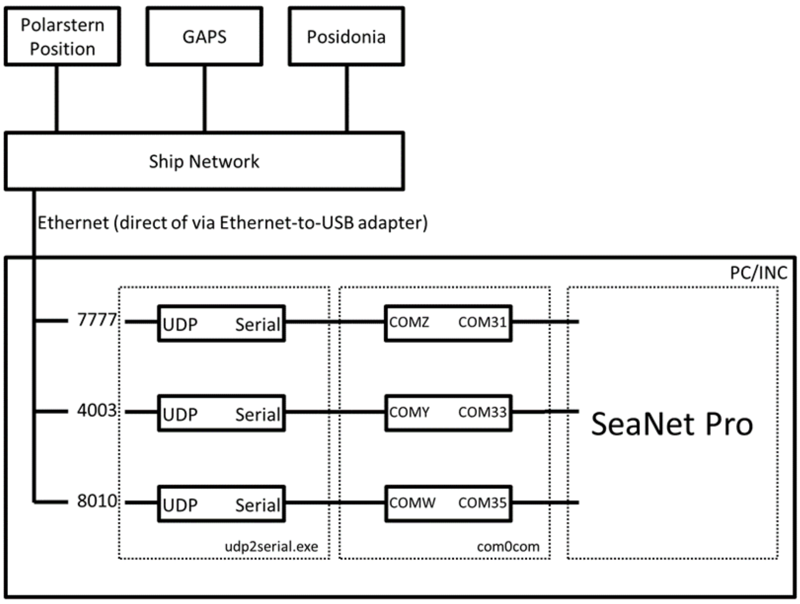

Fig. 2.9: Flow chart of navigational information

During PS117, a UDP broadcast to either the INC or the separate navigation PC was employed. However, during PS129 we could not find a USB-Ethernet adapter that worked with the INC. Hence, we relied on the navigational Laptop only (with com0com[2] and SeaNetPro installed there). In com0com three port pairs were established (Fig. 2. 9):

[2]Null-modem Emulator, creates an unlimited set of virtual COM Port Pairs and connects these with a virtual Null-modem cable. This allows to connect 2 COM based applications with the output of one being the input of the other, and vice-versa.

- Ship GPS position: COMZ ⇔ COM31
- GAPS (ROV) position: COMY ⇔ COM33
- Posidonia (mooring) position: COMW ⇔ COM35

On SeaNet Pro side, the setup was (Utilities → COM Setup):

- GPS COM31 Baud rate 9600
- NAV Beacon B16 COM33 Baud rate 9600
- NAV Beacon B17 COM35 Baud rate 9600

To establish the routing from Ethernet to the emulated COM ports, a C# programme (udp2serial.exe, written during PS117) binds itself to the given UDP (User Datagram Protocol[3]) port and forwards anything to the respective serial port. The source code can be found in the PS117 expedition report. For every port pair given above, a new process of the udp2serial.exe programme has to be started, i.e., three in total. This programme can be started via command line (e.g., "udp2serial.exe 7778 COMZ") or interactively when only issuing udp2serial.exe in a command window.

The UDP setup was as follows:

- Ships UDP port 7778 (navigation PC)
- GAPS UDP port 4003
- Posidonia UDP port 8010

It is recommended to request the "sysman" (computer network operator) to reset the network buffer on your IP for GAPS and Posidonia. This is to make sure that there is no delay in the datagrams received to the current state.

Problems and diagnostics

<u>Network problems</u>: On PS117, datagram problems existed when using the ships position and heading broadcast to UDP ports 7777 to two different PC's (INC and navigation PC). The problem may be overcome by using port 7777 on the INC and port 7778 on the navigation PC.

To check if anything is received on the INC or navigational PC, the software NetCat can be used. In case of the ships position and heading in our setup, the following call has been used from a console window: ncat.exe –ul 7778. The programme ncat.exe is provided with Fiona's documentation. Now all UDP packets that are received on this port are being printed to the terminal.

[3]User Datagram Protocol (UDP) is a communications protocol that is primarily used to establish low-latency and loss-tolerating connections between applications on the internet. UDP speeds up transmissions by enabling the transfer of data before an agreement is provided by the receiving party.

Tab. 2.21: GAPS HIPAP PPR400 protocol (MU Posidonia AN-001-1 – November 2019)

IXBLUE DEEP INSIGHT. SHARPER SENSES.

GAPS – User Guide

G.9 HIPAP HPR 400

Field	Name	Kongsberg Explanation	
$	Start Character		$
PSIMSSB	Address	Prop. Simrad address for SSBL	PSMSSB
,hhmmss.ss	Time	Empty or Time of reception	
,cc	Tp_code	Example: B01, B33, B47	%03d
,A	Status	A for OK and V for not OK	A/V
,cc	Error_code	Empty or a three character error code	ExD/ExM
,a	Coordinate_system	C for Cartesian, P for Polar, U for UTM coordinates	C
,a	Orientation	H for Vessel head up, N for North, E for East	N
,a	SW_filter	M means Measured, F Filtered, P Predicted	M
,x.x	X_coordinate	See table below	Northing
,x.x	Y_coordinate	See table below	Easting
,x.x	Depth	Depth in meters	depth
,x.x	Expected_accuracy	The expected accuracy of the position	Sqrt(Tx2+ty2)
,a	Additional_info	N for None, C Compass, I inclimeter, D Depth, T Time	
,x.x	First_add_value	Empty, Tp compass or Tp x inclination	
,x.x	Second_add_value	Empty or Tp y inclination	
*hh	Checksum	Empty or Checksum	*ck
CRLF	Termination		CRLF

Example: $PSIMSSB,,B01,A,,P,H,M,111.80,63.43,48.50,0.00,N,,*5E

	PSIMSSB fields		PSIMSSB coordinates of TP	
CO-ORD	Coord. system	Orientation	X_coordinate	Y_coordinate
Polar	P	H	Horizontal range	Bearing in °
Cartesian X/Y	C	H	Starboard	Forwards
Cartesian N/E	C	N	North	East
Cartesian E/N	C	E	East	North
UTM N/E	U	N	Northings	Eastings
UTM E/N	U	E	Eastings	Northings

MU-GAPS-AN-005 Ed. F - May 2016

Preliminary results

2.1.18. CTD measurements

Extending our long-term ocean-bottom temperature time series by another 3 years, we reoccupied the 61°S 0°E position for the 16th time, now having 30 years of observations (1992 – 2022). The temperature profile shows the near-linear continuation of the warming in the aged Weddell Sea Bottom Water (WSBW, Fig. 2.10). In the bottom layer of the WSBW, below a depth of 5,300 m, the temperature increased from -0.8435°C (1992) to -0.7759°C during PS129, which corresponds to an increase of 0.0225°C per decade.

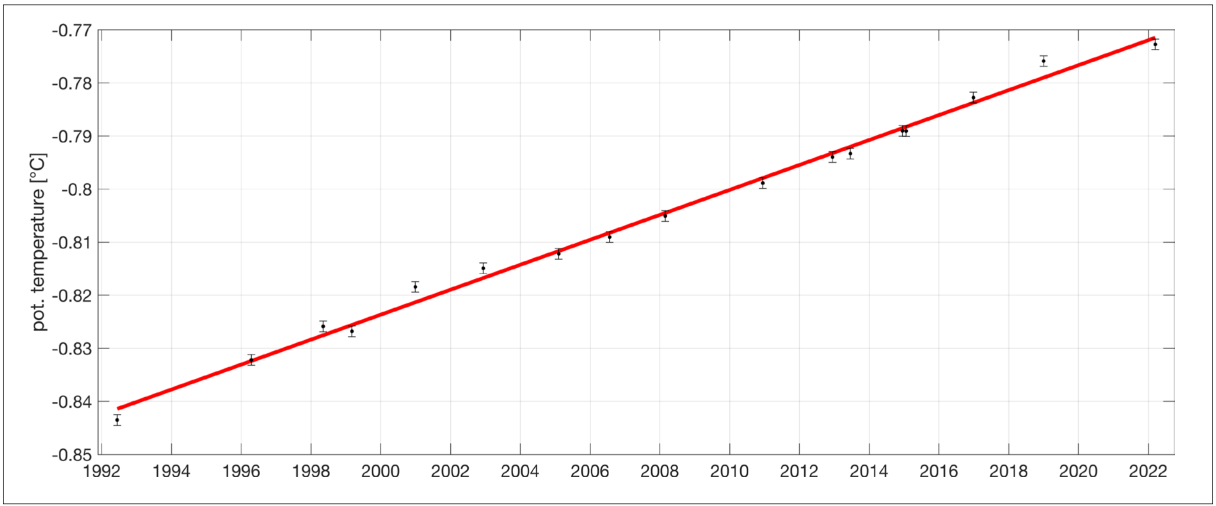

Fig. 2.10: Potential temperature record from past and current CTD casts at nominally 61°S, 0°E. Error bars indicate the measurement accuracy of the temperature sensor (final calibration pending).

Being confronted with significant losses of station time, the decision was taken that the completion of the Weddell Sea hydrographic section SR4 would be given highest priority. While the station spacing had to be stretched somewhat in the open ocean region (Fig. 2.11) a shelf-to-shelf hydrographic section was acquired nevertheless.

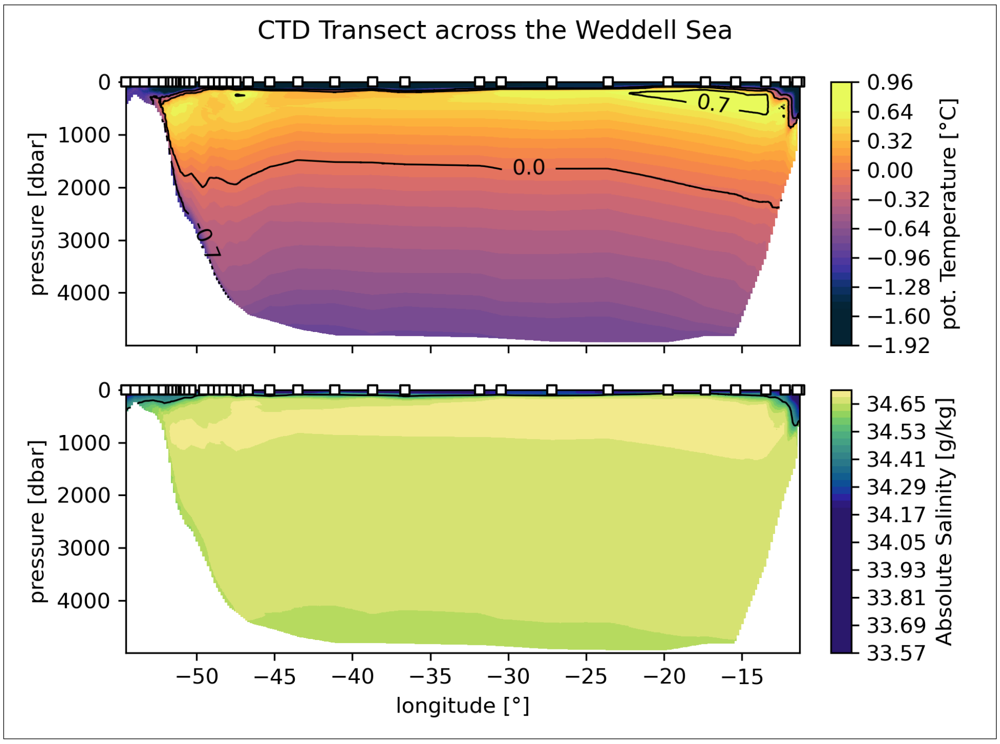

Fig. 2.11: CTD section along SR4 during PS129. In deep waters, station spacing is nominally 60 nmi, while the western outflow region is sampled at a significantly higher rate.

Towards the tip of the Antarctic Peninsula, 20 CTD casts were taken at enhanced horizontal resolution between 46°W to 55°W (Fig. 2.3), repeating a section being occupied there since 1998, resulting in 34 years of coverage.

The surface layer exhibits Antarctic Surface Water offshore and Shelf Water onshore (Fig. 2.11 and Fig. 2.12). Below that, the Warm Deep Water (WDW, with potential temperature >0°C) is centered around 1,000 m depth. It is fed from the ACC, entering the Weddell Sea upstream of the Prime Meridian. The Weddell Sea Deep Water (potential temperature between 0° and -0.7°C) is located below the WDW. The thin sliver of bottom water colder than -0.7°C (Fig. 2.12) at the continental slope is indicative of newly formed Weddell Sea Bottom Water flowing northward along the slope.

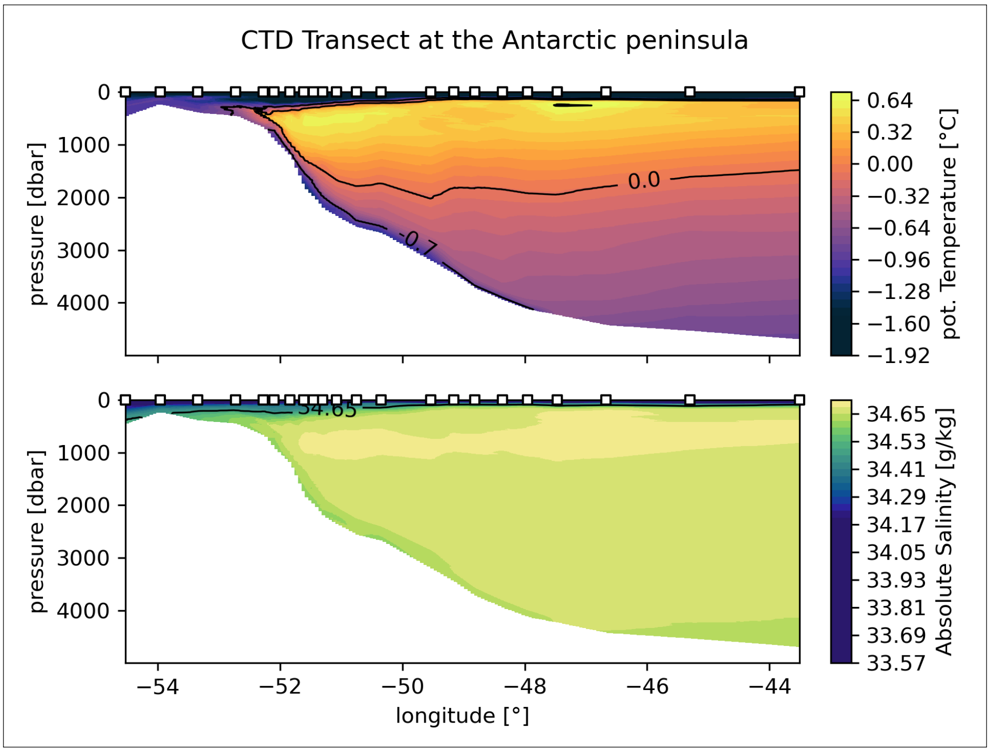

Fig. 2.12: Section of potential temperature and salinity at the tip of the Antarctic Peninsula

2.1.19. Velocity profiles by L-ADCP

Throughout the expedition, L-ADCP measurements were preliminarily analyzed. The SR4 section, with reduced station spacing up the continental slope east of the Antarctic Peninsula confirmed the expected flow patterns (Fig. 2.13). The L-ADCP measurements near the Antarctic Peninsula reveal that the velocity fronts near the 2,000 m isobath are barotropic (Fig. 2.14) while those farther offshore exhibit a strong baroclinicity. However, these preliminary plots have not been corrected for tidal contributions; they only serve to demonstrate data availability.

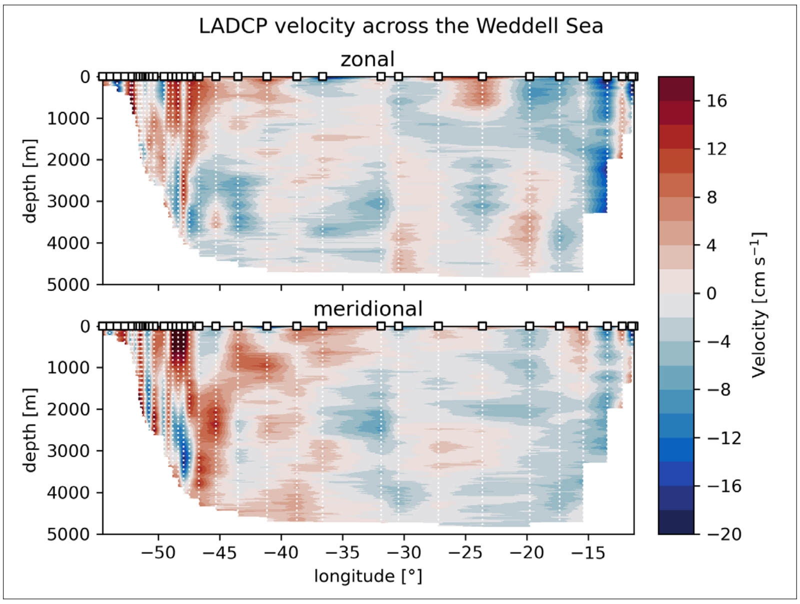

Fig. 2.13: Sections of zonal (top) and meridional (bottom) velocities measured by the L-ADCP along the complete SR4 hydrographic section

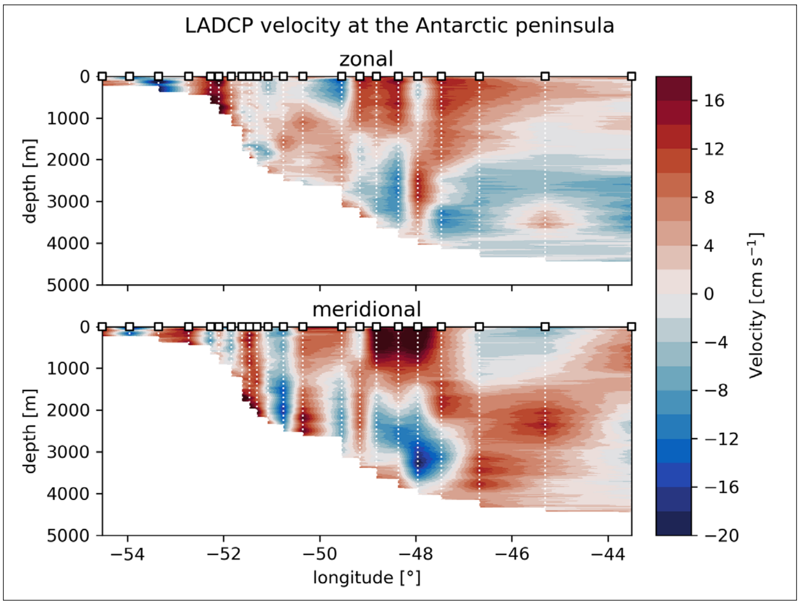

Fig. 2.14: Sections of zonal (top) and meridional (bottom) velocities measured by the L-ADCP along the SR4 hydrographic section off the Antarctic Peninsula (zoom-in of Fig. 2.13)

2.1.20. Thermosalinograph

The thermosalinograph captured the expected hydrographic features (Fig. 2.15). Warm, saline waters reflecting the Agulhas influence near Cape town, a strong reduction in salinity and temperature when crossing the Subtropical Front (characterized by the 10°-isotherm intersecting the sea surface) in the second half of 7 March 2022 and the dominance of sub-zero waters in the southern Weddell Sea. There are two specific observations to be mentioned: 1) the frontal crossing in the first half of 20 March 2022 (with float PS129_01 launched just north of it, and PS129_02 and PS129_03 south of it) at the location of the continental shelf break front; 2) the two instances of increased temperatures on 4-6 April and 13-16 April 2022, when the ship operated to the north of the sea-ice edge.

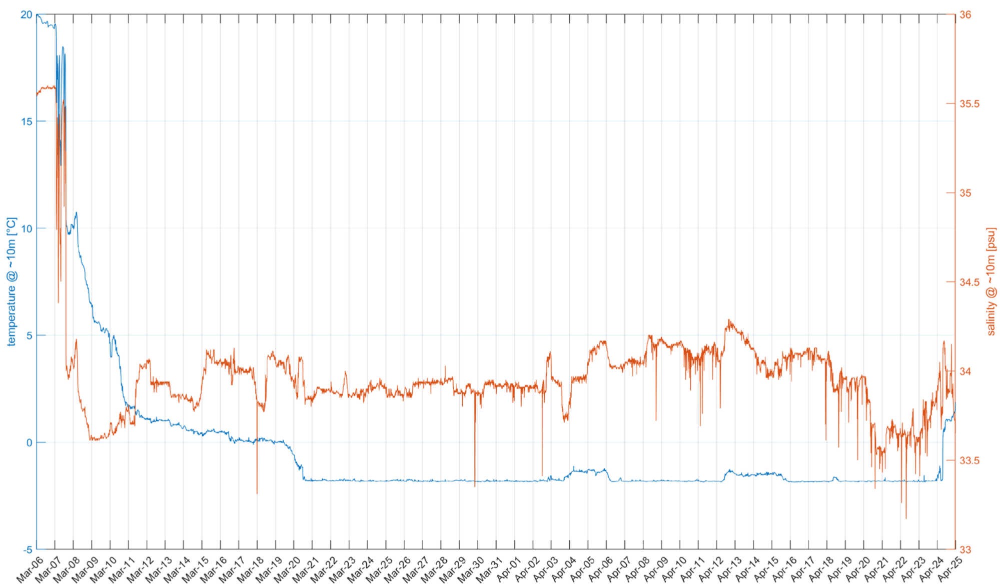

Fig. 2.15: Time series of temperature and salinity as measured by thermosalinograph from sea water continuously drawn at about 11 m depth

Data management

Data from moored oceanographic instrumentation will be uploaded into World Data Center PANGAEA Data Publisher for Earth & Environmental Science (https://www.pangaea.de) after final processing, calibration and quality control. It will be publicly available by latest April 2024. By default, the CC-BY license will be applied.

All data (CTD-, OBOFS-, sADCP- and L-ADCP data) will be uploaded into PANGAEA after final processing, calibration and quality control. It will be publicly available by latest April 2024. P.I.: Sandra Tippenhauer

Float data is available in quasi real time through https://www.ocean-ops.org/board/?t=argo, or https://fleetmonitoring.euro-argo.eu/dashboard?Status=Active. Delayed mode data will be made available through the respective data centres.

This expedition was supported by the Helmholtz Research Programme "Changing Earth – Sustaining our Future": Topic 2, Subtopic 1; Topic 6, Subtopic 3.

In publications based on this expedition, the **Grant No. AWI_PS129_01** will be quoted and the following publication will be cited:

Alfred-Wegener-Institut Helmholtz-Zentrum für Polar- und Meeresforschung (2017) Polar Research and Supply Vessel POLARSTERN Operated by the Alfred-Wegener-Institute. Journal of large-scale research facilities, 3, A119. http://dx.doi.org/10.17815/jlsrf-3-163.

References

Boebel O (2013) The expedition of the research vessel "Polarstern" to the Antarctic in 2012/2013 (ANT-XXIX/2). Berichte zur Polar- und Meeresforschung = Reports on Polar and Marine Research, 671, 99 pp., Bremerhaven, Alfred Wegener Institute for Polar and Marine Research, http://hdl.handle.net/10013/epic.42735.

Boebel O (2015) The Expedition PS89 of the Research Vessel Polarstern to the Weddell Sea in 2014/2015. Berichte zur Polar- und Meeresforschung = Reports on Polar and Marine Research, 689, 151 pp., Bremerhaven, Alfred Wegener Institute for Polar and Marine Research, http://doi.org/10.2312/BzPM_0689_2015.

Boebel O (2017) The Expedition PS103 of the Research Vessel POLARSTERN to the Weddell Sea in 2016/2017. Berichte zur Polar- und Meeresforschung = Reports on Polar and Marine Research, 710, 160 pp., Bremerhaven, Alfred Wegener Institute for Polar and Marine Research https://doi.org/10.2312/BzPM_0710_2017.

Boebel O (2019) The Expedition PS117 of the Research Vessel POLARSTERN to the Weddell Sea in 2018/2019. Berichte zur Polar- und Meeresforschung = Reports on Polar and Marine Research, 732, 205 pp., Bremerhaven, Alfred Wegener Institute for Polar and Marine Research, https://doi.org/10.2312/BzPM_0732_2019.

Klatt O, Boebel O, Fahrbach E (2007) A profiling float's sense of ice. Journal of Atmospheric and Oceanic Technology, 24, 1301-1308.

Rossby T, Dorson D, Fontaine J (1986) The RAFOS system. Journal of Atmospheric and Oceanic Technology, 3, 672-679.

2.2 Ocean Acoustics

Stefanie Spiesecke[1], Clea Parcerisas[2], Irene Torrecilla Roca[1], Olaf Boebel[1]; not on board: Elke Burkhardt[1], Karolin Thomisch[1], Ilse van Opzeeland[1]

[1]DE.AWI
[2]BE.VLIZ

Grant-No. AWI_PS129_01

Objectives

The restricted accessibility of the Southern Ocean throughout most of the year confines our knowledge of the distribution patterns, habitat use and behaviour of marine mammals in this area. Most of the Antarctic marine mammals produce species-specific vocalizations during a variety of behavioral contexts. Hence, passive acoustic monitoring (PAM) offers a valuable tool for research on these species, capable of covering large temporal and spatial scales. Particularly, in remote areas such as the Southern Ocean, moored PAM recorders are the tool of choice, as data can be collected year-round, under poor weather conditions, during darkness and in areas with dense ice cover.

The HAFOS observing system, a large-scale oceanographic mooring array distributed throughout the Weddell Sea, serves as host to numerous passive acoustic recorders which were recovered, refurbished and redeployed during PS129 to continue the long-term collection of passive acoustic data in this area. The basin-wide design of the HAFOS observatory and the multi-year scale of data collection enables unprecedented investigations of the spatio-temporal patterns in marine mammal biodiversity at the different mooring locations. The HAFOS array set-up and design also allows collecting information on the detection range of the various marine mammal sounds. Information on the distance over which marine mammal sounds can be detected by passive acoustic sensors is of vital importance when acoustic presence data are linked to information on environmental parameters in the context of studies of species-specific habitat usage.

Work at sea

2.2.1 Recovery of moored acoustic recorders

In total, 10 passive acoustic recorders moored at 9 different locations were recovered during PS129. Due to temporal limitations resulting from the ship-speed constraints imposed on this expedition, calling at the southwesternmost PAM equipped mooring AWI250-3 was not attempted. Recovery attempts of PAM equipped moorings AWI249-3 and AWI257-2, albeit being on-site, were abandoned after a short while as recoveries under the prevailing quasi-continuous sea-ice conditions would have required an estimated 6-12 hours of shiptime, which we did not have at our disposition. These mooring recoveries were postponed to the next expedition which hopefully will suffer from less severe time constraints.

The recovered recorders comprised 9 SonoVaults (manufactured by Develogic GmbH, Hamburg) and one AURAL (manufactured by MultiElectronique). Nine of these recorders had been deployed during *Polarstern* expedition PS117, while one recorder (SV1024) had been deployed one year prior to PS129 in mooring BGC-1 during *Polarstern* expedition PS124. An overview of the recovery information of all recovered acoustic recorders is provided in Table 2.22 and Figure 2.16, while deployment positions of the recorders are marked in Figure 2.18.

Tab. 2.22: Overview of SonoVault and AURAL recorders recovered during PS129. All SV recorders

For further information see the end of the Chapter.

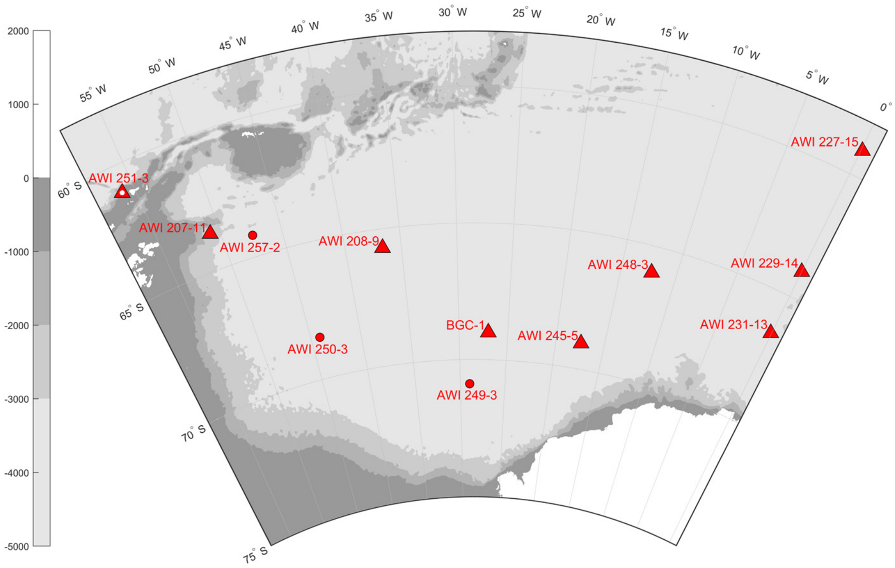

Fig. 2.16: Map of positions of PAM recorders recovered during PS129 (red triangles pointing up) and of moorings with recorders not retrieved (red dots)

After recovery, the acoustic recorders were rinsed with freshwater and cleaned from biological fouling. States of recovered recorders were queried (if possible) by connecting a laptop through a serial connection and using the software 'Develogic Device Control' (Ver 1.0.4.26525, provided by the instrument manufacturer) for the SonoVault recorders and a software provided by Multi-Electronique for the AURAL. The recorders were then left to dry overnight to prevent damage to the electronics from water that was retained in the threading of the recorder's housing. SV1002 and AU0085 from AWI251-03 were opened on the same day due to the lack of time towards the end of the expedition. The area around the openings with the sealings were carefully dried with compressed air and tissues before opening. After opening the recorder housing, the internal power supply was disconnected and its remaining voltage measured. In case of the SonoVaults, all SD cards, which had been labeled prior to deployment with the recorder's serial number, the recording module number and the SD card-slot, were removed and backed up (see below).

Each recovered recorder was calibrated post-recovery to allow calculations of received sound levels. For the calibration of the complete system, including the hydrophone, a Brüel & Kjaer calibrator (Type 4229) with the custom-made adapter (SV.PA manufactured by Develogic) for the TC 4037 hydrophones was used. The calibration frequency is 251.2 Hz ± 0.1% (ISO 266) and the amplitude (at 1013 hPa) is 153.95 dB SPL. Additionally, a gain calibration of the electronic board was performed by connecting a frequency generator (MR Pro, NTI) to the hydrophone input on the electronic board. The generator was set to a sinus of 5 mV amplitude (rms) and the frequencies 100 Hz, 250 Hz, 1 kHz and 10 kHz. For all calibration recordings, the recorder was set to the deployment sampling rate and gain setting to record one file of 5-minute length. All recordings were stored, and signal levels and system gain were calculated. All hydrophones mounted on the recovered SonoVaults were checked individually with an oscilloscope. The B&K pistonphone was used to generate a calibrated signal. Approximately 10 mV_{rms} is expected for the differential hydrophone output. This value, combined with the qualitative check of the symmetry of the positive and negative outputs, was used as an indicator for the hydrophone’s state.

The hard disk with the acoustic data from the AURAL was removed from the instrument. A calibration of this instrument has not yet been performed.

Data retrieval and backup

Five of the nine recovered passive acoustic devices deployed on PS117 recorded for periods ranging between 450 days and 565 days (Fig. 2.17). In 3 recorders (SV1006, SV1060, SV1020), recordings stopped early due to a firmware or electronics error. One recorder (SV1060) had burned internally, presumingly due to a battery failure caused by a deep discharge of one of the lithium cells. The recorder deployed during PS124 reached a recording period of 356 days, having been set to sample at 48 kHz continuously for one year. A total of approximately 28 TB and >3,900 days of passive acoustic data were obtained. Further details are discussed in the section “Preliminary technical results”.

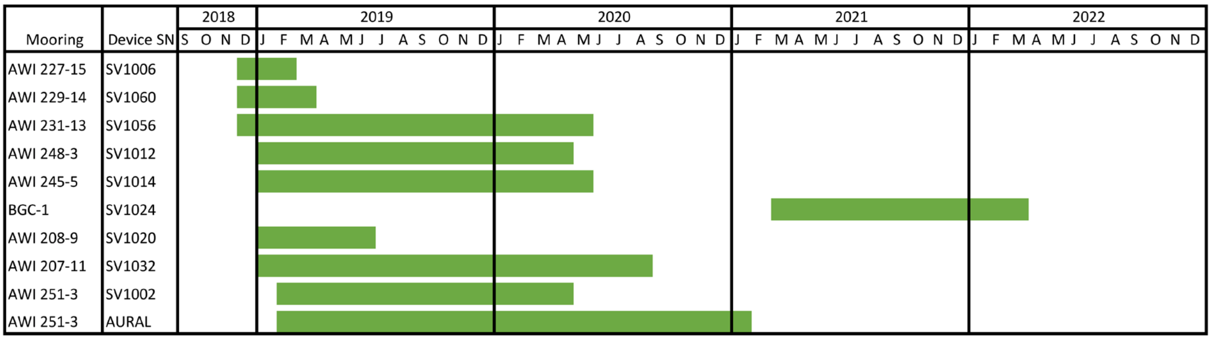

Fig. 2.17: Recording months of passive acoustic recorders retrieved during PS129. Note: granularity equals one month, not days

The SonoVault recorders store data on 35 SD cards (allowing a maximum of 4.4 TB of data storage per recorder for recorders deployed during PS117). After recovery, the SD cards were removed from the recorders and the acoustic data were copied using a custom-written shell script. Up to 5 SD cards were copied simultaneously, with data initially saved with original filenames sorted into monthly and daily folders to one HDD (10 TB WD red) drive. The backup process included the renaming of files based on each files’ internal time stamp (WAV-header) to the file name format ‘YYYYMMDD-HHMMSS_AWIXXX-ZZ_SVXXXX.wav’ (with X representing the IDs of mooring and SonoVault recorder, respectively and Z indicating the consecutive numbering of this mooring, i.e., the number of the current servicing cycle at a respective mooring). After copying was completed, the data were synchronized with a second HDD (10 TB WD red) for backup and copied temporarily to a third external HDD used for the preliminary analysis on board. SD cards from the burnt (SV1060) instrument were treated to prevent further corrosion. They first were rinsed from residues with milli-Q water, wiped dry and left drying over night. In a second step, contacts were cleaned using contact spray for electronics. In a last step the contacts were cleaned using a fiberglass pen. As a result, data from 5 SD cards could be saved. Another two SD cards will have to be sent to a laboratory specializing on data recovery from the embedded microchips.

2.2.1 Deployment of moored acoustic recorders

A total of 15 SonoVault recorders were deployed in 15 moorings during PS129 (Fig. 2.18). These recorders are equipped with electronic version V4.1. All new recorders use the firmware version V4.14. Prior to this expedition, all SonoVault recorders were refurbished by the manufacturer and overpressure valves were installed in all instruments, except for SV1009 and SV1023. The refurbishment included the exchange of O-rings, a pressure test, the exchange of the RTC-clock batteries on the electronics, as well as the test of hydrophones and recording electronics. At the AWI facilities, recorders were equipped with batteries (Tadiran SL-2780) prior to shipping. O-rings were carefully checked, cleaned and greased before closing the housing prior to deployment.

At three moorings (AWI251-04, CWS01-01, WWS02-01), an AURAL recorder (Multi-Electronique, Canada) was deployed alongside a SonoVault recorder for extended recording duration (albeit at a subsampling scheme).

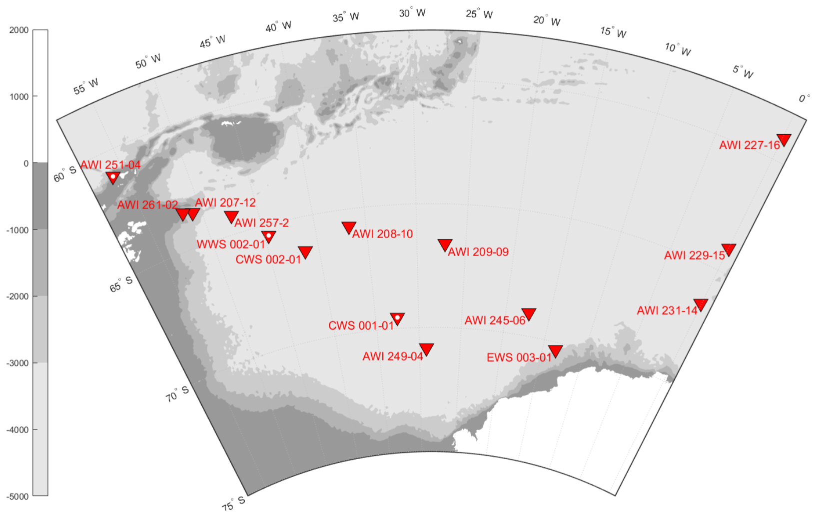

Fig. 2.18: Map of SonoVault (red triangles) and Aural (additional white dot in center of triangle) deployment positions during PS129. A total of 15 SonoVaults and 3 Aural recorders were moored.

Recorders were calibrated prior to deployment in the same manner as the post-recovery calibrations described above, using the Brüel & Kjaer calibrator (Type 4229) and the NTI frequency generator (MR Pro). All hydrophones were checked analog to the recovery check during the preparation for deployment. Three SonoVaults were equipped with new hydrophones of the type D60 (Neptune Sonar). These hydrophones have a slightly lower sensitivity (-195.5 dB re1V/µPa) than the standard TC4037-3 (RESON) (-193 dB re1V/µPa).

Prior to the deployment, newly formatted SD cards were placed into the SD card slots on each recording module. 12 recorders of the type SonoVault now contain 33 SD cards with a capacity of 128 GB each (ATP Industrial Grade SD Cards) and two additional 256 GB (acon Industrial Grade SD Cards), resulting in a total storage capacity of 4.6 TB per recorder, while the three remaining SonoVault recorders use 5 x 7 = 35 SD cards with 128 GB (ATP Industrial Grade SD Cards) resulting in 4.4 TB storage capacity. All SD cards were formatted to FAT32 using the freeware tool 'SDXCformatterFAT32'. On each first SD card (S0) of the first of five recording modules (M0-M4), the recording configuration (e.g., gain setting, sample rate) was stored. Additionally, the module number was copied onto S0 of every recording module to make the set of seven SD cards of this module available for storage.

All SonoVaults were programmed to record at a sampling rate of 48 kHz with 24 bit and to store data in files of 600 seconds duration (Tab. 2.23). A quasi one-day-on/1-day-off scheduling (subsampling scheme) was set with recordings starting at 11:30 every second day to record for 25 hours, then stop for 23 hours. Internal data storage was structured to store data in daily folders. Gain was set to level 7 which in this hardware/firmware release corresponds to about 41-45 dB in all deployed recorders (Tab. 2.23). Every instrument was first tested with its operational setting and then started at least one day prior to the deployment.

AURAL recorders AU0231 and AU0086, model number AURAL-M2, were equipped with a PATA-SATA adapter and a 1 TB hard disc. The scheduling was set to 10-min-long recordings every full hour, starting at 31 December 2022 at 12:00. The internal jumpers were set to a gain of 22 dB. The AURALs were tested for a couple of hours prior to the deployment with a different scheduling (5 minutes every 15 minutes).

AURAL recorder AU0303 at AWI251-04 is the latest AURAL model AURAL-M3. Data is stored on 5 micro-SD-cards and settings are made using a WIFI connection and a browser-based GUI. It was set to record in parallel to the SonoVault with a sampling frequency of 32 kHz, 10 minutes every hour. The new system is expected to use less power and to run for up to 900 days with the current settings. During instrument preparation, its hydrophone behaved erratically, with the AURAL not recording any hydrophone signals. During the last tests, however, this problem did not occur anymore and the instrument was deployed with this hydrophone. We attempted to calibrate the AURAL with its HTI-96-min hydrophone using an adapter for the B&K Pistonphone. However, the system was oversaturated by the signal due to the set gain of 22 dB. Nevertheless, a calibration with the frequency generator was performed, analysis pending.

All recorders were attached to the mooring rope by means of two plastic brackets mounted at two positions around the housing. In comparison with the PS117 deployments, the brackets were placed farther apart. The brackets were then attached to the Dyneema mooring rope. In case of the last 5 deployed recorders, the brackets were attached to a 5 m rope and then rope-shackled in between two mooring lines for easier handling during the deployment. All metal parts are titanium grade 5.

On AWI251-04, additionally, an AZFP (Acoustic Zooplankton and Fish Profiler, ASL) and an ADCP (Acoustic Doppler Current Profiler) were deployed alongside the acoustic recorders for the detection of the presence of prey. The AZFP is using the backscatter of acoustic pings at four different frequencies (38 kHz, 125 kHz, 200 kHz, 455 kHz) to detect zooplankton. AZFP55115 is deployed at 239 m water depth and is set to have bursts every 5 minutes, consisting of 4 pings every 20 seconds. Burst pings will be stored without averaging. The pulse length for every frequency is set to the maximum (1000 µs) to bring the maximum power into the water column. The range for the measurement is set to 280 m, with bin sizes of 0.25 m. A deployment period of 1100 days was assumed for the setup, which was set to start at 12:00 UTC on 24 April 2022. The limiting factor according to the software will be the power consumption.

Furthermore, a 75 kHz ADCP (SN 22858) was deployed in 303 m water depth. The ADCP was started at 14:47 UTC on 24 April 2022 and was set to ping every 10 minutes. With this setting, the ADCP ping and the AZFP pings will not interfere with each other (unless a major clock drift occurs for either of the instruments). Apart from information on the currents at the mooring position, its data is also intended to be used for analysis of presence of zooplankton.

Tab. 2.23: Overview of acoustic recorders deployed during PS129

For further information see the end of the Chapter.

2.2.2 Maintenance of the PALAOA observatory

PALAOA (Perennial Acoustic Observatory in the Antarctic Ocean) located on the Ekström ice shelf since 2005, has collected continuous underwater recordings from the coastal Antarctic environment using a hydrophone deployed at ca. 160 m depth. With the ice shelf advancing by about 150 m per year, the position has been constantly changing.

During the supply of the *Neumayer III* station from 28 until 31 December 2014, an aluminum box, containing modified SonoVault electronics, was installed at the position of the former PALAOA container. It was recessed into the snow and covered with a wooden board and some snow. The box (80 cm x 60 cm x 60 cm) included a Reson input module EC6073 for the active hydrophone (Reson TC4032) and a SonoVault electronics module, similar to those used in the moored recorders. For the power supply, four 90 Ah, 12V batteries were included, two connected in row for each, the active hydrophone and the recording electronics. The battery setup was changed later in 2015 to two batteries in a row and those rows in parallel, supplying both the hydrophone and the recording electronics. Storage capacity is 4.4 TB (35 x 128 GB SDXC). With a sampling rate of 96 kHz at 24 bit and a file size corresponding to of 600 sec (10 min), the PALAOA system was expected to hold recording capacities for up to 6 months. Servicing was provided by the overwintering team of the *Neumayer III* station. Based on their experience, a servicing interval of approximately 3 months proved to be necessary.

For PS129 it was intended to calibrate the hydrophone and recording equipment using a frequency generator attached to the calibration input on the EC6073 input module. However, on 20 March and later on 23 March 2022, when approaching the shelf with *Polarstern*, it seemed as if the hydrophone cable was open-ended at the shelf-ice edge. A helicopter flight to the PALAOA site on 23 March 2022, confirmed this suspicion. The hydrophone cable must have been ripped during a recent calving event of the ice shelf. The recording box was removed and the electronics, including the data storage, was taken back to the ship. Analyzing the recovered acoustic data revealed that the calving event took place on the 27 February 2022 at approximately 08:16 UTC.

On 23 March 2022, i.e., approximately one month after PALAOA's break-off and immediately prior to removing its recording box, the latter's location was determined by handheld GPS as 70.502781°S 08.205716°W.

Preliminary technical results

Preliminary technical evaluation

Recovered SonoVaults had been deployed with mounts, consisting of two plastic brackets, reaching around the instrument housing at two positions spaced by about 1 m, with all metal parts being titanium grade 2. The clamps had been attached directly to the Dyneema rope (though with relatively little spacing of about 1 m, possibly allowing the recorder to vibrate in stronger currents). Upon recovery, no complications with this form of attachment were observed. None of the recovered recorders exhibited signs of corrosion on neither the device nor the mounts. All but the two recorders recovered at AWI251-03 were quasi-free of biofouling. Two recorders at AWI251-03, however, exhibited massive biofouling. The AURAL (AU0085) was completely overgrown, while the SonoVault (SV1002) was overgrown with the exception of the hydrophone, which exhibited only a thin biofilm.

All hydrophones were tested after recovery. Two recovered hydrophones (SN4011021 of recorder SV1020, SN4011040 of recorder SV1024) proved defect. They exhibited asymmetric sinus signals in the oscilloscope reading and the rms amplitude of the signal was lower than the expected 10 mV_{rms}. The underlying damage and its cause remain unknown. The corresponding recorders' system gain deviated accordingly between pre- and post-deployment pistphone calibrations.

Communication with recovered instruments

Communication efforts after recovery were successful with only 1 out of 9 SonoVault and for the single Aural recorder. A computer was connected via RS232 to the instruments. Success of communication efforts and information retrieved from the recorders are listed in Table 2.24.

Tab. 2. 24: Overview of results of preliminary technical and data quality evaluation of recorders recovered during PS129

For further information see the end of the Chapter.

Operation period and failures

All SonoVaults had ceased recording prior to recovery. All devices had been equipped with sufficient power and storage capacity to bridge up to 2 years deployment with recordings. Most of the recovered SonoVaults used the hardware version 4.1, with firmware version 4.13, and were set to Low Power Mode for sampling. The maximum recording duration (620-660 days) did not reach the recording duration from the previous expedition. It is assumed that the new 128 GB SD-cards used during this recent deployment might have had a higher power consumption and led to the shorter recording times.

Recorders SV1006 and SV1020 recorded only for some weeks before stopping to record, presumably due to a software or electronics error, as the log files exhibited good batteries levels at the time of stopping and electronics could be restarted after recovery. The reason for the error is unknown though, as recorders ran for several days prior to the deployment without fault and were checked only hours before the deployment.

Clock drift and post calibration

Where possible, the status of the system, the clock drift of the precision clock, voltage and SD-card status were checked using the communication software. To post-calibrate the hardware in combination with the hydrophone, a laboratory power supply was connected to the hardware. A post calibration of each recovered recorder was performed to ensure the correct calculation of signal levels after recovery (see Tab. 2.23, Gain PHS and MRPro).

Preliminary data quality evaluation

Two of the SonoVault recordings exhibited distinct peaks in the spectra (Fig. 2.19), representing tonal noise within the frequency range 25 Hz up to the Nyquist frequency, which likely is caused by the electronics. No cause of this noise could yet be determined, but will be under investigation. Table 2.25 summarizes the occurrence and type of noise found during the preliminary analysis of the recovered data.

Tab. 2.25: Overview of PAM recorders data quality

AWI22715_SV1006	Some electronic noise, order of 2 dB
AWI23113_SV1056	No electronic noise discernable in annual spectra.
AWI24803_SV1012	No electronic noise discernable in annual spectra.
AWI245-05_SV1014	No electronic noise discernable in annual spectra.

BGC-1_SV1024	“Flat” spectrum” for f > 3 Hz, possibly broken hydrophone
AWI 208-9_SV1020	“Flat” spectrum” for f > 3 Hz, possibly broken hydrophone
AWI 207-11_SV1032	Pronounced electronic noise, order of 10 dB
AWI 251-3_SV1002	No electronic noise discernable in annual spectra.
AWI 251-3_AU	pending

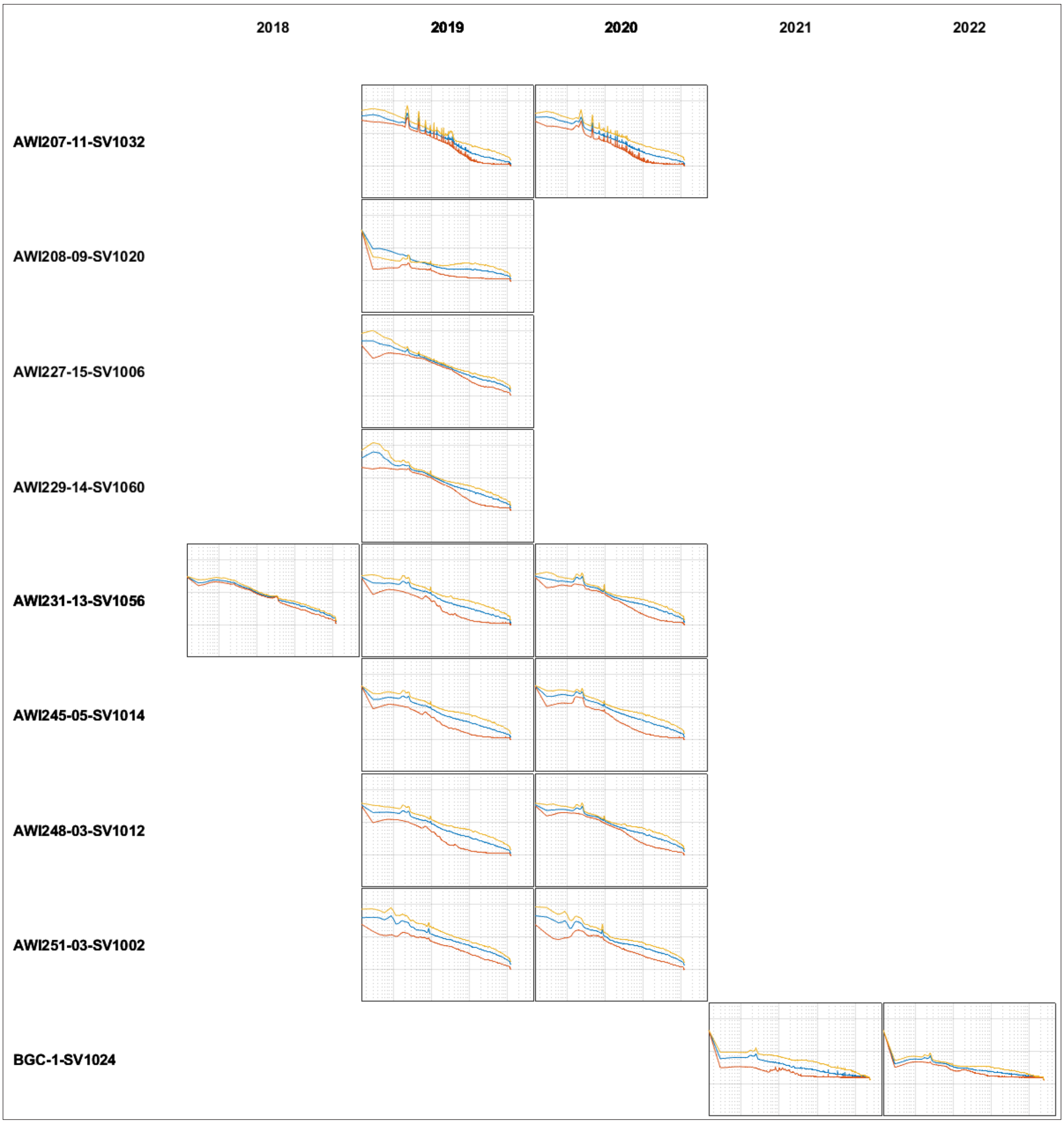

Fig. 2.19: Annual spectra of recorded data. Actual recording length varies with recorder and years. The logarithmic frequency (x-) axis ranges from 1 Hz to 50 kH, the sound pressures spectral density from 40 to 110 dB re 1 µPa2Hz.

Preliminary scientific results

Recordings were examined using the OPUS analysis tools (opus.aq) to calculate annual spectrograms (Figs. 2.20). Spectrograms indicate that tonal noise existed in AWI207 11_SV1032 throughout the recording period and throughout the short recording period of AWI227 15_SV1006. "Flat" spectra prevail for AWI208-9_SV1020 and BGC_SV1024 for the duration of their recordings. The remaining 9 recordings exhibit enhanced energy in the fin and blue whale bands and frequent broadband events, probably related to storms and cryophonic sound.

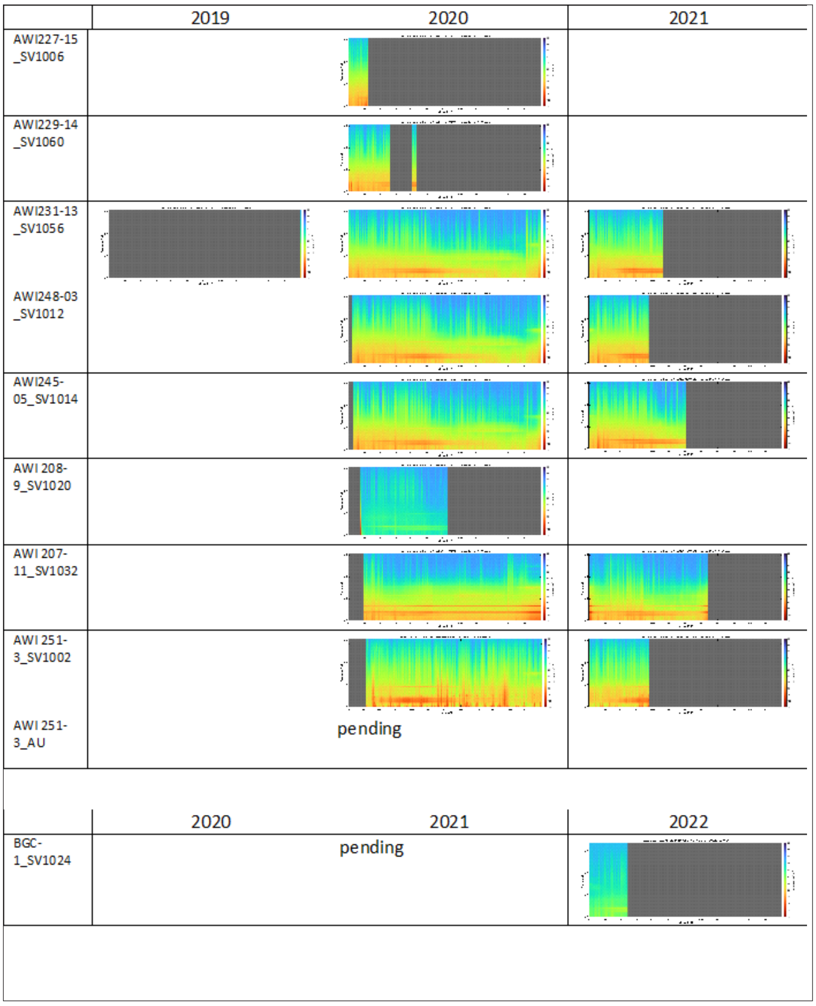

Fig. 2.20: Annual spectrograms of acoustic recordings captured by recorders deployed during previous expedition PS117 (top) and PS124 (bottom)

We randomly sampled 52 days over one complete year of recording per recovered mooring. We then systematically selected twelve 10-min acoustic files from the sampled day (one 10-min file out of every two hours) to ensure the representativity of the acoustic activity during that day. This made a total of about 600 files per mooring when recordings from the complete year where available. We manually analyzed every sample (10-min file) using Raven Pro 1.5 (Cornell Lab of Ornithology, Ithaca, USA) to visually and aurally identifying the presence/absence of species-specific calls from spectrograms. Spectrogram calculations employed various parameter settings to optimize visual contrasts of signal to noise gradients. Due to time constrains, data from AWI251-3 were not included in the analysis.

For each recorder, we computed the acoustic-presence proportion of every single species over the studied year (or shorter periods if data was missing). This allowed us to coarsely assess the marine mammal community composition at the recording sites and the species distribution over the studied area (Fig. 2.21).

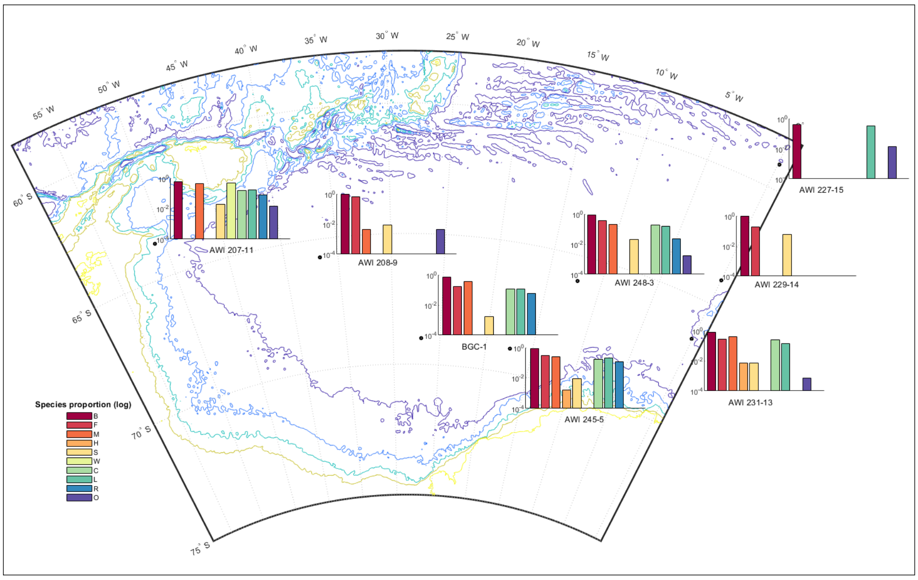

Fig. 2.21: Spatial distribution of marine mammal community composition

We also computed the species daily proportion of acoustic presence to assess the temporal variation in the structure of the communities at the specific sites (Fig. 2.22).

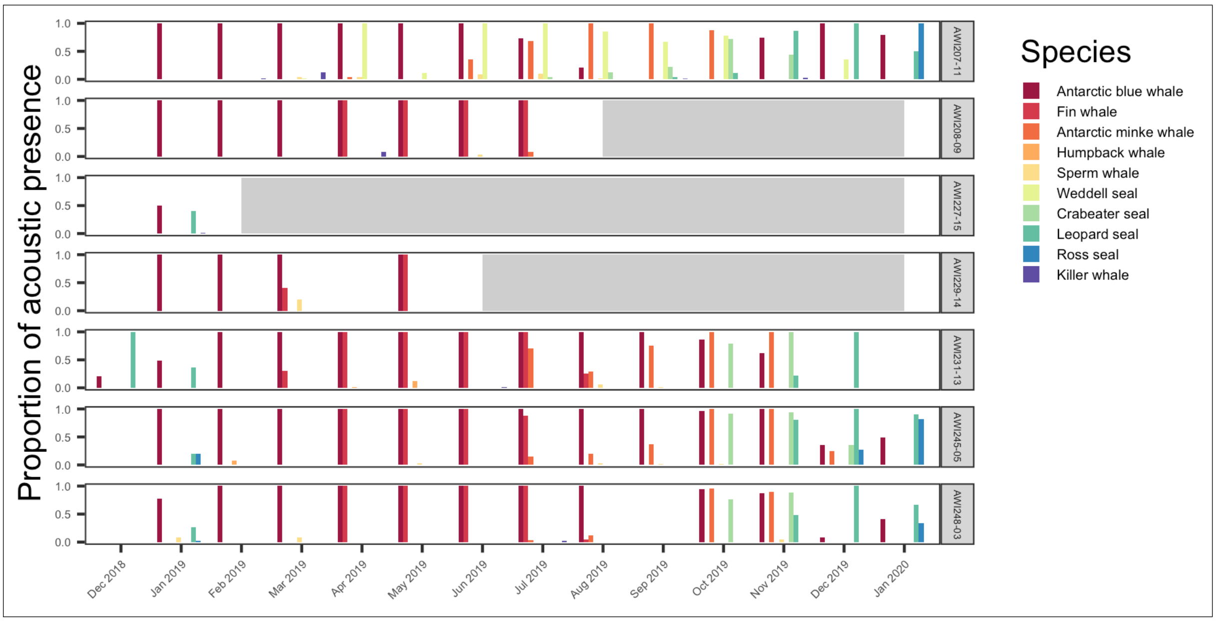

Fig. 2.22: Species daily proportion of acoustic presence

Pinnipeds

Only considering the random subset of data that was analyzed, Weddell seals (*Leptonychotes weddellii*) were exclusively detected at AWI207-11 in 2019. However, their acoustic presence was recurrent at the station lasting from April to December. On all analyzed sites with data available during the austral summer (4/7), we detected crabeater seals (*Lobodon carcinophaga*), leopard seals (*Hydrurga leptonyx*) and Ross seals (*Ommatophoca rossii*), except for AWI231-13, where no acoustic activity from Ross seals was detected. In all cases, the pack-ice related *pinniped* species followed a similar temporal pattern, with crabeater seals being acoustically conspicuous at the sites from September to December, leopard seals from October/November to January and Ross seals from the end of December to January. Only on AWI207-11 did we observe crabeater seal calls from July on.

Cetaceans

Single vocalizations and/or choruses of Antarctic blue whales (*Balaenoptera musculus intermedia*), fin whales (*B. physalus*) and Antarctic minke whales (*B. bonaerensis*) were very common at almost all recording positions. Fin whales were not detected at AWI227-15, probably because data from 2019 were missing from February on there and this species showed to be acoustically active from February to August at the remaining stations. They were also not observed at AWI207-11, but due to the pervasive mechanical noise present in these recordings it may also be possible that we were not able to distinguish their acoustic signature in the spectrograms. Most likely, the absence of Antarctic minke whale calls at AWI227-15 and AWI229-14 was also due to the lack of recordings during their acoustically active period in the Weddell Sea. Humpback whale (*Megaptera novaeangliae*) songs were only observed occasionally at the two southernmost sites, AWI245-5 and AWI231-13.

Sperm whale (*Physeter macrocephalus*) clicks were observed, even though not very frequently, in almost all recording positions. Killer whale (*Orcinus orca*) clicks and whistles were observed at 5 out of the 7 locations, however, their frequency was also very low.

Other sound sources

Pervasive tonal mechanical noise was detected in all recordings from AWI207-11 in 2019. Recordings from all sites, especially those located along the Greenwich Meridian transect and in the central Weddell Sea, presented intense and frequent noises with varying frequency and temporal patterns. The probable source of these noises was sea-ice related, either from the interaction between different sorts of sea-ice floes, the melting or hardening of the ice, or the calving/breaking off from close-by iceberg. Nevertheless, the precise source of each of these noises still needs to be determined.

Data management

Passive acoustic data will be transferred to the AWI silo and made accessible through the OPUS.aq webpage and will be archived, published and disseminated according to international standards by the World Data Center PANGAEA Data Publisher for Earth & Environmental Science (https://www.pangaea.de) within two years after the end of the expedition at the latest. By default, the CC-BY license will be applied. P.I.'s: Ilse van Opzeeland and Olaf Boebel.

This expedition was supported by the Helmholtz Research Programme "Changing Earth – Sustaining our Future" topic 6, subtopic 4. In all publications based on this expedition, the **Grant No. AWI_PS129_01** will be quoted and the following publication will be cited:

Alfred-Wegener-Institut Helmholtz-Zentrum für Polar- und Meeresforschung (2017) Polar Research and Supply Vessel POLARSTERN Operated by the Alfred-Wegener-Institute. Journal of large-scale research facilities, 3, A119. http://dx.doi.org/10.17815/jlsrf-3-163.

References

Steiner WW, Hain JH, Winn HE, Perkins PJ (1979) Vocalizations and feeding behavior of the killer whale (*Orcinus orca*). Journal of Mammalogy, 60, 823-827.

Backus RH, Schevill WE (1966) Physeter clicks. In: Norris KS (ed), Whales, dolphins and porpoises. University of California Press, Berkely and Los Angeles, U.S.A., p. 510-528.

Tab. 2.2: Instrumentation of moorings recovered during PS129. The column “CTD” gives the station number of the CTD casts carried out near the mooring location at deployment and recovery.

					Deploy				Recover				Instrument		
Mooring	Latitude	Longitude	EK80 Reading	Corr. depth [m]	Station # PS117_ Moor	Station # PS117_ CTD	Date	Time	Station # PS129_ Moor	Station # PS129_ CTD	Date	Time	Type	S/N	Depth (m)
AWI227-15	59°03.02’S	000°06.44’E		4605	22-4	22-2	2018-12-13	10:10	18-1	18-7	2022-03-12				
								09:58				08:23	SonoVault	1006	285
								08:26				10:30	SBE37SMP	12479	4560
AWI229-14	64°00.49’S	000°00.84'W		5060	24-2	none	2019-01.01	22:38	25-2	25-8	2022-03-15				
								20:10				09:39	SBE56	9494	82
								20:15				09:37	SBE56	9495	133
								20:20				09:37	SBE56	9496	184
								20:30				09:33	SBE56	9497	235
								20:36				09:33	Nortec	12654	256
								20:36				09:33	SBE56	9492	256
								20:45				09:44	SonoVault	1060	1060
								20:47				09:50	SBE56	2385	2098
								20:52				09:53	SBE56	2382	2385
								20:56				09:55	SBE56	2396	2382
								21:00				09:56	SBE56	3811	2396
								21:05				09:59	SBE56	3811	3811
								21:05				09:59	Aquadopp	12658	12658
								22:27				11:11	SBE37SMP	2092	12481
AWI231-13	66°31.03’S	000°04.48’W		4580	15-5	15-1	2018-12-27	18:34	27-5	27-2	2022-03-17				
								18:14				08:38	SonoVault	1056	303
								16:11				10:18	SBE37SMP	10944	4536
AWI244-06	69°00.08’ S	07°01.65’ W		2900	33-4	33-6	2019-01-05	20:01	**PS126** _116-1		2021-03-20	15:00			
													PAM	1049	300
													SBE37	8122	2903
AWI248-03	65°58.12’S	12°13.84’W		4950	34-5	34-2	2019-01-07	10:37	30-2	30-1	2022-03-19				
								18:14				09:10	SonoVault	1012	350
								16:11				10:30	SBE37SMP	8123	4906
AWI245-5	69°03.64’S	17°23.49’W		4734	35-4	35-6	2019-01-08	14:20	65-2	65-1	2022-04-04				
								14:12				11:10	SonoVault	1014	300
								12:10				12:57	SBE37SMP	8124	4691

Mooring	Latitude	Longitude	EK80 Reading	Corr. depth [m]	Deploy: Station # PS117_ Moor	Deploy: Station # PS117_ CTD	Deploy: Date	Deploy: Time	Recover: Station # PS129_ Moor	Recover: Station # PS129_ CTD	Recover: Date	Recover: Time	Instrument: Type	Instrument: S/N	Instrument: Depth (m)
BGC-1	69°00.03'S	27°00.29'W		CTD→4676		PS124_ 117-2	2021-03-24	13:13	72-2	72-1	2022-04-07	15:01	Lab on Chip	7	
												15:01	Nitrate		
												15:01	CO2	219	
												15:02	RAS-500	12073	
												15:02	Ecotriplet	17c	
												15:02	SBE37SMP	21026	132 ist
												15:03	RDI WH300	12667	
								13:06				15:10	SBE56	7824	
								13:00				15:15	SBE37SMP	2100	
								12:55				15:19	SBE56	7825	
								12:24				15:23	SBE37SM	449	
								12:00				15:30	Octopus		
								12:00				15:30	Suna	449	
								12:00				15:30	Vp6	7LP	
								12:00					SBE56	6513	
								12:02				15:46	Sediment trap	2009404	
								11:50				16:06	SonoVault	1024	
								11:27				16:39	Sediment trap	2009406	
AWI249-3	70°53.22'S	28°56.97'W		4362	53-3	53-4	2019-01-20	11:20			skipped				
								09:52					SonoVault	1010	307
								11:10					SBE37	8126	4319
AWI208-9	65°41.78'S	36°41.01'W		4714	56-6	56-2	23.01.2019	16:00	86-2	86-1	2022-04-14				
								15:47				12:31	SonoVault	1020	294
								15:28				11:03	Aquadopp	12685	794
								15:26				11:03	SBE37SMP	3812	797
								13:58				10:48	SBE37SMP	9841	4758
AWI250-3	68°28.85'S	44°05.94'W		4100	57-4	57-3	24.01.2019	20:28			skipped				
								20:16					SonoVault	1048	294
								20:08					Aquadopp	12718	795
								20:08					SBE37SMP	3813	797
								18:40					SBE37SMP	9839	4057

					Deploy				Recover				Instrument		
Mooring	Latitude	Longitude	EK80 Reading	Corr. depth [m]	Station # PS117_		Date	Time	Station # PS129_		Date	Time	Type	S/N	Depth (m)
					Moor	CTD			Moor	CTD					
AWI257-2	64°12.94'S	47°29.38'W		4292	64-2	64-4	27.01.2019	17:50			skipped				
								17:38					PAM		311
								17:24					RCM8	11888	813
								17:24					SBE37SMP	9831	813
								16:05					SBE37SMP	9493	4285
AWI207-11	63°39.36'S	50°48.66'W		2510	72-2	72-3	29.01.2019	17:08	109-1	109-3	2022-04-22				
												02:01	SBE37SMP	10934	250
								17:00				02:10	QM150	23548	291
								16:53				02:10	SonoVault	1032	300
								16:36				02:30	Aquadopp	12745	
								16:36				02:30	SBE37SMP	6928	
								16:05					SBE37SMP	10937	
								16:00				03:18	RCM8	3517	
												03:18	SBE39	8641	
												03:11	SBE39	8642	
								15:47				03:11	SBE39	8643	
												03:28	SBE37SMP	10943	
								15:37				03:38	QM6000	24053	
AWI251-03	61°01.38'S	55°58.68'W	335		99-2	99-3	2019-02-01	18:30	127-1	127-3	2022-04-24				
								18:25				14:25	Aural	0085	148
								18:21				14:38	SonoVault	1002	153

Tab. 2.3: Instrumentation of mooring deployments during PS129

					Deploy				Recover				Instrument		
Mooring	Latitude	Longitude	EK80 Reading	Corr. depth [m]	Station # PS129_ Moor	Station # PS129_ CTD	Date	Time	Station # Moor	Station # CTD	Date	Time	Type	S/N	Depth (m)
AWI227-16	59° 03.02'S	00° 06.44'E	4632	4587	18-2		2022-03-12	14:21							
								14:04					SonoVault	1005	282
								12:43					SBE37	1232	782
								11:28					SBE37	10933	4542
AWI229-15	64° 01.26'S	00° 00.83'E	5173	5146	25-3		2022-03-15	15:25					SBE37SMP	10929	252
AWI229-15	64° 01.26'S	00° 00.83'E	5173	5146	25-3		2022-03-15	15:25					SBE37SMP	10929	252
								15:19					SonoVault	1009	296
								15:11					SBE37SMP	10930	377
								15:07					SBE37SM	225	450
								15:02					SBE37SMP	10931	550
								14:58					SBE37SM	230	650
								14:49					SBE37SMP	10932	750
								12:24					SBE37SM	238	5102
AWI231-14	66° 31.03'S	00° 04.48'W	4602	4557	27-6		2022-03-17	13:40					SonoVault	1021	307
AWI231-14	66° 31.03'S	00° 04.48'W	4602	4557	27-6		2022-03-17	13:40					SonoVault	1021	307
								13:16					SBE37SMP	9848	800
								11:14					SBE37SM	239	4514
EWS 001-01	70° 47.87'S	12° 13.05'W	706	683	58-1		2022-04-02	09:11					SBE56SMP	10940	324
EWS 001-01	70° 47.87'S	12° 13.05'W	706	683	58-1		2022-04-02	09:11					SBE56SMP	10940	324
								09:11					ADCP QM150	23807	324
								09:07					SBE 37SMP	10941	329
								08:59					SBE56	7826	383
								08:52					SBE56	7827	443
								08:45					SBE 37SMP	10942	503
								08:40					SBE56	7828	563
													ADCP WH600	1002	635
													SBE56	7829	676
								08:33					SBE 37SMP	10928	676
EWS 002-01	70° 35.17'S	12° 51.46'W	1423	1348	59-2		2022-04-02	16:50					ADCP QM150	22283	289
								16:50					SBE 37SMP	10946	289
								16:45					SBE 37SMP	10947	

					Deploy				Recover				Instrument		
Mooring	Latitude	Longitude	EK80 Reading	Corr. depth [m]	Station # PS129_ Moor	Station # PS129_ CTD	Date	Time	Station # Moor	Station # CTD	Date	Time	Type	S/N	Depth (m)
								16:34					SBE56	7830	448
								16:28					SBE56	7831	548
													SBE56	7833	648
								16:11					SBE 37SMP	9490	748
								16:01					SBE56	6368	848
								15:56					SBE56	6986	948
								15:52					SBE 37SMP	2088	1048
													SBE56	6988	1148
								15:35					ADCP WH300	951	1250
								15:35					SBE56	6989	1250
								15:19					SBE 37	11420	1341
													SBE53	439	1348
EWS 003-01			3359	3304	62-5		2022-04-03	12:18					SonoVault	1008	244
								11:50					SoSo	0061	800
								11:46					Aquadopp	16505	799
								11:44					SBE 37	3814	799
								10:32					SBE 37	224	3296
													SBE53	438	3304
AWI245-06	69° 03.64'S	17° 23.49'W	4762	4721	65-3		2022-04-04	15:43					SonoVault	1022	285
								15:26					SoSo	2025	806
								15:20					Aquadopp	16600	807
								15:19					SBE37SMP	9838	807
								13:54					SBE37SM	218	4678
AWI249-04	70° 53.22'S	28° 56.97'W	4420	4374	74-3		2022-04-08	18:35					SonoVault	1026	300
								18:15					SoSo	43	809
								18:12					Aquadopp	16581	809
								18:11					SBE37SMP	9832	809
								16:29					SBE37SM	235	4319
CWS01-01	69° 57.55'S	36° 43.87'W	4476	4430	77-1		2022-04-10	22:18					Aural	0231	255
								22:08					SonoVault	1031	314
								21:47					SoSo	0018	817
								21:44					Aquadopp	16544	818
								21:41					SBE37SMP	2090	818
								19:53					SBE37SM	233	4387

					Deploy				Recover				Instrument		
Mooring	Latitude	Longitude	EK80 Reading	Corr. depth [m]	Station # PS129_ Moor	Station # PS129_ CTD	Date	Time	Station # Moor	Station # CTD	Date	Time	Type	S/N	Depth (m)
AWI209-09	66° 36.45'S	27° 07.29'W	4861	4821	80-1		2022-04-12	16:45					SonoVault	1025	299
								16:31					SBE37SMP	9491	799
								14:55					SBE37SM	440	4813
AWI208-10	65° 41.78'S	36° 41.01'W	4756	4715	86-3		2022-04-14	15:10					SonoVault	1049	300
								14:00					SBE37SMP	9487	796
								13:26					SBE37SM	442	4758
CWS02-01 (1)			4566	4524	91-1		2022-04-16						SonoVault	1030	1030
													SoSo	0017	798
													Aquadopp	16550	799
													SBE37SMP	2101	799
													SBE37SM	444	4481
WWS02-01	66° 34.62'S	44° 00.91'W	4463	4416	94-1		2022-04-17	20:30					Aural	0086	257
								20:22					SonoVault	1027	310
								20:09					SoSo	0066	812
								20:01					AquaD	16572	814
								20:01					SBE37SMP	9488	814
								18:42					SBE37SM	232	4408
													SBE53	437	4416
AWI257-03	64° 12.94'S	47° 29.38'W	4197	4142	100-2		2022-04-19	20:24					SonoVault	1034	310
								20:01					SoSo	0045	812
													AquaD	11330	813
													SBE37SMP	7690	813
								18:20					SBE37SM	435	4134
AWI207-12	63° 39.36'S	50° 48.66'W	2555	2502	109-2		2022-04-21	23:38					SM37SMP	2089	249
								23:33					QM150	23456	290
								23:31					SonoVault	1013	300
								23:06					SM37SMP	11421	805
								22:18					SM37SMP	2094	2200
								22:16					AquaD	11348	2203
								22:15					SBE39	7862	2210
								22:14					SBE39	7861	2260
								22:00					SBE39	7860	2310
								21:53					SM37SMP	2234	2410
								21:50					QM150	24052	2500

					Deploy				Recover				Instrument		
Mooring	Latitude	Longitude	EK80 Reading	Corr. depth [m]	Station # PS129_ Moor	CTD	Date	Time	Station # Moor	CTD	Date	Time	Type	S/N	Depth (m)
								21:50					SBE37SMP	2020	2500
													SBE53	436	
AWI261-02	63° 30.87'S	50° 38.20'W	1660	1618	114-1		2022-04-22	21:01					SonoVault	1023	255
								20:24					SBE37SMP	9840	755
								20:32					SBE56	6990	1268
								20:24					SBE37SMP	2092	1318
								20:20					SBE56	6991	1368
								20:05					SBE37SMP	2093	1409
								19:56					SBE56	7068	1468
								19:49					SBE37SMP	9834	1518
								19:45					SBE56	7069	1568
								19:38					SBE37SMP	12478	1609
								19:36					ADCP QM150	14088	1609
AWI251-04	61° 01.38'S	55° 58.68'W	323	311	127-2		2022-04-24	16:08					Aural	303	148
								16:08					SonoVault	1054	153
								15:49					AZFP	55115	239
								15:38					ADCP LR 075	22858	303
								15:38					SBE37SMP	2359	330

(1) Originally, it was planned to exchange mooring AWI250-3 with AWI250-4. However, due to temporal constraints, calling at AWI250 was cancelled. Instead, CWS02-01 was deployed further north and AWI250-3 was left untouched

Abbreviations for Tables 2.2 and 2.3:

ADCP LR075	RD Instruments Doppler Current Profiler, Type Long Ranger 75 kHz
ADCP QM150	RD Instruments Doppler Current Profiler, Type Quarter Master 150 kHz
ADCP WH600	RD Instruments Doppler Current Profiler, Type Workhorse 600 kHz
AquaD	Nortek Aquadopp Acoustic Current Meter
Aural	Multi-Electronique (MTE) Aural Passive Acoustic Recorder
AVT	Aanderaa Current Meter with Temperature Sensor
AZFP	ASL Environmental Sciences Acoustic Zooplankton and Fish Profiler
PAM	Passive Acoustic Monitor (Type: AURAL or SONOVAULT)
RCM11	Aanderaa Doppler Current Meter (acoustic)
SBE37	SeaBird Electronics MicroCat Conductivity and Temperature Logger
SBE39	SeaBird Electronics Temperature Logger
SBE56	SeaBird Electronics Temperature Logger
SonoVault	Develogic SonoVault Passive Acoustic Recorder
SOSO	Develogic RAFOS Sound Source
Ecotriplet	Fluorescence sensor
ISUS	Nitrate Sensor
LOC	Lab on Chip sensors
RAS-500	Remote Access Sampler RAS-48-500
Sediment trap	KUM sediment traps
Suna	Nitrate Sensor
VVP6	Underwater Vision Profiler 6

Tab. 2.5: CTD casts of PS129

Station ID	LADCP Cast	Date-Time in water	Date-Time at depth	Latitude	Longitude	EK80 depth [reading]	Corr. Depth [m]	Altim [m]	CTD max. pressure [dbar]	Config	Comment
014_01	2	2022-03-11T10:15:30	2022-03-11T10:26:09	55°56.57'S	002°56.11'E	3524.9	3466	98.7	153	1	Test cast Most bottles leaking
018_07	4	2022-03-12T23:39:32	2022-03-13T03:20:08	59°05.52'S	000°07.33'E	4668.7	4730	94.9	4682	1	Winch problems. Stopped at about 2350 meters for 2.5 h. Beam transmission decrased strongly during the cast Altimeter did not work
023_01	5	2022-03-14T05:56:45	2022-03-14T07:50:12	61°00.13'S	000°00.01'E	5373	5343	8.1	5468	2	Calibration cast. 2nd oxygen sensor broken during cast
025_08	6	2022-03-16T01:15:47	2022-03-16T03:18:31	64°04.42'S	000°04.66'E	5177.5	5148	10.6	5264	3	2nd oxygen sensor spiky
027_02	7	2022-03-16T21:59:05	2022-03-16T23:32:36	66°28.90'S	000°04.28'W	4444.5	4394	28.1	4476	3	2nd oxygen sensor spiky. Altimeter did not work. Cast stopped 90m above bottom, visible from LADCP
030_01	8	2022-03-19T03:08:16	2022-03-19T04:59:12	65°56.13'S	012°11.92'W	5037.7	5005	14.2	5109	3	2nd oxygen sensor spiky
040_02	9	2022-03-21T13:12:33	2022-03-21T13:41:23	70°45.07'S	010°49.84'W	928	902	4.8	918	3	Calibration cast. 2nd oxygen sensor spiky
041_02	10	2022-03-23T18:08:00	2022-03-23T18:19:35	70°31.76'S	008°12.20'W	226.9	221	4.8	223	3	2nd oxygen sensor spiky
042_01	11	2022-03-24T01:23:12	2022-03-24T01:44:13	70°50.51'S	010°35.35'W	253.3	241	4.1	252	3	2nd oxygen sensor spiky
047_01	13	2022-03-25T16:52:45	2022-03-25T17:10:07	70°47.18'S	010°45.14'W	617.3	599	9.8	594	3	2nd oxygen sensor spiky
049_01	14	2022-03-26T12:13:07	2022-03-26T12:29:05	70°56.61'S	010°32.16'W	296.4	289	4.8	295	3	2nd oxygen sensor spiky
053_03	15	2022-03-28T05:54:41	2022-03-28T06:06:47	70°52.41'S	010°28.94'W	234.7	221	3.9	234	4	New 2nd oxygen sensor
054_03	16	2022-03-29T01:56:27	2022-03-29T02:29:39	70°39.23'S	011°00.34'W	1376.3	1333	9.7	1352	4	
058_02	18	2022-04-02T10:17:56	2022-04-02T10:41:37	70°53.18'S	011°17.42'W	691.5	667	5.7	693	4	Wrong LADCP cast number in CTD header
059_01	19	2022-04-02T12:39:25	2022-04-02T13:21:02	70°50.07'S	011°24.61'W	1429.4	1392	4.3	1396	4	
060_01	20	2022-04-02T19:33:38	2022-04-02T20:16:59	70°36.09'S	012°13.03'W	2024.4	1972	4.7	2012	4	Calibration cast. Bottle 23 leaked
062_04	21	2022-04-03T07:07:44	2022-04-03T08:28:27	70°18.01'S	013°26.76'W	3319.1	3265	7.5	3349	4	Bottle 1 did not close
064_02	22	2022-04-03T18:07:51	2022-04-03T19:50:36	69°42.75'S	015°24.25'W	4756.5	4720	9.2	4821	4	Calibration cast

Station ID	LADCP Cast	Date-Time in water	Date-Time at depth	Latitude	Longitude	EK80 depth [reading]	Corr. Depth [m]	Altim [m]	CTD max. pressure [dbar]	Config	Comment
065_01	23	2022-04-04T04:46:16	2022-04-04T06:21:27	69°05.11'S	017°20.09'W	4759.1	4720	9.9	4823	4	
068_01	24	2022-04-05T08:26:52	2022-04-05T06:10:32	68°13.30'S	019°44.36'W	4873.6	4832	7.7	4942	4	Bottle 23 and 24 did not close. CTD was started again, with the filename PS129_068_02
070_01	25	2022-04-05T19:23:22	2022-04-05T21:02:59	67°15.95'S	023°35.76'W	4874.9	4832	10.8	4940	4	
071_02	26	2022-04-07T10:16:34	2022-04-07T10:28:05	68°43.04'S	027°03.11'W	4723.7	4679	98.7	317	4	shallow cast
072_01	27	2022-04-07T13:56:48	2022-04-07T14:12:51	68°58.13'S	026°59.64'W	4708.7	4669	98.7	456	4	shallow cast
072_03	29	2022-04-07T19:28:03	2022-04-07T19:43:15	69°00.11'S	027°02.51'W	4705.3	4669	98.7	406	4	Shallow cast, cast was delayed, LADCP was turned off again to save battery
074_04	30	2022-04-08T20:34:32	2022-04-08T20:48:43	70°49.09'S	029°14.72'W	4426.2	4384	98.7	405	4	Shallow calibration cast
080_02	31	2022-04-12T17:47:52	2022-04-12T19:24:19	66°36.91'S	027°12.42'W	4859.5	4821	9.3	4926	4	ADCP Battery changed, calibration cast
082_01	32	2022-04-13T05:43:37	2022-04-13T07:21:41	66°14.96'S	030°26.13'W	4804.6	4760	8.9	4868	4	Communication failure with the CTD, bottles couldn't be closed, for the upcast the file "PS129_82_01_upcast" was created
083_02	33	2022-04-13T13:16:12	2022-04-13T15:00:40	66°06.29'S	031°49.82'W	4784.8	4740	9.7	4846	4	Change to the winch SE32.1 to reestablish communication with the CTD
086_01	34	2022-04-14T05:08:36	2022-04-14T06:45:15	65°40.08'S	036°36.78'W	4760	4720	9.8	4819	4	Winch SE32.1 was used
087_01	35	2022-04-14T21:27:08	2022-04-14T23:07:07	65°21.29'S	038°43.16'W	4750.1	4709	9.6	4808	4	Changed back to winch EL31
088_01	36	2022-04-15T08:28:39	2022-04-15T10:10:33	65°02.45'S	041°08.32'W	4746.6	4699	6.6	4807	4	
096_01	40	2022-04-18T08:44:44	2022-04-18T10:25:25	64°44.32'S	043°30.60'W	4637.7	4597	9.2	4691	4	LADCP problems at the startup, erroneous measurement at 360m
097_01	42	2022-04-18T21:47:20	2022-04-18T23:25:20	64°28.82'S	045°18.02'W	4479.4	4445	5.5	4530	4	
099_01	43	2022-04-19T08:25:56	2022-04-19T09:54:47	64°18.02'S	046°40.10'W	4383.2	4333	10	4424	4	Depth for bottle 3 was miscalculated at first, CTD was lowered a few meters to the correct depth
100_03	44	2022-04-19T21:32:09	2022-04-19T22:56:57	64°16.74'S	047°28.15'W	4192.1	4151	9.1	4231	4	
102_01	46	2022-04-20T05:05:03	2022-04-20T06:30:09	64°07.96'S	047°57.24'W	4091.9	4040	5	4126	4	New grease was applied to the LADCP plugs, LADCP was restarted because of a delay in the search for a suitable hole in the ice
103_01	47	2022-04-20T11:18:08	2022-04-20T12:37:56	64°04.66'S	048°21.91'W	3924.6	3868	8.3	3949	4	

Station ID	LADC P Cast	Date-Time in water	Date-Time at depth	Latitude	Longitude	EK80 depth [reading]	Corr. Depth [m]	Altim [m]	CTD max. pressure [dbar]	Config	Comment
104_01	49	2022-04-20T17:30:09	2022-04-20T18:45:32	63°59.66'S	048°49.17'W	3709.2	3687	9.8	3722	4	
105_01	50	2022-04-21T01:10:31	2022-04-21T02:20:44	63°52.59'S	049°09.13'W	3445.3	3395	10.7	3452	4	Faulty 2nd oxygen sensor; because of ice conditions station was changed to a location of equal depth less than 3nm away
106_01	51	2022-04-21T06:41:04	2022-04-21T07:49:09	63°48.88'S	049°32.68'W	3206.2	3135	10	3202	5	New 2nd oxygen sensor was installed
107_01	52	2022-04-21T15:15:16	2022-04-21T16:12:49	63°44.06'S	050°21.05'W	2683.4	2628	4.5	2677	5	Calibration cast, new 2nd oxygen sensor was not working, CTD was covered in jelly fish tentacles
109_03	53	2022-04-22T04:19:46	2022-04-22T05:16:26	63°40.47'S	050°45.23'W	2575.7	2515	9.9	2560	5	Bottles 14 and 18 didn't close
110_01	55	2022-04-22T09:24:12	2022-04-22T10:14:50	63°36.97'S	051°04.43'W	2379.1	2328	9.9	2363	5	LADCP was restarted during the search for better ice conditions
111_01	56	2022-04-22T13:02:49	2022-04-22T13:51:06	63°34.32'S	051°18.08'W	2225.4	2180	9.6	2207	5	
112_01	58	2022-04-22T16:11:51	2022-04-22T16:55:41	63°31.92'S	051°27.35'W	2013.3	1963	9.8	1992	5	
114_02	59	2022-04-22T22:23:17	2022-04-22T23:02:22	63°28.67'S	051°36.84'W	1823.3	1775	10.2	1819	5	
116_01	61	2022-04-23T02:17:17	2022-04-23T03:25:03	63°28.85'S	051°50.40'W	1231.3	1196	9.9	1210	5	CTD got frozen on deck during repositioning, cast 115_01 was restarted due to technical problems
117_01	62	2022-04-23T06:05:50	2022-04-23T06:28:59	63°27.96'S	052°05.79'W	940.2	912	9.7	922	5	
119_01	63	2022-04-23T08:40:48	2022-04-23T09:00:58	63°24.59'S	052°16.37'W	687.2	667	10.2	673	5	Bottles 8,7 and 15 were not registered as fired and didn't close
120_01	64	2022-04-23T12:16:27	2022-04-23T12:30:37	63°21.06'S	052°43.66'W	459.1	444	10.6	447	5	
121_01	65	2022-04-23T17:19:38	2022-04-23T17:32:43	63°15.64'S	053°20.99'W	394.9	376	7.9	386	5	
122_01	66	2022-04-23T21:26:18	2022-04-23T21:38:26	63°10.12'S	053°57.26'W	236.9	221	9.7	231	5	
123_01	67	2022-04-24T00:20:38	2022-04-24T00:35:50	63°05.47'S	054°31.42'W	479	463	9.8	466	5	
127_03	68	2022-04-24T16:57:38	2022-04-24T17:10:27	61°00.07'S	055°59.73'W	380.5	366	10.64	379	5	Calibration cast

Tab. 2.6: OFOBS CTD deployments

		Profile start		Profile end			CTD SN	Comment
Station name	**Date**	**Latitude south**	**Longitude west**	**Latitude south**	**Longitude west**	**File name**		
PS129_040_05	22-03-21T21:56	70.732825	10.916521	70.725818	10.912191	SBE37SM-RS232_03707727_2022_03_21.hex	7727	
PS129_043_03	24-03-22T08:39	70.86189	10.748137	70.852686	10.667725	SBE37SM-RS232_03707727_2022_03_24.hex	7727	Didn't record
PS129_047_04	25-03-22T23:24	70.778072	10.743258	70.779168	10.624015	SBE37SM-RS232_03709494_2022_03_26.hex	9494	
PS129_049_03	26-03-22T14:45	70.940804	10.523132	70.935392	10.497735	SBE37SM-RS232_03709494_2022_03_26.hex	9494	
PS129_050_01	27-03-22T01:23	70.942587	10.574757	70.933009	10.550206	SBE37SM-RS232_03709494_2022_03_27.hex	9494	
PS129_053_02	28-03-22T02:51	70.871975	10.519886	70.885567	10.471686	SBE37SM-RS232_03709494_2022_03_28.hex	9494	
PS129_054_02	28-03-22T23:09	70.64989	10.968565	70.640635	10.958279	SBE37SM-RS232_03709494_2022_03_29.hex	9494	
PS129_057_04	30-03-22T03:44	70.910549	11.183418	70.895211	11.137764	SBE37SM-RS232_03709494_2022_03_30.hex	9494	

Tab. 2.8: Metadata of RAFOS sound sources deployed during PS129

Mooring	Sound Source Position	Sound Source S/N	Position LAT	Position LON	Corr. water depth [m]	Deploy depth [m]	Deployment date /time [UTC]	Sweep Time [UTC]	1st sweep [UTC]	Configuration *)
EWS 003-01	W22	D0048 EI0061 ZBP2052	70° 17.905' S	013° 26.779' W	3304	800	2022-04-03 T12:41:00	12:40	20220401T12:40:00 [1)]	repeat=0xffff; Amp=95%; Tuning Coil = ON
AWI245-06	W09	D0046 EI0043 ZBP2050	69° 03.636' S	017° 23.455' W	4721	806	2022-04-04 T16:03:00	13:00	20220404T13:00:00 (checked with Dummy Load)	repeat=0xffff; Amp=95%; Tuning Coil = ON
AWI249-04	W13	D0043 EI0047 ZBP2122	70° 49.932' S	029° 07.930' W	4374	821	2022-04-08 T19:50:00	13:20	20220409T13:20:00	repeat=0xffff; Amp=95%; Tuning Coil = ON
CWS 001-01	W21	D0018 EI0050 ZBP2056	69° 33.349' S	032° 28.620' W	4430	817	2022-04-10 T22:36:00	12:40	20220410T12:40:00 (checked with Dummy Load)	repeat=0xffff; Amp=95%; Tuning Coil = ON
CWS 002-01	W23	D0017 EI0058 ZBP2053	66° 22.766' S	041° 23.502' W	4524	797	16.04.2022 T17:05:22	13:00	20220416T13:00:00	repeat=0xffff; Amp=95%; Tuning Coil = OFF [2)]
WWS 002-01	W20	D0030 EI0066 ZBP2054	65° 25.985'S	044° 35.575'W	4416	812	17.04.2022 T20:44:00	13:20	20220417T13:20:00 (checked with Dummy Load)	repeat=0xffff; Amp=95%; Tuning Coil = ON
AWI257-2	W10	D0045 EI0065 ZBP2116	64° 14.420' S	047° 29.114' W	4142	810	2022-04-19T20:42:39	12:40	20220419T12:40:00 (checked with Dummy Load)	repeat=0xffff; Amp=95%; Tuning Coil = ON

Standard Configuration: interval=86400000ms; f=259.38-260.9Hz; duration=80000ms;
*) Sound source deployment configuration tested prior to deployment, but at half-hourly intervals and connected to Dummy Load
1) First sweep on deck with Dummy Load (two days prior to deployment) OK, second sweep (one day prior to deployment) aborted. Amplifier set to 95% instead of 100% Additional tests at half hourly intervals OK; deployment configuration changed accordingly to 95%
2) Test sweep with dummy load did not work, presumably caused to the tuning coil. The tuning coil switched off for deployment

Tab. 2.9: Ice resilient APEX float tests and clock readings

internal ID	Apex S/N	WMO	IMEI	TestTdate	Test result	Float Time	iPhone Time	Offset [s]	Comment
PS129_01	9215	7900990	300125061143710	19.03.2022T17:06	PASSED	16:41:06	16:41:00	+6	1)
PS129_02	9224	7900999	300125061162760	19.03.2022T20:42	PASSED	20:07:12	20:07:00	+12	
PS129_03	9223	7900998	300125061162770	19.03.2022T19:56	PASSED	19:19:16	19:19:00	+16	
PS129_04	9216	7900991	300125061163760	27.03.2022T11:52	PASSED	11:21:02	11:21:00	+2	2)
PS129_05	9220	7900995	300125061144830	23.03.2022T10:14	PASSED	09:37:00	09:37:00	+0	
PS129_17	8893	7900986	300125061813240	23.03.2022T09:25	PASSED	08:43:34	08:44:00	-26	3)
PS129_06	9217	7900992	300125061246210	26.03.2022T12:33	PASSED	11:44:05	11:44:00	+5	
PS129_07	9218	7900993	300125061165760	27.03.2022T11:12	PASSED	10:25:10	10:26:00	+10	
PS129_08	9213	7900988	300125061142720	26.03.2022T11:36	PASSED	10:41:05	10:51:00	+5	
PS129_09	9221	7900996	300125061167760	23.03.2022T15:24	PASSED	14:41:17	14:41:00	+17	
PS129_10	8888	7900981	300125061323740	26.03.2022T10:18	PASSED	09:31:05	09:31:00	+5	
PS129_11H	8889	7900982	300125061326720	23.03.2022T17:29	PASSED	16:41:05	16:41:00	+5	
PS129_12	9222	7900997	300125061163750	26.03.2022T09:23	PASSED	08:38:16	08:38:00	+16	
PS129_13	8892	7900985	300125061810140	21.03.2022T16:41	PASSED	16:01:18	16:01:00	+18	
PS129_14	8891	7900984	300125061321740	23.03.2022T12:34	PASSED	11:50:05	11:50:00	+5	
PS129_15	8890	7900983	300125061321650	23.03.2022T11:41	PASSED	10:56:09	10:56:00	+9	
PS129_17	9212	7900987	300125061140800	21.03.2022T15:30	PASSED	15:31:02	15:31:00	+2	
PS129_16	9219	7900994	300125061148800	23.03.2022T16:31	PASSED	15:43:11	15:43:00	+11	
PS129_18	8878	7900971	300125061811150	25.03.2022T10:33	PASSED	09:44:08	09:44:00	+8	
PS129_19	8879	7900972	300125061814250	23.03.2022T13:25	PASSED	12:45:09	12:45:00	+9	
PS129_20	8887	7900980	300125061324710	23.03.2022T14:29	PASSED	13:45:09	13:45:00	+9	
PS129_21	8886	7900979	300125061326710	25.03.2022T11:52	PASSED	10:43:16	10:43:00	+16	4)
	9214	7900989	300125061756090	-	FAILED	-	-	-	

1) self-test only partially logged

2) self-test passed only on second try, touched ice flow when dropped, presumably at damper disk

3) log sheet not completed

4) self-test passed only on third try

Time(iPhone) - Time(WempeClock) = -2s

Tab. 2.10: Ice resilient APEX float deployments, all featuring Ice Sensing Algorithm (ISA) and RAFOS receivers

Apex S/N	WMO	deployment Datetime	Station PS129_	deployment latitude	deployment longitude	EK80 depth reading	CDT cast	sea ice	Corrected depth	Profiles sent until 2022-05-23	Comments Profiles
9215	7900990	2022-03-20T07:22	35-1	69° 22,491' S	009° 15,944' W	3296	none	none	3241	5	
9224	7900999	2022-03-20T12:27	37-1	70° 02,821' S	008° 39,546' W	2546	none	pancake, >95%	2493		
9223	7900998	2022-03-20T13:03	38-1	70° 03,543' S	008° 43,664' W	2087	none	pancake, >95%	2039		
9216	7900991	2022-04-02T21:40	60-2	70° 36,081' S	012° 12,871' W	2024	60-1	none	1976		
9220	7900995	2022-04-02T23:17	61-1	70° 27,893' S	012° 48,739' W	2359	none	none	2308	3	
8893	7900986	2022-04-03T12:49	62-6	70° 17,714' S	013° 26,526' W	3367			3312		
9217	7900992	2022-04-03T17:33	64-1	69° 44,786' S	015° 17,740' W	4754	64-2	none	4713	1	
9218	7900993	2022-04-04T22:07	65-8	69° 01,739' S	017° 28,411' W	4766	65-1	none	4725	3	
9213	7900988	2022-04-08T06T12	73-1	69° 57.538' S	027° 56,895' W	4606	none	pancake, >95%	4564		
9221	7900996	2022-04-09T23:46	74-9	70° 38.030' S	029° 19.800' W	4620	74-4	floes, >95%	4577		
8888	7900981	2022-04-10T10:00	75-1	70° 08.015' S	030° 59.889' W	4514	none	floes, >95%	4469		
8889	7900982	2022-04-10T12:11	helicopter	70° 44.855' S	031° 10.573'W	none	none		none		by helicopter
9222	7900997	2022-04-10T16:36	76-1	69° 46.013' S	032° 01.362' W	4270	none	floes, >95%	4221		
8892	7900985	2022-04-10T22:54	77-2	69° 33.229' S	032° 28.230' W	4477	none	new ice, > 95%	4431		no plugs
8891	7900984	2022-04-11T08:48	78-1	68° 59.702' S	031° 56.559' W	none	none	new ice, > 95%	none		no plugs, 6)
8890	7900983	2022-04-11T12:32	88-2	65° 62.050' S	041° 08.439' W	4745	88_1	none	4704	1	no plugs
9212	7900987	2022-04-16T17:20	90-1	66° 22,784' S	041° 23,910' W	4567	none	new ice, > 95%	4523		
9219	7900994	2022-04-16T01:51	91-2	66° 04,892' S	041° 45,811' W	4492	none	floes, >95%	4447		
8878	7900971	2022-04-17T05:02	92-1	66° 02,222' S	043° 30,435' W	4472	none	100%	4426		5)
8879	7900972	2022-04-17T21:00	94-2	65° 25,966' S	044° 36,015' W	4469	283.2	100%	4424		no plugs
8887	7900980	2022-04-18T04:40	95-1	65° 00,179' S	043° 54,511' W	4618	none	100%	4575		no plugs
8886	7900979	2022-04-18T12:38	96-2	65° 25,966' S	044° 36,015' W	4638	96-1	100%	4595	1	
9214	7900989										

5) dropped into turbulent wake, float not seen under water
6) EK80 gives false readings, float ice cage touched A-frame when lifting over reeling

Tab. 2.11: ARVOR float deployments. *Ice Sensing Algorithm (ISA)

internal ID	ARVOR S/N	WMO	Datetime time	Station PS129_	deployment latitude	deployment longitude	EK80 depth reading	CDT cast	Sea ice	Corrected depth [m]
PS129-BSH1	AI2600-22DE001	6904211	2022-03-07T20:51	PS129_4-1	45° 00.219' S	011° 25.364' E	4888.4	none	none	4887
PS129-BSH2	AI2600-22DE002	6904210	2022-03-08T11:09	PS129_7-1	46° 59.714' S	010° 01.181' E	4556.9	none	none	4543
PS129-BSH3	AI2600-22DE003	6904209	2022-03-09T12:42	PS129_10-1	50° 00.791' S	007° 46.020' E	4451.2	none	none	4426
PS129-BSH4	AI2600-22DE004	6904208	2022-03-11T21:55	PS129_16-1	57° 37.450' S	001° 20.715' E	4226.2	none	none	4182
PS129-BSH5	AI2600-22DE005	6904207	2022-03-13T20:18	PS129_21-1	59° 31.759' S	000° 00.447' W	4659.7	none	none	4617
PS129-BSH6	AI2600-21DE018	6904130	2022-03-13T22:18	PS129_22-1	59° 50.669' S	000° 00.001' E	5381.7	none	none	5355

Tab. 2.12: SOCCOM float deployments

SOCCOM float S/N	Datetime time	Station PS129_	deployment latitude	deployment longitude	EK80 depth reading	CDT cast PS129_	Sea ice	Corrected depth	Comment
19014	05.03.2022T12:56	PS129_1-1	37° 30.256´ S	016° 19.712´ E		none	none		Subtropical
19302	07.03.2022T11:05	PS129_3-1	43° 37.687´ S	012° 21.926´ E		none	none		Subtropical
19996	13.03.2022T05:57	PS129_18-8	59° 06.633´ S	000° 06.225´ E		18-7	none		Subpolar
19598	17.03.2022T19:10	PS129_27-9	66° 33.886´ S	000° 17.519´ W		27-2	none		Subpolar
19951	19.03.2022T10:51	PS129_30-3	65° 58.121´ S	012° 11.299´ W		30-1	none		Subpolar
19378	04.04.2022T22:00	PS129_65-7	69° 02.091´ S	017° 27.749´ W		65-1	none		Subpolar
19045	07.04.2022T12:02	PS129_71-4	68° 42.809´ S	027° 04.704´ W		71-2	brown pancakes 100%		Subpolar.
19445	12.04.2022T21:59	PS129_80-3	66° 36.996´ S	027° 12.743´ W		80-2	none		Subpolar
19441	14.04.2022T15:44	PS129_86-4	65° 41.710´ S	036° 41.039´ W		86-1	none		Subpolar

Tab. 2.13: Salinity measurements by salinometer. Numbers printed red indicate values that exhibited a discontinuity in the OPS reading, resulting in their exclusion from the calibration process.

									Salinity from CTD		Deviation	
Station Nr.	Date	OTE Bottle	Press [dbar]	Salinity OPS	Measured	Operator	Bottle Nr.	Remark	Sensor 1	Sensor 2	to Sensor 1	to Sensor 2
PS129_018_07	12-03-2022T23:39	3	4509	34.6447	18.03.2022	ST	132	OPS006	34.6468	34.6453	-0.0021	-0.0006
PS129_018_07	12-03-2022T23:39	3	4509	34.6450	18.03.2022	ST	16-6	OPS006	34.6468	34.6453	-0.0018	-0.0003
PS129_018_07	12-03-2022T23:39	3	4509	34.6455	08.04.2022	ST	171	OPS007	34.6468	34.6453	-0.0013	0.0002
PS129_018_07	12-03-2022T23:39	3	4509	34.6450	08.04.2022	ST	157	OPS007	34.6468	34.6453	-0.0018	-0.0003
PS129_018_07	12-03-2022T23:39	3	4509	34.6453	08.04.2022	ST	141	OPS007	34.6468	34.6453	-0.0015	0.0000
PS129_018_07	12-03-2022T23:39	3	4509	34.6456	08.04.2022	ST	169	OPS007	34.6468	34.6453	-0.0012	0.0003
PS129_018_07	12-03-2022T23:39	4	4354	34.6453	18.03.2022	ST	144	OPS006	34.6470	34.6457	-0.0017	-0.0004
PS129_018_07	12-03-2022T23:39	4	4354	34.6451	18.03.2022	ST	150	OPS006	34.6470	34.6457	-0.0019	-0.0006
PS129_023_01	14-03-2022T05:56	1	5466	34.6443	18.03.2022	ST	4	OPS006	34.6460	34.6439	-0.0017	0.0004
PS129_023_01	14-03-2022T05:56	1	5466	34.6442	18.03.2022	ST	8-46	OPS006	34.6460	34.6439	-0.0018	0.0003
PS129_023_01	14-03-2022T05:56	1	5466	34.6439	18.03.2022	ST	113	OPS006	34.6460	34.6439	-0.0021	0.0000
PS129_023_01	14-03-2022T05:56	1	5466	34.6444	18.03.2022	ST	122	OPS006	34.6460	34.6439	-0.0016	0.0005
PS129_023_01	14-03-2022T05:56	3	5099	34.6448	18.03.2022	ST	127	OPS006	34.6463	34.6446	-0.0015	0.0002
PS129_023_01	14-03-2022T05:56	3	5099	34.6444	18.03.2022	ST	142	OPS006	34.6463	34.6446	-0.0019	-0.0002
PS129_023_01	14-03-2022T05:56	3	5099	34.6453	16.04.2022	ST	181	OPS006	34.6463	34.6446	-0.0010	0.0007
PS129_023_01	14-03-2022T05:56	3	5099	34.6454	16.04.2022	ST	201	OPS006	34.6463	34.6446	-0.0009	0.0008
PS129_023_01	14-03-2022T05:56	3	5099	34.6460	16.04.2022	ST	153	OPS006	34.6463	34.6446	-0.0003	0.0014
PS129_023_01	14-03-2022T05:56	3	5099	34.6458	16.04.2022	ST	165	OPS006	34.6463	34.6446	-0.0005	0.0012
PS129_023_01	14-03-2022T05:56	4	4491	34.6456	18.03.2022	ST	136	OPS006	34.6486	34.6468	-0.0030	-0.0012
PS129_023_01	14-03-2022T05:56	4	4491	34.6458	18.03.2022	ST	166	OPS006	34.6486	34.6468	-0.0028	-0.0010
PS129_023_01	14-03-2022T05:56	5	4077	34.6493	18.03.2022	ST	125	OPS006	34.6517	34.6502	-0.0024	-0.0009
PS129_023_01	14-03-2022T05:56	5	4077	34.6499	18.03.2022	ST	148	OPS006	34.6517	34.6502	-0.0018	-0.0003
PS129_025_08	16-03-2022T01:15	1	5261	34.6445	18.03.2022	ST	156	OPS006	34.6474	34.6452	-0.0029	-0.0007
PS129_025_08	16-03-2022T01:15	1	5261		18.03.2022	ST	170	OPS006, invalid	34.6474	34.6452		
PS129_025_08	16-03-2022T01:15	1	5261	34.6459	03.04.2022	ST	134	OPS006	34.6474	34.6452	-0.0015	0.0007

									Salinity from CTD		Deviation	
Station Nr.	Date	OTE Bottle	Press [dbar]	Salinity OPS	Measured	Operator	Bottle Nr.	Remark	Sensor 1	Sensor 2	to Sensor 1	to Sensor 2
PS129_025_08	16-03-2022T01:15	1	5261	34.6457	03.04.2022	ST	117	OPS006	34.6474	34.6452	-0.0017	0.0005
PS129_025_08	16-03-2022T01:15	2	5009		18.03.2022	ST	48	OPS006, invalid	34.6498	34.6479		
PS129_025_08	16-03-2022T01:15	2	5009	34.6478	18.03.2022	ST	100	OPS006	34.6498	34.6479	-0.0020	-0.0001
PS129_025_08	16-03-2022T01:15	3	4695	34.6518	18.03.2022	ST	164	OPS006	34.6545	34.6527	-0.0027	-0.0009
PS129_025_08	16-03-2022T01:15	3	4695	34.6516	18.03.2022	ST	179	OPS006	34.6545	34.6527	-0.0029	-0.0011
PS129_025_08	16-03-2022T01:15	5	4081	34.6518	18.03.2022	ST	180	OPS006	34.6546	34.6531	-0.0028	-0.0013
PS129_025_08	16-03-2022T01:15	5	4081	34.6517	18.03.2022	ST	159	OPS006	34.6546	34.6531	-0.0029	-0.0014
PS129_025_08	16-03-2022T01:15	5	4081				20-4	pending	34.6546	34.6531		
PS129_025_08	16-03-2022T01:15	5	4081				115	pending	34.6546	34.6531		
PS129_025_08	16-03-2022T01:15	5	4081				154	pending	34.6546	34.6531		
PS129_025_08	16-03-2022T01:15	5	4081				161	pending	34.6546	34.6531		
PS129_027_02	16-03-2022T21:58	1	4473	34.6515	18.03.2022	ST	167	OPS006	34.6542	34.6522	-0.0027	-0.0007
PS129_027_02	16-03-2022T21:58	1	4473	34.6516	18.03.2022	ST	137	OPS006	34.6542	34.6522	-0.0026	-0.0006
PS129_027_02	16-03-2022T21:58	1	4473	34.6521	03.04.2022	ST	152	OPS006	34.6542	34.6522	-0.0021	-0.0001
PS129_027_02	16-03-2022T21:58	1	4473	34.6522	03.04.2022	ST	168	OPS006	34.6542	34.6522	-0.0020	0.0000
PS129_027_02	16-03-2022T21:58	2	4316	34.6524	18.03.2022	ST	81-6	OPS006	34.6542	34.6524	-0.0018	0.0000
PS129_027_02	16-03-2022T21:58	2	4316	34.6520	18.03.2022	ST	126	OPS006	34.6542	34.6524	-0.0022	-0.0004
PS129_027_02	16-03-2022T21:58	3	4101	34.6524	18.03.2022	ST	119	OPS006	34.6543	34.6529	-0.0019	-0.0005
PS129_027_02	16-03-2022T21:58	3	4101	34.6524	18.03.2022	ST	114	OPS006	34.6543	34.6529	-0.0019	-0.0005
PS129_027_02	16-03-2022T21:58	3	4101				8-15	pending	34.6543	34.6529		
PS129_027_02	16-03-2022T21:58	3	4101				155	pending	34.6543	34.6529		
PS129_027_02	16-03-2022T21:58	3	4101				346	pending	34.6543	34.6529		
PS129_027_02	16-03-2022T21:58	3	4101				111	pending	34.6543	34.6529		
PS129_027_02	16-03-2022T21:58	4	3874	34.6529	18.03.2022	ST	124	OPS006	34.6549	34.6533	-0.0020	-0.0004
PS129_027_02	16-03-2022T21:58	4	3874	34.6526	18.03.2022	ST	128	OPS006	34.6549	34.6533	-0.0023	-0.0007
PS129_030_01	19-03-2022T03:09	2	5006	34.6438	03.04.2022	ST	4-6	OPS006	34.6459	34.6441	-0.0021	-0.0003

									Salinity from CTD		Deviation	
Station Nr.	Date	OTE Bottle	Press [dbar]	Salinity OPS	Measured	Operator	Bottle Nr.	Remark	Sensor 1	Sensor 2	to Sensor 1	to Sensor 2
PS129_030_01	19-03-2022T03:09	2	5006	34.6438	03.04.2022	ST	8-46	OPS006	34.6459	34.6441	-0.0021	-0.0003
PS129_030_01	19-03-2022T03:09	3	4800				144	pending	34.6468	34.6453		
PS129_030_01	19-03-2022T03:09	3	4800				150	pending	34.6468	34.6453		
PS129_030_01	19-03-2022T03:09	3	4800				16-6	pending	34.6468	34.6453		
PS129_030_01	19-03-2022T03:09	3	4800				132	pending	34.6468	34.6453		
PS129_030_01	19-03-2022T03:09	3	4800	34.645	03.04.2022	ST	127	OPS006	34.6468	34.6453	-0.0018	-0.0003
PS129_030_01	19-03-2022T03:09	3	4800	34.6451	03.04.2022	ST	136	OPS006	34.6468	34.6453	-0.0017	-0.0002
PS129_030_01	19-03-2022T03:09	4	4223	34.6510	03.04.2022	ST	166	OPS006	34.6531	34.6517	-0.0021	-0.0007
PS129_030_01	19-03-2022T03:09	4	4223	34.6506	03.04.2022	ST	125	OPS006	34.6531	34.6517	-0.0025	-0.0011
PS129_030_01	19-03-2022T03:09	5	3771	34.6533	03.04.2022	ST	148	OPS006	34.6558	34.6547	-0.0025	-0.0014
PS129_030_01	19-03-2022T03:09	5	3771	34.6532	03.04.2022	ST	142	OPS006	34.6558	34.6547	-0.0026	-0.0015
PS129_040_02	21-03-2022T13:13	6	861	34.6284	03.04.2022	ST	175	OPS006	34.6279	34.6276	0.0005	0.0008
PS129_040_02	21-03-2022T13:13	6	861	34.6287	03.04.2022	ST	174	OPS006	34.6279	34.6276	0.0008	0.0011
PS129_040_02	21-03-2022T13:13	6	861				10-46	pending	34.6279	34.6276		
PS129_040_02	21-03-2022T13:13	6	861				123	pending	34.6279	34.6276		
PS129_040_02	21-03-2022T13:13	6	861				116	pending	34.6279	34.6276		
PS129_040_02	21-03-2022T13:13	6	861				5-8	pending	34.6279	34.6276		
PS129_040_02	21-03-2022T13:13	8	776	34.6065	03.04.2022	ST	170	maybe forgot to wipe the intake manifold, OPS006	34.6062	34.6058	0.0003	0.0007
PS129_040_02	21-03-2022T13:13	8	776	34.6070	03.04.2022	ST	176	OPS006	34.6062	34.6058	0.0008	0.0012
PS129_059_01	02-04-2022T12:38	6	1355	34.6760	03.04.2022	ST	156	OPS006	34.6749	34.6742	0.0011	0.0018
PS129_059_01	02-04-2022T12:38	6	1355	34.6733	03.04.2022	ST	164	jump in reading	34.6749	34.6742	-0.0016	-0.0009
PS129_059_01	02-04-2022T12:38	6	1355				120	pending	34.6749	34.6742		
PS129_059_01	02-04-2022T12:38	6	1355				137	pending	34.6749	34.6742		
PS129_059_01	02-04-2022T12:38	6	1355				4-8	pending	34.6749	34.6742		
PS129_059_01	02-04-2022T12:38	6	1355				119	pending	34.6749	34.6742		

									Salinity from CTD		Deviation	
Station Nr.	Date	OTE Bottle	Press [dbar]	Salinity OPS	Measured	Operator	Bottle Nr.	Remark	Sensor 1	Sensor 2	to Sensor 1	to Sensor 2
PS129_059_01	02-04-2022T12:38	7	1235	34.6760	03.04.2022	ST	100	OPS006	34.6778	34.6772	-0.0018	-0.0012
PS129_059_01	02-04-2022T12:38	7	1235	34.6761	03.04.2022	ST	179	OPS006	34.6778	34.6772	-0.0017	-0.0011
PS129_059_01	02-04-2022T12:38	8	1051	34.6747	03.04.2022	ST	128	OPS006	34.6760	34.6756	-0.0013	-0.0009
PS129_059_01	02-04-2022T12:38	8	1051	34.6747	03.04.2022	ST	126	OPS006	34.6760	34.6756	-0.0013	-0.0009
PS129_060_01	02-04-2022T19:33	6	1907				81-6	pending	34.6679	34.6672		
PS129_060_01	02-04-2022T19:33	6	1907				180	pending	34.6679	34.6672		
PS129_060_01	02-04-2022T19:33	6	1907				124	pending	34.6679	34.6672		
PS129_060_01	02-04-2022T19:33	6	1907				7-1	pending	34.6679	34.6672		
PS129_060_01	02-04-2022T19:33	6	1907	34.6682	08.04.2022	ST	159	OPS007	34.6679	34.6672	0.0003	0.0010
PS129_060_01	02-04-2022T19:33	6	1907	34.6682	08.04.2022	ST	114	OPS007	34.6679	34.6672	0.0003	0.0010
PS129_060_01	02-04-2022T19:33	7	1644	34.6717	08.04.2022	ST	167	OPS007	34.6712	34.6709	0.0005	0.0008
PS129_060_01	02-04-2022T19:33	7	1644	34.6721	08.04.2022	ST	500	OPS007	34.6712	34.6709	0.0009	0.0012
PS129_060_01	02-04-2022T19:33	8	1411	34.6738	08.04.2022	ST	400	Wax, OPS007	34.6731	34.6727	0.0007	0.0011
PS129_060_01	02-04-2022T19:33	8	1411	34.6738	08.04.2022	ST	401	Wax, OPS007	34.6731	34.6727	0.0007	0.0011
PS129_062_04	03-04-2022T07:07	2	3258	34.6578	08.04.2022	ST	405	Wax, OPS007	34.6584	34.6576	-0.0006	0.0002
PS129_062_04	03-04-2022T07:07	2	3258	34.6575	08.04.2022	ST	407	Wax, OPS007	34.6584	34.6576	-0.0009	-0.0001
PS129_062_04	03-04-2022T07:07	2	3258	34.6578	08.04.2022	ST	411	Wax, OPS007	34.6584	34.6576	-0.0006	0.0002
PS129_062_04	03-04-2022T07:07	2	3258		08.04.2022	ST	412	Not degassed, Wax, OPS007, invalid	34.6584	34.6576		
PS129_062_04	03-04-2022T07:07	2	3258		08.04.2022	ST	408	Not degassed. Wax, OPS007, invalid	34.6584	34.6576		
PS129_062_04	03-04-2022T07:07	2	3258		08.04.2022	ST	413	Not degassed. Wax, OPS007, invalid	34.6584	34.6576		
PS129_062_04	03-04-2022T07:07	3	3104	34.6578	08.04.2022	ST	406	Wax, OPS007	34.6585	34.6579	-0.0007	-0.0001
PS129_062_04	03-04-2022T07:07	3	3104	34.6585	08.04.2022	ST	410	Wax, OPS007	34.6585	34.6579	0.0000	0.0006
PS129_062_04	03-04-2022T07:07	4	2957	34.6585	08.04.2022	ST	409	Wax, OPS007	34.6593	34.6586	-0.0008	-0.0001
PS129_062_04	03-04-2022T07:07	4	2957	34.6586	08.04.2022	ST	404	Wax, OPS007	34.6593	34.6586	-0.0007	0.0000
PS129_064_02	03-04-2022T18:08	2	4593	34.6516	08.04.2022	ST	127	OPS007	34.6533	34.6521	-0.0017	-0.0005

									Salinity from CTD		Deviation	
Station Nr.	Date	OTE Bottle	Press [dbar]	Salinity OPS	Measured	Operator	Bottle Nr.	Remark	Sensor 1	Sensor 2	to Sensor 1	to Sensor 2
PS129_064_02	03-04-2022T18:08	2	4593	34.6517	08.04.2022	ST	136	OPS007	34.6533	34.6521	-0.0016	-0.0004
PS129_064_02	03-04-2022T18:08	2	4593				4-6	pending	34.6533	34.6521		
PS129_064_02	03-04-2022T18:08	2	4593				8-46	pending	34.6533	34.6521		
PS129_064_02	03-04-2022T18:08	2	4593				168	pending	34.6533	34.6521		
PS129_064_02	03-04-2022T18:08	2	4593				152	pending	34.6533	34.6521		
PS129_064_02	03-04-2022T18:08	3	4385	34.6532	08.04.2022	ST	403	Wachsflasche, OPS007	34.6545	34.6534	-0.0013	-0.0002
PS129_064_02	03-04-2022T18:08	3	4385	34.6533	08.04.2022	ST	402	Wax, OPS007	34.6545	34.6534	-0.0012	-0.0001
PS129_064_02	03-04-2022T18:08	4	4082	34.6541	08.04.2022	ST	414	Wax, OPS007	34.6554	34.6543	-0.0013	-0.0002
PS129_064_02	03-04-2022T18:08	4	4082	34.6539	08.04.2022	ST	415	Wax, OPS007	34.6554	34.6543	-0.0015	-0.0004
PS129_065_01	04-04-2022T04:45	2	4696				421	Wax, OPS007	34.6494	34.6480		
PS129_065_01	04-04-2022T04:45	2	4696				422	Wax, OPS007	34.6494	34.6480		
PS129_065_01	04-04-2022T04:45	2	4696				430	Wax, OPS007	34.6494	34.6480		
PS129_065_01	04-04-2022T04:45	2	4696				428	Wax, OPS007	34.6494	34.6480		
PS129_065_01	04-04-2022T04:45	2	4696	34.6477	08.04.2022	ST	439	no Wax, OPS007	34.6494	34.6480	-0.0017	-0.0003
PS129_065_01	04-04-2022T04:45	2	4696	34.6476	08.04.2022	ST	126	Wax, OPS007	34.6494	34.6480	-0.0018	-0.0004
PS129_065_01	04-04-2022T04:45	3	4314	34.6533	08.04.2022	ST	425	Wax, OPS007	34.6547	34.6537	-0.0014	-0.0004
PS129_065_01	04-04-2022T04:45	3	4314	34.6532	08.04.2022	ST	423	Wax, OPS007	34.6547	34.6537	-0.0015	-0.0005
PS129_065_01	04-04-2022T04:45	4	4184	34.6532	08.04.2022	ST	134	OPS007	34.6551	34.6541	-0.0019	-0.0009
PS129_065_01	04-04-2022T04:45	4	4184	34.6531	08.04.2022	ST	117	OPS007	34.6551	34.6541	-0.0020	-0.0010
PS129_068_01	05-04-2022T04:32	2	4912				148	pending	34.6473	34.6458		
PS129_068_01	05-04-2022T04:32	2	4912				125	pending	34.6473	34.6458		
PS129_068_01	05-04-2022T04:32	2	4912				164	pending	34.6473	34.6458		
PS129_068_01	05-04-2022T04:32	2	4912				176	pending	34.6473	34.6458		
PS129_068_01	05-04-2022T04:32	2	4912	34.6462	14.04.2022	ST	179	OPS006	34.6473	34.6458	-0.0011	0.0004
PS129_068_01	05-04-2022T04:32	2	4912	34.6462	14.04.2022	ST	170	OPS006	34.6473	34.6458	-0.0011	0.0004
PS129_068_01	05-04-2022T04:32	3	4341	34.6525	16.04.2022	ST	426	OPS006	34.6534	34.6524	-0.0009	0.0001

									Salinity from CTD		Deviation	
Station Nr.	Date	OTE Bottle	Press [dbar]	Salinity OPS	Measured	Operator	Bottle Nr.	Remark	Sensor 1	Sensor 2	to Sensor 1	to Sensor 2
PS129_068_01	05-04-2022T04:32	3	4341	34.6545	16.04.2022	ST	424	OPS006	34.6534	34.6524	0.0011	0.0021
PS129_068_01	05-04-2022T04:32	4	3976	34.6542	16.04.2022	ST	420	OPS006	34.6551	34.6540	-0.0009	0.0002
PS129_068_01	05-04-2022T04:32	4	3976	34.6538	16.04.2022	ST	417	OPS006	34.6551	34.6540	-0.0013	-0.0002
PS129_070_01	05-04-2022T19:23	2	4800				100	pending	34.6472	34.6457		
PS129_070_01	05-04-2022T19:23	2	4800				128	pending	34.6472	34.6457		
PS129_070_01	05-04-2022T19:23	2	4800				174	pending	34.6472	34.6457		
PS129_070_01	05-04-2022T19:23	2	4800				156	pending	34.6472	34.6457		
PS129_070_01	05-04-2022T19:23	2	4800	34.6457	16.04.2022	ST	175	OPS006	34.6472	34.6457	-0.0015	0
PS129_070_01	05-04-2022T19:23	2	4800	34.6459	16.04.2022	ST	142	OPS006	34.6472	34.6457	-0.0013	0.0002
PS129_070_01	05-04-2022T19:23	3	4615	34.6469	16.04.2022	ST	433	OPS006	34.6480	34.6467	-0.0011	0.0002
PS129_070_01	05-04-2022T19:23	3	4615	34.6473	16.04.2022	ST	416	OPS006	34.6480	34.6467	-0.0007	0.0006
PS129_070_01	05-04-2022T19:23	5	3976	34.6620	16.04.2022	ST	418	OPS006	34.6537	34.6529	0.0083	0.0091
PS129_070_01	05-04-2022T19:23	5	3976	34.6618	16.04.2022	ST	427	OPS006	34.6537	34.6529	0.0081	0.0089
PS129_080_02	12-04-2022T17:48	2	4620				134	pending	34.6481	34.6468		
PS129_080_02	12-04-2022T17:48	2	4620				126	pending	34.6481	34.6468		
PS129_080_02	12-04-2022T17:48	2	4620				122	pending	34.6481	34.6468		
PS129_080_02	12-04-2022T17:48	2	4620				167	pending	34.6481	34.6468		
PS129_080_02	12-04-2022T17:48	2	4620	34.6474	14.04.2022	ST	127	OPS006	34.6481	34.6468	-0.0007	0.0006
PS129_080_02	12-04-2022T17:48	2	4620	34.6476	14.04.2022	ST	117	OPS006	34.6481	34.6468	-0.0005	0.0008
PS129_080_02	12-04-2022T17:48	3	4449	34.6491	14.04.2022	ST	404	OPS006	34.6499	34.6487	-0.0008	0.0004
PS129_080_02	12-04-2022T17:48	3	4449	34.6857	14.04.2022	ST	431	OPS006	34.6499	34.6487	0.0358	0.037
PS129_080_02	12-04-2022T17:48	4	3966	34.6534	14.04.2022	ST	429	OPS006	34.6544	34.6533	-0.001	1E-04
PS129_080_02	12-04-2022T17:48	4	3966	34.6535	14.04.2022	ST	410	OPS006	34.6544	34.6533	-0.0009	0.0002
PS129_083_02	13-04-2022T13:15	2	4697				159	pending	34.6461	34.6449		
PS129_083_02	13-04-2022T13:15	2	4697				166	pending	34.6461	34.6449		
PS129_083_02	13-04-2022T13:15	2	4697				171	pending	34.6461	34.6449		

									Salinity from CTD		Deviation	
Station Nr.	Date	OTE Bottle	Press [dbar]	Salinity OPS	Measured	Operator	Bottle Nr.	Remark	Sensor 1	Sensor 2	to Sensor 1	to Sensor 2
PS129_083_02	13-04-2022T13:15	2	4697				439	pending	34.6461	34.6449		
PS129_083_02	13-04-2022T13:15	2	4697	34.6454	14.04.2022	ST	157	OPS006	34.6461	34.6449	-0.0007	0.0005
PS129_083_02	13-04-2022T13:15	2	4697	34.6454	14.04.2022	ST	169	OPS006	34.6461	34.6449	-0.0007	0.0005
PS129_083_02	13-04-2022T13:15	3	4490	34.6465	14.04.2022	ST	406	OPS006	34.6473	34.6462	-0.0008	0.0003
PS129_083_02	13-04-2022T13:15	3	4490	34.6466	14.04.2022	ST	407	OPS006	34.6473	34.6462	-0.0007	0.0004
PS129_083_02	13-04-2022T13:15	4	4287	34.6485	14.04.2022	ST	403	OPS006	34.6493	34.6483	-0.0008	0.0002
PS129_083_02	13-04-2022T13:15	4	4287	34.6486	14.04.2022	ST	405	OPS006	34.6493	34.6483	-0.0007	0.0003
PS129_086_01	14-04-2022T05:08	2	4618	34.6454	18.04.2022	ST	136	OPS006	34.6461	34.6448	-0.0007	0.0006
PS129_086_01	14-04-2022T05:08	2	4618	34.6453	20.04.2022	ST	141	OPS006	34.6461	34.6448	-0.0008	0.0005
PS129_086_01	14-04-2022T05:08	2	4618	34.6453	20.04.2022	ST	113	OPS006	34.6461	34.6448	-0.0008	0.0005
PS129_086_01	14-04-2022T05:08	2	4618	34.6454	20.04.2022	ST	114	OPS006	34.6461	34.6448	-0.0007	0.0006
PS129_086_01	14-04-2022T05:08	2	4618	34.6454	20.04.2022	ST	411	OPS006	34.6461	34.6448	-0.0007	0.0006
PS129_086_01	14-04-2022T05:08	2	4618	34.6545	18.04.2022	ST	438	OPS006	34.6461	34.6448	0.0084	0.0097
PS129_086_01	14-04-2022T05:08	3	4492	34.6455	18.04.2022	ST	409	OPS006	34.6461	34.6450	-0.0006	0.0005
PS129_086_01	14-04-2022T05:08	3	4492	34.6757	18.04.2022	ST	432	OPS006	34.6461	34.6450	0.0296	0.0307
PS129_086_01	14-04-2022T05:08	4	4180	34.6488	18.04.2022	ST	401	OPS006	34.6500	34.6488	-0.0012	0
PS129_086_01	14-04-2022T05:08	4	4180	34.6834	18.04.2022	ST	436	OPS006	34.6500	34.6488	0.0334	0.0346
PS129_087_01	14-04-2022T21:25	2	4697	34.6441	19.04.2022	ST	169	OPS006	34.6455	34.6443	-0.0014	-0.0002
PS129_087_01	14-04-2022T21:25	2	4697	34.6441	19.04.2022	ST	157	OPS006	34.6455	34.6443	-0.0014	-0.0002
PS129_087_01	14-04-2022T21:25	2	4697	34.6438	19.04.2022	ST	403	OPS006	34.6455	34.6443	-0.0017	-0.0005
PS129_087_01	14-04-2022T21:25	2	4697	34.7156	19.04.2022	ST	435	OPS006	34.6455	34.6443	0.0701	0.0713
PS129_087_01	14-04-2022T21:25	2	4697	34.6444	18.04.2022	ST	410	OPS006	34.6455	34.6443	-0.0011	0.0001
PS129_087_01	14-04-2022T21:25	2	4697	34.6601	18.04.2022	ST	434	OPS006	34.6455	34.6443	0.0146	0.0158
PS129_087_01	14-04-2022T21:25	3	4490	34.645	18.04.2022	ST	170	maybe forgot to wipe the intake manifold, OPS006	34.6472	34.6461	-0.0022	-0.0011
PS129_087_01	14-04-2022T21:25	3	4490	34.646	18.04.2022	ST	179	OPS006	34.6472	34.6461	-0.0012	-0.0001

									Salinity from CTD		Deviation	
Station Nr.	Date	OTE Bottle	Press [dbar]	Salinity OPS	Measured	Operator	Bottle Nr.	Remark	Sensor 1	Sensor 2	to Sensor 1	to Sensor 2
PS129_087_01	14-04-2022T21:25	4	4227	34.6476	18.04.2022	ST	407	OPS006	34.6505	34.6496	-0.0029	-0.0020
PS129_087_01	14-04-2022T21:25	4	4227	34.649	18.04.2022	ST	429	OPS006	34.6505	34.6496	-0.0015	-0.0006
PS129_088_01	15-04-2022T08:28	5	4698				408	pending	34.6433	34.6421		
PS129_088_01	15-04-2022T08:28	5	4698				400	pending	34.6433	34.6421		
PS129_088_01	15-04-2022T08:28	5	4698				415	pending	34.6433	34.6421		
PS129_088_01	15-04-2022T08:28	5	4698				423	pending	34.6433	34.6421		
PS129_088_01	15-04-2022T08:28	5	4698	34.6424	18.04.2022	ST	413	OPS006	34.6433	34.6421	-0.0009	0.0003
PS129_088_01	15-04-2022T08:28	5	4698	34.6425	18.04.2022	ST	425	OPS006	34.6433	34.6421	-0.0008	0.0004
PS129_088_01	15-04-2022T08:28	6	4492	34.6444	18.04.2022	ST	406	OPS006	34.6453	34.6442	-0.0009	0.0002
PS129_088_01	15-04-2022T08:28	6	4492	34.7224	18.04.2022	ST	437	OPS006	34.6453	34.6442	0.0771	0.0782
PS129_088_01	15-04-2022T08:28	7	4181	34.6476	18.04.2022	ST	414	OPS006	34.6487	34.6477	-0.0011	-0.0001
PS129_088_01	15-04-2022T08:28	7	4181	34.6475	18.04.2022	ST	500	OPS006	34.6487	34.6477	-0.0012	-0.0002
PS129_096_01	18-04-2022T08:44	2	4593	34.6432	19.04.2022	ST	127	OPS006	34.6447	34.6435	-0.0015	-0.0003
PS129_096_01	18-04-2022T08:44	2	4593	34.6433	19.04.2022	ST	402	OPS006	34.6447	34.6435	-0.0014	-0.0002
PS129_096_01	18-04-2022T08:44	2	4593				405	pending	34.6447	34.6435		
PS129_096_01	18-04-2022T08:44	2	4593				412	pending	34.6447	34.6435		
PS129_096_01	18-04-2022T08:44	2	4593				419	pending	34.6447	34.6435		
PS129_096_01	18-04-2022T08:44	2	4593				181	pending	34.6447	34.6435		
PS129_096_01	18-04-2022T08:44	3	4434	34.6458	19.04.2022	ST	20-1	OPS006	34.6470	34.6458	-0.0012	0.0000
PS129_096_01	18-04-2022T08:44	3	4434	34.6457	19.04.2022	ST	153	OPS006	34.6470	34.6458	-0.0013	-0.0001
PS129_096_01	18-04-2022T08:44	4	4176	34.648	19.04.2022	ST	142	OPS006	34.6496	34.6485	-0.0016	-0.0005
PS129_096_01	18-04-2022T08:44	4	4176	34.6479	19.04.2022	ST	165	OPS006	34.6496	34.6485	-0.0017	-0.0006
PS129_097_01	18-04-2022T21:47	5	4387				170	pending	34.6473	34.6460		
PS129_097_01	18-04-2022T21:47	5	4387	34.6461	20.04.2022	ST	410	OPS006	34.6473	34.6460	-0.0012	0.0001
PS129_097_01	18-04-2022T21:47	5	4387				437	pending	34.6473	34.6460		
PS129_097_01	18-04-2022T21:47	5	4387	34.646	20.04.2022	ST	438	OPS006	34.6473	34.6460	-0.0013	0.0000

									Salinity from CTD		Deviation	
Station Nr.	Date	OTE Bottle	Press [dbar]	Salinity OPS	Measured	Operator	Bottle Nr.	Remark	Sensor 1	Sensor 2	to Sensor 1	to Sensor 2
PS129_097_01	18-04-2022T21:47	5	4387				429	pending	34.6473	34.6460		
PS129_097_01	18-04-2022T21:47	5	4387				175	pending	34.6473	34.6460		
PS129_097_01	18-04-2022T21:47	6	4177	34.6504	20.04.2022	ST	117	OPS006	34.6514	34.6500	-0.001	0.0004
PS129_097_01	18-04-2022T21:47	6	4177	34.6501	20.04.2022	ST	136	OPS006	34.6514	34.6500	-0.0013	0.0001
PS129_097_01	18-04-2022T21:47	7	3877	34.653	20.04.2022	ST	426	OPS006	34.6543	34.6532	-0.0013	-0.0002
PS129_097_01	18-04-2022T21:47	7	3877	34.6529	20.04.2022	ST	431	OPS006	34.6543	34.6532	-0.0014	-0.0003
PS129_099_01	19-04-2022T08:25	4	4129	34.6523	20.04.2022	ST	179	OPS006	34.6536	34.6526	-0.0013	-0.0003
PS129_099_01	19-04-2022T08:25	4	4129				432	pending	34.6536	34.6526		
PS129_099_01	19-04-2022T08:25	4	4129				404	pending	34.6536	34.6526		
PS129_099_01	19-04-2022T08:25	4	4129				413	pending	34.6536	34.6526		
PS129_099_01	19-04-2022T08:25	4	4129				436	pending	34.6536	34.6526		
PS129_099_01	19-04-2022T08:25	4	4129	34.6523	20.04.2022	ST	500	OPS006	34.6536	34.6526	-0.0013	-0.0003
PS129_099_01	19-04-2022T08:25	5	3769	34.6543	20.04.2022	ST	434	OPS006	34.6555	34.6545	-0.0012	-0.0002
PS129_099_01	19-04-2022T08:25	5	3769	34.6543	20.04.2022	ST	416	OPS006	34.6555	34.6545	-0.0012	-0.0002
PS129_099_01	19-04-2022T08:25	6	3405	34.6558	20.04.2022	ST	417	OPS006	34.6568	34.6558	-0.001	0.0000
PS129_099_01	19-04-2022T08:25	6	3405	34.6563	20.04.2022	ST	427	OPS006	34.6568	34.6558	-0.0005	0.0005
PS129_100_03	19-04-2022T21:32	4	3975	34.6535	20.04.22, 2	ST	20-1	OPS006	34.6545	34.6533	-0.001	0.0002
PS129_100_03	19-04-2022T21:32	4	3975				153	pending	34.6545	34.6533		
PS129_100_03	19-04-2022T21:32	4	3975				127	pending	34.6545	34.6533		
PS129_100_03	19-04-2022T21:32	4	3975				407	pending	34.6545	34.6533		
PS129_100_03	19-04-2022T21:32	4	3975				406	pending	34.6545	34.6533		
PS129_100_03	19-04-2022T21:32	4	3975	34.6533	20.04.22, 2	ST	420	OPS006	34.6545	34.6533	-0.0012	0.0000
PS129_100_03	19-04-2022T21:32	5	3693	34.6542	20.04.22, 2	ST	418	OPS006	34.6554	34.6544	-0.0012	-0.0002
PS129_100_03	19-04-2022T21:32	5	3693	34.6543	20.04.22, 2	ST	409	OPS006	34.6554	34.6544	-0.0011	-0.0001
PS129_100_03	19-04-2022T21:32	6	3359	34.6559	20.04.22, 2	ST	401	OPS006	34.6568	34.6558	-0.0009	0.0001
PS129_100_03	19-04-2022T21:32	6	3359	34.6559	20.04.22, 2	ST	433	OPS006	34.6568	34.6558	-0.0009	0.0001

									Salinity from CTD		Deviation	
Station Nr.	Date	OTE Bottle	Press [dbar]	Salinity OPS	Measured	Operator	Bottle Nr.	Remark	Sensor 1	Sensor 2	to Sensor 1	to Sensor 2
PS129_102_01	20-04-2022T05:05	5	3982	34.6494	22.04.2022	ST	402	OPS006	34.6503	34.6494	-0.0009	0.0000
PS129_102_01	20-04-2022T05:05	5	3982	34.6492	22.04.2022	ST	165	OPS006	34.6503	34.6494	-0.0011	-0.0002
PS129_102_01	20-04-2022T05:05	6	3873	34.6535	22.04.2022	ST	435	OPS006	34.6545	34.6534	-0.001	0.0001
PS129_102_01	20-04-2022T05:05	6	3873	34.6534	22.04.2022	ST	157	OPS006	34.6545	34.6534	-0.0011	0.0000
PS129_102_01	20-04-2022T05:05	7	3617	34.6542	22.04.2022	ST	169	OPS006	34.6554	34.6545	-0.0012	-0.0003
PS129_102_01	20-04-2022T05:05	7	3617	34.6542	22.04.2022	ST	403	OPS006	34.6554	34.6545	-0.0012	-0.0003
PS129_103_01	20-04-2022T11:17	5	3667	34.6541	22.04.2022	ST	424	OPS006	34.6551	34.6542	-0.001	-0.0001
PS129_103_01	20-04-2022T11:17	5	3667	34.654	22.04.2022	ST	410	OPS006	34.6551	34.6542	-0.0011	-0.0002
PS129_103_01	20-04-2022T11:17	7	3051	34.6569	22.04.2022	ST	414	OPS006	34.6578	34.6569	-0.0009	0.0000
PS129_103_01	20-04-2022T11:17	7	3051	34.6569	22.04.2022	ST	431	OPS006	34.6578	34.6569	-0.0009	0.0000
PS129_104_01	20-04-2022T17:29	5	3483	34.6529	22.04.2022	ST	142	OPS006	34.6540	34.6532	-0.0011	-0.0003
PS129_104_01	20-04-2022T17:29	5	3483	34.6531	22.04.2022	ST	425	OPS006	34.6540	34.6532	-0.0009	-0.0001
PS129_104_01	20-04-2022T17:29	6	3360	34.654	26.04.2022	ST	500	OPS007	34.6554	34.6546	-0.0014	-0.0006
PS129_104_01	20-04-2022T17:29	6	3360	34.6536	26.04.2022	ST	179	OPS007	34.6554	34.6546	-0.0018	-0.0010
PS129_105_01	21-04-2022T01:09	5	3005	34.6564	22.04.2022	ST	401	OPS006	34.6570	34.6565	-0.0006	-0.0001
PS129_105_01	21-04-2022T01:09	5	3005	34.6563	22.04.2022	ST	409	OPS006	34.6570	34.6565	-0.0007	-0.0002
PS129_105_01	21-04-2022T01:09	6	2816	34.6575	22.04.2022	ST	433	OPS006	34.6580	34.6575	-0.0005	0.0000
PS129_105_01	21-04-2022T01:09	6	2816	34.6575	22.04.2022	ST	434	OPS006	34.6580	34.6575	-0.0005	0.0000
PS129_106_01	21-04-2022T06:40	5	2521	34.6591	22.04.2022	ST	417	OPS006	34.6589	34.6584	0.0002	0.0007
PS129_106_01	21-04-2022T06:40	5	2521	34.6586	22.04.2022	ST	411	OPS006	34.6589	34.6584	-0.0003	0.0002
PS129_106_01	21-04-2022T06:40	5	2521	34.6587	22.04.2022	ST	427	OPS006	34.6589	34.6584	-0.0002	0.0003
PS129_106_01	21-04-2022T06:40	6	3041	34.6292	22.04.2022	ST	418	OPS006	34.6296	34.6291	-0.0004	0.0001
PS129_106_01	21-04-2022T06:40	6	3041	34.6292	22.04.2022	ST	136	OPS006	34.6296	34.6291	-0.0004	0.0001
PS129_106_01	21-04-2022T06:40	6	3041	34.629	22.04.2022	ST	420	OPS006	34.6296	34.6291	-0.0006	-0.0001
PS129_107_01	21-04-2022T15:15	5	2295	34.6571	26.04.2022	ST	417	OPS007	34.6574	34.6571	-0.0003	0.0000
PS129_107_01	21-04-2022T15:15	5	2295	34.6571	26.04.2022	ST	416	OPS007	34.6574	34.6571	-0.0003	0.0000

									Salinity from CTD		Deviation	
Station Nr.	Date	OTE Bottle	Press [dbar]	Salinity OPS	Measured	Operator	Bottle Nr.	Remark	Sensor 1	Sensor 2	to Sensor 1	to Sensor 2
PS129_107_01	21-04-2022T15:15	6	1974	34.6611	26.04.2022	ST	438	OPS007	34.6614	34.6612	-0.0003	-0.0001
PS129_107_01	21-04-2022T15:15	6	1974	34.6609	26.04.2022	ST	20-1	OPS007	34.6614	34.6612	-0.0005	-0.0003
PS129_109_03	22-04-2022T04:19	5	1814	34.6638	26.04.2022	ST	113	OPS007	34.6640	34.6637	-0.0002	0.0001
PS129_109_03	22-04-2022T04:19	5	1814	34.6639	26.04.2022	ST	114	OPS007	34.6640	34.6637	-0.0001	0.0002
PS129_109_03	22-04-2022T04:19	6	1431	34.673	26.04.2022	ST	426	OPS007	34.6727	34.6726	0.0003	0.0004
PS129_109_03	22-04-2022T04:19	6	1431	34.6728	26.04.2022	ST	141	OPS007	34.6727	34.6726	0.0001	0.0002
PS129_112_01	22-04-2022T16:12	5	1419	34.6616	26.04.2022	ST	6	OPS007	34.6606	34.6615	0.001	0.0001
PS129_112_01	22-04-2022T16:12	5	1419	34.6621	26.04.2022	ST	7	OPS007	34.6606	34.6615	0.0015	0.0006
PS129_112_01	22-04-2022T16:12	6	926	34.6841	26.04.2022	ST	8	OPS007	34.6832	34.6834	0.0009	0.0007
PS129_112_01	22-04-2022T16:12	6	926	34.6843	26.04.2022	ST	9	OPS007	34.6832	34.6834	0.0011	0.0009
PS129_114_02	22-04-2022T22:23	5	1622	34.619	26.04.2022	ST	157	OPS007, repeat	34.6175	34.6183	0.0015	0.0007
PS129_114_02	22-04-2022T22:23	5	1622	34.619	26.04.2022	ST	402	OPS007	34.6175	34.6183	0.0015	0.0007
PS129_114_02	22-04-2022T22:23	6	1603	34.6202	26.04.2022	ST	435	OPS007	34.6194	34.6186	0.0008	0.0016
PS129_114_02	22-04-2022T22:23	6	1603	34.6201	26.04.2022	ST	165	OPS007	34.6194	34.6186	0.0007	0.0015
PS129_116_01	23-04-2022T02:56	5	926	34.6692	26.04.2022	ST	136	OPS007	34.6682	34.6684	0.001	0.0008
PS129_116_01	23-04-2022T02:56	5	926	34.6692	26.04.2022	ST	418	OPS007	34.6682	34.6684	0.001	0.0008
PS129_116_01	23-04-2022T02:56	6	521	34.67	26.04.2022	ST	420	OPS007	34.6693	34.6699	0.0007	0.0001
PS129_116_01	23-04-2022T02:56	6	521	34.67	26.04.2022	ST	424	OPS007	34.6693	34.6699	0.0007	0.0001
PS129_117_01	23-04-2022T06:05	5	660	34.6333	26.04.2022	ST	410	OPS007	34.6322	34.6324	0.0011	0.0009
PS129_117_01	23-04-2022T06:05	5	660	34.6332	26.04.2022	ST	169	OPS007	34.6322	34.6324	0.001	0.0008
PS129_117_01	23-04-2022T06:05	6	505	34.6616	26.04.2022	ST	401	OPS007	34.6600	34.6603	0.0016	0.0013
PS129_117_01	23-04-2022T06:05	6	505	34.6615	26.04.2022	ST	403	OPS007	34.6600	34.6603	0.0015	0.0012
PS129_119_01	23-04-2022T08:40	5	663	34.6222	26.04.2022	ST	431	OPS007	34.6206	34.6203	0.0016	0.0019
PS129_119_01	23-04-2022T08:40	5	663	34.6222	26.04.2022	ST	409	OPS007	34.6206	34.6203	0.0016	0.0019
PS129_119_01	23-04-2022T08:40	6	642	34.6218	26.04.2022	ST	414	OPS007	34.6204	34.6203	0.0014	0.0015
PS129_119_01	23-04-2022T08:40	6	642	34.6215	26.04.2022	ST	427	OPS007	34.6204	34.6203	0.0011	0.0012

									Salinity from CTD		Deviation	
Station Nr.	Date	OTE Bottle	Press [dbar]	Salinity OPS	Measured	Operator	Bottle Nr.	Remark	Sensor 1	Sensor 2	to Sensor 1	to Sensor 2
PS129_120_01	23-04-2022T12:15	5	356	34.5981	26.04.2022	ST	433	OPS007	34.5958	34.5968	0.0023	0.0013
PS129_120_01	23-04-2022T12:15	5	356	34.5978	26.04.2022	ST	142	OPS007	34.5958	34.5968	0.002	0.0010
PS129_120_01	23-04-2022T12:15	6	319	34.5829	26.04.2022	ST	434	OPS007	34.5811	34.5818	0.0018	0.0011
PS129_120_01	23-04-2022T12:15	6	319	34.5826	26.04.2022	ST	425	OPS007	34.5811	34.5818	0.0015	0.0008
PS129_121_01	23-04-2022T17:19	5	303	34.5342	26.04.2022	ST	117	OPS007	34.5321	34.5322	0.0021	0.0020
PS129_121_01	23-04-2022T17:19	5	303	34.5342	26.04.2022	ST	411	OPS007	34.5321	34.5322	0.0021	0.0020

Tab. 2.20 : List of common problems of L-ADCP casts by station number

Station ID	LADCP cast	File Names	Large up-down compass difference (>15°)	Found no SADCP data in time window	Found LARGE timing difference between ADCPs	Found x ADCP w deviating more than 2.5 m/s from w-CTD.	Increased error because of shear-inverse difference	shifted CTD time series by x seconds	Comments
014_01	2	002DN000.000	-	-	-	-		-	test cast
018_07	4	004DN000.000 004UP000.000	-	-	-	-	X	-	-
023_01	5	005DN000.000 005UP000.000	-	-	-	-	X	-	
025_08	6	006DN000.000 006UP000.000	-	-	-	8	X	-	
027_02	7	007DN000.000 007UP000.000	-	-	-	-	X	-	
030_01	8	008DN000.000 008UP000.000	-	-	-	-	X	-	
040_02	9	009DN000.000 009DN001.000 009UP000.000 009UP001.000	18.4714	-	-	-	X	-	
041_02	10	010DN000.000 010UP000.000	-	X	-	-	X	-	
042_01	11	011DN000.000 011UP000.000	-	-	-	-	X	-	
047_01	13	013DN000.000 013UP000.000	-	-	-	-	X	-	
049_01	14	014DN000.000 014UP000.000	-	-	-	-	X	-	
053_03	15	015DN000.000 015UP000.000	-	-	-	-	X	-	
054_03	16	016DN000.000 016UP000.000	-	-	-	-	X	-	
058_02	18	018DN000.000 018UP000.000	-	-	-	-	X	-	
059_01	19	019DN000.000 019UP000.000	-	-	-	-	X	-	
060_01	20	020DN000.000 020UP000.000	-	-	-	1	X	-	

Station ID	LADCP cast	File Names	Large up-down compass difference (>15°)	Found no SADCP data in time window	Found LARGE timing difference between ADCPs	Found x ADCP w deviating more than 2.5 m/s from w-CTD.	Increased error because of shear-inverse difference	shifted CTD time series by x seconds	Comments
062_04	21	021DN000.000 021DN001.000 021DN002.000 021DN003.000 021UP000.000 021UP001.000 021UP002.000	-	-	-	-	X	-	data gap during upcast between 2,100m and 1,800m
064_02	22	022DN000.000 022DN001.000 022UP000.000 022UP001.000 022UP002.000	-	-	-	1	X	-	data gap during upcast between 2,400m and 2,300m
065_01	23	023DN000.000 023UP000.000	-	-	-	-	X	-	battery change
068_01	24	024DN000.000 024UP000.000 024UP001.000	-	-	-	1	X	-	
070_01	25	025DN000.000 025DN001.000 025UP000.000	-	-	-	-	X	-	only down looker contained data
071_02	26	026DN000.000 026UP000.000	-	-	-	-	X	-	
072_01	27	027DN000.000 027UP000.000	-	-	-	-	X	-	
072_03	29	029DN000.000 029UP000.000	-	-	-	-	X	-	
074_04	30	030DN000.000 030UP000.000	-	-	-	-	X	-	
080_02	31	031DN000.000 031UP000.000	-	-	-	-	X	-	ADCP battery was changed
082_01	32	032DN000.000 032UP000.000	-	-	-	1	X	-	a new CTD file, was created for the up cast

Station ID	LADCP cast	File Names	Large up-down compass difference (>15°)	Found no SADCP data in time window	Found LARGE timing difference between ADCPs	Found x ADCP w deviating more than 2.5 m/s from w-CTD.	Increased error because of shear-inverse difference	shifted CTD time series by x seconds	Comments
083_02	33	033DN000.000 033DN001.000 033UP000.000 033UP001.000	-	-	-	-	X	-	data gap during upcast between 1,400m and 1,000m
086_01	34	034DN000.000 034UP000.000	-	-	-	-	X	-	
087_01	35	035DN000.000 035UP000.000	-	-	-	37	X	-	large tilt values
088_01	36	036DN000.000 036DN001.000 036DN002.000 036UP000.000 036UP001.000 036UP002.000	16.7237	-	-	1	X	-	L-ADCP measured only below 2,500m on the downcast
096_01	40	040DN000.000 040UP000.000	-	-	-	-	X	-	error message at the L-ADCP start: date out of range
097_01	42	042DN000.000 042UP000.000	-	-	-	-	X	-	
099_01	43	043DN000.000 043UP000.000 043UP001.000	-	-	-	-	X	-	
100_03	44	044DN000.000 044DN001.000 044UP000.000 044UP001.000	-	-	-	-	X	14	data gap during the upcast between 1,800m and 300m
102_01	46	046DN000.000 046UP000.000	-	-	-	-	X	18	
103_01	47	047DN000.000 047UP000.000	-	-	-	-	X	-	
104_01	49	049DN000.000 049UP000.000	-	-	-	-	X	-	
105_01	50	050DN000.000 050UP000.000	-	-	-	-	X	-	

Station ID	LADCP cast	File Names	Large up-down compass difference (>15°)	Found no SADCP data in time window	Found LARGE timing difference between ADCPs	Found x ADCP w deviating more than 2.5 m/s from w-CTD.	Increased error because of shear-inverse difference	shifted CTD time series by x seconds	Comments
106_01	51	051DN000.000 051UP000.000	-	-	-	-	X	-	
107_01	52	052DN000.000 052UP000.000	-	-	-	-	X	-	
109_03	53	053DN000.000 053UP000.000	-	-	-	-	X	-	
110_01	55	055DN000.000 055DN001.000 055DN002.000 055UP000.000 055UP001.000 055UP002.000	-	-	-	-	X	31	2 data gaps during the upcast, between 1,600 and 1,500, and between 950 and 900m
111_01	56	056DN000.000 056UP000.000	-	-	-	-	X	-	
112_01	58	058DN000.000 058DN001.000 058DN002.000 058DN003.000 058UP000.000 058UP001.000 058UP002.000 058UP003.000	-	-	-	-	X	-	data gap between 850m and 700m
114_02	59	059DN000.000 059UP000.000	-	-	-	-	X	-	
116_01	61	061DN000.000 061DN001.000 061UP000.000	-	-	-	-	X	-	
117_01	62	062DN000.000 062UP000.000	-	-	-	-	X	-	
119_01	63	063DN000.000 063UP000.000	-	-	-	-	X	-	
120_01	64	064DN000.000 064UP000.000	-	-	-	-	X	-	

Station ID	LADCP cast	File Names	Large up-down compass difference (>15°)	Found no SADCP data in time window	Found LARGE timing difference between ADCPs	Found x ADCP w deviating more than 2.5 m/s from w-CTD.	Increased error because of shear-inverse difference	shifted CTD time series by x seconds	Comments
121_01	65	065DN000.000 065UP000.000	-	-	-	-	X	-	
122_01	66	066DN000.000 066UP000.000	-	-	-	-	X	-	
123_01	67	067DN000.000 067UP000.000	-	-	-	-	X	-	
127_03	68	068DN000.000 068UP000.000	-	-	-	-	X	-	

Tab. 2.22: Overview of SonoVault and AURAL recorders recovered during PS129. All SV recorders

Mooring	Device SN	Latitude	Longitude	Deployment depth/m	Deployment date /time (UTC)	Recovery date	Gain /dB *)	Setup	Condition
AWI 227-15	SV1006	59°03.02'S	000°06.44'E	285	2018-12-31T10:10	2022-03-12T10:32:00	44.2/44.4	24 kHz; 24 bit; LowPower mode	b), e)
AWI 229-14	SV1060	64°00.49'S	000°00.84'W	329	2019-01-01T22:38	2022-03-15T09:39:00	44.3/--	24 kHz; 24 bit; LowPower mode	b), c)
AWI 231-13	SV1056	66°31.03'S	000°04.48'W	303	2018:12:27T18:34	2022-03-18T08:29:00	44.5/44.7	24 kHz; 24 bit; LowPower mode	b), a)
AWI 248-3	SV1012	65°58.12'S	12°13.84'W	350	2019-01-07T10:37	2022-03-19T09:10:00	44.4/44.5	24 kHz; 24 bit; LowPower mode	b), a)
AWI 245-5	SV1014	69°03.64'S	17°23.49'W	300	2019-01-08T14:20	2022-04-04T09:27:00	44.3/44.1	24 kHz; 24 bit; LowPower mode	b), a)
BGC-1	SV1024	69°00.03'S	27°00.29'W	918	2021-03-24T13:13	2022-04-07T15:09:00	41.4/ 24.8	48 kHz; 24 bit; LowPower mode	d)
AWI249-3	**SV1010**	**70°53.22'S**	**28°56.97'W**	**307**	**2019-01-20T12:00**	**aborted due to ice**	–	–	–
AWI 208-9	SV1020	65°41.78'S	36°41.01'W	294	2019-01-23T16:01	2022-04-14T10:04:00	44.5/20	24 kHz; 24 bit; LowPower mode	b), a)
AWI 250-3	**SV1048**	**68°28.85'S**	**44°05.94'W**	**294**	**2019-01-24T20:28**	**position not reached**	–	–	–
AWI 257-2	**SV1033**	**64°12.94'S**	**47°29.38'W**	**311**	**2019-01-27T17:50**	**aborted due to ice**	–	–	–
AWI 207-11	SV1032	63°39.36'S	50°48.66'W	300	2019-01-29T17:08	2022-04-22T01:37:00	45.1/45.0	24 kHz; 24 bit; LowPower mode	b), a)
AWI 251-3	SV1002	61°01.38'S	55°58.68'W	181	2019-02-01T18:30	2022-04-24T13:52:39	41.3/40.5	24 kHz; 24 bit; LowPower mode	b), a)
AWI 251-3	AU0085	61°01.38'S	55°58.68'W	179	2019-02-01T18:30	2022-04-24T13:52:39	--/--	32 kHz; 16 bit;	b), a)

a) system in good condition; b) no communication established directly after recovery; c) electronics damaged, batteries burned, SD cards readable; d) hydrophone defect;
e) stopped early due to electronics failure (watchdog); f) problems with electronics during test and calibration after recovery;
*) Calibration before/after recovery, using a B&K Pistonphone at 251.2 Hz ± 0.1% (ISO 266) with amplitude of 153.95 dB SPL (at 1013 hPa air pressure);
1) Not calibrated;
2) calibration pending; 3) calibration not possible.

Tab. 2.23: Overview of acoustic recorders deployed during PS129

Mooring	Acoustic Recorder SN	Position Latitude	Position Longitude	water depth true [m]	Deploy. Depth [m]	Deploy. date /time (UTC)	hydrophone type	Gain PHO and MRPro /dB *)	Configuration	Start date recordings
AWI 227-16	SV1005	59° 02.977' S	000° 06.483' E	4587	282	2022-03-12T14:21	D60	43.3 a) / 40.7 b)	1) , 2)	2022-03-10T11:30
AWI 229-15	SV1009	64° 01.222' S	000° 00.820' E	5146	296	2022-03-15T15:41	TC4032	40.5 a) / 40.8 b)	1) , 2)	2022-03-10T11:30
AWI 231-14	SV1021	66° 31.043' S	000° 04.477' W	4557	307	2022-03-17T13:55	TC4032	40.5 a) / 40.8 b)	1) , 2)	2022-03-10T11:30
EWS 003-01	SV1008	70° 17.905' S	013° 26.779' W	3304	346	2022-04-03T12:41	TC4032	40.5 a) / 40.8 b)	1) , 2)	2022-03-22T11:30
AWI 245-06	SV1022	69° 03.636' S	017° 23.455' W	4721	285	2022-04-04T16:03	TC4032	40.1 a) / 40.9 b)	1) , 2)	2022-03-30T11:30
AWI 249-04	SV1026	70° 49.932' S	029° 07,930' W	4374	312	2022-04-08T19:50	TC4032	41.7 a) / -	1) , 2)	2022-04-05T11:30
CWS 001-01	SV1031	69° 33.349' S	032° 28.620' W	4430	314	2022-04-10T22:36	D60	43.6 a) / 40.8 b)	1) , 2)	2022-04-06T11:30
as above	AU0231	69° 33.349' S	032° 28.620' W	4430	268	2022-04-10T22:36	HTI-96-min	-	3)	2022-12-31T12:00
AWI 209-09	SV1025	66° 36.444' S	27° 07.279'W	4821	299	2022-04-12T17:06	TC4032	44.1 a) / 44.9 b)	1) , 2)	2022-04-12T11:30
AWI 208-10	SV1049	65° 41.760' S	36° 40.971 'W	4715	298	2022-04-14T15:34	TC4032	44.1 a) / 44.5 b)	1) , 2)	2022-04-12T11:30
CWS 002-01	SV1030	66° 22,766' S	041° 23,502' W	4524	298	2022.04.16T17:05	TC4032	40.3 a) / 40.9 b)	1) , 2)	2022-04-14T11:30
WWS 002-01	SV1027	65° 25.985'S	044° 35.575'W	4416	310	2022-04-17T20:44	TC4032	40.8 a) / 40.9 b)	1) , 2)	2022-04-13T11:30
as above	AU0086	65° 25.985'S	044° 35.575'W	4416	257	2022-04-17T20:44	HTI-96-min	-	3)	2022-12-31T12:00
AWI 257-2	SV1034	64° 14,420' S	047° 29,114' W	4142	308	2022-04-19T20:42	TC4032	44.8 a) / 44.8 b)	1) , 2)	2022-04-16T11:30
AWI 207-12	SV1013	63° 37,749' S	050° 47,457' W	2502	276	2022-04-21T23:50	TC4032	44.5 a) / 44.9 b)	1) , 2)	2022-04-15T11:30
AWI 261-02	SV1023	63° 29,929' S	051° 38,229' W	1618	255	2022-04-22T21:12	D60	46.8 a) / 44.9 b)	1) , 2)	2022-04-21T11:30
AWI 251-04	SV1054	61° 01,376' S	055° 58,665' W	311	153	2022-04-24T16:20	TC4032	40.9 a) / 41.2 b)	1) , 2)	2022-04-19T11:30
as above	AU0303	61° 01,376' S	055° 58,665' W	311	148	2022-04-24T16:20	HTI-96-min	-	3), 4)	2022-04-23T20:00

*) Calibration before deployment, using a a) B&K Pistonphone at 251.2 Hz ± 0.1% (ISO 266) and 153.95 dB SPL amplitude (at 1013 hPa air pressure) and b) a signal generator MR Pro at 1kHz with V0p=7.1mV connected to the hydrophone connector on the electronics board;
1) 48 kHz; 24 bit; Low Power Mode;
2) Schedule: 25 hrs ON / 23 hrs OFF (11:30-12:30 +1d);
3) Schedule: 10min every full hour, 32 kHz;
4) VLP WB2 OSR 128 (Very low power, wide band 2, over-sampling-rate 128)

Tab. 2. 24: Overview of results of preliminary technical and data quality evaluation of recorders recovered during PS129

Mooring	Recorder [SN]	Deployment Expedition	Deployment [datetime]	Recording end [date time]	com ms	Battery status end (start)	Clock drift [sec / ann]	Quality data [days]	Missing records	Recording status	Electronic noise <u>(preliminary results)</u>
AWI 227-15	SV1006	PS117	2018-12-31T10:10	2019-02-08T08:05:50	No	13.9 (25)	nn	38	none	end, possibly electronic failure, reason unknown	4)
AWI 229-14	SV1060	PS117	2019-01-01T22:38	2019-05-10T12:39:28	No	nn	nn	127	From 22/03 to 02/05 2019 2 SD Cards not readable	burned out	no
AWI 231-13	SV1056	PS117	2018:12:27T18:34	2020-05-20T06:10:06	No	8.45 (25)	nn	509	none	end: battery low	no
AWI 248-3	SV1012	PS117	2019-01-07T10:37	2020-04-23T07:06:02	No	7.52 (25)	nn	470	none	end: battery low	no
AWI 245-5	SV1014	PS117	2019-01-08T14:20	2020-07-03T06:31:00	No	7.14 (25)	nn	540	none	end: battery low	no
BGC-1	SV1024	PS124	2021-03-24T13:13	2022-03-15T20:51:08	Yes	24.6 (25)	363	349	none	storage full	6)
AWI 208-9	SV1020	PS117	2019-01-23T16:01	2019-07-08T00:23:00				75	none	end, possibly electronic failure, reason unknown	6)
AWI 207-11	SV1032	PS117	2019-01-29T17:08	2020-08-14T13:32:52	No	6.83 (25)	7	561	none	end: battery low	4, 5)
AWI 251-3	SV1002	PS117	2019-02-01T18:30	2020-04-25T03:25:15	No	10.85 (25)	380	449	1)	end: battery low	1)
AWI 251-3	AURAL	PS117	2019-02-01T18:30	2021-02-04T03:00:00				734	1)	end: battery low	1)

to be analyzed
Comms: communication established after recovery
battery: voltage at recovery [V] (voltage at deployment [V]
tonal electronic noise
broadband instrument or mooring noise
hydrophone malfunction

3. NUTRIENTS, DOC AND POC

Martin Graeve[1], Kai-Uwe Ludwichowski[1]   [1]DE.AWI

Grant-No. AWI_PS129_03

Objectives

The determination of nutrients and biogeochemical parameters is closely connected with physical and biological investigations. The development of phytoplankton blooms and particulate organic matter flux is especially dependent on the available nutrients. Nutrients are also well suited as tracers for the identification of water masses. This work was carried out to continue the investigation of the seasonal as well as the interannual variability of nutrients in the Antarctic Circumpolar Current (ACC) and the Weddell Gyre. In comparison to similar transects of former years, our work focused especially on the transect from Kapp Norvegia to Joinville Island (Hoppema et al., 2015). Providing baseline values for $\delta^{13}C$ and $\delta^{15}N$ isotopes of particulate organic matter (POM) is a further major aspect of this part of the HAFOS project. Significantly higher ^{13}C enrichment in ice algae relative to pelagic phytoplankton allows for the tracking of carbon from ice algae and pelagic phytoplankton to higher trophic levels (Pinault et al., 2013). The values are depending on various regional aspects of phytoplankton blooms and thus of the POM composition. The results will be used as baseline values for Bayesian multisource stable isotope mixing models (SIAR; Parnell et al., 2010).

Work at sea

Equipment and method-nutrients were analyzed with a SEAL AA 500, continuous flow auto-analyser (Strickland and Parsons, 1968). Water samples were drawn from the CTD/rosette and were measured unfiltered. Measurements were made simultaneously on five channels of the auto-analyzer for phosphate, silicate, nitrate, nitrite and ammonium. (Grasshoff et al., 1983, Murphy and Riley, 1962). All measurements were calibrated with a five-nutrient standard cocktail solution (all from Merck, traceable to SRM from NIST) diluted in artificial seawater (ASW), while ASW was also used as rinse water between the samples. Data were all standardized by the same in-house reference material based on a batch of water from the deep ocean. In each run we checked our measurements and standards against the reference material for nutrients in seawater (CRM 7602-a + CRM 7603a) produced by the National Meteorological Research Institute, Japan. Our standards and methods have been verified by intercalibration exercises like ICES and Quasimeme, and last year's RMNS exercise organized by Dr. Michio Aoyama of the National Meteorological Research Institute. At selected stations, 6 L of sample water for POC analysis (2 x 2 L at the chlorophyll maximum and 1 x 2 L at 10 m depth) were taken from the Niskin bottles, filtered on Whatman GF/F filters (0.7 µm pore size) and stored at -80° C.

Preliminary results

During this cruise we measured 954 samples for nutrients and 160 ones for ^{13}C and ^{15}N stable isotopes. The nutrients are important parameters (4,770 data points) allowing other parameters to be related to biological activity such as primary production and remineralization. Nutrients can also be used as tracers of water masses. Analysis of $\delta^{13}C$ and $\delta^{15}N$ of POM will highlight the interaction between sympagic and pelagic phytoplankton communities. This will be done by isotope ratio mass spectrometry in combination with an elemental analyser.

Data management

All nutrient data are available among all cruise participants. For quality measures, after the cruise some re-analysis and quality management will take part. We plan that the full data set will be available as soon as possible, but the latest one year after the cruise. Data will be archived, published and disseminated according to international standards by the World Data Center PANGAEA Data Publisher for Earth & Environmental Science (https://www.pangaea.de) within two years after the end of the cruise at the latest. By default, the CC-BY license will be applied. Data on carbon and nitrogen isotope ratios of POC will be provided upon request to all cruise participants and later also uploaded to the PANGAEA data archive.

This expedition was supported by the Helmholtz Research Programme “Changing Earth – Sustaining our Future” Topic 6, Subtopic 2. In all publications based on this expedition, the **Grant No. AWI_PS129_03** will be quoted and the following publication will be cited:

Alfred-Wegener-Institut Helmholtz-Zentrum für Polar- und Meeresforschung (2017) Polar Research and Supply Vessel POLARSTERN Operated by the Alfred-Wegener-Institute. Journal of Large-Scale Research Facilities, 3, A119. http://dx.doi.org/10.17815/jlsrf-3-163.

References

Grasshoff K., Erhardt M, Kremling K (1983) Methods of seawater analysis. Second, revised and extended edition, Verlag Chemie GmbH, Weinheim, 419 pp.

Hoppema M, Bakker K, van Heuven SMAC, van Ooijen JC, de Baar HJW (2015) Distributions, trends and inter-annual variability of nutrients along a repeat section through the Weddell Sea (1996–2011). Marine Chemistry, 177, 545–553.

Murphy J, Riley JP (1962) A modified single solution method for the determination of phosphate in natural waters. Analytica Chimica. Acta, 27, 31-36.

Parnell AC, Inger R, Bearhop S, Jackson AL (2010) Source partitioning using stable isotopes: Coping with too much variation. PloS One, 5, e9672.

Pineault S, Tremblay J-E, Gosselin M, Thomas H, Shadwick E (2013) The isotopic signature of particulate organic C and N in bottom ice: Key influencing factors and applications for tracing the fate of ice-algae in the Arctic Ocean. Journal of Geophysical Research: Oceans, 118, 287-300.

Strickland JDH, Parsons TR (1968) A practical handbook of seawater analysis. First edition. Bulletin Fisheries Research Board of Canada, 167, 65

4. THE CARBON SYSTEM OF THE WEDDELL SEA

M. González-Dávila[1], M. Santana-Casiano[1]   [1]ES.ULPGC

Grant-No. AWI_PS129_02

Objectives

The Southern Ocean is a key region for our understanding of the global carbon cycle and how it will respond under predicted future climate change. Antarctic Bottom Water (AABW) fills approximately 36 % of the global deep ocean basins (Johnson, 2008), and its circulation comprises the deepest limb of the global overturning circulation (Orsi et al., 1999; Talley, 2013). The Weddell Sea supplies 40 – 50 % of the Antarctic Bottom Water and therefore exerts significant influence over global circulation and climate (Stewart, 2021). Recent studies have suggested that the Southern Ocean is taking up around 30 – 40 % of the anthropogenic (i.e., excess) CO_2 (C_{ant}), followed by an important and efficient transport of this C_{ant} by intermediate- and deep-water formation in this area. The uptake and accumulation of C_{ant} is mainly controlled by the ocean circulation and water mass mixing, in particular the deepest penetrations associated with convergence zones. This is why the Southern Ocean is one of the most conspicuous places of the global ocean. One of the main objectives of the HAFOS project and this research cruise was to study the formation of intermediate, deep and bottom water masses together with the upwelling of old waters takes place through complex dynamical processes.

Work at sea

This cruise has provided a new set of carbon dioxide data for this area that will increase our knowledge of the amount of anthropogenic carbon being incorporated by the different water masses and will be compared with previous results for this area to compute the anthropogenic carbon inventory, the concentration in deep and bottom layers and its storage and evolution.

In order to achieve these objectives, the Marine Chemistry group (QUIMA) from the Instituto de Oceanografía y Cambio Global (IOCAG) at the Universidad de Las Palmas de Gran Canaria has measured for each CTD cast and in the whole water column two carbon dioxide parameters: the total alkalinity (A_T) and the total dissolved inorganic carbon concentration (C_T; also known as DIC), making the value traceable to the highest standards by using Certified Reference Material (CRM) for CO_2 analyses. During the cruise, the QUIMA group was also in charge of analyzing the concentration of dissolved oxygen on discrete samples.

Dissolved oxygen

The dissolved oxygen content (DO) in the water column was analyzed in discrete samples from the Niskin bottles. The DO determined from water samples will be used to calibrate the oxygen sensor on the CTD/rosette (see Chapter 2, Physical Oceanography).

Seawater samples for DO determination were the first samples taken from the 12 L Niskin bottles of the CTD/rosette after coming on board to avoid gas exchange with the air during the time of sampling. The seawater samples were collected in pre-calibrated wide-neck glass bottles that were previously rinsed three times with the seawater sample, avoiding air bubbles. The temperature of the water was recorded during the sampling. Reagent 1 ($MnCl + 4H_2O$) and reagent 2 ($NaOH + NaI$) were then added and thoroughly mixed with the seawater sample. The mixed samples were kept in a dark box during 6 hours to allow the precipitate to settle at the bottom of the bottle.

Sampling for DO analysis was performed for all depths at stations 14-87, except for station 83. From stations 87 to 127, sampling for oxygen (and carbonate system variables) and their analysis could not be done for all Niskin bottles available due to time limitation. A total of 430 samples for DO were analysed, corresponding to 49 % of the number of Niskin bottles (881) available for oxygen analysis during the cruise. A total of 95 samples were analysed at the Prime Meridian section, 88 in the EWOS box, 29 at ice stations and 218 samples at the Weddell Sea section.

DO was determined from the seawater samples using the Winkler method, introduced by Winkler (1888) and optimized by Carritt and Carpenter (1966). A Metrohm 785 Titrando amperometric electrode to determine the end point was used for the titration (Culberson and Huang, 1987). Three reagents were used: fixative reagent 1 ($MnCl + 4H_2O$) and reagent 2 ($NaOH + NaI$) at sampling and reagent 3 (H_2SO_4) immediately before starting the titration. A 0.01N solution of thiosulfate was used as titrant and a 0.01N solution of KIO_3 as a standard solution. All the reagents and solutions used during the cruise for DO determination were prepared on board following the procedures described by Dickson (1994). Reagent 3 was added at least 6 hours after sampling and immediately before starting the titration to acidify the sample, which was stirred after the addition. A standardization of the thiosulphate was performed every two days with seawater and the standard solution of KIO_3. The possible impurities of the reagents were controlled by determining a blank titration every two days. The calibration values for standardization and blanks obtained during the cruise were better than ± 0.0021 mL for the three different thiosulfate solutions prepared and 17 standardizations done. Concentration of thiosulfate solutions was 0.0577 ± 0.0001 M during the cruise.

CO_2 system parameters

The distribution of the CO_2 system in the water column was studied all along the cruise track. Discrete seawater samples from the Niskin bottles were analysed on board for Total Alkalinity (A_T) and Total Dissolved Inorganic Carbon (C_T). The sampling, data collection methodology, quality control and calculation procedures were done according to the manual for ocean CO_2 analysis (Dickson et al., 2007).

Seawater samples for A_T and C_T determination were taken from the 12 L Niskin bottles placed in the CTD/rosette immediately after the sampling for DO determination and collected together in 500 mL glass bottles. The samples were stored in the dark until they were put into a 25º C water bath to keep the temperature constant during the analysis.

The sampling for A_T and C_T was performed for all depths of each station. A total of 51 stations with 881 samples were analysed during the cruise. A 100 % data collection was achieved. A total of 95 samples were analysed at the Prime Meridian section, 88 in the EWOS box, 29 at the ice stations and 669 samples at the Weddell Sea section. Moreover, 32 samples (until station 127) from the continuous underwater pump system of the COMA project (section 5) were sampled and analysed for A_T and C_T. After station 127, samples were taken and fixed with 100 µL concentrated $HgCl_2$ solution and preserved for analyses at Gran Canaria Laboratory facilities.

A_T and C_T (in µmol $kg^{-}1$) were determined on board by a VINDTA 3C system (Marianda™) that allows the determination of both A_T by potentiometric titration (Dickson et al., 2007) using a 719 Titrino titrator with a three-electrodes system, and C_T by coulometric titration in a glass cell with Pt cathode and silver anode. This titration system requires a cell preparation time of about 2 hours and analysis time of approximately 15 minutes per sample (including rinsing and sample preparation). It provides A_T and C_T measurements with an estimated uncertainty of 1.5 µmol kg^{-1} (based on reproducibility studies).

In order to provide data with the highest accuracy, Certified Reference Material, acquired from Andrew Dickson's facilities at Scripps Institution of Oceanography (U.S.A.), was analysed in duplicate for a total of 19 bottles (38 measurements). CRM batch #196 was analysed with a frequency of about 2 days to test the performance of the titration system and improve the accuracy of the system, correcting the experimental values for the changes in burette volumes and acid concentration (A_T) and system performance. Correcting factor was lower than 1.0003 for both parameters according to the measured CRM values.

The computation of other carbonate system variables will be done from pairs of A_T and C_T data using the Excel programme CO2SYS.

Preliminary results

Using the experimentally measured Dissolved Oxygen ($O_{2,\ meas}$) data together with data from the CTD sensor for oxygen SBEox0 ($O_{2,sens}$), a linear relationship was obtained with a correlation coefficient r^2 = 0.9988 and with a standard error of estimate in DO of 0.045 mL L^{-1}. (1)

The fitting can be slightly improved with a quadratic polynomial equation (Fig. 4.1) with a correlation coefficient r^2 = 0.9993 and with a standard error of estimate in DO of 0.035 mL $L^{-1.}$ (2)

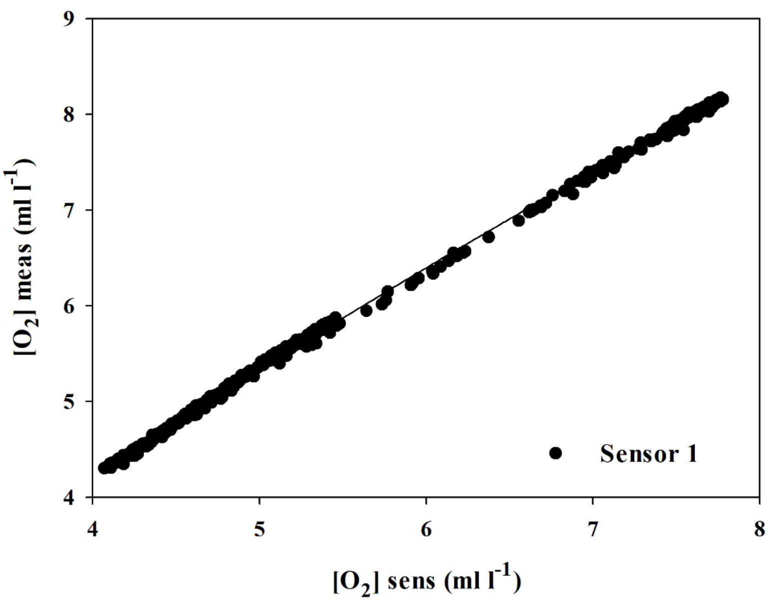

Fig. 4.1: Plot of dissolved oxygen measured by the sensor on the CTD versus dissolved oxygen measured by Winkler titration

Fig. 4.2 shows the results of the CRM analysis for C_T during the cruise period with indication of the average value of 2018.99 ± 1.09 µmol kg^{-1} and one and two sigma deviations. The certified value for CRM #196 is 2018.83 µmol kg^{-1}. Moreover, it is observed that, on average, that the reproducibility for the duplicate analysis of C_T was 1.06 µmol kg^{-1} , with maximum deviation of 2.0 µmol kg^{-1}.

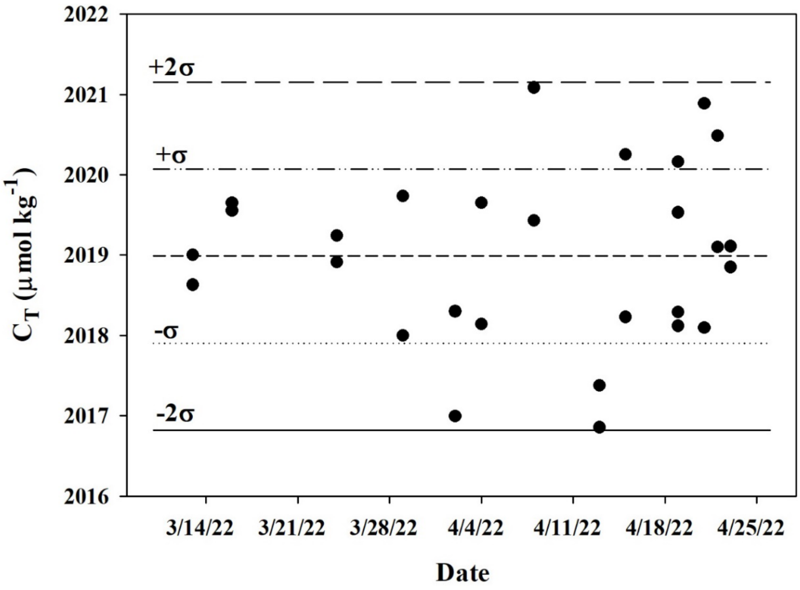

Fig. 4.2: The C_T concentrations determined for CRM #196 together with average and 1 and 2 standard deviations

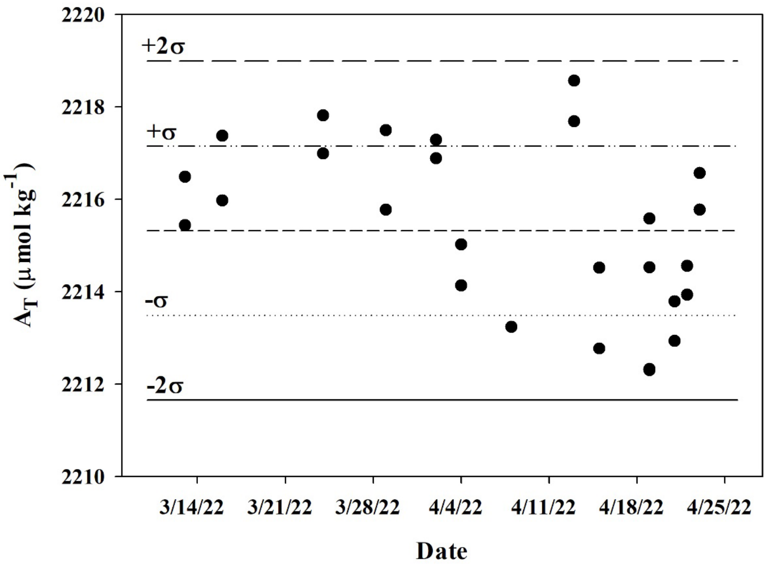

Fig. 4.3: The A_T concentrations determined for CRM #196 together with average and 1 and 2 standard deviations

Fig. 4.3 shows a similar plot for the A_T values for CRM #196 during the cruise period. The average value (2215.40 ± 1.82 µmol kg^{-1}) is almost identical to the certified one (2215.32 µmol kg^{-1}) and the reproducibility for the duplicate analysis was on average 0.88 µmol kg^{-1}, with a maximum difference of 1.7 µmol kg^{-1}.

Data management

Environmental data will be archived, published and disseminated according to international standards by the World Data Center PANGAEA Data Publisher for Earth & Environmental Science (https://www.pangaea.de) within two years after the end of the cruise at the latest. By default, the CC-BY license will be applied. Any other data will be submitted to an appropriate long-term archive that provides unique and stable identifiers for the datasets and allows open online access to the data.

Results will be used for publication in an international peer-reviewed journal in a collaborative AWI-ULPGC paper including the ULPGC members M. González-Dávila, J.M. Santana-Casiano (both on board) and D. González-Santana (on land).

In all publications based on this expedition, the Grant No. AWI_PS129_02 will be quoted and the following publication will be cited:

Alfred-Wegener-Institut Helmholtz-Zentrum für Polar- und Meeresforschung (2017) Polar Research and Supply Vessel POLARSTERN Operated by the Alfred-Wegener-Institute. Journal of large-scale research facilities, 3, A119. http://dx.doi.org/10.17815/jlsrf-3-163.

References

Culberson CH, Huang S (1987) Automated amperometric oxygen titration. Deep-Sea Research, 34, 875-880.

Dickson AG (1994) Determination of dissolved oxygen in seawater by Winkler titration. Technical report, WOCE operations manual, WOCE report 68/91, Revision 1.

Dickson AG, Sabine CL, Christian JR (2007) Guide to best practices for ocean CO_2 measurements. PICES Special Publ. 3, 191 pp.

Carritt DE, Carpenter JH (1966) Comparison and evaluation of currently employed modifications of the Winkler method for determining dissolved oxygen in seawater; a NASCO Report. Journal of Marine Research, 24, 286-318.

Johnson GC (2008) Quantifying Antarctic Bottom Water and North Atlantic Deep Water volumes. Journal of Geophysical Research, 113, C05027, https://doi.org/10.1029/2007JC004477

Orsi AH, Johnson GC, Bullister JL (1999) Circulation, mixing, and production of Antarctic Bottom Water. Progress in Oceanography, 43, 55-109, https://doi.org/10.1016/S0079-6611(99)00004-X

Stewart AL (2021) Mesoscale, tidal, and seasonal/interannual drivers of the Weddell Sea overturning circulation. Journal of Physical Oceanography, 51, 3695-3722, https://journals.ametsoc.org/ view/journals/phoc/51/12/JPO-D-20-0320.1.xml

Talley LD (2013) Closure of the global overturning circulation through the Indian, Pacific, and Southern Oceans: Schematics and transports. Oceanography, 26, 80–97. http://www.jstor.org/ stable/24862019

Winkler LW (1888) Die Bestimmung des in Wasser gelösten Sauerstoffen. Berichte der Deutschen Chemischen Gesellschaft, 21-2, 2843-2354, https://doi.org/10.1002/cber.188802102122

5. IDENTIFYING THE CARBON THAT MATTERS: CHEMICAL CONTROLS ON ORGANIC MATTER AGGREGATION (COMA)

Jan Tebben[1], Mario Hoppema[1], Kai-Uwe Ludwichowski[1], Martin Graeve[1], Melchor González-Dávila[3], Magdalena Santana-Casiano[3], Boris Koch[1,2]
Not on board: Alessandro Tagliabue[4], Stéphane Pesant[5]

[1]DE.AWI
[2]DE.HSB
[3]ES.ULPGC
[4]UK.UNI-Liverpool-EOE
[5]UK.EBI

Grant-No. AWI_PSXXX_07

Outline

The biological pump and its transport of particulate organic matter (POM) from the photic zone to the ocean floor and the formation and downwelling of CO_2 and recalcitrant dissolved organic matter (DOM) in the Southern Ocean are key regulators of the transfer of atmospheric CO_2 to long-term storage of carbon. The composition and distribution of organic matter is controlled by primary production and microbial activity, water-mass mixing, physico-chemical degradation and aggregation processes (Koch et al., 2014). DOM undergoes aggregation and binds to particles (e.g., cells, fecal pellets and detritus), which contributes to deposition and sequestration of carbon and creates a major sink in the global carbon cycle. Despite the significant role of aggregation, very little is known about the accumulation rates and binding of low-molecular organic matter and colloidal matter on macromolecules and particles.

Objectives

This project addresses some of the central questions of the global carbon cycle, namely to derive a mechanistic understanding whether certain chemical classes within the DOM pool predominantly drive aggregation in the Southern Ocean and therefore impact the sequestration of atmospheric CO_2. The central objectives of this project, therefore, are to sample, isolate and structurally identify bacterially produced molecules that, 1) act as coagulants and drive particle aggregation, and 2) sample, isolate and structurally identify bacterially produced ligands that complex trace metals such as iron. A consequential objective is then to correlate the genetic diversity of bacteria and phytoplankton (e.g., Bucklin et al., 2016) with aggregation rates and environmental parameters (such as iron stress, salinity and temperature).

Work at sea

The filtration and concentration of large amounts of particulate and dissolved organic matter is a prerequisite for the chromatographic isolation and identification of organic matter components as well as the exploration of the genetic diversity (DNA barcoding). Both phytoplankton species and clonal lines of bacterial strains will be isolated from single cells on board to be used in co-inoculation experiments in the home laboratories. All materials were washed with 10 % hydrochloric acid followed by pure water unless stated otherwise. Water was sampled from the ship's moonpool at 11 m water depth using a "snorkel" equipped with a teflon head protruding

~0.5 m below the ships edge, a 40 m x 1 inch suction hose with polyethylene tubing inlay (suction side), and a teflon pneumatic pump equipped with pulsation dampening (Tapflo). The water flow was divided with a T-valve (pressure side post-pump) to a half inch polyethylene tubing and 4 mm PTFE tubing piped in under a laminar flow cabinet inside a clean room container (Tab. 5.1).

Large volume samples (LVS) were prefiltered using polypropylen filter socks in a 10-inch polypropylene filter housing (Fuhr, 1 µm pore size) and were collected in 1 m³ intermediate bulk containers. The latter were washed with about 100 L at each station and the wash-water discarded. 950-L samples were then collected over about 30 min, equivalent to a distance of approximately 5 nmi and acidified to pH=3 using concentrated hydrochloric acid (12 M, Carl Roth). The water was pumped at 20 L h^{-1} through a pre-combusted (500° C, 5 h) glass fibre filter (Whatman, GFF, 142 mm) in a polycarbonate filter-holder and a manually packed and precleaned (methanol, LichroSolv followed by ultrapure water pH=2) solid phase extraction cartridge containing a 17 g of bulk solid phase adsorber material (BondElut ENV, Agilent, or PPL, Agilent, respectively). While the large volume sample bulk container was filled, the divided sample flow was simultaneously sampled in a clean room lab container for Fe^{3+} (0.5 L, 0.2 µm filtered over Sartobran 300), Fe^{2+} (0.25 L), ligands (0.5 L), live bacterial cultures (15 mL), nutrients (20 mL), dissolved organic carbon (DOC, 20 mL), dissolved inorganic carbon (DIC, 0.2 L), alkalinity (0.2 L), fluorescence (FL, 20 mL) analysis, particulate organic carbon (POC, 2 L), eDNA (20 L; Gorsky et al., 2019) and small volume (0.5 L) solid phase extractions for the molecular characterization of dissolved organic matter. The acidified and pre-filtered water in each intermediate bulk container was additionally sampled for DOC (1 L).

Tab. 5.1: Sample types derived from underway sampling (through the snorkel)

Parameter	Treatment	Sample volume	Storage container	Storage condition
Large volume samples, DOM, POM	Prefiltered 1 um	950 L	1 m³ Intermediate bulk container	Frozen -20°C (Chromatographic resin and GF/F filter)
Fe^{2+}	Unfiltered, sampling under laminar flow in clean room container	500 mL	HDPE bottle	Frozen -20°C
Ligands	Unfiltered, sampling under laminar flow in clean room container	500 mL	HDPE bottle	Frozen -20°C
Fe^{3+}	0.8/0.2 µm filtration (Sartobran 300) under laminar flow in clean room container	250 mL	HDPE bottle	Acidified, 4°C
DOC	GF/F filtered, sampling under laminar flow in clean room container	20 mL	HDPE bottle	Frozen -20°C
SPE-DOM	GF/F filtered, acidified	500 mL	ppl resin/PP cartridge	Frozen -20°C
Fluorescence	GF/F filtered	20 mL	HDPE bottle	Frozen -20°C
Nutrients	Unfiltered, sampling under laminar flow in clean room container	20 mL	HDPE bottle	Direct analysis
Alkalinity	Unfiltered	0.2 L	Glass bottle	Direct analysis
Inorganic carbon	Unfiltered	0.2 L	Glass bottle	Direct analysis

Parameter	Treatment	Sample volume	Storage container	Storage condition
Bacterial culture	Unfiltered	15 mL	Sterile falcon tube	Agar plating
eDNA	Unfiltered, 3 μm, 0.2 μm filtration. $FeCl_3$ precipitate (12 h) filtered onto 0.8 μm	20 L	5 mL cryotube	Snap frozen in liquid N_2, then -80°C

The Niskin water bottles from the CTD/rosette were sampled using acid-washed glass bottles (1L or 2 L, Schott Duran) that were thoroughly rinsed with sample water (Tab. 5.2). For the surface layer depths (chlorophyll maximum and surface) samples were collected using acid-washed PE sample bottles (2 L) to avoid iron contamination and additional samples for bacteria were taken in sterile 50 mL centrifuge vials.

For all DOC and fluorescence samples, at least 1 L of water was filtered using pre-combusted (450° C, 5 h) glass fibre filters (Whatman, GFF, 42 mm diameter) and a glass filtration unit). Samples were filled into pre-cleaned and thoroughly rinsed high-density polyethylene HDPE bottles (50 mL). For POC samples, 2 L of water was filtered using the same method and filters were wrapped in aluminum foil. All samples were stored at -30° C until further analyses. Inorganic nutrient samples were measured unfiltered directly onboard (see Chapter 3 – Nutrients, Doc and POC). Small volume extraction was performed using 0.5 L of the filtrate of the DOC samples and precleaned SPE cartridges (PPL, Agilent, 200 mg).

Tab. 5.2: Sample types taken from the CTD/rosette

Parameter	Treatment	Sample volume	Storage container	Storage condition
DOC	GF/F filtered, sampling under laminar flow in clean room container	20 mL	HDPE bottle	Frozen -20°C
SPE-DOM	GF/F filtered, acidified	500 mL	ppl resin/PP cartridge	Frozen -20°C
Fluorescence	GF/F filtered	20 mL	HDPE bottle	Frozen -20°C
Nutrients	Unfiltered, sampling under laminar flow in clean room container	20 mL	HDPE bottle	Direct analysis
Bacterial culture	Unfiltered	15 mL	Sterile falcon tube	Agar plating
eDNA	Unfiltered, 3 μm, 0.2 μm filtration. $FeCl_3$ precipitate (12 h) filtered onto 0.8 μm	20 L	5 mL cryotube	Snap frozen in liquid N_2, then -80°C

Blanks

- Ultrapure water pH2
- SPE process blank
- GFF Filtration blank

Structure elucidation of refractory DOM

250 L and 45 L of seawater from 400 m depth were sampled on stations PS129_72-1 and PS129_74-4, respectively (Figs. 5.1). The samples were transferred into an acid-washed intermediate bulk container (high-density polyethylene, HD-PE), filtered with an inline pre-combusted glass fibre filter (142 mm, GFF, Whatman) to a second intermediate bulk container. The entire filtrate (~270 L) was acidified to pH=6.6 using hydrochloric acid (30 %, suprapure, Merck). Two solid-phase extraction cartridges (HhD-PE; inner diameter: 36 mm) were pre-cleaned with methanol (LiCHrosolv) and filled with adsorber material (20 g each, PPL, Agilent). SPE cartridges were conditioned with methanol and rinsed with ultrapure water (not acidified). On each cartridge, 136 L of seawater was extracted at a flow rate of 7.5 L h^{-1} (125 mL per minute; verified by repeated volume flow measurements).

The permeate of the first extraction was collected in an intermediate bulk container and acidified to pH=3.95. The pump system was used to circulate the water for one hour to allow for complete mixing. Two additional cartridges were filled with 15 g PPL and conditioned with MeOH (2 cartridge fillings) and ultrapure water (1 cartridge filling) and the extraction of the pH=4 permeate was started. After extraction, the adsorber was washed with two cartridge fillings ultrapure water (pH=4, total volume about 400 mL), dried under nitrogen gas (5.0 purity) and transferred into HDPE vials.

In a third step, the resulting permeate was acidified to pH=2.14 and extracted in duplicate with two cartridges loaded with 10 g PPL each. The cartridges were again conditioned with methanol and this time with ultrapure water acidified to pH=2.

Additional three small volume extractions were carried out for the original sample adjusted to pH=2 (and GFF filtered), the pH=3.9 permeate (no additional filtration) and the pH=2.0 permeate (no additional filtration). For each extraction, additional DOC samples were collected. The extraction of pH=6.6 permeate got lost. DOC samples for the permeate were taken from each individual cartridge at the beginning, in the middle and at the end of the extraction. In addition, permeate DOC samples were collected from each desalting step (MQ; second wash).

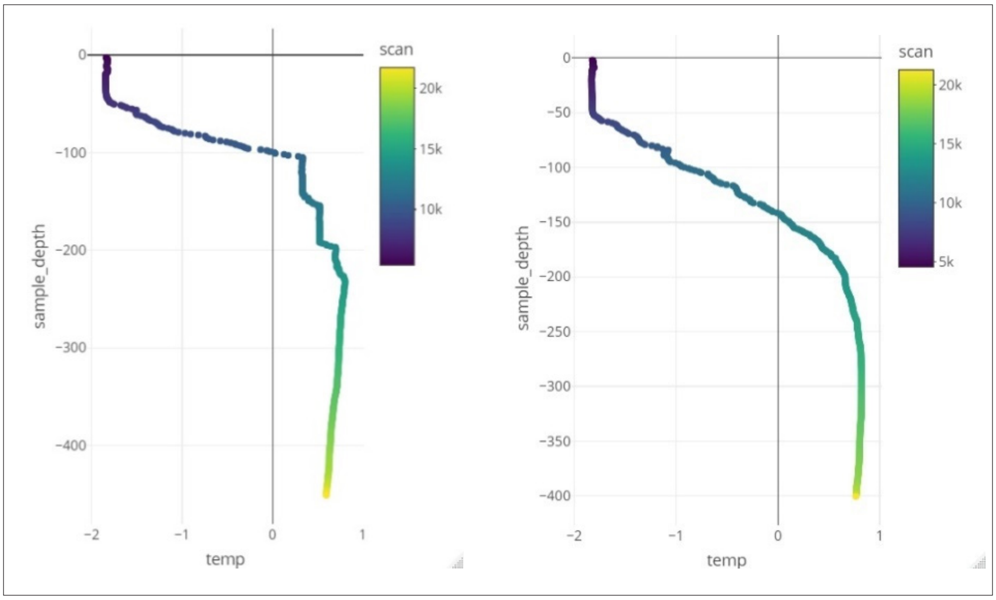

Fig. 5.1: Temperature profiles of stations PS129_72-1 (left) and PS129-74-4 (right). Sample water was collected from 400 m water depth in the Warm Deep Water.

Preliminary results

All analyses for the COMA project will be carried out after the cruise. Here, we provide an overview on the types, number and volumes of samples taken (Fig. 5.2 and Tab. 5.3).

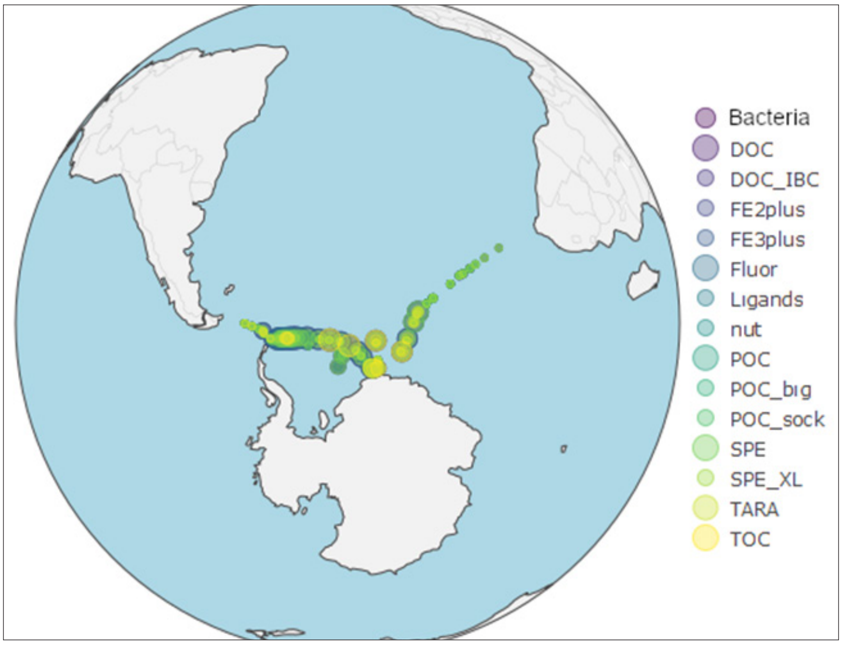

Fig. 5.2: Location of samples taken within the project. Size represents the number of samples taken at each location. Bacteria: isolated bacterial colonies; DOC: dissolved organic carbon; DOC_IBC: dissolved organic carbon procedural control; Fe2plus: samples for iron (II) quantification; Fe3plus: samples for iron (III) quantification; Fluor: samples for total fluorescence determination; Ligands: quantification of total (iron) ligand concentration; nut: nutrient concentration (analyzed on board); POC: particulate organic carbon; POC_sock: particulate organic carbon (prefiltration); SPE: samples obtained by solid phase extraction for analysis of dissolved organic matter (0.5 L); SPE_XL: samples obtained by large volume solid phase extraction for analysis of dissolved organic matter (~950 L); TARA: samples for eDNA analysis; TOC: samples for total organic carbon analysis

Tab. 5.3: Overview on samples collected during PS129

Parameter	Number of samples	Total volume (L)
DOC	168	56
POC	51	947
SPE_XL	20	17800
POC_big	19	0
POC_sock	17	2600
FE2plus	15	8
FE3plus	15	8
Ligands	15	8
SPE	121	0
nut	13	26
bugs	27	0

Parameter	Number of samples	Total volume (L)
DOC_IBC	14	28
Fluor	153	40
TARA	32	0
TOC	68	12

Data management

Environmental data will be archived, published and disseminated according to international standards by the World Data Center PANGAEA Data Publisher for Earth & Environmental Science (https://www.pangaea.de) within two years after the end of the cruise at the latest. By default, the CC-BY license will be applied.

Molecular data (DNA and RNA data) will be archived, published and disseminated within one of the repositories of the International Nucleotide Sequence Data Collaboration (INSDC, www.insdc.org) comprising of EMBL-EBI/ENA, GenBank and DDBJ). Any other data will be submitted to an appropriate long-term archive that provides unique and stable identifiers for the datasets and allows open online access to the data.

In all publications, based on this cruise, the Grant No. AWI_PS129_07 will be quoted and the following *Polarstern* article will be cited: Alfred-Wegener-Institut Helmholtz-Zentrum für Polar- und Meeresforschung (2017) Polar Research and Supply Vessel POLARSTERN Operated by the Alfred-Wegener-Institute. Journal of large-scale research facilities, 3, A119. http://dx.doi.org/10.17815/jlsrf-3-163.

This expedition was supported by the Helmholtz Research Programme “Changing Earth – Sustaining our Future” Topic 6, Subtopic 6.1, 6.2 and 6.3.

Third party funding for the following projects supporting this expedition is provided by the Priority Programme 1158 Antarctic Research with Comparable Investigations in Arctic Sea Ice Areas:

“Recognition, signalling and response of the diatom Fragilariopsis to epibiotic bacterial colonization” for T. Harder and J. Tebben;

“Siderophore mediated iron acquisition of psychrophilic Antarctic marine bacteria” for J. Tebben, T. Harder and C. Völker;

“Identifying the carbon that matters: Chemical controls on organic matter aggregation (COMA)” for M. Hoppema, B. Koch and J. Tebben.

References

Bucklin A, Lindeque PK, Rodriguez-Ezpeleta N, Albaina A, Lehtiniemi M (2016) Metabarcoding of marine zooplankton: prospects, progress and pitfalls. Journal of Plankton Research, 38, 393-400.

Koch BP, Kattner G, Witt M, Passow U (2014) Molecular insights into the microbial formation of marine dissolved organic matter: recalcitrant or labile? Biogeosciences, 11, 4173-4190.

Gorsky G et al. (2019) Expanding Tara Oceans protocols for underway, ecosystemic sampling of the ocean-atmosphere interface during Tara Pacific Expedition (2016–2018). Frontiers in Marine Science, 6, 750.

6. DEFIANT (DRIVERS AND EFFECTS OF FLUCTUATIONS IN SEA ICE IN THE ANTARCTIC)

Jeremy Wilkinson[1], Povl Abrahamsen[1], Robbie Mallett [2]

[1]UK.BAS
[2]UK.UCL

Grant-No. AWI_PS129_01

Outline

While climate models suggest that Antarctic sea-ice extent should reduce in response to rising atmospheric CO_2, satellite observations reveal that during 1979-2015 the opposite was in fact true. The trend in Antarctic sea-ice extent has been a small increase of approximately 1.5 % per decade. In 2016, however, this increase was abruptly interrupted by a dramatic reduction in sea-ice extent that was far outside the previously observed range. Neither the increasing trend nor the rapid decline are authentically simulated by climate models, casting doubt on their ability to represent associated processes, including Southern Ocean heat and carbon uptake, melting of the Antarctic ice sheet and many other aspects of the Southern Hemisphere climate.

Since the extreme event in 2016, Antarctic sea-ice extent has almost returned to its pre-2016 values, but this year it plummeted to a new summer minimum, thus highlighting the significant variability in Antarctic sea-ice conditions that can occur from one year to the next. Understanding the reasons behind these dramatic changes is essential, as sea ice is the glue that binds all parts of the unique Antarctic marine ecosystem together, and variations in sea- ice extent can impact the Earth's climate. These recent extreme swings in Antarctic sea-ice extent and the challenge of accurately predicting, understanding and modelling them emphasise the need to:

- increase our knowledge of the processes that drive Antarctic sea-ice variations, including extreme events, and
- understand the drivers and climate implications of Antarctic sea-ice loss over different time-scales, from weeks to decades.

Addressing this knowledge gap requires a significant research programme, one that takes year-round observations, including throughout the harsh Antarctic winter, and is effective in improving the underlying processes in the latest computer climate models. Our project, known as DEFIANT (Drivers and Effects of Fluctuations in sea Ice in the ANTarctic), will embark on one of the most ambitious campaigns aimed at understanding Antarctic sea-ice variability. This £5 million project unites sea-ice physicists, oceanographers, meteorologists and modellers in order to assess the consequences of Antarctic sea-ice variability over different spatial and temporal scales. Through this interlinked programme of observations, model development and model evaluation, DEFIANT will deliver a step change in our understanding of the Antarctic sea-ice system.

Objectives

Freeze-up is the season where substantial changes occur in the upper ocean. For example, the warm, fresh summer surface layer must have its temperature reduced to the freezing point to allow ice formation to progress. Thus, monitoring autumn mixing rates, heat fluxes, sea ice/snow mass balance and upper-ocean properties is essential to understand sea-ice formation and variability. Collaboration with AWI's HAFOS project through PS129 provided the DEFIANT team broad access to the Weddell Sea during freeze-up. With this in mind, we had five interconnected objectives. These were:

1. to quantify ocean and under-ice turbulence using microstructure measurements,
    a. large-scale survey of microstructure temperature variance (Chi-pods), and
    b. parameterisations of fine-scale shear/strain to directly and indirectly quantify the intensity of turbulence
2. to perform on-ice surveys of radar reflectivity of snow properties (Ku/Ka band radar)
3. to understand the partitioning of solar radiation into incoming, reflected and transmitted, to better understand the attenuation of light through snow and sea ice
4. to deploy two clusters of two ice-tethered assets (i.e., four buoys on two floes)
5. to perform 18O measurements of the upper-ocean.

In addition to the above-mentioned objectives, we were also sent daily, high-resolution satellite images of the Weddell Sea, in order to improve our day-to-day tactical planning for our on-ice operations. We were able to provide support for the autonomous vehicles used within the EU Horizon 2020 funded SO-CHIC (Southern Ocean Carbon and Heat Impact on Climate) project.

Work at sea

To perform their work, the DEFIANT team were reliant on the *Polarstern* being within the sea ice zone. When not is this zone, the team were available to help with CTD sampling. It was planned that most of the objectives of the sea-ice work would be performed during the two legs to the southern region of the Weddell Sea (stations 71-79 and 89-95). Ideally this work was to be ship-time neutral, as the team would use helicopter support to establish ice stations whilst the ship was involved with other tasks. The only exception was the deployment of the ice tethered profiler (ITP) buoy, which would need some ship time as it is a difficult and complex deployment.

The combination of (i) bad weather, (ii) over-runs in timings of science operations within the schedule, and (iii) the non-closure of the Posidonia window (which limited the ship to a maximum of speed to 5 kt in the ice) meant that the schedule for on-ice operations was squeezed. Because of these time constraints, the southern legs where the ship would venture deeper into the sea ice could not extend as far south as originally planned. This was disappointing, as it was during these legs that the main areas of the DEFIANT project would perform their work. The decision had a detrimental impact on the amount of sea ice-based work we could achieve.

Additional sea-ice work from the helicopter was possible on the western stations of the Weddell Sea, as the ice had begun to form in these regions. Unfortunately, DEFIANT was not alone in the call on helicopter time whilst the ship was in the ice. There were five groups that also needed to use the helicopter. The combination of the weather and the number of teams needing to use the helicopter, the result was a squeeze on helicopter time available to us. A breakdown of all the ship and helicopter ice-based work performed by the DEFIANT team can be seen in Table 6.1. We had two aborted flights due to bad weather, on 8 April 2022 (no measurements) and 23 April (one ice core obtained).

Tab. 6.1: DEFIANT ice operations during PS129

Date in 2022	Start operation time	Stop operation time	Approximate science time on ice**	Description
17 March	08:00	08:40	0.5 hrs of radar operation	Radar Ship: Radar survey of pancake ice from Polarstern’s mummy chair
9 April	11:20	13:57	2.5 hrs of flying ITP equipment to floe	ITP deployment Helo: Moving people and ITP equipment to floe, around 5 flights
9 April	14:50	18:00*	5 hrs for deploying ITP	ITP deployment (continued) Ship: Moving ITP heavy equipment to floe. Stayed with us whilst we installed ITP. Second buoy instalment (WIMBO) failed due to mechanical failure of ice drills.
11 April	09:00	11:45	3 hrs of radar and light measurements	Radar and buoy deployment Ship: Deployment of WIMBO buoy and Radar measurements using ship’s mummy chair.
16 April	13:11	18:43*	2.5 hrs of radar and light measurements	Radar and light measurements Helo: Radar and light measurements (performed with the ice coring team). Three flights needed
17 April	12:12	18:04*	3.25 hrs of radar and light measurements	Radar and light measurements Helo: Radar and light measurements (performed with the ice coring team). Two flights needed
19 April	11:44	17:10*	2.25 hrs of radar and light measurements	Radar and light measurements Helo: Radar and light measurements. Two flights needed
22 April	12:57	18:44*	3.5 hrs of radar and light measurements	Radar measurements Helo: Radar measurements. Two flights needed. Performed with the under-iceberg team

** Note: Stop operation is when the helicopter was finished for the day. In most instances it was performing other work during this time, such as marine mammal surveys, and thus does not reflect when the DEFIANT team were back on the ship.*

*** Note: For helo-based work, the science time is based upon when radar was turned on at start of the day’s measurements and turned off just before pickup. For actual time on the ice could add 40 minutes to include setup and breakdown of radar.*

Besides the on-ice work, the DEFIANT team also installed high-frequency temperature sensors (chi-pods) on the CTD and obtained water samples for ^{18}O measurements to quantify sources of freshwater in the upper ocean.

Preliminary results

The preliminary results from the five objectives are as follows:

1. Upper-ocean and under-ice turbulence

We aimed to use two different systems to quantify oceanic turbulence, from the ship and beneath ice floes. These were Chi-Pods and Sea and Sun Technology MSS90L microstructure profilers. Each is explained below:

1a. Chi-pod measurements

Two "χ-pod" (chi-pod) high-frequency temperature loggers were installed on the CTD/rosette to measure turbulence in the water column. These loggers were developed by, and borrowed from, Jonathan Nash at Oregon State University (U.S.A.). The loggers measure temperature and vertical and horizontal components of acceleration continuously at 100 Hz. These data are merged with the CTD data, aligning the accelerometer data with the CTD's 24-Hz pressure measurements. This is used to derive the dissipation rate of temperature variance (χ), which in turn can be used to derive the diffusivity of heat. Using the assumption that the diffusivities of density and heat are equal, the dissipation rate of turbulent kinetic energy ε can also be estimated.

The systems consist of a logger housing, which holds two lithium D cells (we used SAFT LS33600 cells) and three circuit boards (logger, acceleration and temperature boards). The logger has two wet-pluggable Seacon bulkhead connectors, a four-pin connector on the top, which is connected to a USB port on the logger board and a four-pin connector on the bottom, two pins of which are used as a switch for the power going to the logger (the negative battery wire passes through these pins, which are shorted in the connector on the logger cable) and two pins which are used to measure the resistance across an FP07 thermistor. The thermistor is housed inside an aluminium housing with two o-rings, connected with a four-pole phone jack, with a two-pin connector on the bottom. Either a four-foot or six-foot cable connects the logger housing and sensor holder.

Work at sea

The two logger housings were mounted on the rosette behind Niskin bottles 16 and 17. An upward-looking instrument was mounted on a steel pole attached to the side of the rosette near bottles 20-21, protruding 26 cm above the top of the rosette itself, 204 cm above the base of the rosette. A downward-looking instrument was mounted on a pole on the inside of the rosette, 3 cm above the bottom of the rosette frame. 6-ft cables were run from the sensors to the bulkhead connector on the bottom of the loggers. Because of the geometry of the rosette, a Niskin bottle had to be removed or lowered to access the bulkhead connectors on the top of the loggers. The locations of the sensors and loggers on the rosette at the start of the cruise are shown in Figure 6.1. The downward-looking logger and sensor were removed after station 59. After station 94, the upward-looking chi-pod logger was moved to the outside of the rosette, on the inside of a stanchion between bottles 20 and 21, making access to the logger for data downloads considerably easier.

Fig. 6.1: Photographs of the upward-looking sensor, logger housings and downward-looking sensor on the CTD/rosette at the start of the cruise

The loggers start logging five minutes after the sensor cable is plugged in, providing electricity to the logger board. Before the cable is unplugged, logging needs to be stopped by connecting a USB cable to the bulkhead connector on the top of the logger and stopping acquisition manually. Unless acquisition is stopped before unplugging, file system corruption can occur if power is lost while data are being written to the memory card. After station 102, the power connectors on the upward-looking logger were reconfigured to circumvent the bulkhead connector, with power supplied directly from the batteries to the logger board.

Tab. 6.2: Chi-pod instrumentation used on PS129

Housing	Logger	Sensor holder	Sensor cable	Sensor
Ti44-2 (down)	2018	1 (1-49)	24-6-5 (1-40)	11-67DAS (1-40)
			24-6-4 (41,47-49)	10-06MP (41,47-49)
		4 (58-59)	24-6-4 (58-59)	10-06MP (58-59)
Ti44-11 (up)	2030 (1-59)	4 (1-49)	24-6-7 (1-88)	14-33D (1-40)
				14-34D (42-49)
		7 (58-70)		11-67DAS (58-70)
	2008 (60-88)	4 (71-74)		10-06MP (71-74)
		7 (80)		14-18D (80)
		4 (86-123)		14-14D (86-123)
	2030 (96-123)		24-4-4 (96-123)	
Ti44-8 (spare)	2008 (1-59)	n/a	n/a	n/a

The instruments had previously been used on a cruise by Woods Hole Oceanographic Institution (WHOI, U.S.A.) and had not been serviced or inspected before use on this cruise. Some of the equipment was in poor condition, with one sensor holder flooded on arrival, and severe corrosion on the two others supplied. The sensor/power bulkhead connector on a third logger housing had an intermittent loose connection affecting both power and signal; this was not used, except occasionally in the lab for testing spare sensors.

To enable us to use the damaged sensor holders, we potted the sensors into the holders, covering the corroded areas with Sikaflex 291i marine adhesive sealant. Once this had cured for at least 12 hours, it was covered with self-amalgamating rubber tape (Scotch 23 or generic) and Scotch 33+ vinyl electrical tape. This provided a waterproof repair that appeared to work for much of the cruise.

After several good casts, the upward-looking instrument exhibited an increasing amount of spiking and shifts in temperature during stations 27-40. The holder was removed during station 41, while the sensor was changed from 14-33D to 14-34D. This appeared to solve the problem, though there was severe temperature spiking at the end of station 42, possibly because the instrument was partially out of the water during the near-surface bottle stop at the end of the cast. On stations 47 and 49, the data were noisy and full of shifts. The sensor holder was removed on station 52.

The downward-looking instrument provided good data on the first four deep casts, but then exhibited poor calibration on station 30. On station 40 the temperature voltage increased to the maximum and stayed flat when the instrument was submerged below approximately 70 dbar, partially recovering when the instrument reached 60 dbar on the upcast, indicating a short circuit at higher pressures. Since some corrosion was visible on the connector end of the instrument, including near the bulkhead connector, and since the other sensor holder appeared to have epoxy around the connector, Sikaflex was applied around the connector, and once cured this was covered with self-amalgamating tape and vinyl tape. In addition, the sensor cable was replaced with a spare. However, this did not solve the problem, and the short circuit appeared worse on station 49. The sensor holder was removed on station 52.

After station 52, the sensor holders were inspected. Sensor holder 1 was disassembled. The metal of the holder body was in poor condition because of corrosion. The brass bulkhead connector was oxidised, but the o-ring and thread were in good condition and there was no sign of water ingress. Resistance across the two terminals was approximately 25 MΩ. The wires soldered onto the phone jack socket were not insulated, though it is unclear whether this could have contributed to the short circuit problem.

Sensor holder 7 was also disassembled; apart from some pitting on the outside of the case the metal was in good condition. The bulkhead connector at the end of the case was in poor condition: the o-ring was considerably deformed and the thread and base had signs of corrosion. Resistance between the two terminals varied across the day between 450 kΩ and 3 MΩ, but with 2-3 MΩ resistance from the terminals to the housing. This connector was not considered serviceable. The phone jack socket was in surprisingly good condition for being immersed in seawater for two months. The sensor holder was rebuilt using the bulkhead connector and phone jack socket from holder 1 (with electrical tape applied around the outside of the terminals on the phone jack socket to prevent contact with the housing). To check whether the short circuit could be in the bulkhead connector on the logger or in the sensor holder, holder 4 was installed as the downward-looking sensor, while holder 7 was installed looking up. Sensor 10-06MP was potted into sensor holder 4, while sensor 11-67DAS was installed into holder 7 without any additional waterproofing applied. The four best o-rings from the spare sensors were chosen to minimise the risk of water ingress.

The chi-pods were used again on stations 58 and 59. After station 59, the USB cable was plugged into upward-looking logger 2030 and logging was stopped. A directory listing was performed and upload was started. However, at that stage the software crashed and when communications were attempted with the logger afterwards, it refused to display a prompt. Eventually, the logger was removed from the rosette and brought into the lab. Here attempts to communicate through the bulkhead USB cable and the mini-USB connector on the circuit board both had the same result: occasionally the logger displayed its serial number and time when communications were established, but a prompt was never displayed. The clock battery was also disconnected to remove all power, but without any change (apart from resetting the time). At this stage, logger 2008 was installed into housing Ti44-11 to ensure that a working logger was on the rosette in advance of the next CTD cast.

Eventually, the memory card from logger 2030 was removed and inserted into the computer. A directory listing was performed with the “ChiPod2File.exe” program, but this only listed the first 127 files, while the latest file on the chipod was number 137. Attempts to manually download the file failed, as the software appears to be unable to read file numbers above 127. A blank memory card was installed into logger 2030, which promptly booted and appeared to work correctly. The remaining files were extracted from the memory card after reverse engineering the (very simple) format of the file system.

Data were downloaded from logger 2018 without problems, though these showed a short circuit on the temperature sensor throughout. While still connected to the rosette, but with the sensor cable disconnected, the logger still showed a high, constant temperature voltage. The logger was then brought into the lab, resistance was checked across the bulkhead connector and the pins were found to have resistance on order of a few tens of kΩ. When the bulkhead connector was disconnected, raw readings decreased to just over 1000 counts (as expected for a disconnected sensor), but with the bulkhead connector connected to the temperature circuit board, these increased to over 25000 counts. The spare temperature board was tested with and without the wire to the bulkhead connector, with the same result. As a result, logger 2018 was not replaced onto the rosette and the downward-looking sensor holder was also removed from the rosette before station 60.

With the sensor still giving noisy data, the sensor holder was swapped again before station 80. However, on this station the upward-looking sensor holder (number 7) flooded. The holder was removed and on station 86 it was replaced with holder 4, fitted with sensor 14-14D. On the first cast, the sensor cap was accidentally left on. On the second cast, the logger saved only zeros (and time stamps) and the third cast had poor data quality.

At this stage, the logger was removed from the system again, along with the upward-looking cable. Logger 2008 was removed from the housing and logger 2030 was re-installed, with a blank SD card. One of the wires on the plug from the bulkhead connector to the temperature board was found to be in poor condition, with only two strands of the wire remaining. When this was inspected further, these also broke. The end of the wire was then soldered onto the end of the crimp terminal from the connector.

On the following cast, station 96, the bulkhead connector was shorted at depth. Low resistance was measured between the two sensor wires when pins are inserted into the female connector (either a dummy plug or a connector cable). The endcap from Ti44-2 (where the bulkhead connector had previously failed in a similar way) was installed onto Ti44-11 as a test. Although there are problems with calibration, with noticeable drift on some casts (presumably from varying resistance in the connector), this resulted in some usable data in later casts.

On stations 100 and 102, the loggers stopped collecting data during the casts. This is assumed to be a problem with the pins switching the power through the bulkhead connector. As a result, the battery pack was wired directly to the logger, circumventing the switch in the sensor cable. This resulted in data being continuously collected from the morning of 20 April onward, except while downloading data files. The last cast was collected on station 123. After this cast, the batteries had to be removed from the data logger for shipping back to AWI, so there are no chi-pod data on station 127.

In summary, we collected chi-pod data on 51 CTD stations, resulting in five successful downward-looking profiles and 20 successful upward-looking profiles (Tab. 6.3). Because of problems with the loggers and sensors, many of the other casts likely do not have usable data. However, it might be possible to process some further casts to obtain usable microstructure data. Analysis of these data will be led by Gwyn Evans and Alberto Naveira Garabato at the University of Southampton, and Eleanor Frajka-Williams (formerly at the National Oceanography Centre, Southampton, now at the University of Hamburg).

Recommendations

The chi-pod loggers should be fully checked and overhauled, with new bulkhead connectors fitted for the sensor connections. On future cruises, spare bulkhead connectors should be supplied, along with spare o-rings for the sensors and blanking plugs for the sensor end of the sensor cables. The sensor holders should be replaced, ideally with ones made from a more durable material, and all sensors checked or replaced. The wire connectors from the bulkhead connector onto the temperature board and battery wires are vulnerable to damage when the endcap is screwed on, and several were broken during the cruise. A better solution needs to be found for this, perhaps involving a strain relief for the wires on the end of the circuit board, or use of a pressure housing that does not twist the wires when the endcap is installed.

It is unclear whether the loggers can support more than 128 files: they appeared to function with more files, but one eventually crashed and the software supplied does not support downloading extended files. Better documentation of the disk format and file numbering and more stable software would be welcome. For trouble-shooting purposes, it would be useful if the software had a feature to save the communications log.

The processing scripts in Matlab contained several bugs and inconsistencies that made data processing more difficult. The changes from this cruise will be submitted as a pull request to GitHub to benefit future users of this instrumentation.

Tab. 6.3: Cast status. Legend: green = good; yellow = issues, possibly fixable in software; orange = poor data quality; red = bad, unusable data; grey = not installed

Cast	Downward status (2018)	Upward status (2030/2008)
014_01	Good (shallow test cast)	Good (shallow test cast)
018_07	Good	Good
023_01	Good	Good
025_08	Good	Good
027_02	Good	Spikes, offset at times
030_01	Poor calibration	Lots of spikes
040_02	Flat lined temperature at depth	Spikes at start, poor calibration
041_02	Flat lined temperature at depth	Not installed
042_01	Not installed	Good except near surface at end
047_01	Flat lined temperature at depth	Spikes and shifts throughout
049_01	Flat lined temperature throughout	Few spikes, but shifts throughout

Cast	Downward status (2018)	Upward status (2030/2008)
053_03	Not installed	Not installed
058_02	Flat lined temperature throughout	Good
059_01	Flat lined temperature throughout	Good
060_01	Not installed	Good
062_04	Not installed	Good
064_02	Not installed	Good
065_01	Not installed	Good
068_01	Not installed	Good
070_01	Not installed	Spikes and shifts throughout
071_02	Not installed	Spikes and shifts, but processes
072_01	Not installed	Spikes and shifts throughout
072_03	Not installed	Spikes and shifts, but processes
074_04	Not installed	Spikes and shifts throughout
080_02	Not installed	Sensor holder flooded – flat line
081_01	Not installed	Not installed
083_02	Not installed	Not installed
086_01	Not installed	Forgot to remove sensor cover
087_01	Not installed	Chi-pod saved nothing but zeros
088_01	Not installed	Noisy mess
096_01	Not installed	Flat lined temperature at depth
097_01	Not installed	Spiky, poorly calibrated
099_01	Not installed	Less spiky, but poorly calibrated
100_03	Not installed	Poorly calibrated, stopped early
102_01	Not installed	Poorly calibrated, stopped early
103_01	Not installed	Spikes on downcast, poorly calibrated
104_01	Not installed	Spikes, shifts, poorly calibrated
105_01	Not installed	Few spikes, one big shift on downcast
106_01	Not installed	Lots of spikes, poorly calibrated
107_01	Not installed	Lots of spikes, poorly calibrated
109_03	Not installed	Lots of spikes, poorly calibrated
110_01	Not installed	Lots of spikes
111_01	Not installed	Lots of spikes
112_01	Not installed	Lots of spikes, but still processes
114_02	Not installed	Good
115_02	Not installed	CTD sensor frozen, no calibration
116_01	Not installed	Good
117_01	Not installed	Spikes in start, then better
119_01	Not installed	Good
120_01	Not installed	Good
121_01	Not installed	Some spikes, rest might be OK
122_01	Not installed	Some spikes, rest might be OK
123_01	Not installed	Lots of spikes, poorly calibrated
127_03	Not installed	Not installed

1b. Microstructure measurements under sea ice

There were plans to conduct microstructure measurements beneath sea ice, to measure the turbulent mixing during sea-ice formation. The goal was to take multiple profiles over several hours using a Sea and Sun Technology MSS90L microstructure profiler. However, several factors prevented this work from being carried out. Two people were required to conduct this work (one to run the computer and winch, another to handle the wire) and the equipment was a full helicopter-load: the profiler itself plus a spare, Zarges boxes containing the winch, wire, winch control box, cables, laptop, deck unit and tools, a generator, and a drill and drill flights.

An ice drill capable of creating a hole of at least 255 mm diameter (the outer diameter of the sensor protection cage) was required. Because of the failure of the two Jiffy drills supplied by WHOI and the ship's small Echo EA-410 drill turning the opposite direction to the Jiffy drills, the only drill we had available was the ship's large Stihl BT 360 drill, which would require a further helicopter load and four or five people to safely operate.

Unfortunately, the time required to conduct long stations on the ice was not available to us during the cruise (with the exception of the combined radar and ROV ice station on 22 April 2022), and the limit of five people working on the ice at any time made it impossible to conduct more than two types of measurement at once (e.g., light and radar, radar and ROV). If we had full days for ice stations while the ship was occupied with measurements in the ice, this would be possible, but with only a few hours and pressure to conduct other measurements with the limited personnel numbers able to go onto the ice, the microstructure measurements were not carried out.

2. Radar reflectivity of snow properties

Satellite-mounted radar altimeters emit radar waves and detect their reflections. In the case of snow-covered sea ice, it is unclear where these reflections come from in some radar frequency ranges (the Ku and Ka bands). Some power seems to be reflected from the snow–air interface, and some from the snow–ice interface. Power can also be reflected from layering in the snow. We brought a high-resolution, Ku- and Ka-band sled-mounted radar 'KuKa' to investigate this. By emitting short pulses of radar energy and precisely timing their return, it is possible to calculate the distance from which they were reflected.

Our goal was to deploy 'KuKa' on snow-covered sea ice and measure the power returned to the radar instrument as a function of height. By then digging coincident snow pits, we aim to understand how snow properties influence radar reflectivity. In particular, we aimed to quantify the fraction of returned power that was reflected from the ice–snow interface at Ku-band, and the fraction that returned from the snow–air interface for Ka-band. It is commonly assumed that Ku (Ka) band satellite altimeters receive reflections solely from the ice–snow (air–snow) interface.

We also designed a short pilot study to establish the features of Ku/Ka backscatter from thin pancake ice and characterise the sensitivity of radar waveform shape to target range. This study was conducted using the ship's crane.

Work at sea

At each site, a patch of snow was scanned at the two radar frequencies (one after the other). The snow depth was then measured, and its stratigraphy was characterised. Key properties of its layers were then measured: temperature and density. At some sites the snow grain types were analysed. Photographs were also taken of the snow patches and pits.

In total six floes were visited with the radar, with only five measured as the first visit was aborted immediately due to impending bad weather. The first floe that was measured was visited by ship, with the subsequent four visited by helicopter. The five floes that were measured will be labelled in this report as F1-F5 (Tab. 6.4).

Tab. 6.4: Ice floes surveyed with KuKa radar during PS129

Date	Floe code	# Pits	Approx. Position	Duration of KuKa operation	Time first KuKa measurement (UTC)	Time last KuKa measurement
11/4	F1	2	68.983°S 31.939°W	2h24m	09:21	11:45
16/4	F2	2	66.447°S 41.402°W	2h18m	14:38	16:56
17/4	F3	5	65.763°S 44.794°W	3h18m	13:17	16:35
19/4	F4	3	64.306°S 47.367°W	2h09m	13:15	15:24
22/4	F5	5	63.508°S 51.385°W	3h25m	14:05	17:30

F1 was accessed by mummy chair from *Polarstern* and measurements were performed by R. Mallett and David Barnes (BAS). F2-5 were accessed by helicopter with measurements performed by R. Mallett and J. Wilkinson.

Radar/crane

In addition to the above surveys, a crane-based radar survey was taken over thin pancake ice. During the survey the radar in the crane was moved in 1 m increments up to a height of 16 m above the surface and then back down to 2 m from the surface. At this point the ship moved off at 1 kt while the radar scanned the surface.

Mallett and Wilkinson conducted this survey beginning at 8:00 UTC 28 March 2022 and ending at 9:00. Both were present in the mummy chair along with the radar. The crane was operated by a member of the crew, who was communicating with Mallett via shortrange radio. The radar had a downward-looking GoPro mounted on the Ku-band arm. Two additional downward looking GoPros were attached to either side of the mummy chair, with the intention of inferring ice roughness using structure-from-motion. Unfortunately, one of them didn't function correctly due to a loose battery connection. Furthermore, the mummy chair experienced larger vertical motion than expected due to the heave of the ship and stretch in the crane cable. This meant that the photography interval on the two remaining GoPros was too low for effective structure from motion. The radar instrument functioned nominally throughout the pilot.

Preliminary results: Radar reflectivity of snow properties

Crane work

Preliminary results of the crane-based pilot study reveal the expected sensitivity of both radar frequencies to open-water coverage within the footprint of the radar. Because the footprint of the radar increases with height, some simple modelling will be required to further investigate this and also to rectify the downward-looking GoPro images to visually retrieve the open-water fraction. It also appears that the shape of the returned radar waveform from the surface is sensitive to height, indicating that the pulse-limited footprint of the radar is relevant (as well as its beam limited footprint). This may provide valuable information on how to upscale our *in situ* radar surveys to the airborne and satellite-mounted scales.

Ice floe work – Snow pits

Snow stratigraphy at all floes could be characterised by a layer of cold-season (recent) snow over a layer of older snow that was remnant from the summer. In the southern hemisphere these snow conditions are largely endemic to the Weddell Sea. The remnant snow was often undiggably hard due to extended metamorphosis and melting. Coring at floes 3 and 5 revealed that it often featured a smooth transition to almost solid, fresh ice near the base.

Ice floe work – Density and salinity measurments

56 Snow density samples were taken across the 17 snow pits. As well as indicating the stratigraphy of the snow, these samples are essential for adjusting radar ranges for the reduced speed of electromagnetic wave propagation in snow. Density samples were taken with a 250-cc tube-cutter from SnowMetrics and were weighed on board.

A salinity measurement was taken for each snow density sample. In addition, the salinity was also derived from scrapings of several interfaces that were too hard for a density sample. Preliminary analysis indicates that the snow was fresh by comparison to that over first year ice.

Finally, four snow cores were transported back to the ship from F5. Visually, these illustrated the transition in the remnant snow of low-density snow near the top to almost solid ice near the base. Density and salinity profiles were derived from these cores, although it was often unclear whether they extended to the sea ice surface.

Ice floe work – Radar

Frequency-modulated continuous wave (FMCW) radars such as ‘KuKa’ suffer from a phenomenon known as range sidelobes. These are peaks in the power-range plot that do not correspond to physical positions where radar power is reflected. Instead, they are artefacts from the radar processing. One source of these sidelobes is non-linearity in the frequency ramping of the emitted radar chirp. This can be accounted for using data from radar scans of a large metal plate, which were periodically performed in the field. These data are then used to deconvolve returns from snow, and produce “cleaner” waveforms. It was not possible to perform this deconvolution process in the field or on board.

Because of the above issue, at most snow pits an A4 metal plate was placed on the snow surface and scanned prior to digging the snow pit. Attempts were made to vary the placement of this plate between Ku and Ka horns. The visibility of the plate in the waveforms is useful for unambiguously detecting the peak corresponding to the snow surface and distinguishing it from sidelobes.

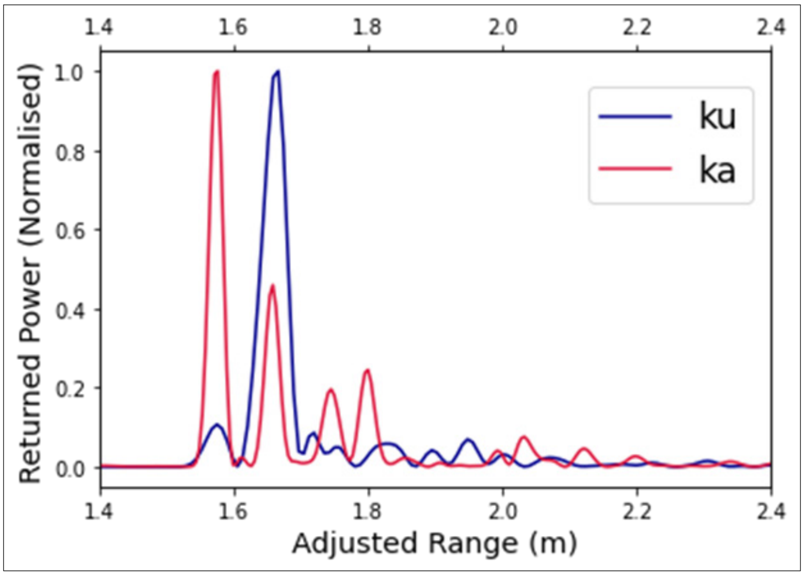

Fig. 6.2: Radar reflections from floe 3 snow pit 3 at Ka- and Ku-frequency. Most Ka band power returns from the snow-air surface (1.57 m radar range), and less returns from the surface of the icy snow below (1.66 m radar range). This is not the case for the Ku-frequency, where most power returns from the surface of the icy snow and considerably less returns from the snow-air interface. No clear peak is associated with the true sea-ice surface, which would be seen between 2 and 2.4 m range (depending on snow density).

Figure 6.2 is an example of the radar data that will ultimately be available for all 17 snow pits that were scanned with 'KuKa' (although it is un-deconvolved). When combined with the observed stratigraphy from the snow pits, we hope to characterise the layering from which radar will and will not reflect. When combined with photos and images from a GoPro camera mounted on the horns of the radar, we also hope to qualitatively characterise snow reflectivity as a function of snow-air interface roughness.

We also carried out an experiment where we artificially smoothed and roughened the snow by hand. The preliminary results of this are promising. At Ku-band frequency there appears to be a relationship between the power reflected by the snow-air interface and its roughness. This relationship is more complex at Ka-band, although the ratio between the reflections from the cold-season snow and the remnant snow are the same at both frequencies.

3. Partitioning of solar radiation

The ice-albedo feedback (driven by solar radiation) is one of the dominant forces that influences sea-ice melt and -growth processes. For example, the more the ice pack opens up, the more solar radiation enters the water column and the stronger the coupling between the ocean and atmosphere becomes. In addition, light is one of the critical drivers of primary production in and under sea ice; it acts as a trigger for sea-ice algae and phytoplankton blooms. We are working with the AWI EWOS II team to determine how chlorophyll content of sea ice impacts the attenuation/absorption of light through Antarctic snow and sea ice. With our measurements, we aim to better understand the partitioning of solar radiation into its three components; incoming, reflected and transmitted in order to better understand the amount of solar energy reaching the ice bottom.

A standard protocol was used for all sea-ice stations. Photographs were taken at all stages to document the conditions, all people handling the ice cores wore latex gloves. Hyperspectral light measurements were made with the TriOS RAMSES sensors. The process ran as follows:

Step 1: site set-up

- Find a level site and check ice thickness
- Drill first 9 cm core (core 0)
- Remove core, visual inspection and photograph core.
- Measure temperature at 20 cm intervals down core.
- Cut core up into 20 cm sections and place in separate bags for salinity and possibly nutrient analysis.

Step 2: radiation measurements

- Measure the incoming and reflected light field and deploy L-Arm through core 0 hole to measure under ice light in 3 positions, see Figure 6.3 (0 degrees: Core 1; 90 degrees: Core 2 and 180 degrees: Core 3) in the direction desired. We ensured the sun was in front of us and no shadowing of the readings occurred.
- Mark the position of the previous L-arm measurements (with pencils in the snow); these will be 1.05 m from core 0.

Step 3: cores 1 to 3

- At each corresponding point of the under-ice L-arm measurements, drill and extract an ice core (labelled core 1 to 3).
- Photograph each core and place in a plastic bag for chlorophyll analysis.
- measure ice thickness, freeboard and snow depth at each core site.

Step 4: snow and ice thickness

- Measure ice thickness, freeboard and snow depth at each core site.
- Put GoPro down hole to video under-ice conditions.

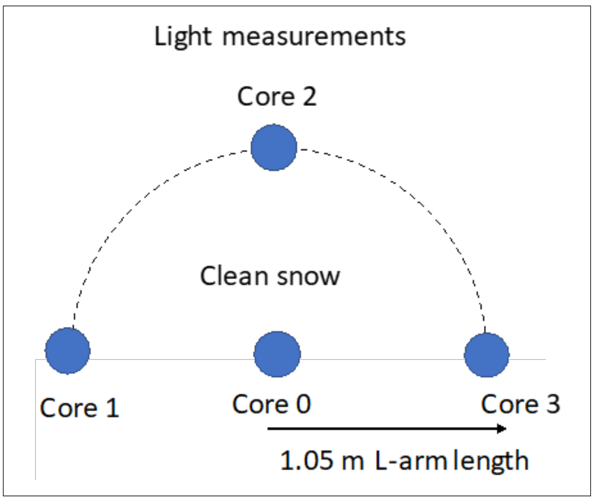

Fig. 6.3: Layout of radiation measurement sites with core locations

Work at sea

Due to the limited time available on the ice, we were able to perform detailed snow/ice/light measurements on just three ice floes. The locations are given in Table 6.5.

Tab. 6.5: Location of light measurement sites

Location name	Date	Latitude	Longitude	Measurement sites
PS129-91	16 April	S66° 27.412’	W41° 24.487’	1 site: labelled A
PS129-93	17 April	S65° 45.683’	W44° 47.775’”	2 separate sites: labelled A & B
PS129-99	19 April	S64° 18.616’	W47° 21.649’	1 site: labelled A

Interestingly, all these sites were on young ice between 30-50 cm thick. As they had only a limited snow cover (just a few cm) these readings will provide valuable information on the light transmission through newly formed ice. An example of photographs from PS129-93 ice light station 1 site A is shown in Figure 6.4.

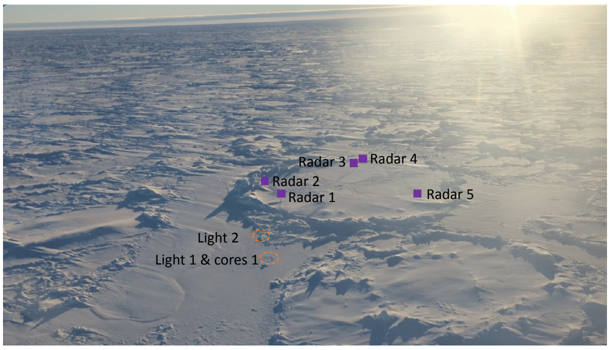

General ice conditions surrounding the light measurements which were obtained on a newly frozen lead next to multiyear ice.
Photo: R. Mallett

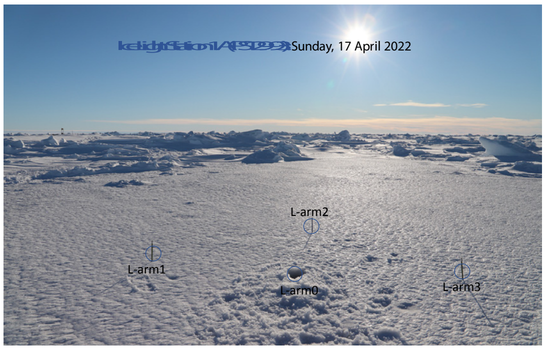

Local snow surface surrounding the L-Arm measurements; note core 0 has already been drilled.
Photo: Hauke Flores (AWI)

Under-ice conditions at the measurement site
Photo: J. Wilkinson

Core 1: Ice thickness (Nut) L-Arm0
Photo: Hauke Flores (AWI)

Fig. 6.4: Example of photographs from PS129-93 ice light station 1 site A

4. Deploy two clusters of two ice-tethered assets

The major task was the deployment of four on-ice buoy systems. These systems were co-ordinated to be deployed together in pairs (known as clusters) on two separate floes. Each cluster contained:

- Cluster A: ITP-V (Ice tethered profiler velocity) buoy + WIMBO-RAD (weather, waves, ice mass balance and ocean- solar radiation) buoy
- Cluster B: WIMBO-TS (weather, waves, ice mass balance and ocean – temperature - salinity via a 120 m chain) + WIMBO-RAD (weather, waves, ice mass balance and ocean- solar radiation) buoy

A short description of the buoys is as follows:

ITP-V: Profiles of temperature, salinity and velocity, and burst measurements of turbulent fluxes of heat and momentum are obtained from a profiler that crawls along a wire suspended from a surface buoy. The ITP-V has an 800 m wire (hence deep-water deployment) and will float after the ice melts. Profiles will be taken every four hours.

WIMBO-TS: Monitors meteorological parameters including incoming solar radiation, wind speed and direction, air temperature, pressure and humidity; ice and snow properties via an ice mass balance (IMB) sensor string, freeboard sensor and sonar; upper-ocean properties via a 120 m T-S chain with temperature (0.25 m) and salinity/pressure (5 m) and wave properties via an IMU. The system has a 360˚ underwater and in-air camera, and floats after the ice melts. As with their Arctic deployments, WIMBOs will sample every 10 minutes in summer (when sun is up) and hourly in winter.

WIMBO-RAD: Similar to the WIMBO-TS, but without T-S chain. It is connected to a series of radiometers recording incoming, reflected and transmitted solar radiation.

Once deployed, the ITP-V is powered by lithium batteries, whilst the WIMBO systems have an upper frame with three solar panels mounted vertically to recharge internal lead acid batteries to provide power during the daylight months; and primary alkaline batteries to power the system through the dark winter. The system measures battery and solar charging voltages continuously and automatically. The two-way Iridium RUDICS communication protocol is used by the ITP-V, whilst the WIMBO system uses the new Iridium CERTUS system for communication. Both can be remotely configured over the satellite link as desired.

The plan was for cluster A to be on a floe near the mooring site during the first southerly excursion to the Weddell Sea, and the second deployment, cluster B, was to be on a floe at the second southerly excursion to the Weddell Sea. These deployment combinations were aimed at allowing us to monitor the near-surface atmosphere; the ice itself and the water beneath (i.e., atmosphere-ice-ocean interactions) over a wider distance. The deployment of two clusters of ice-tethered assets allows us to sample through the crucial winter period. It is expected that each cluster will take over 12 months to drift through the Weddell Sea.

Work at sea

At the start of the cruise all buoys were unpacked, built and tested to ensure they worked. The ITP-V surface unit was strapped to the railing on the monkey island and the WIMBOs were all build up and each sensor tested (Fig. 6.5).

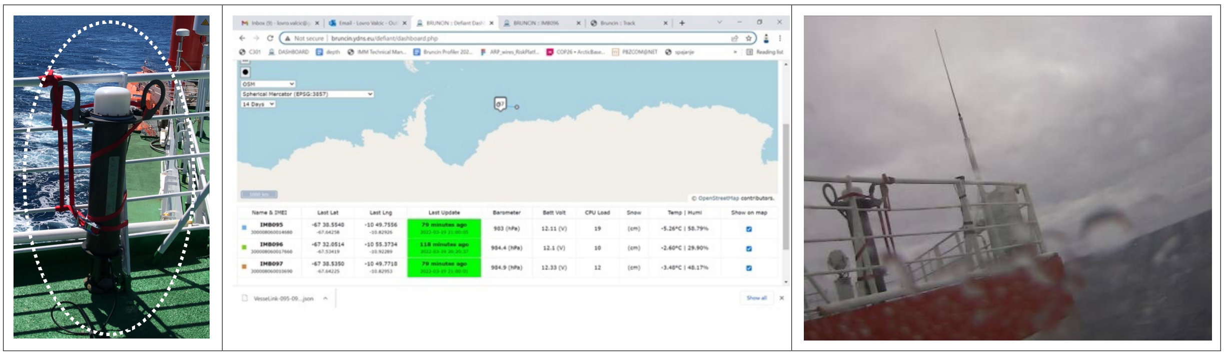

Fig. 6.5: Photographs of the ITP deck unit, WIMBO control centre and a photograph taken from a WIMBO buoy during on-board testing: ITP-V deck unit test (left), WIMBO control centre showing green. All WIMBOs functioning correctly (middle), Photograph from a WIMBO during the on-board tests (right)

Deployment of cluster A: the opportunity to deploy the two buoys that made up cluster A became available on 9 April 2022 (Fig. 6.6). The assembled deployment team were: Team ITP: Jeremy, Povl and Mareike; Team WIMBO: Robbie and Marie.

ITP-V: Initially, Povl and Jeremy were flown out to the floe, followed by the equipment, then Robbie, Mareike and Marie joined. The reel that held the ITP wire was too heavy for the helicopter so that had to be craned off the *Polarstern* and onto our floe.

As soon as the team was on the ice, we started to drill the hole for the deployment (Fig. 6.6), after which Robbie and Marie broke off to deploy the WIMBO. Whilst the ITP-V is not difficult, there are many steps involved. By the time we were finished, it was getting dark (Fig. 6.6). The status of the ITP-V at present is that it is profiling as expected, however there is a potential issue with the pump on the CTD. It seems to have stopped working, resulting in attenuation of both temperature and conductivity data, as water does not flow freely past the sensors. It is unclear whether these data will be usable with some further processing.

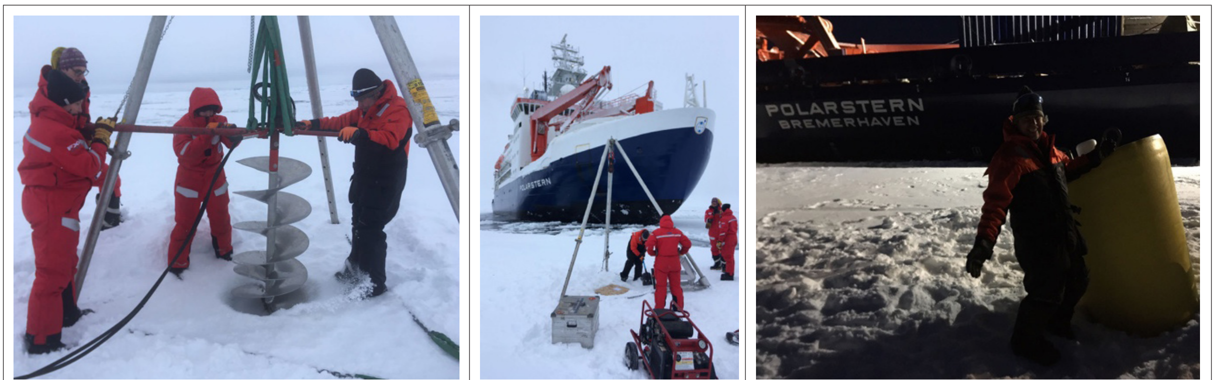

Drilling the hole for the ITP-V	*Polarstern* coming alongside to drop off the wire reel	A long day, finally the ITP-V is fully deployed

Fig. 6.6: Photographs of ITP-V deployment during PS129

WIMBO-RAD: We decided to deploy WIMBO-RAD:095 next to the ITP-V. During the drilling of the holes for the WIMBO-RAD the starter cords of both Jiffy drills broke. This was a strange thing to happen as it was not that cold, but the plastic housing surrounding the starter cord shattered. This issue meant the motors could not be started and as a result the deployment of the WIMBO-RAD had to be aborted until we could fix or find another drill.

A second chance to deploy WIMBO-RAD:095 came on 11 April 2022 with an ice station. There were three teams involved in the station: Team Radar: Robbie and Dave; Team Coring: Hauke, Mareike and Anton and Team WIMBO: Jeremy and Povl. The floe was next to the ship and it was around 1.6 m thick and fairly level. To make the craning of the W095 easier, team WIMBO selected location near the ship (see Fig. 6.7). The plan was to deploy the buoy in four stages:

1. Drill the 12-inch holes that W095 would sit in

2. Crane the W095 to the hole

3. Attach and deploy the underwater sensors

4. Phone the manufacturer (Lovro) to check the system was deployed and check all was well.

Despite some problems with the 12-inch drills we were able to complete stage 1 in a timely fashion and thus we had two holes ready for the next stage. It was decided that we would crane W095 directly into the first hole, and after a small bit of manoeuvring by the crane W095 was seated in its hole, with the other hole being for the L-Arm deployment. There was a bit of bumping of the foot of the buoy on the snow, but nothing that would register concern. We then attached the underwater sensors to the L-Arm (stage 3) and proceeded to deploy it through the second hole. The deployment of the L-arm went smoothly except for the radiometer as it was slightly wider than the hole. We were able to overcome this by chiselling out the hole slightly. Once the L-Arm was deployed we then connected all the sensor cables to the buoy and the manufacturer confirmed that the system worked successfully in every 3 hours as expected, but had missed its last call. This was not much of a concern as the Certus System often misses calls and this would not be unexpected as the ship was blocking access to half the sky. In hindsight this was a mistake as at present we have not been able to communicate with the system and are looking at understanding what went wrong.

Fig. 6.7: Photographs of WIMBO deployment on PS129

Cluster B: unfortunately, the time required to deploy cluster B in the southern Weddell Sea was not available to us during the cruise. Given the drift of the sea ice within the Weddell Sea it did not make scientific sense to deploy this cluster in the western or northern regions as the ice in these regions will drift fairly quickly into open water.

5. ^{18}O measurements of the upper ocean

Seawater samples were obtained from the CTD/rosette for analysis of the stable isotopes of oxygen in the water molecules. The purpose of these measurements is to differentiate sources of freshwater, in conjunction with measurements of salinity. This is done using a mass balance with three endmembers, typically a generic oceanic endmember, sea-ice meltwater and meteoric meltwater from glacial or precipitation sources (Östlund and Hut 1984). The resulting fractions show the contributions of sea-ice melting or -formation and glacial sources to the freshwater in the upper ocean.

A total of 309 samples were collected from the rosette: 35 on the Greenwich Meridian section, 240 from the SR4 Weddell section, 26 south of the SR4 section, and 8 in Drake Passage near Elephant Island. Samples were collected in the upper 900 m on the Greenwich Meridian, and in the upper 300 m on the remaining stations (with a few stations additionally sampled at 400 m). The deeper samples on the Greenwich Meridian were to see any residual signature of deep convection resulting from sea-ice formation at Maud Rise in recent years. The distribution of samples along the ship's track is shown in Figure 6.8.

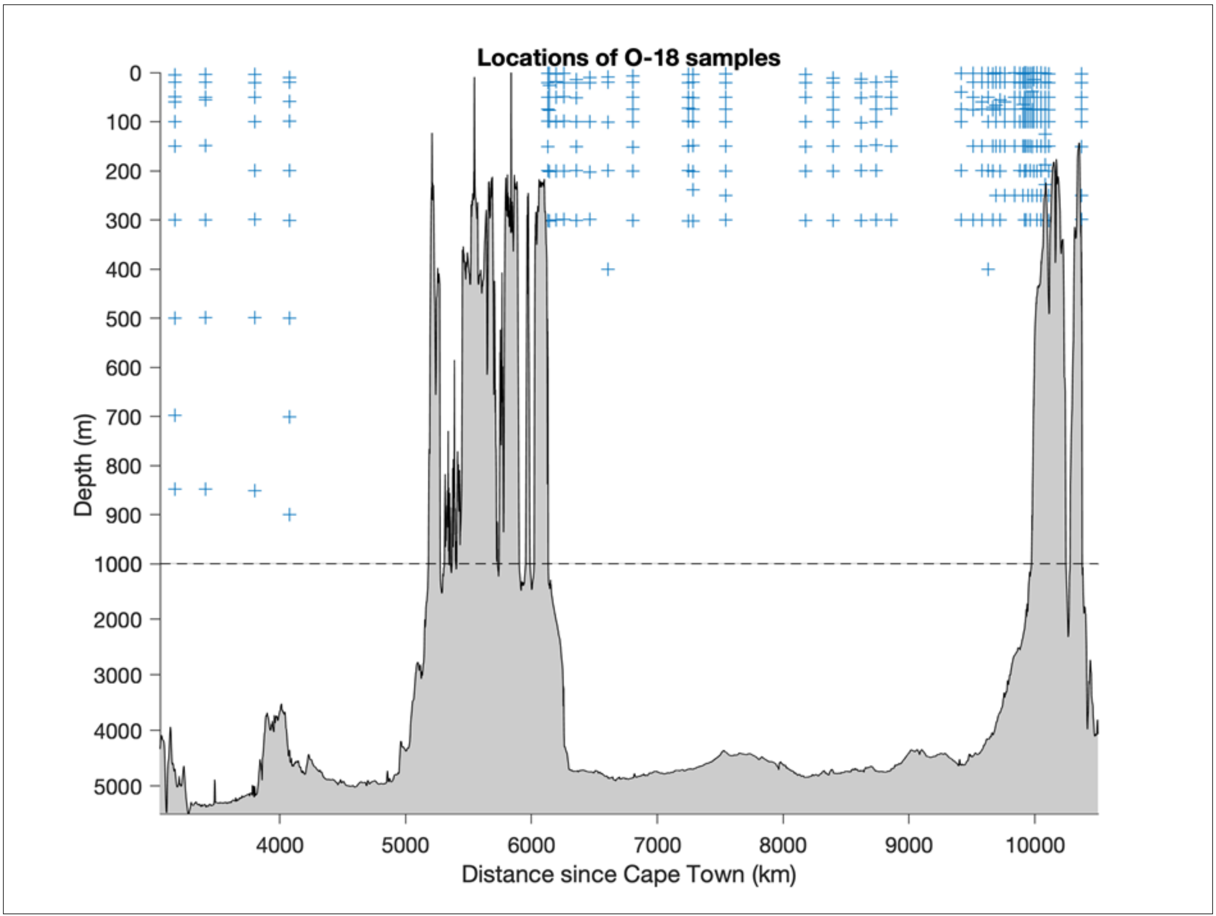

Fig. 6.8: Distribution of ^{18}O samples on the PS129 cruise track, with bottom depths from GEBCO_2014

Additionally, seven samples were obtained at station PS129_89-1. A core from a pancake ice floe sampled at this station was divided into six segments, which were melted in double plastic bags and poured into bottles. A bucket of surface water near the ice floe was also sampled.

Samples from the CTD/rosette were sampled in 50-mL glass injection vials, which were rinsed twice before filling to the neck of the vial. A rubber stopper was then inserted and held in place by an aluminium crimp seal. The samples from station PS129_89 1 were collected in 30-mL HDPE wide-neck Nalgene bottles, which were filled to the brim, with lids screwed on tightly and covered with overlapping layers of electrical tape.

The samples have been consigned to the British Antarctic Survey as refrigerated cargo to avoid evaporation during the transit through the tropics. They will be analysed at the UK's National Environmental Isotope Facility at the British Geological Survey, Keyworth. The oxygen isotope composition ($\delta^{18}O$, the standardized ratio of ^{18}O to ^{16}O relative to VSMOW standard) will be measured using the CO_2 equilibration method with an IsoPrime100 mass spectrometer with an Isoprime AquaPrep on-line sample preparation system, which will equilibrate the samples with CO_2 before passing the equilibrated gas from the headspace of each vial through a cryogenic water trap into the inlet of the mass spectrometer. Isotope measurements will be calibrated against internal and international standards, including VSMOW2 and VSLAP2. Based on duplicate analysis, analytical reproducibility of around 0.02 ‰ is expected for these samples.

Additional measurements – Autonomous vehicles (Slocum gliders and Sailbuoy)

We recovered one offshore sensing (OS) Sailbuoy autonomous surface vehicle, which was later redeployed and we deployed two Teledyne Webb Research (TWR) Slocum G2 oceanographic gliders. These were all part of the EU SO-CHIC project. A cruise for the SO-CHIC project took place on SA Agulhas II in December 2021 to January 2022. However, because of logistical problems two containers with gliders and mooring equipment from the UK did not arrive in time for the ship's departure from South Africa. Sailbuoy "Kringla" (s/n 1812) from the University of Gothenburg was deployed on this cruise, along with two seagliders. We were asked to recover Kringla to download the data from its sensors. Three TWR Slocum G2 gliders (s/n 631, 632 and 633) were sent on the cruise, with 632 as a backup in case of problems with the others. Unlike 631 and 633, 632 was not fitted with an extra battery bay and extended lithium batteries. The two gliders were deployed on 12 March 2022 on station 18; the Sailbuoy was recovered on 15 March on station 25, and redeployed on 17 March on station 27.

The three gliders were all supplied by the British Antarctic Survey (PI: Alex Brearley); their specifications are shown in Table 6.6. After unpacking, they were tested. The clock batteries on both Rockland Scientific International (RSI) MicroRider microstructure probes were replaced and the cable connecting the MicroRider to glider 633 was replaced with a slightly shorter cable. All gliders were run through the standard TWR functional checkout procedure, in addition to separate bench tests of the MicroRider probes. The Argos transmitter on the glider was found to interfere with the MicroRider, creating a large spike on multiple channels every 90 seconds. Once this was disabled in software, the spikes disappeared. MicroRider 224 still exhibited larger noise levels than MicroRider 221; this will need to be investigated at a later stage.

Tab. 6.6: Glider specifications, configuration, and deployment information for PS129

Glider	TWR Slocum G2 631	TWR Slocum G2 632	GWR Slocum G2 633
Maximum depth	1000 m	1.000 m	1.000 m
Batteries	Extended lithium 4S (12500 Wh)	Standard lithium 3S (8424 Wh)	Extended lithium 4S (12500 Wh)
CTD	Sea-Bird GPCTD (pumped) s/n 9359	Sea-Bird unpumped s/n 0256	Sea-Bird unpumped s/n 0260
Fluorometer	WetLabs FLBB-SLC (Chl, scatter) s/n 4504	WetLabs FLBBCD-SLC (Chl, CDOM, scatter) s/n 4559	WetLabs FLBBCD-SLC (Chl, CDOM, scatter) s/n 4561

Glider	TWR Slocum G2 631	TWR Slocum G2 632	GWR Slocum G2 633
Microstructure	n/a	RSI MicroRider s/n 224 standard configuration, probes not installed	RSI MicroRider s/n 221 with Ti-anodised probe holders and extra anodes T1: T1889 T2: T1891 sh1: M1240 sh2: M1241
PAR	Biospherical s/n 50246	n/a	n/a
Recovery system	Nose recovery system	n/a	n/a
Thruster	10W hybrid thruster	n/a	n/a
Deployment event	PS129_018-4	n/a	PS129_018-05
Deployment time	12-3-2022 22:44:40	n/a	12/3/2022 23:11:43
Deployment position	59° 05.517' S 000° 07.336' E	n/a	59° 05.544' S 000° 07.458' E

Both gliders were deployed from the starboard side, using strops fitted into a quick releaser on the main crane. Glider 631 was deployed first and released cleanly, though one strop subsequently wrapped itself around the aft section of the glider. However, this quickly disentangled and the ship moved away for the next deployment. Glider 633 was also launched smoothly, though the glider subsequently turned slightly towards the ship. A boat hook had to be used to fend off the gilder, on the hull between the wing and MicroRider. However, no contact was seen with the probes.

Both gliders are piloted from the United Kingdom by BAS glider pilots via Iridium RUDICS using TWR's Slocum fleet mission control website software on a BAS server (with a backup server at TWR). The intention was to recover both gliders in late 2022. However, at the time of writing, glider 633 has developed problems with its science computer and may need to be recovered at an earlier stage. Glider 631 is still working well.

Additional measurements – Sailbuoy

OS Sailbuoy "Kringla" was supplied by the University of Gothenburg (PI: Sebastiaan Swart). It was fitted with an AIRMAR weather sensor on a short mast, a Doppler current profiler beneath the hull with two beams on each side of the keel, and a temperature/conductivity sensor inside the keel bulb.

Tab. 6.7: Sailbuoy configuration, and recovery/deployment information for PS129

Surface vehicle	OS Sailbuoy 1812 "Kringla"	
Conductivity/temperature sensor	AADI 4319 s/n 1758	
Wind/air temperature/GPS/ acceleration/attitude sensor	AIRMAR 200WX-IPX7 s/n 60065078	
Doppler current profiler sensor	AADI 5400 (600 kHz) s/n 472	
Recovery/deployment event	PS129_025-1	PS129_027-7
Recovery/deployment time	15-3-2022 08:10:00	17-3-2022 15:05:03
Recovery/deployment position	64° 01.000' S 000° 05.492' W	66° 31.082' S 000° 11.162' W

The vehicle has two Iridium SBD modems, used for the flight and science computers, respectively. It is piloted from Gothenburg via OS's Iridium data service server. Kringla was piloted to 64°S 0°E in anticipation of *Polarstern*'s arrival, and was sighted just before dawn, with regular positions being sent to the ship. When the ship approached the vehicle, it was apparent that the upper part of the sail had been damaged. The vehicle was recovered by lowering a rope lasso over the sail using a boat hook, as recommended by the manufacturer. The rope was then pulled up by hand; it would probably have been better to lift the vehicle using a gantry or crane, although no damage appeared to be caused by pulling the vehicle up along the hull of *Polarstern*.

After recovery the Sailbuoy was rinsed with freshwater, the sail was removed. All data from the science computer were downloaded using the cable supplied by the University of Gothenburg and photographs of the sail were sent to Gothenburg, where the owner discussed the best course of action with the manufacturer. Repair materials were available on *Polarstern*, with some glass cloth, polyester/glass filler from the carpenter's workshop. Heli Service had newer aviation grade epoxy. We were asked to perform a repair, and helicopter mechanic Timo Hecken assisted with cutting 28 cm off the top of the sail, plus removing an additional 1 cm of the outer layer of carbon fibre below this cut. The foam core was then smoothed and shaped with sandpaper, with a small section of damaged foam replaced with foam from the removed section. To compensate for the weight lost with the end of the sail, 14 small TWR Slocum ballast weights were recessed into holes drilled into the top of the foam of the sail. The tops of the holes were covered with filler; this was allowed to dry and then sanded flush again. Then two layers of woven glass cloth, with an extra layer at the ends of the sail, were applied using approximately 40 g of Henkel Loctite EA9396 QT Aero epoxy, with the repair overlapping the original carbon fibre by approximately 1.5 cm. After this had cured overnight, excess glass cloth was cut back to the overlapping area, and the joint was sanded flush. The balance of the sail was still good, and the sail was refitted to the Sailbuoy.

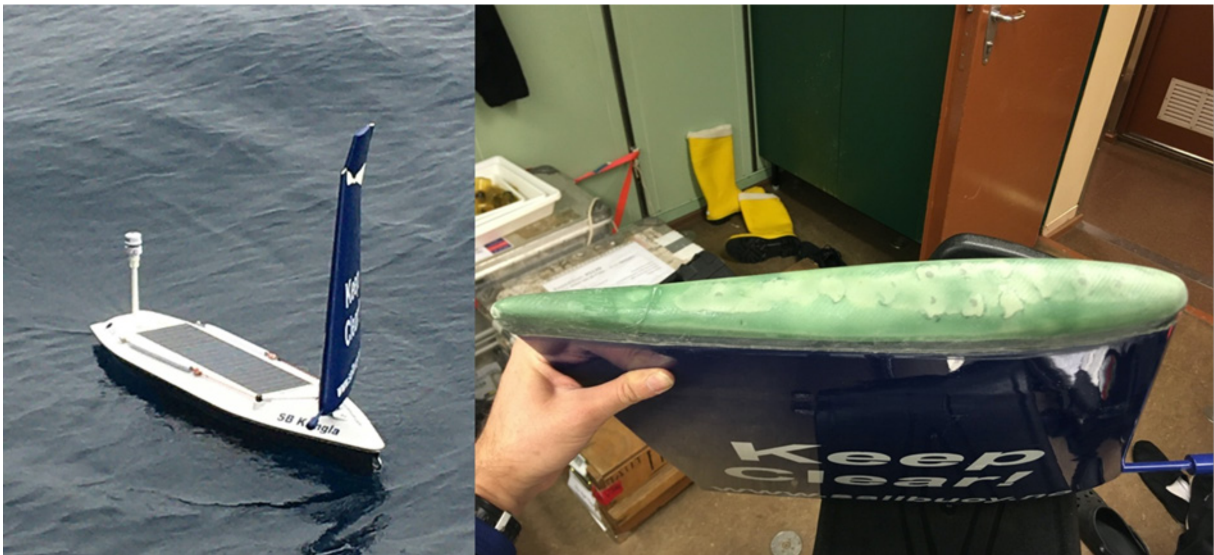

Fig. 6.9: Sailbuoy Kringla before recovery with the damaged sail and the top of the sail after repair

After Iridium communications with the Sailbuoy were confirmed by the team in Gothenburg, it was launched from the after gantry on the starboard side of the vessel while steaming slowly ahead; the Sailbuoy subsequently turned to starboard, turning behind the ship. It was piloted north toward its recovery position, and at the time of writing is still sailing well with its truncated sail.

Additional measurements –Remote sensing

Through a collaboration between BAS (Andrew Fleming and Gaelle Veyssiere) and the Norwegian Meteorological Institute (Nick Hughes), we were sent daily satellite images of the Weddell Sea. These include SAR images from various suppliers as well as ice concentration images and ice drift maps. These images were invaluable in day-to-day tactical planning when we were in the ice (Fig. 6.10). They allowed us to better understand the ice conditions, the movement of the ice and ice extent. An example of the SAR Image coverage near the western side of the Weddell Sea when we were in the vicinity. Under these images is the ice concentration map for that day.

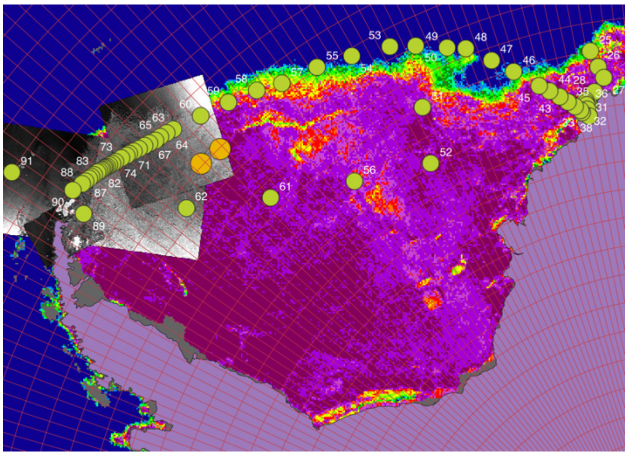

Fig. 6.10: Example of SAR image coverage near the western side of the Weddell Sea, superimposed on ice concentrations from passive microwave satellite data and planned station positions

Data management

Oceanographic data (^{18}O and chi-pod) will be submitted to the British Oceanographic Data Centre (BODC, https://www.bodc.ac.uk) and PANGAEA Data Publisher for Earth & Environmental Science (https://www.pangaea.de) within two years after the end of the cruise at the latest.

Other environmental data will be archived, published and disseminated according to international standards by the World Data Center PANGAEA Data Publisher for Earth & Environmental Science (https://www.pangaea.de) within two years after the end of the cruise at the latest. By default, the CC-BY license will be applied.

Any other data will be submitted to an appropriate long-term archive that provides unique and stable identifiers for the datasets and allows open online access to the data.

The DEFIANT project's participation on this expedition was supported by the UK Natural Environment Research Council grant NE/W004747/1.

References

Östlund HG, Hut G (1984) Arctic Ocean water mass balance from isotope data. Journal of Geophysical Research, 89, 6373-6381, https://doi.org/10.1029/JC089iC04p06373

7. PILOT STUDY FOR AN EASTERN WEDDELL SEA OBSERVATION SYSTEM (EWOS)

Felix C. Mark[1], Hauke Flores[1], Heike Link[2], Mareike Bach[3], David Barnes[4], Kerstin Beyer[1], Lisa Chakrabarti[5], Michiel van Dorssen[6], Gabriel Erni-Cassola[7], Bram Fey[8], Christopher Gebhardt[2], Christoph Held[1], Christopher D. Jones[9], Marie Kaufmann[1], Nils Koschnick[1], Susanne Kühn[10], Kevin Leuenberger[7], Sarah Kempf[1], André Meijboom[10], Malte Pallentin[1], Chiara Papetti[11], Martin Powilleit[2], Autun Purser[1], Anton van de Putte[12], Henning Schröder[1], Martina Vortkamp[1]
not on board: Patricia Holm[7], Jürgen Laudien[1], Magnus Lucassen[1], Dieter Piepenburg[1], Judith Piontek[13], Claudio Richter[1], Fokje Schaafsma[10], Jacqueline Stefels[3], Gritta Veit-Köhler[14]

[1]DE.AWI
[2]DE.UNI-Rostock
[3]NL.RUG
[4]UK.BAS
[5]UK.NOTTING
[6]NL.DORSSEN
[7]CH.UNIBAS
[8]NL.NIOZ
[9]GOV.NOAA
[10]NL.WUR
[11]IT.UNIPD
[12]BE.IRSNB
[13]DE.IOW
[14]DE.SENCKENBERG

Grant-No. AWI_PS129_04; AWI_PS129_05; AWI_PS129_06

Outline

General introduction to EWOS

The Weddell Sea features rich and diverse ecosystems and complex sea-ice dynamics. It plays a central role for global ocean circulation, sea-level change and carbon sequestration, and life in this unique stable and cold habitat contributes to global marine diversity and ecosystem services. Nonetheless, systematic long-term studies on ecosystem dynamics are largely lacking for the East Antarctic Southern Ocean, although it is well recognized that such investigations are indispensable to identify the ecological impacts and risks of environmental change and also for the establishment of marine protected areas. A pilot study for an **E**astern **W**eddell Sea **O**bservation **S**ystem (EWOS) was conceived to provide the scientific basis and a proof-of-concept for evaluating whether there is need for further coordinated biological observations in form of a potential long-term observation/ecological research framework (Gutt el al., 2022), which would be strongly related to the existing Hybrid Antarctic Float Observing System (HAFOS) programme carried out by AWI (see Chapter 2). The proposed scientific activities aimed to collect biological baseline data in the Eastern Weddell Sea, which will be analysed together with already existing data from the area in order to observe changes and trends in the development of the marine environment and ecosystems.

Specifically, this EWOS expedition aimed to complement HAFOS with biological analyses of carbon and nutrient fluxes and cycles between atmosphere, sea-ice, water column and the respective biota, including marine living resources, such as Antarctic krill and Antarctic toothfish. Three work areas were foreseen: i) along the Prime Meridian transect; ii) the shelf and inflow region off Kapp Norvegia, and iii) across the central Weddell Sea. The expected results will provide a quantitative assessment of the biogeochemical fluxes between phytoplankton, zooplankton and benthic communities as well as of marine living resources such as krill and Antarctic toothfish in relation to environmental drivers, and associated passive and trophic carbon fluxes from the surface into the deep ocean. EWOS constitutes a pilot study to coordinate and harmonize the methodology as a general proof-of-concept for a potential continuation of sustained measurements in the future. The expected results by themselves will already provide valuable quantitative information for ecosystem functions such as carbon export and secondary production from a rarely studied region and will also constitute an important baseline for the decision about the need for a long-term EWOS observatory.

The EWOS studies were conducted to assess whether a sensitive ‘change-detection’ array at a site off Kapp Norvegia – the so-called ‘EWOS Box’ – can be established in the future, which could expand offshore with transects crossing the Weddell Gyre and at the Greenwich Meridian, aiming at coordinated, systematic observations of the sympagic, pelagic and benthic part of the ecosystem.

EWOS was conceived as a multinational initiative carried by several national and international institutions. This is reflected in the numerous international cruise participants from seven different countries. Our work builds upon the knowledge and experience gained in the course of numerous research activities performed during the past decades in the region (e.g., EPOS, EASIZ, BENDEX, LAKRIS, SIPES). The aims of the EWOS pilot study are to instigate and assess a set of coordinated measurements enabling to observe and predict alteration of Weddell Sea biological diversity and evaluate the risk for critical transitions in marine ecosystem functionality. EWOS can thus offer a highly resolved view into a representative ecosystem and make an important contribution to the establishment and implementation of a large marine protected area in the Weddell Sea (WSMPA), which the EU, Germany and Norway are actively pursuing under the Convention of the Conservation of Antarctic Marine Living Resources (CCAMLR; cf. Jones et al., 2022).

The general EWOS sampling scheme with station positions is listed in Tables 7.1 and 7.2 and shown in Figure 7.1.

Tab. 7.1: Planned and realized EWOS station work. For gear abbreviations, see Table 7.2

Lat (N)	Lon (E)	PS129 station	EWOS site	Planned gear	Deployed gear
-59.378	0.019	PS129_20	GM_01	MN, RMT, SUIT	MN, RMT, SUIT
-62.000	0.000	cancelled	GM_02	ICE, MN, RMT, SUIT	--
-64.092	0.073	PS129_25	GM_03	ICE, MN, RMT, SUIT	MN, RMT, SUIT
-66.487	-0.065	PS129_27	GM_04	ICE, MN, RMT, SUIT	MN, RMT, SUIT
-68.000	0.000	cancelled	GM_05	ICE, MN, RMT, SUIT	--
-70.746	-10.797	PS129_40/48	EWOS_01	AGT, Lander, LL, MG, MN, OFOBS, RMT, SUIT, TV-MUC	AGT, Lander, LL, MG, MN, OFOBS, RMT, TV-MUC
-70.840	-10.581	PS129_42/44	EWOS_02	ICE, MG, OFOBS, TV-MUC	MG, TV-MUC
-70.862	-10.754	PS129_43	EWOS_03	Lander, MG, OFOBS	MG, OFOBS

Lat (N)	Lon (E)	PS129 station	EWOS site	Planned gear	Deployed gear
-70.89	-10.698	cancelled	EWOS_04	MG, TV-MUC	--
-70.943	-10.535	PS129_49/50	EWOS_05	Lander, MG, OFOBS, TV-MUC	Lander, MG, OFOBS, TV-MUC
-70.947	-10.514	PS129_49/52	EWOS_06	AGT, ICE, Lander, MG, MN, OFOBS, RMT, SUIT, TV-MUC	AGT, Lander, MG, MN, OFOBS, RMT, SUIT
-70.877	-10.487	PS129_53	EWOS_07	AGT, ICE, Lander, MG, OFOBS, TV-MUC	AGT, Lander, MG, OFOBS
-70.786	-10.749	PS129_47	EWOS_08	AGT, Lander, LL, MG, MN, OFOBS, RMT, SUIT, TV-MUC	AGT, MG, MN, OFOBS, RMT
-70.886	-11.122	PS129_57	EWOS_09	ICE, Lander, MG, OFOBS, TV-MUC	MG, OFOBS, TV-MUC
-70.654	-11.0190	PS129_54	EWOS_10	AGT, Lander, LL, MN, OFOBS, RMT, SUIT	ICE, LL, MN, OFOBS, RMT
-68.713	-27.050	PS129_71	WS_09	ICE	ICE
-68.977	-27.066	PS129_72	WS_10	MN, RMT, SUIT	RMT
-70.636	-29.397	PS129_74	WS_11	MN, RMT, SUIT	SUIT
-69.553	-32.440	PS129_77	WS_12	ICE	ICE
-68.970	-31.929	PS129_79	WS_13		ICE
-65.454	-41.374	PS129_89	WS_19	ICE	ICE
-66.447	-41.402	PS129_91	WS_20	MN, RMT, SUIT	ICE
-65.763	-44.794	PS129_93	WS_21		ICE
-64.306	-47.367	PS129_99	WS_24		ICE
-70.509	-8.181	PS129_39			IceROV
-70.499	-8.339	PS129_39			IceROV
-70.530	-8.204	PS129_41		IceROV	IceROV
-70.993	-10.624	PS129_51		IceROV	IceROV
-70.805	-10.568	PS129_55		IceROV	IceROV
-70.791	-10.563	PS129_55		IceROV	IceROV
-70.797	-10.529	PS129_55			IceROV
-68.638	-31.271	D_HAOE 19			IceROV
-68.638	-31.271	D_HAOE 19			IceROV
-64.843	-44.253	D_HAOE 25			IceROV
-63.540	-51.387	D_HAOE 36			IceROV
-63.540	-51.387	D_HAOE 37			ICEROV
-63.8620	-55.5333	cancelled	repeated station	TV-MUC, AGT	—

Tab. 7.2: Sampling gear and methods used by EWOS, regions and realised vs. planned deployments. Region I: Prime Meridian transect; II: EWOS box off Kapp Norvegia; III: central Weddell Sea transect

Sampling device	Full name	Region	Realised / planned deployments
Top predator census		continuous	n.a.
CTD	Conductivity Temperature Depth	I, II, III	18/18
SUIT	Surface under ice trawl	I, II, III	5/12
RMT	Multi-Rectangular midwater trawl	I, II, III	8/12
MN	Multinet	I, II, III	7/12
ICE	Ice station	I, II, III	6/11
AGT	Agassiz Trawl	II, III	4/6
TV-MUC	TV-Multicorer	II, III	7/12
OFOBS	Ocean Floor Observation System	II	9/9
MG	Multi-Grab	II	9/9
Lander	Lander with baited fish traps	II	4/10
LL	Long-lines	II	2/3
ROV	BlueROV	II	11/4
TOTAL			90/118

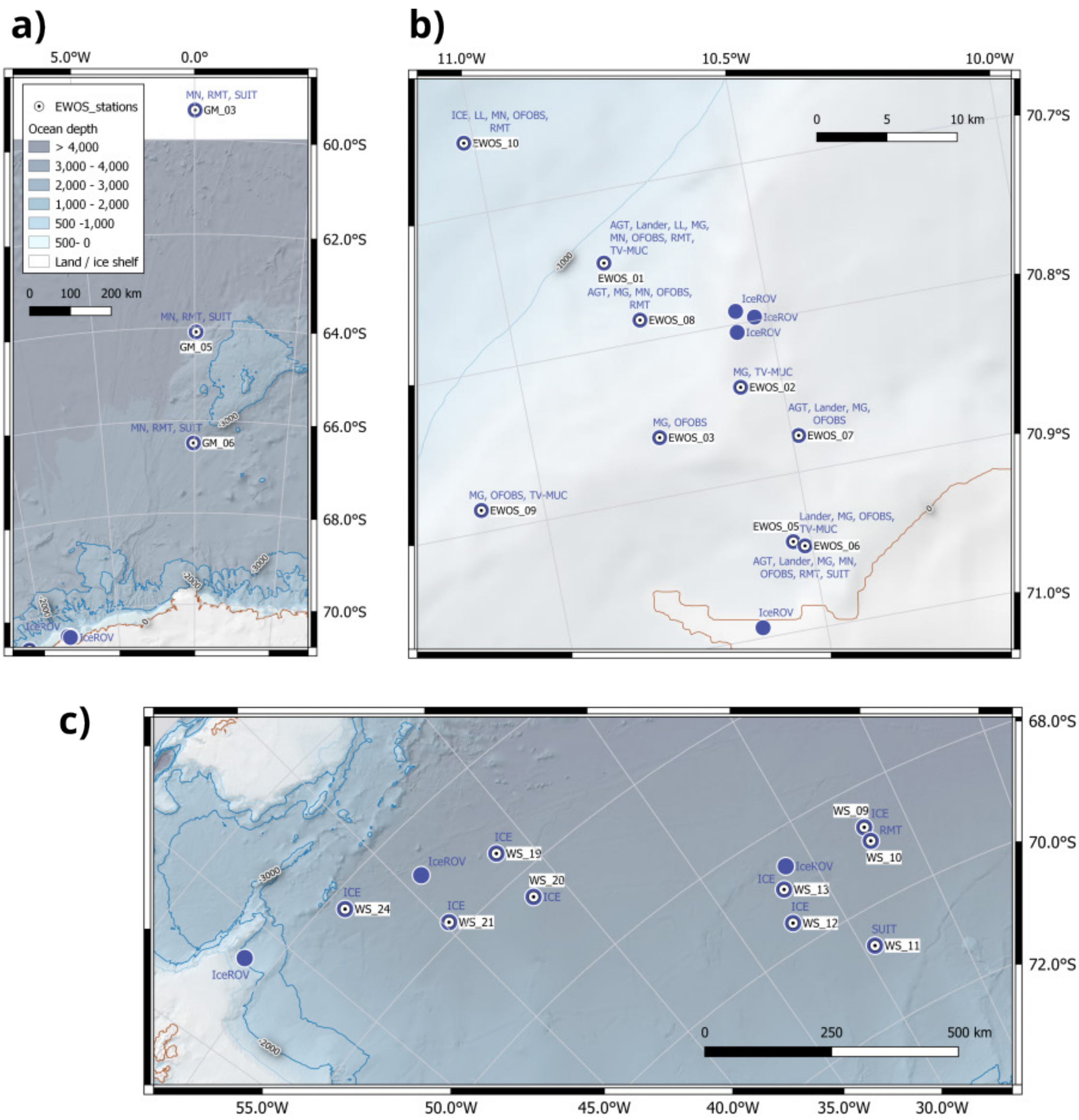

Fig. 7.1: EWOS sampling stations along the (a) Greenwich Meridian, (b) in the EWOS box, and (c) across the Weddell Sea

7.1. EWOS I

Felix C. Mark, Chiara Papetti, Christopher D. Jones, Gabriel Erni-Cassola, Kevin Leuenberger, Lisa Chakrabarti, Nils Koschnick, Sarah Kempf
Not on board: Magnus Lucassen, Patricia Holm

Grant-No. AWI_PS129_04

Objectives

- Study of key species responsible for the carbon and nutrient transfer, especially for carbon export to assess the role of the Southern Ocean sea-ice zone for global climate regulation.
- Determine the abundance, biomass and diversity of benthic fauna on the shelf and the shelf break in relation to organic carbon availability, seafloor substrate and bottom current regime as a baseline to compare future change against.

- Assess and explain taxonomic and functional biodiversity and composition of ice-associated-, pelagic- and benthic biota encompassing a wide range of trophic levels (microbes to top predators), including energy flow, production and species interactions (symbioses).
- Identify key species for monitoring (ecologically important, all trophic levels), observe their stress response and assess their adaptive scope: genetic diversity, gene flow, and ecophysiological plasticity, adaptive strategies and capacities.
- Assess robustness or sensitivity of Weddell Sea ecosystems with respect to changes in biodiversity and energy flow.
- Direct human impact and conservation: protect sympagic, pelagic and benthic ecosystems as potential refugia for, inter alia, top predators (e.g., marine mammals and seabirds), commercially exploited species (e.g., krill and Antarctic toothfish), fish and other ice-dependent species, in order to maintain and/or enhance their resilience and ability to adapt to the effects of climate change. Identify scientific reference areas to monitor the effects of climate change, human activities (fishing, pollution) in representative Antarctic ecosystems and thereby support the establishment and implementation of the WSMPA.
- Indirect anthropogenic impacts such as global pollution by plastic debris (macro-, micro- and small microplastics): study the occurrence of plastic debris (microplastic (MP, 300 µm - 5 mm) and small microplastic (SMP, 10-300 µm).

Work at sea

Owing to weather conditions, logistic- and time constraints, we were only able to realise 10 of the planned 25 gear deployments (40% realisation rate, cf. Tab. 7.3). Positions of the deployments are shown in Figure 7.2.

Tab. 7.3: Overview of gear deployed in EWOS I

Gear	Approved deployments	Realised Deployments
Agassiz-Trawl	12	4
Fish Trap-Lander	10	4
Longlines	3	2

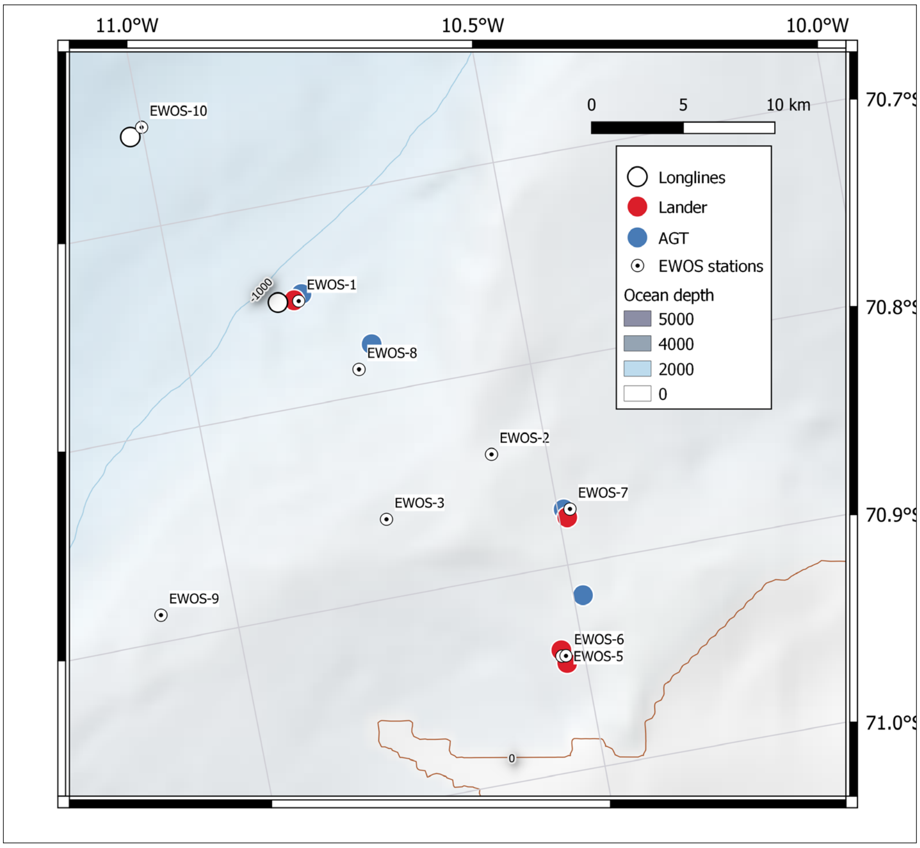

Fig. 7.2: Map of EWOS I gear deployment at EWOS box stations off Kapp Norvegia

Agassiz trawl catches

Tab. 7.4: Metadata of AGT deployments

Date	Station	EWOS	Latitude	Longitude	Depth	Catch
23.03.22 00:15	PS129_40-12	EWOS_01	-70.745748	-10.814778	931 m	40 kg
25.03.22 20:22	PS129_47-3	EWOS_08	-70.776271	-10.726429	691 m	30 kg
27.03.22 22:35	PS129_52-6	EWOS_06	-70.915883	-10.485963	218 m	650 kg
28.03.22 13:32	PS129_53-6	EWOS_07	-70.872826	-10.490958	233 m	440 kg

The first two AGT hauls at depths (Tab. 7.4) below the sponge communities (station 40-12 and 47-3) were small and contained only few individuals as is typical for deep stony ground. They contained fish, invertebrates and a few individual sponges. The other two stations 52-6 and 53-6 between stranded icebergs contained a higher volume of biological material – several juvenile notothenioid fish, a high diversity of invertebrates and huge masses of loose, dead bottom material comprised of bryozoans, encrusting algae and sponge spicules, impressively documenting the destruction of the benthic comunities in this shallow area by iceberg scouring.

The individual catches contained (Tab. 7.4):

Station 40-12: 12 fish (9 Notothenioidei and 3 Macrouridae), invertebrates including Crustacea (Decapoda, Isopoda, Amphipoda), Echinodermata (Holothuroidea, Ophiuridea, Echinoidea, Crinoidea), Polychaeta, Pycnogonida, Anthozoa, Porifera

Station 47-3: 13 fish (exclusively Notothenioidei), 1 Octopus (*Pareledone spec*) and further invertebrates including Crustacea (Decapoda, Euphausiacea, Isopoda, Amphipoda), Echinodermata (Holothuroidea, Ophiuridea, Asteroidea, Echinoidea, Crinoidea), Polychaeta, Pycnogonida, Anthozoa, Porifera, Hemichordata, Bryozoa, Bivalvia, Gastropoda

Station 52-6: 34 fish (exclusively Notothenioidei, of which 10 juveniles < 2,0 g), 3 Octopus (*Pareledone spec*) and further invertebrates including Crustacea (Decapoda, Euphausiacea, Isopoda, Amphipoda), Porifera, Echinodermata (Holothuroidea, Ophiuridea, Asteroidea, Echinoidea, Crinoidea), Polychaeta, Pycnogonida, Anthozoa, Bryozoa, Bivalvia, Gastropoda, Tunicata

Station 53-6: 43 fish (1 ray (released) and Notothenioidei, of which 20 juveniles < 2,0 g), 1 Octopus (*Pareledone spec*) and further invertebrates including Crustacea (Decapoda, Euphausiacea, Isopoda, Amphipoda), Porifera, Echinodermata (Holothuroidea, Ophiuridea, Asteroidea, Echinoidea, Crinoidea), Polychaeta, Pycnogonida, Anthozoa, Bryozoa, Bivalvia, Gastropoda, Tunicata, Brachiopoda

Subsamples of AGT catches have not yet been fully examined and therefore this summary may not be complete.

Fish trap catches

Tab. 7.5: Metadata of fish trap lander deployments

Date	Station	EWOS	Latitude	Longitude	Depth (m)	Time (h)	Fish	Amphi-poda
21.03.22 15:44	PS129_40-3	EWOS_01	-70.74808	-10.827228	934,2	39	31	0
26.03.22 13:22	PS129_49-2	EWOS_05	-70.940375	-10.532759	286,9	30	6	5
26.03.22 19:22	PS129_49-5	EWOS_06	-70.947056	-10.527647	282,2	21,5	0	20
28.03.22 00:06	PS129_53-1	EWOS_07	-70.87705	-10.487915	234,3	15	0	50

We originally planned to deploy the landers at all 10 stations within the EWOS box and leave them on the ground for 18-30 h. For recovering, weights were dropped via an acoustic releaser and the lander would rise at a speed of approximately 1-1.5 m s^{-1} to the surface, where it was picked up by the ship's crane and hauled on board. The catch was immediately recovered from the traps and brought to the expedition aquaria –no mortalities were recorded during this procedure. Due to ice coverage, overall weather conditions and station logistics, only 4 of the planned 10 deployments could be realized (cf. Tab. 7.5). Only the first deployment at a greater depth (station 40-3, 934 m) proved successful in terms of catching organisms, while the other three deployments at shallower depths (230-280 m) brought up empty nets. This may either be attributed to the time of year, weather conditions and depth or to overall bottom time, which had to be compromised due to time shortage.

The single trap deployments caught the following specimens (Tab. 7.5):

Station 40-3/13: 3 *Muraenolepis microps*, 1 *Chionobathyscus dewitti*, 24 *Pachycara brachycephalum*, 4 *Trematomus loennbergii*

Station 49-2/50-2: empty

Station 49-5/52-4: empty

Station 53-1/7: empty

Longlines

Tab. 7.6: Metadata of longline deployments

Date	Station	EWOS	Latitude	Longitude	Depth
21.03.22 16:22	PS129_40-4	EWOS_01	-70.747661	-10.851292	962.7 m
28.03.22 18:16	PS129_54-1	EWOS_10	-70.654589	-11.019067	1.384.3 m

Longlines could only be deployed and recovered twice due to meteorological and technical problems (Tab. 7.6). They were placed horizontally on the sea bottom and consisted of an anchor weight connected to a line (1,000 and 1,500 m, respectively), followed by 500 m of baited line. It consisted of a main line, into which we clipped a 5 m rope with 7 baited hooks on 50 cm snoods (70 cm between snoods) every 10 m (see Fig. 7.3), resulting in a total of 350 baited hooks per deployment.

The baited line was connected to 500 m of slack towards the second anchor weight, which was attached to the line by a releaser. The releaser also held a line (water depth 300 m) with flotation (250 kg buoyancy) for later recovery. We chose not to use surface or ice buoys due to the extreme and rather unpredictable ice conditions.

Soaking time was 96 and 24 hours. In both cases, the individuals caught were moribound or dead, indicating that soaking time was on the long side and should be reduced to <24 hours.

Fig. 7.3: Deployment of longlines. Main line is visible on the left (black) and side line (green), which carries the snoods and baited hooks supported by a float (orange). Picture: Felix Mark

Species caught with the longlines:

Station 40-4/46-1: *Dissostichus mawsoni*, *Chionobathyscus dewitti*, *Macrourus whitsoni*

Station 54-1/56-1: *Chionobathyscus dewitti*, *Chionodraco myersi*, *Macrourus whitsoni*

Laboratory work

Cell biology

Mitochondrial respirometry is a highly sensitive methodology that allows us to understand the cellular response to a change in environmental temperature that a species inhabits. Changes in mitochondrial function can be early signs that an organism is not able to produce the energy that is required to maintain its metabolic processes. Mitochondrial function can be adversely affected by changes in temperature, which we can simulate in our protocols to predict the effects of climate change on particular fish. For the EWOS work on board PS129 we carried out measurements on freshly dissected fish tissues including red muscle, heart and isolated mitochondria from liver. These measurements of respiration need to be performed on tissues that are fresh, where the organelles are intact and can continue to work to produce ATP – currently this is the only way in which these methodologies can be employed. We compared mitochondrial metabolism of members of the family of Channichthyidae against members of the Nototheniidae (mostly Trematominae) and assayed mitochondrial capacities, efficiencies and ATP/O ratios under thermal stress (Fig. 7.6) by means of Oroboros O2k oxygraphs (Oroboros Instruments GmbH, Innsbruck, Austria).

Live-cell based observations based on microscopy or interrogating metabolic pathways 'on the fly' are not straightforward since the high-quality microscopes we would wish to use would not work onboard of a moving vessel. One strategy to overcome some of these hurdles is to generate primary cell cultures from the fish of interest. The cell lines can be maintained in our home laboratories and used to conduct experiments to extend the work done during PS129 and to inform and optimise proposals for future expeditions. During PS129, we started to culture primary cells from icefish and red-blooded notothenioids. Sixteen different fish were targeted for cell preparation over several weeks and the cultures have been maintained for the entirety of the expedition. We cultured cells from heart and red muscle from each of the animals. If we are successful in returning the cultures to the lab in Bremerhaven (with the assistance of a group member who was staying on board), then these will be the first reported Antarctic icefish cultured cells. We will continue to maintain and characterise the cells in the United Kingdom and at AWI.

Notothenioid retina function

The retina of the eye is unusual in that it is the most externally exposed part of the nervous system. The optic nerve travels through the retina and is one of the cranial nerves; these have a direct connection to the hind brain. Environmental changes that affect neuronal function can first be noticed in the eyes. The retina is a beautifully ordered tissue with rows of photoreceptors, ganglion cells and connecting neurons, any disturbance to the order of this structure is readily identified and can be investigated. The Antarctic icefish are extraordinary in their lack of haemoglobin. Vascular input to the eye in red-blooded animals is essential to maintain retinal health, however, it is still not really clear how oxygen delivery to hypoxia sensitive tissues like the retina is achieved. A detailed study to document the structure and function of the retina during the lifespan of icefish and compare this with closely related red-blooded notothenioids was identified early on during PS129.

We have proceeded to collect eyes from 87 fish of which 18 are icefish (including *Chionobathyscus dewitti, Chionodraco hamatus, Chionodraco myersi*) for comparison with 30 red blooded notothenioid (including *Trematomus loennbergi* and *hansoni*, *Pleuragramma antarcticum*) eyes. For each animal, one eye was flash frozen and stored at -80 °C. The other eye was placed in formalin and eye cups prepared to expose the retina to fixative. The experimental idea is to look at retinal histology of the fixed specimens and correlate this with mitochondrial proteomic analyses of the frozen retina tissues. Otoliths from each of the fish have also been retained and will be used to find the ages of each animal. We expect to construct a detailed and informative picture of this sensitive neural tissue in the context of the unique oxygen niche that the icefish inhabits. This will form a baseline for studies in the future where rising ocean temperatures are likely to change the ability for the icefish to maintain normoxia for mitochondrial and retinal function.

Microplastics in seawater

Surface water for microplastic analyses was obtained using two methods: via the snorkel and pump of the COMA project (see Chapter 5), and the Klaus Union Sealex Centrifugal Pump (Bochum, Germany) via ship's own stainless steel seawater system.

Sampling via the ship's continuous water supply was conducted in wetlab 1. The water was drawn from ca. 11.2 m depth and led through a 1/2" PTFE-lined hose into a stainless-steel pressure filter holder (Pieper Filter GmbH, H293SSI) with a 10 µm stainless-steel filter (diameter: 293 mm; Körner, 1076420) to collect the suspended particles >10 µm. Water was filtered during ship steaming, as well as stationary work sections to assess whether ship movement affects incidence of sample contamination with paint particles (Leistenschneider et al., 2021). Filtered volumes were measured with a Gardena flowmeter attached to the outflow of the filter holder. The filters were replaced when the ship changed between steaming and stationary work, or water flow had noticeably (visually) decreased within sampling event. The 10 µm filters with the retained solids were folded, wrapped in non-stick baking paper, aluminium foil and stored at +4 °C for analysis in Basel, Switzerland. Sampling via the ship's snorkel employed the identical filtration system, but instead the water was fed from the pump into the filter holder with a PP hose.

Opportunistic samples of bottom water were obtained from two CTD/rosette casts within the EWOS box research area. From the Niskin bottles the water was led with a silicone tube into PP and LDPE containers. The water was then filtered onto 10 µm mesh filters (diameter: 25 mm, Körner) using a medical syringe and attached filter holder (Millipore Swinnex-25). The filters with the retained material were stored in glass petridishes at +4 °C.

Microplastic incidence in fish intestinal tracts

Digestive tracts of fish were removed by ventrally opening each fish from the pectoral fins to the anus, taking care not to damage the digestive tract; tracts were removed with cuts each at the opening of the stomach and the end of the intestines. Samples were then directly transferred into glass petridishes or aluminium foil and frozen at -20° C. To prepare samples for transport, they were defrosted and all external parts were rinsed with ultrapure water (Milli-Q) to remove potential contamination from the dissection process. After rinsing, the samples were transferred into 50 mL falcon tubes or glass jars covered with aluminium foil and submerged in syringe filtered (0.22 µm) ethanol (96 %) and stored at +4° C.

Microbial colonization of plastic

To study microbial colonization of plastics in the Weddell Sea, an experimental set-up was designed to mimic plastics floating in surface seawater. Polyethylene (PE) was used as substrate, as it is among the most commonly found plastic polymers in the environment, thereby employing "pristine" and surface oxidized PE (Erni-Cassola et al., 2020), as well as glass as an inert control substrate. As the experiment could not be performed on the working deck, alternative set-ups were used, namely (I) aquarium (60 L) in a container with controlled temperature (1° C) and replenishing water every 3 h during the day, and (II) aquarium in wetlab 1 with high water flow rate (>6 L/min) and with a light source (10 W 500 mm, SolarStinger LED sunstrip; wrapped in a cotton bag to provide some shading) to promote growth of photosynthetic organisms. Seawater was obtained via the ship's stainless steel continuous supply system from ca. 11.2 m depth.

The PE and glass slides (2.5 x 7.5 cm) were attached to stainless-steel frames, which were inserted in the aquarium. Samples (n = 4 per substrate) were recovered after 2, 7 and 14 days of incubation. To obtain the biofilms for DNA analyses, samples were then sonicated in filter sterilized sea water, biofilm material pelleted via centrifugation and resuspended in lysis buffer (MBL, Qiagen). Samples for microscopy and biofilm thickness measurements were fixed in 4 % formaldehyde solution (ROTI Histofix 4 %, Roth). All samples were stored at -20 °C.

Quality control measures

Several quality control and -assurance measures were applied. All materials were copiously rinsed with Milli-Q water before use and whenever possible, work was conducted on a clean bench. Potential background contamination during microplastic work was assessed with filter paper as done previously (e.g., Bosshart et al., 2020). To further reduce contamination risk during dissection, the digestive tracts were among the first samples to be removed.

Preliminary results

Fish species composition

First results of fish species research are shown in Figures 7.4, 7.5 and 7.6 below:

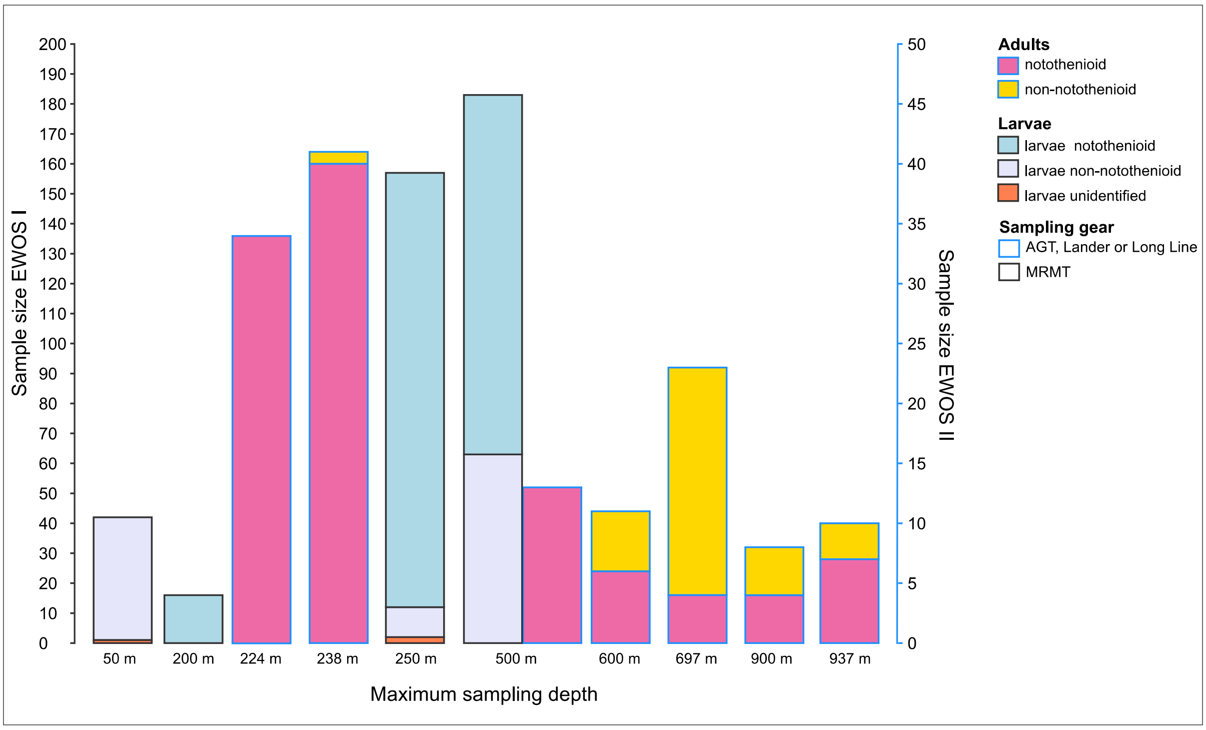

Fig. 7.4: Statistics of fish species composition from AGT, fish traps and longlines (benthic, blue frames), also including data from the Multi-RMT (EWOS II (Section 7.2), pelagic, black frames)

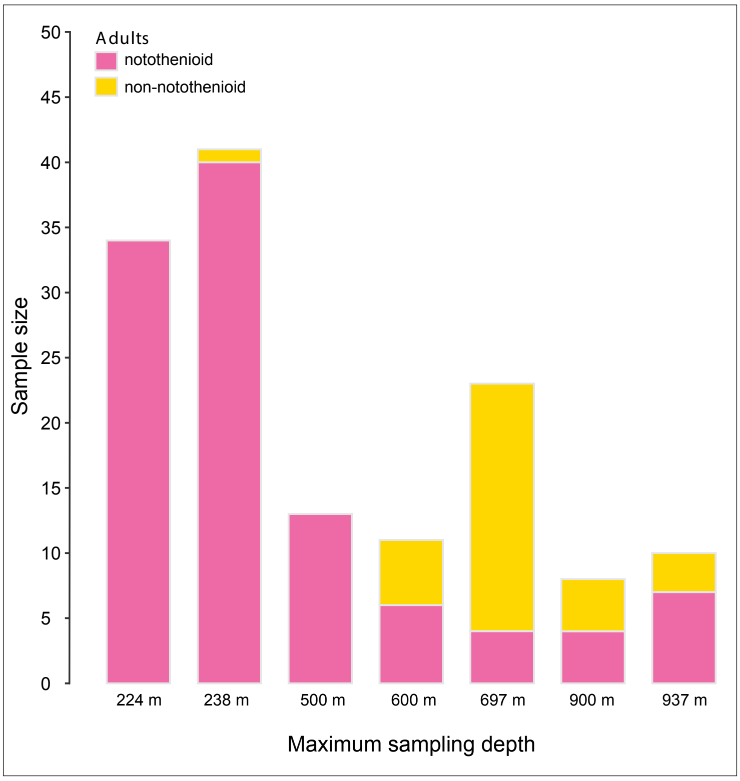

Fig. 7.5: Distribution of fish catches of benthic gear (AGT, traps, longlines). The distribution of adult notothenioids (pink) and non-notothenioids (yellow) is depth dependent, with nn-nothenioid species mostly occurring in the deeper and warmer water layers on the shelf slope below 500 m.

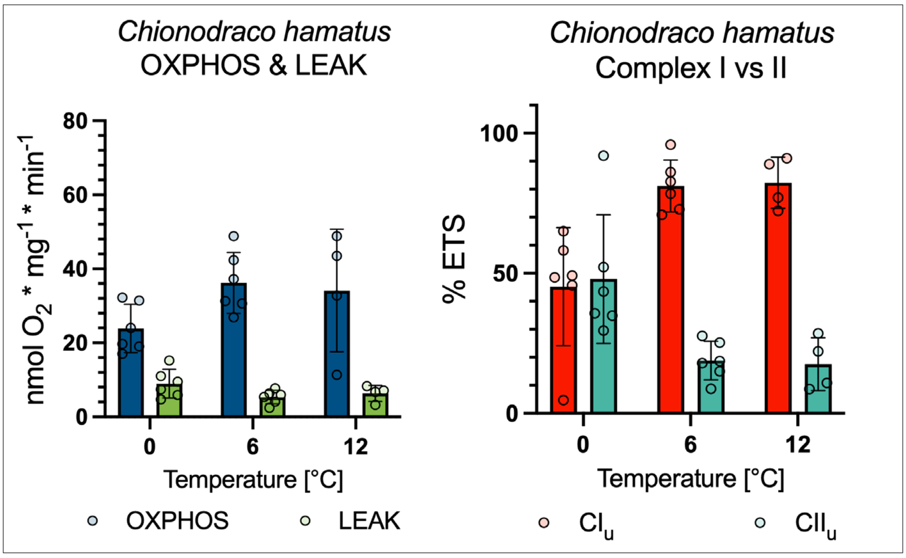

Fig. 7.6: Examples of preliminary results on notothenioid fish mitochondrial energetics, as measured in permeabilized heart fibers of the icefish C. hamatus. Left panel: oxidative phosphorylation (OXPHOS, blue) and LEAK respiration (green) at 0, 6, and 12°C. Right panel: contribution of mitochondrial complex I (NADH dehydrogenase, red) and complex II (succinate dehydrogenase, petrol) to total mitochondrial electron transport

Microplastics in seawater

The 18 collected surface water samples represent 83 m^3 of filtered seawater (Tab. 7.7). Most of this (83 %) was obtained through the Klaus Union Sealex Centrifugal Pump system. Deep water samples from the CTD totaled 22.5 L (from 940 m depth), and 21.7 L (from 630 m depth). We expect to find microplastics predominantly in the surface water samples >10 µm.

Tab. 7.7: Description of the surface water samples taken

For further information see the end of the Chapter 7.1.

Microplastic incidence in fish intestinal tracts

A total of 103 specimens representing 24 species were sampled for microplastic ingestion (Tab. 7.8). Based on low environmental microplastic contamination, we do not expect to find high microplastic ingestion incidence.

Tab. 7.8: Fish gut samples for microplastic analyses

Species	Family	Quantity
Artedidraco orianae	Artedidraconidae	4
Pogonophryne sp.	Artedidraconidae	1
Bathydraco marri	Bathydraconidae	1
Cygnodraco mawsoni	Bathydraconidae	1
Prionodraco evansii	Bathydraconidae	17
Racovitzia glacialis	Bathydraconidae	1
Chionobathyscus dewitti	Channichthyidae	10
Chionodraco hamatus	Channichthyidae	1
Chionodraco myersi	Channichthyidae	5
Pagetodes (formerly Cryodraco) antarcticus	Channichthyidae	1
Pagetopsis macropterus	Channichthyidae	1
Macrourus whitsoni	Macrouridae	8
Muraenolepis microps	Muraenolepididae	4
Electrona antarctica	Myctophidae	3
Aethotaxis mitopteryx	Nototheniidae	1
Lepidonotothen kempi	Nototheniidae	1
Pleuragramma antarcticum	Nototheniidae	5
Trematomus hansoni	Nototheniidae	1
Trematomus lepidorhinus	Nototheniidae	3
Trematomus loennbergi	Nototheniidae	5
Trematomus nicolai	Nototheniidae	1
Trematomus pennellii	Nototheniidae	1
Trematomus scotti	Nototheniidae	4
Pachycara brachycephalum	Zoarcidae	23

Microbial colonization of plastic

In total, we collected 108 DNA samples and 36 fixed samples. Preliminary visual inspection of the colonized surfaces indicates limited growth. Diatoms were observed to colonize and preliminary observations suggest that these may be primarily *Fragilariopsis* sp.

Tab. 7.7: Description of the surface water samples taken

Sample ID	Date	Latitude Start	Longitude Start	Latitude Stop	Longitude Stop	Volume filtered L	Wind m/s	Ship speed kn	Water source	condition
filt_1	14.3.2022	61° 24.559’ S	00° 00.000’ E	NA	NA	2006.5	13.7	8.6	snorkel	steaming
filt_2	16.3.2022	66° 04.693’ S	00° 03.517’ E	66° 29.208’ S	00° 04.101’ E	2000.5	12.0	10.4	snorkel	steaming
filt_3	19.3.2022	66° 34.803’ S	11° 43.806’ W	66° 54.515’ S	11° 27.337’ W	2013.2	13.3	10.4	snorkel	steaming
filt_4	24.3.2022	70° 51.128’ S	10° 33.947’ W	70° 47.195’ S	10° 40.676’ W	9083.9	27.1	1.3	KlausUnion	stationary
filt_5	25.3.2022	70° 46.907’ S	10° 44.607’ W	70° 47.251’ S	10° 40.198’ W	6851.9	15.0	0.7	KlausUnion	stationary
filt_6	26.3.2022	70° 49.155’ S	10° 40.775’ W	70° 56.328’ S	10° 32.424’ W	1319.9	7.7	9.2	KlausUnion	steaming
filt_7	26.3.2022	70° 56.324’ S	10° 31.383’ W	70° 56.822’ S	10° 30.901’ W	6254.1	6.2	0.6	KlausUnion	stationary
filt_8	28.3.2022	70° 52.379’ S	10° 28.939’ W	70° 52.600’ S	10° 29.734’ W	7790.3	6.1	0.1	KlausUnion	stationary
filt_9	28.3.2022	70° 51.938’ S	10° 30.980’ W	70° 39.060’ S	11° 00.0’ W	2025.2	6.0	8.7	KlausUnion	steaming
filt_10	29.3.2022	70° 47.644’ S	10° 39.287’ W	70° 39.256’ S	11° 06.754’ W	2086.8	14.9	8.8	KlausUnion	steaming
filt_11	30.3.2022	70° 51.741’ S	10° 31.150’ W	70° 51.706’ S	10° 30.403’ W	11107	19.5	0.6	KlausUnion	stationary
filt_12	31.3.2022	70° 51.717’ S	10° 30.331’ W	70° 51.626’ S	10° 30.902’ W	11205	14.8	0.2	KlausUnion	stationary
filt_13	2.4.2022	70° 50.057’ S	11° 30.036’ W	70° 36.284’ S	12° 13.486’ W	3491.4	15.1	9.3	KlausUnion	steaming
filt_14	3.4.2022	70° 17.114’ S	13° 28.567’ W	69° 42.577’ S	15° 23.454’ W	4973.8	9.6	10	KlausUnion	steaming
filt_15	3.4.2022	69° 42.769’ S	15° 24.106’ W	69° 42.676’ S	15° 25.038’ W	6031.2	18.5	1	KlausUnion	stationary
filt_16	5.4.2022	68° 12.394’ S	19° 47.919’ W	67° 44.206’ S	21° 42.755’ W	2170	8.6	11.6	KlausUnion	steaming+ stationary
filt_17	5.4.2022	67° 40.880’ S	21° 49.821’ W	67° 15.943’ S	23° 35.728’ W	1134.8	10.4	10.9	KlausUnion	steaming+ stationary
filt_18	6.4.2022	68° 11.834’ S	25° 34.267’ W	68° 01.083’ S	25° 45.059’ W	1113.3	12.9	5-7	KlausUnion	steaming

7.2. EWOS II

Hauke Flores, Anton Van de Putte, Susanne Kühn, Christoph Held, Mareike Bach, David Barnes, Michiel van Dorssen, Bram Fey, André Meijboom, Martina Vortkamp
Not on board: Fokje Schaafsma, Jacqueline Stefels

Objectives

- Identification of key variables and drivers that structure the main ecosystem compartments sea ice and water column, including seabirds and mammals. Study of key variables of carbon, nutrient and trace-element fluxes, and cycling within and between these compartments, as well as the key species responsible for the carbon and nutrient transfer.
- Assess and explain taxonomic and functional biodiversity and composition of ice-associated and pelagic biota, encompassing a wide range of trophic levels (microbes to top predators), including energy flow, production and species interactions.
- Assess sympagic, pelagic and cryobenthic ecosystems as potential refugia for, inter alia, top predators (e.g., marine mammals and seabirds), commercially exploited species (e.g., krill and Antarctic toothfish), fish and other ice dependent species, in order to maintain and/or enhance their resilience and ability to adapt to the effects of climate change.
- Quantify primary production and DMSP production in sympagic and pelagic ecosystems. Study of taxonomic and functional biodiversity to identify the key algal species contributing to DMSP production within these ecosystems.

Work at sea

Pelagic and sympagic fauna sampling

A multiple opening Rectangular Midwater Trawl (M-RMT 8+1) was used to investigate deeper-dwelling macrofauna key species of the pelagic food web, such as euphausiids, amphipods, and myctophids. The M-RMT consisted of a nominal 8 m^2 rectangular net with a mesh size of 5 mm mounted below a nominal 1 m^2 opening rectangular net with a mesh size of 0.3 mm. A CTD recorded temperature and salinity profiles during each M-RMT haul. The three standard sampling strata of the M-RMT were 500-200 m, 200-50 m and 50-0 m, where the water was deep enough. In shallower waters the maximum depth of the deepest stratum was set to 10 m above the seafloor. In total, we conducted 8 M-RMT hauls: 3 on the Greenwich Meridian (GM_01 – GM_03), 4 in the EWOS box (EWOS_1, EWOS_6, EWOS_8, EWOS_10) and one in the Weddell Sea (WS_01) (Fig. 7.8, Tab. 7.9). A multinet (Hydrobios) with an opening size of 0.25 m^2 and a mesh size 0.1 mm was deployed at 7 sampling stations to sample the mesozooplankton community. The 5 standard sampling strata sampled with the multinet were 1000-500 m, 500-200 m, 200-100 m, 100-50 m and 50-0 m. In shallower waters, the maximum depth of the deepest stratum was set to 10 m above the seafloor.

A Surface and Under-Ice Trawl (SUIT) was used to sample the pelagic fauna within the top 2 m layer of the ocean under the ice and in open surface waters. During SUIT tows, data from the physical environment were recorded, including chlorophyll a concentration, water temperature, salinity and ice thickness. We conducted altogether 5 SUIT deployments, 3 on the Greenwich Meridian in open water, 1 deployment in the EWOS box under newly forming sea ice and 1 deployment under young sea ice in the central Weddell Sea (Fig. 7.9, Tab. 7.9).

In addition, *Polarstern*'s EK80 echosounder profiled the distribution of pelagic animals in the water column continuously. The 4 nominal sampling frequencies (38 KHz, 70 KHz, 120 KHz, 200 KHz) were recorded in broadband (fm) mode. The EK80 profiling was working from 6

March to 25 April 2022, with few interruptions. A calibration of the EK80 system was conducted on 9 April 2022 in free drift in open water.

Sea ice work and protist communities

At ice stations, ice cores were collected for physical sea-ice parameters, including salinity, temperature and ice thickness; biogeochemical sea-ice parameters, including pigment analysis (HPLC), nutrients, PAM-fluorometry and particulate organic carbon (POC); as well as dimethylsulfide (DMS) and dimethylsulfoniopropionate (DMSP). Primary productivity and DMSP production of the bottom sea-ice communities were investigated during five stable isotope addition experiments on board. We collected young ice from the mummy chair, pancake ice from pancake ice floes scooped from the sea surface with a metal basket and sampled on board, and from ice floes accessed either from the ship or with a helicopter. To minimize the time spent on the ice, ice cores were collected in plastic core bags and subsequently sectioned on board. The same parameters were collected from seawater obtained from the CTD/rosette at 4 depths (surface, chlorophyll maximum, 50 m, 100 m). Additional samples were filtered from water and melted ice cores for DNA analysis of microbial sea-ice communities. Furthermore, DNA samples from the surface water were collected from the ship's seawater intake with the Autofim (Isitec) sampler at 3-hour intervals.

Top predator censuses

During steaming, surveys of top-predator densities were conducted mainly from observation posts installed on the flying bridge. In addition, helicopter surveys were conducted. During PS129, helicopter transects were restricted to 80 nmi per flight due to the expected low reliability of the weather during the autumn season. All surveys covered both seabirds and marine mammals. For ship-based counts, usually a 300 m band-transect count with snapshots for flying birds and additional line transect count for marine mammals is used. The helicopter counts were band transects only, set on 250 m bandwidth.

Shelf-ice habitats

Where the ice sheet covering nearly all of Antarctica's land mass meets the ocean, it flows into the coastal seas as floating ice shelves, which may reach more than 200 m in thickness. The vast 1.6 million km^2 habitat underneath these ice shelves is virtually unknown, with just a few tiny peeks at the water and seabed below through exploratory hot-water drill holes (Fig. 7.7).

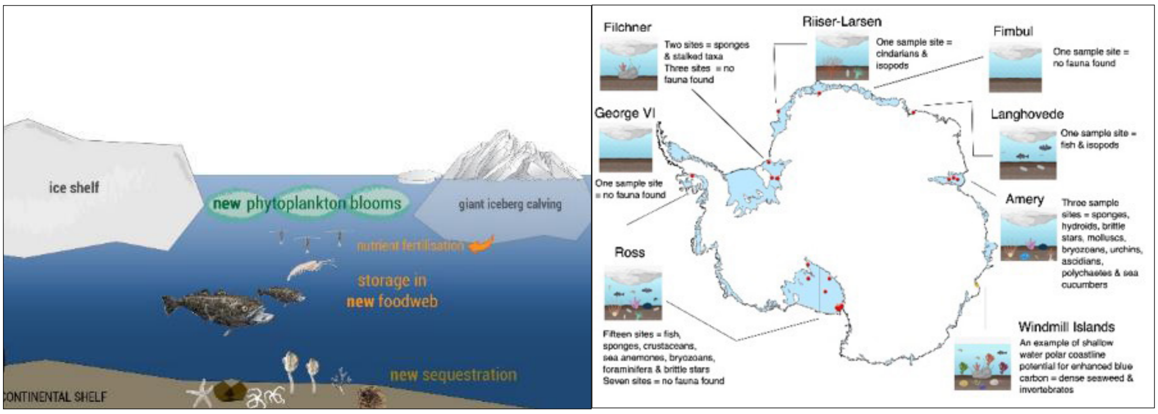

Fig. 7.7: Ice shelf environment and sites of the few biological investigations (taken from Barnes et al., 2021)

There is one environment on Earth even more poorly known than the seabed below ice shelves and that is the potential habitat of the underside of the ice shelf itself. Northwards of this, the underside of seasonal sea ice (the freezing sea surface) is known to be an important habitat for many autotroph algae, such as diatoms and some organisms that feed on these, such as amphipods and a limited foodweb (Thomas, 2017). A single study in the Ross Sea reported an anemone living on the underside of the Ross Ice shelf (Daly et al., 2013), but otherwise the underside of the ice of this vast habitat has remained uninvestigated, yet may be one of our planet's most threatened environments in an era of rapid greenhouse-mediated warming and marine ice losses.

The remote operated vehicle (ROV) is a BlueROV2 made by Blue Robotics modified with extra thrusters, twin battery capacity and two types of tethers (each 400 m in length). Each battery allows 35-45 min running time. The tether was attached to a Toughbook laptop run either from *Polarstern*'s winch control room or remotely in ice stations. The camera view was seen livescreen on the Toughbook with depth information and the ROV could carry and operate a pump to take water samples (for eDNA analysis) and a separate top-mounted 'slurp gun'. The latter device is a perspex tube of ~8 cm diameter terminating in a spare ROV thruster with a compartment separated by mesh and a back pointing valve at the suction point. This was aimed at collecting live specimens of animals. Finally, a 30 cm long measuring wire was made to project 40 cm ahead of the ROV to measure physical structuring of the ice and perpendicular particle movement in the water (flow rate). The ROV was either deployed from the starboard midships side of the vessel or from suitable ice floes adjacent to tabular icebergs, following helicopter reconnaissance and field deployment onto temporary ice stations.

Preliminary results

Pelagic and sympagic fauna sampling

We sampled pelagic macrofauna with the M-RMT at 3 stations on the Greenwich Meridian, at 4 stations in the EWOS box and at 1 station on the Weddell Sea transect (Fig. 7.8; Tab. 7.9). Hence, we could realize 67% of the planned net deployments (12 stations; only 33 % in the Weddell Sea). The species composition was dominated by krill (Euphausiidae) at 50 % of the stations (25, 40, 45, 54), whereas at other stations (20, 27, 49, 72) gelatinous zooplankton (jellyfish, chaetognaths and salps) dominated (Fig. 7.9a, b). The omnivorous krill *Thysanoessa macrura* occurred throughout the sampling area. In oceanic waters, Antarctic krill *Euphausia superba* was by far the most abundant krill species. Notably, the highest numbers of these krill species were often sampled in the lowest depth stratum (500-200 m), which is below the standard sampling depth of CCAMLR krill surveys. Salps were more abundant in the EWOS box and the Weddell Sea than on the Greenwich Meridian. The two species *Salpa thompsoni* and *Ihlea racovitzai* occurred in different depth strata. Particularly high numbers were found at station 72 in the inner Weddell Sea, where a massive ice-algae bloom in the marginal sea-ice zone stained the surface water and pancake ice in yellowish-green colours (see below, Fig. 7.13). In oceanic waters, mesopelagic fish sampled with the M-RMT were predominantly myctophids (*Electrona antarctica, Gymnoscopelus* spp.), *Bathylagus antarcticus* and larval *Notolepis* spp (Fig. 7.9b). On the shelf-slope and shelf of the EWOS box, notothenioid larvae were abundant, with a sharp increase of larval *Pleuragramma antarctica* numbers from deep waters > 1,000 m towards the inner shelf (Fig. 7.10a). Likewise, the dominance of the shelf-associated krill *Euphausia crystallorophias* increased with decreasing water depth (Fig. 7.10b).

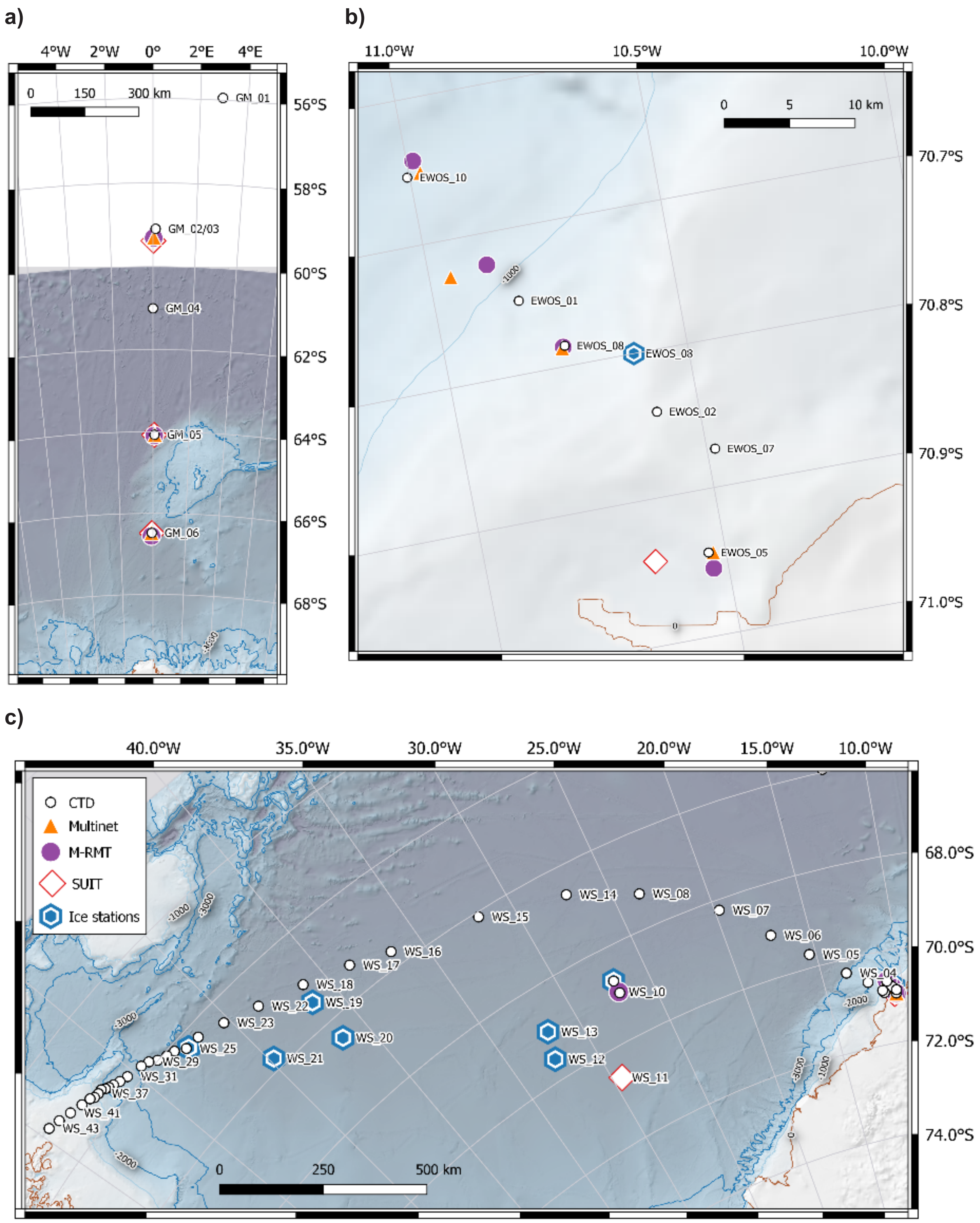

Fig. 7.8: Distribution of sampling locations for M-RMT, Multinet, SUIT, CTD and ice stations on: (a) the Greenwich Meridian, (b) in the EWOS box, and (c) in the Weddell Sea

The multinet was deployed at 7 stations, of which we performed 3 on the Greenwich Meridian and 4 in the 'EWOS box'. The 35 mesozooplankton samples obtained from this operation were brought to the home laboratory at AWI for in-depth taxonomic analysis. This equals about 60 % of the planned sampling effort (12 stations).

Fig. 7.9: Examples of M-RMT catches: krill from (a) station 25-4, (b) salps from station 54-4, and (c) myctophids from station 72-4

We sampled under-ice- and surface-dwelling fauna with the SUIT at 3 open ocean stations on the Greenwich Meridian, at one ice-covered station in the EWOS box, and at one ice-covered station in the inner Weddell Sea (Fig. 7.8; Tab. 7.9). This equals only about 40% of the planned sampling effort (12 stations). Antarctic krill dominated the catch in 2 out of 3 stations on the Greenwich Meridian (25 and 27). The SUIT in the EWOS box (station 52) yielded only few animals, because frazil ice had clogged the entire net from the mouth to the codend. At station 74 in the inner Weddell Sea, the under-ice species community was numerically dominated by pteropods (*Limacina helicina*), followed by ice amphipods (*Eusirus spp.*) and Antarctic krill. We collected altogether 924 samples of zooplankton species for size distribution, population genetics, trophic biomarker and stable isotope measurements.

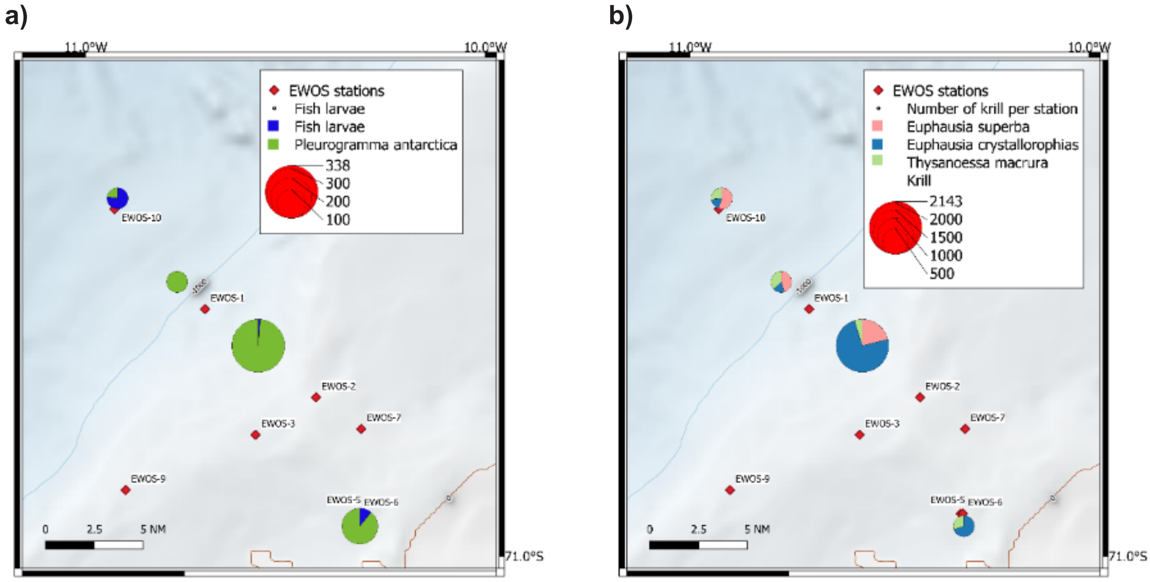

Fig. 7.10: Depth-associated change in fish larvae composition (a) and krill species composition (b) in the EWOS box. Numbers shown are non-quantitative raw catch numbers.

The distribution of acoustic backscatter of zooplankton and fish in the water column down to 1,000 m depth was recorded with the ship's new Simrad EK80 echosounder between 6 March and 25 April 2022. The recording was only occasionally interrupted. Altogether, we collected over 14 TB of hydroacoustic data in broadband (fm) mode around the four nominal frequencies 38, 70, 120 and 200 KHz. Preliminary screening of the data showed a deep-scattering layer between 200 and 700 m depth. In the EWOS box, this scattering layer remained at mesopelagic depth and did not follow the bottom topography onto the shelf (Fig. 7.11). The vertical distribution of scatterers followed a diel pattern with deeper distribution at day and many scatterers reaching the surface at night (Fig. 7.11).

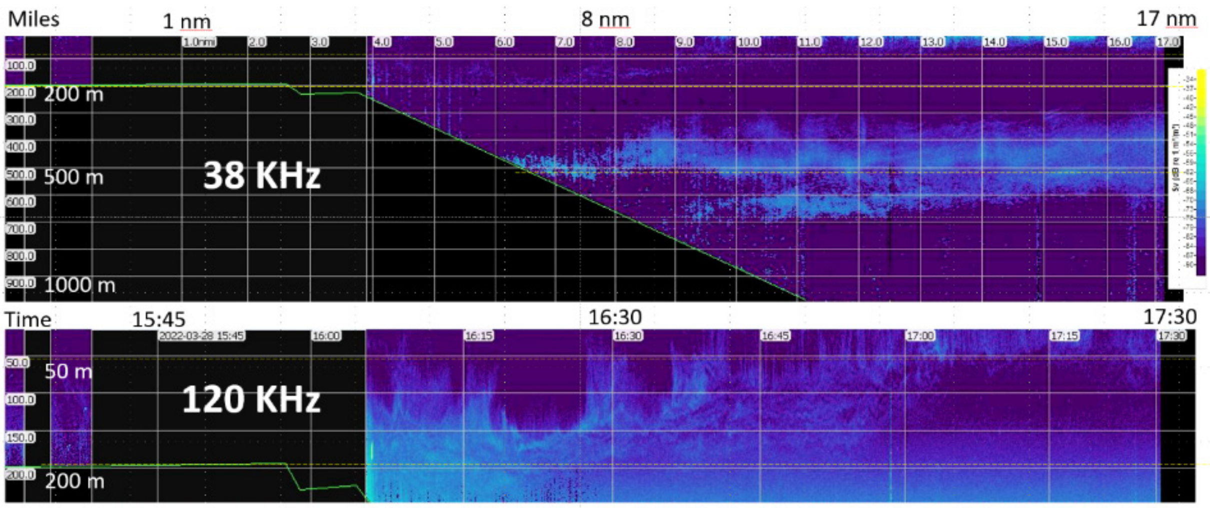

Fig. 7.11: Echograms of volume backscatter (Sv) along a transect from the deep sea to the shelf of the EWOS box at 38 KHz (top panel) and 120 KHz (bottom panel)

A calibration of the transducer signals was attempted on 21 March 2022 (station 40-1) in ice-covered waters. During this attempt, we aimed to balance the calibration sphere in the transducer beams between a starboard-mounted calibration winch and a BlueROV launched from the starboard side of the ship. This attempt was unsuccessful, because the tether of the ROV and the line from the calibration winch were pushed against the ship by sea ice. During a second calibration attempt in the night from 8 to 9 April 2022 (station 74-7), we balanced the Tungtsen Carbide calibration sphere between a fishing rod and the ship's ROV Biber, both operated through the moon pool ("Brunnenschacht"; Fig. 7.12). This attempt was successful; the net operation time of the calibration was 6 hours.

Fig. 7.12: Calibration of the EK80 transducer signal through the moonpool. The sphere is attached between a fishing rod and the ship's ROV "Biber" underneath the ship. Persons: Olaf Hüttebräuker (holding ROV controller), Felix Mark (holding fishing rod), Ilias Nasis. Picture: Hauke Flores

Tab. 7.9: Parameters of pelagic fauna sampling stations and numbers of samples per taxonomic group for each device operation

For further information see the end of Chapter 7.2.

Sea ice work and protist communities

At the beginning of the expedition, no sea ice was present in the eastern part of the research area from the Greenwich Meridian to the 'EWOS box'. During the work in the 'EWOS box', ice formation started rapidly. Altogether, we sampled 8 ice stations along the Weddell Sea transect (Fig. 7.8; Tab. 7.10). This equals about 75% of the planned sampling effort.

The first ice station was conducted with the ship's man basket on 29 March 2022 near the site of EWOS_10 (Station 55-1; Tab. 7.10). Here, the about 60 cm thick ice consisted of up to

8 pancakes stacked on top of each other. While passing through the newly forming marginal sea-ice zone on 6 April 2022, we crossed a wide band of pancake ice with an intense greenish-yellow coloration, indicating extremely high ice-algae biomass (Fig. 7.13a). The algal biomass appeared to be associated with the pancakes and brash ice in-between, whereas the water appeared to contain only low concentrations of biomass (Fig. 7.13b).

a) **b)**

Fig. 7.13: Ice-algae bloom in new pancake ice. (a) Overview picture, (b) close-up of pancake ice floes with high algae content. Picture: Hauke Flores

a) **b)**

Fig. 7.14: Pancake ice floes sampled from the ship. (a) Example of a pancake before sampling, seen from the bottom side, (b) sampling a pancake ice floe with an ice corer. Persons from left to right: Jeremy Wilkinson, Povl Abrahams, Anton Van de Putte, Mareike Bach. Picture: Hauke Flores

During the next crossing of this ice-algae bloom on 7 April 2022, we collected 3 pancakes with an iron basket operated with the ship's crane (station 71; Fig. 7.14, Tab. 7.10). The passage time of this ice-algae bloom was over 6 hours. The pancakes where 63, 90 and 98 cm wide. Ice cores for pigment analysis, DMSP measurements, DNA, POC/trophic biomarkers, nutrient concentration, production measurements and salinity profiles were sampled from each pancake. Progressing further into the inner Weddell Sea, we performed three more ice stations from the ship: One sampling thin new ice from the man basket (station 77), one sampling multi-year ice during a buoy deployment (station 79) and another pancake sampling with the ship's crane (station 89) (Tab. 7.10). In the western part of the Weddell Sea transect, we used the helicopter to reach ice floes for sampling light transmission through sea ice with a RAMSES spectroradiometer mounted on an L-Arm, and corresponding chlorophyll content. At all three stations (91, 93, 99), we sampled relatively thin ice adjacent to a multi-year ice floe (about 20-60 cm, Tab. 7.10). At station 93, we measured spectral radiation and sampled chlorophyll cores at 2 different sites.

Tab. 7.10: Ice cores sampled for biological sea-ice parameters during PS129.The parameters were: High-Pressure Liquid Chromatography (HPLC: chlorophyll a and other pigments), dimethylsulfide (DMS), environmental DNA (DNA), particulate organic carbon and trophic biomarkers (POC), nurient concentrations (NUT: nitrate, silicate, phosphate), temperature and salinity profiles (TS), optical properties (light)

Device operation	EWOS site	Station type	Date (UTC)	Latitude (N)	Longitude (E)	Ice thickness (min-max, cm)	HPLC / DMS	DNA / POC	Experiments	NUT	TS	Light
PS129_55	EWOS_10	Ice station (ship)	2022-03-29	-70.800	-10.613	60-64	x			x		
PS129_71-1	WS_09	Pancake (ship)	2022-04-07	-68.713	-27.050	12-23	x	x	x	x		
PS129_77-3	WS_12	Ice station (ship)	2022-04-10	-69.553	-32.440	18-20	x	x	x	x	x	
PS129_79-1	WS_13	Ice station (ship)	2022-04-11	-68.970	-31.929	178-179	x	x	x	x	x	
PS129_89-1	WS_19	Pancake (ship)	2022-04-15	-65.454	-41.374	30-39	x	x	x	x	x	
PS129_91-0	WS_20	Ice station (heli)	2022-04-16	-66.447	-41.402	49-59	x	x		x	x	x
PS129_93_0	WS_21	Ice station (heli)	2022-04-17	-65.763	-44.794	23-33	x	x		x	x	x
PS129_99_0	WS_24	Ice station (heli)	2022-04-19	-64.306	47.367	32-45	x				x	x

For water column parameters, we sampled 50 stations at 2 to 4 depths including the surface layer, the depth of the chlorophyll maximum, 50 m, and below the mixed layer depth. Samples for pigment analysis (HPLC), nutrients, PAM-fluorometry, particulate organic carbon (POC)/ trophic biomarkers, as well as dimethylsulfide (DMS) and dimethylsulfoniopropionate (DMSP) were collected acrosss the Greenwich Meridian, the EWOS box and the Weddell Sea. Additional POC/trophic biomarker samples were taken on the CTD transect on the shelf slope of the Antarctic Peninsula at the end of the expedition (stations 97-123; Tab. 7.13). Nutrients were sampled at every CTD of the expedition by the HAFOS project (see Chapter 2). After solving minor technical difficulties, the Autofim sampled eDNA in the EWOS box and across the Weddell Sea.

Tab. 7.11: Stations sampled for biological water column parameters during PS129. The parameters were: High-Pressure Liquid Chromatography (HPLC: chlorophyll a and other pigments), dimethylsulfide (DMS) and dimethylsulfoniopropionate (DMSP), environmental DNA (DNA), particulate organic carbon and trophic biomarkers (POC), nutrient concentrations (NUT: nitrate, silicate, phosphate)

Device operation	EWOS site	Date (UTC)	Latitude (N)	Longitude (E)	HPLC	DMS(P)	DNA	POC	NUT
PS129_14-1	GM_01	2022-03-11	-55.943	2.936	x	x	x		x
PS129_18-7	GM_02	2022-03-13	-59.092	0.123	x	x	x		x
PS129_23-1	GM_04	2022-03-14	-61.002	0.001	x	x	x		x
PS129_25-8	GM_05	2022-03-16	-64.073	0.085	x	x	x		x
PS129_27-2	GM_06	2022-03-16	-66.482	-0.071	x	x	x		x
PS129_30-1	GM_07	2022-03-19	-65.935	-12.197	x	x	x		x
PS129_40-2	EWOS_01	2022-03-21	-70.750	-10.827	x	x	x		x
PS129_41-2	NM_02	2022-03-23	-70.529	-8.203	x	x			x
PS129_42-1	EWOS_02	2022-03-24	-70.842	-10.588	x	x	x		x
PS129_47-1	EWOS_08	2022-03-25	-70.786	-10.751	x				x
PS129_49-1	EWOS_05	2022-03-26	-70.943	-10.536	x	x	x		x
PS129_53-3	EWOS_07	2022-03-28	-70.874	-10.483	x			x	x
PS129_54-3	EWOS_10	2022-03-29	-70.653	-11.005	x	x	x	x	x
PS129_58-2	WS_01	2022-04-02	-70.885	-11.291	x	x	x	x	x
PS129_59-1	WS_02	2022-04-02	-70.832	-11.385				x	x
PS129_60-1	WS_03	2022-04-02	-70.601	-12.217	x	x	x	x	x
PS129_62-4	WS_04	2022-04-03	-70.301	-13.442				x	x
PS129_64-2	WS_05	2022-04-03	-69.713	-15.407				x	x
PS129_65-1	WS_06	2022-04-04	-69.085	-17.335	x	x	x	x	x
PS129_68-1	WS_07	2022-04-05	-68.221	-19.743	x			x	x
PS129_70-1	WS_08	2022-04-05	-67.266	-23.595				x	x
PS129_71-2	WS_09	2022-04-07	-68.717	-27.050	x	x	x	x	x
PS129_72-3	WS_10	2022-04-07	-69.001	-27.043	x	x	x	x	x
PS129_80-2	WS_14	2022-04-12	-66.615	-27.207	x	x	x	x	x
PS129_83-2	WS_15	2022-04-13	-66.104	-31.836				x	x
PS129_86-1	WS_16	2022-04-14	-65.667	-36.610	x		x	x	x
PS129_87-1	WS_17	2022-04-14	-65.356	-38.709				x	x
PS129_88-1	WS_18	2022-04-15	-65.041	-41.139				x	x
PS129_96-1	WS_22	2022-04-18	-64.740	-43.507	x	x	x	x	x
PS129_97-1	WS_23	2022-04-18	-64.480	-45.300				x	x
PS129_99-1	WS_24	2022-04-19	-64.300	-46.668				x	x
PS129_100-3	WS_25	2022-04-19	-64.279	-47.469	x		x	x	x

Device operation	EWOS site	Date (UTC)	Latitude (N)	Longitude (E)	HPLC	DMS(P)	DNA	POC	NUT
PS129_102-1	WS_26	2022-04-20	-64.133	-47.954				x	x
PS129_103-1	WS_27	2022-04-20	-64.078	-48.365				x	x
PS129_104-1	WS_28	2022-04-20	-63.994	-48.819				x	x
PS129_105-1	WS_29	2022-04-21	-63.876	-49.152				x	x
PS129_106-1	WS_30	2022-04-21	-63.815	-49.545				x	x
PS129_107-1	WS_31	2022-04-21	-63.734	-50.351				x	x
PS129_109-3	WS_32	2022-04-22	-63.674	-50.754	x		x	x	x
PS129_110-1	WS_33	2022-04-22	-63.616	-51.074				x	x
PS129_111-1	WS_34	2022-04-22	-63.572	-51.301				x	x
PS129_112-1	WS_35	2022-04-22	-63.532	-51.456				x	x
PS129_114-2	WS_36	2022-04-22	-63.478	-51.614				x	x
PS129_116-1	WS_37	2022-04-23	-63.481	-51.840				x	x
PS129_117-1	WS_38	2022-04-23	-63.466	-52.096				x	x
PS129_119-1	WS_39	2022-04-23	-63.410	-52.273				x	x
PS129_120-1	WS_40	2022-04-23	-63.351	-52.728				x	x
PS129_121-1	WS_41	2022-04-23	-63.261	-53.350				x	x
PS129_122-1	WS_42	2022-04-23	-63.169	-53.954				x	x
PS129_123-1	WS_43	2022-04-24	-63.091	-54.524				x	x

Top predator censuses

After leaving Cape Town, calibration counts where carried out and standardized daylight surveys started at 44°S, well north of the Polar Front. The ship set course to southwest and later followed the Prime Meridian from approximately 59°S. By passing the Polar Front, water got colder and marine life changed. North of Bouvet Island, the first (crested) penguins were encountered. Around the Polar Front, hourglass dolphins, long-finned pilot whales, humpback whales and southern right whales were sighted. A single emperor penguin was counted in open waters. Occasionally, large groups of snow petrels (>300 ind.) were found resting in the vicinity of icebergs (Fig. 7.15a). Within the EWOS box, the distances between sampling points were short, therefore only a minimum of ship-based transect counts were possible. To account for that, six helicopter surveys covering the area were conducted. Weddell seals were found close to the shelf resting on the limited amounts of available thicker ice floes. Crabeater and leopard seals as well as Adélie and emperor penguins were found in a band with thicker ice floes north of the EWOS box (Fig. 7.16). Within the sea-ice area of the Weddell Sea, the densities of top predators were low compared to earlier summer expeditions. Penguins, snow petrels, Antarctic petrels and Antarctic minke whales were found close to the ice edges. However, as soon as the ice closed up, most marine mammals and birds, except penguins, were absent. All top predator surveys had to stop on the 21 April 2022 due to a request by the ship to timely packing of materials. Therefore, no data from the vicinity of the Antarctic Peninsula could be collected.

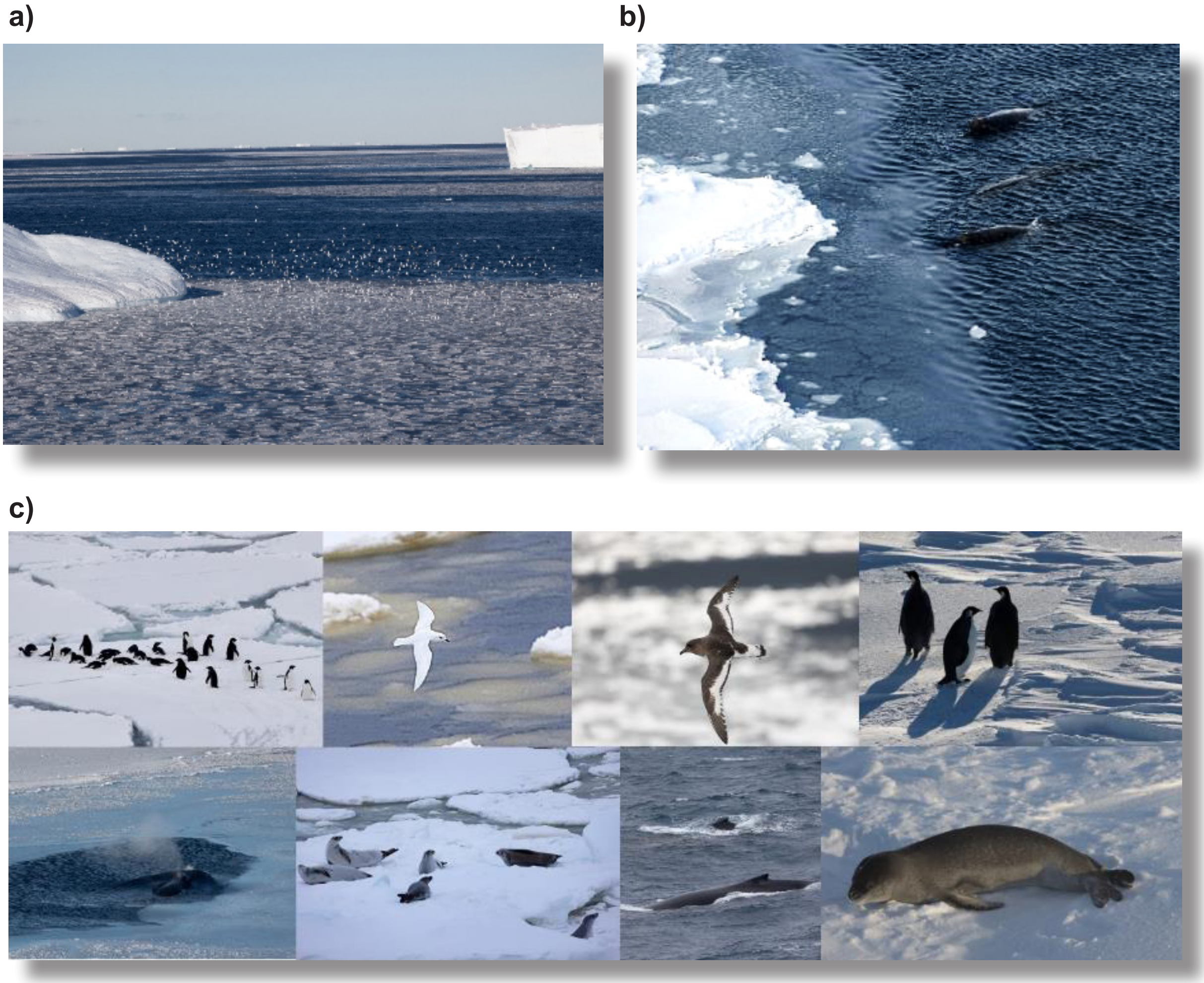

Fig. 7.15: Marine birds and mammals observed during PS129. (a) Flock of snow petrels, (b) group of Arnoux' beaked whales, and (c) collection of common Antarctic species (from left to right, top row: Adélie penguins, snow petrel, Antarctic petrel, emperor penguins. Bottom row: Antarctic minke whale, crabeater seals, humpback whale, leopard seal. Pictures: Susanne Kühn, André Meijboom, Bram Fey

In total, 15 top predator helicopter surveys were conducted during PS129 (Tab. 7.12), six of which took place in the EWOS box (see above). One flight (D-HAOE 16) had to be aborted early, due to snow showers and associated low visibility. The first flight took place over open water, all other flights were conducted at least partly above sea ice. During one helicopter survey (D-HAOE 18) on the Weddell Sea transit, four of the rarely observed Arnoux's beaked whales were found within the transect (Fig. 7.15b). Later and more to the western part of the Weddell Sea, two other groups were encountered in small leads within the sea-ice (D-HAOE 33 and 34). Closer to the peninsula, with decreasing water depth, large groups of Adélie penguins and seals were encountered, together with small groups of Orcas within the sea ice.

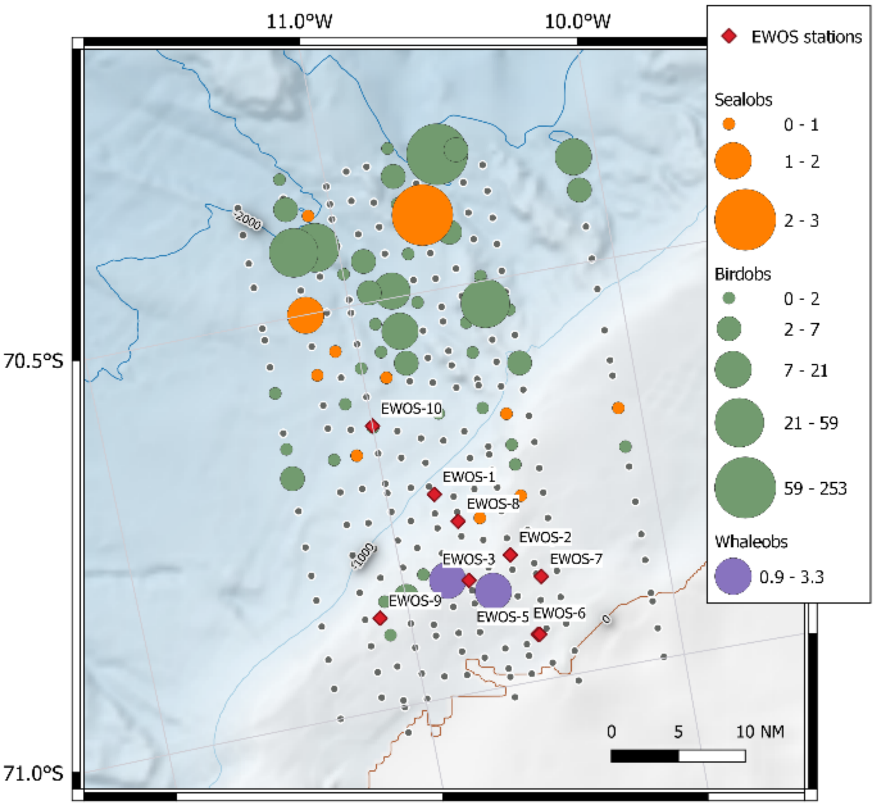

Fig. 7.16: Helicopter observations of marine birds and mammals in the 'EWOS box'. The numbers shown are non-quantitative numbers of sightings per observation block.

Tab. 7.12: Overview of helicopter censuses for top predators. Censuses usually consisted of two parallel 40 nmi tracks with ca. 8 nmi in between.

Flight Number	Date	Position Start Transect (S/W)		Survey nmi	Notes
D-HARK 1 18-03-2022		66.21	06.50	80	Open water
D-HARK 3	21-03-2022	70.45	10.35	80	EWOS box
D-HARK 6-7	23-03-2022	70.36	09.08	120	Neumayer station
D-HARK 9	25-03-2022	70.44	10.50	80	EWOS box
D-HARK 10	25-03-2022	70.44	10.55	80	EWOS box
D-HARK 11-12	26-03-2022	70.45	10.40	80	EWOS box
D-HAOE 13	27-03-2022	70.59	11.10	80	EWOS box
D-HAOE 14	28-03-2022	70.52	10.30	80	EWOS box
D-HAOE 16	03-04-2022	70.18	13.28	28	Aborted due to snow
D-HAOE 17	10-04-2022	70.05	31.02	20	
D-HAOE 18	11-04-2022	68.59	31.52	80	
D-HAOE 26	17-04-2022	65.29	45.00	40	Short due to sunset
D-HAOE 27	18-04-2022	64.39	44.10	80	
D-HAOE 33	19-04-2022	64.13	47.30	80	
D-HAOE 34	21-04-2022	63.44	50.23	80	

Between the start of the official survey on 5 Mar 2022 until the end on 21 Apr 2022, almost 200 hours of steaming time were covered by the top predator survey. This is considerably less time than in earlier surveys, due to the autumn season and associated shorter daylight. During the helicopter flights, 1088 nmi were surveyed and flight time was 27 hours. In total, 58 taxa were encountered during the surveys from the ship and the helicopter (Fig. 7.15c). This includes 40 bird taxa and 18 marine mammal species, of which 11 whale species and 7 seal species. All species are listed in Table 7.13. At a later stage, the distribution the abundance of species will be calculated. With this knowledge, energy requirements by top predators can be linked to food availability, which can be retrieved from fishing activities and EK80 data collected during PS129.

Tab. 7.13: Seabird and marine mammal taxa (English and scientific names) encountered during the top predator censuses both from ship and helicopter. In some cases, closely related species are combined, as identification at sea is challenging.

Seabirds				**Marine mammals**	
English name	***Scientific name***	**English name**	***Scientific name***	**English name**	***Scientific name***
Emperor penguin	*Aptenodytes forsteri*	Great-winged petrel	*Pterodroma macroptera*	Crabeater seal	*Lobodon carcinophagus*
Chinstrap penguin	*Pygoscelis antarctica*	Kerguelen petrel	*Pterodroma brevirostris*	Leopard seal	*Hydrurga leptonyx*
Adelie penguin	*Pygoscelis adeliae*	Soft-plumaged petrel	*Pterodroma mollis*	Weddell seal	*Leptonychotes weddellii*
Crested penguin sp.	*Eudyptes sp.*	Atlantic petrel	*Pterodroma incerta*	Ross seal	*Ommatophoca rossii*
Wandering albatross	*Diomedea exulans*	Grey petrel	*Procellaria cinerea*	S. elephant seal	*Mirounga leonina*
White-capped albatross	*Diomedea cauta*	White-chinned petrel	*Procellaria aequinoctialis*	Subant. fur seal	
Atl. yellow-nosed albatross	*Thalassarche chlororhynchos*	Prion sp.	*Pachyptila spp*	Antarctic fur seal	*Arctocephalus gazella*
Indian yellow-nosed albatross	*Thalassarche carteri*	White-headed petrel	*Pterodroma lessonii*	Ant. minke whale	*Balaenoptera bonaerensis*
Black-browed albatross	*Diomedea melanophris*	Grey petrel	*Procellaria cinerea*	Sei whale	*Balaenoptera borealis*
Grey-headed albatross	*Diomedea chrysostoma*	Cory's shearwater	*Calonectris borealis*	Fin whale	*Balaenoptera physalus*
Light-mantled sooty albatross	*Phoebetria palpebrata*	Sooty shearwater	*Puffinus griseus*	Humpback whale	*Megaptera novaeangliae*
Sooty albatross	*Phoebetria fusca*	Great shearwater	*Puffinus gravis*	Southern right whale	*Eubalaena australis*
Southern giant petrel	*Macronectes giganteus*	Subantarctic shearwater	*Puffinus assimilis*	Sperm whale	*Physeter macrocephalus*
Southern fulmar	*Fulmarus glacialoides*	Wilson's stormpetrel	*Oceanites oceanicus*	Long- finned pilot whale	*Globicephala melaena*
Antarctic petrel	*Thalassoica antarctica*	Black-bellied stormpetrel	*Fregetta tropica*	Hourglass dolphin	*Lagenorhynchus cruciger*
Cape petrel	*Daption capense*	White/ black-bellied stormpetrel	*Fregetta spp*	Orca	*Orcinus orca*

Seabirds				Marine mammals	
English name	***Scientific name***	**English name**	***Scientific name***	**English name**	***Scientific name***
Snow petrel	*Pagodroma nivea*	Diving petrel sp.	*Pelecanoides sp.*	Arnoux's beaked whale	Berardius arnouxii
Blue petrel	*Halobaena caerulea*	Tern sp	Sterna sp.	Southern Bottlenose whale	*Hyperoodon planifrons*
Antarctic prion	*Pachyptila desolata*	South polar skua	*Catharacta maccormicki*		
Thin-billed prion	*Pachyptila belcheri*	Brown skua	*Catharacta (skua) lonnbergi*		

Shelf-ice habitats

Thirteen deployments of the ROV were attempted of which 11 were actually made in the water. This means that we could realize 300 % of the originally planned sampling effort (4 stations). The failed deployments included one from vessel (ROV electrical fault) and one from helicopter (cloud ceiling dropped too low for sea-ice landing). Four deployments were made under the ice shelf, three under near ice-shelf icebergs which had calved off, three under distant icebergs and one under seasonal sea ice adjacent to one of these distant icebergs.

Tab. 7.14: Details of ROV deployments during PS129

Dive no.	Device operation/ Helicopter flight number	Date	Latitude	Longitude	Type	Notes
1	39-1	20/03/2022	70° 30.547‘ S	08° 10.892‘ W	Ice shelf	Scalloping of ice undersurface
2	39-2	20/03/2022	70° 29.974‘ S	08° 20.345‘ W	Ice shelf	Strong currents going inwards
3	41-1	23/03/2022	70° 31.806‘ S	08° 12.251‘ W	Ice shelf	Last Atka Bay deployment
4	51-1	27/03/2022	70° 59.606‘ S	10° 37.448‘ W	Ice shelf	Lighting problems (flood)
5	55-2	28/03/2022	70° 48.314 , S	10° 34.078 , W	Near iceberg	Possibly grounded, changed angle?
6	55-3	28/03/2022	70° 47.51 , S	10° 33.815 , W	Near iceberg	Possibly grounded, changed angle?
7	55-4	28/03/2022	70°47.858 , S	10° 31.768 , W	Near iceberg	Possibly grounded, changed angle?
8	D_HAOE 19	11/04/2022	68°38.325‘ S	31°16.267 , W	Far iceberg	Abyssal sea depth underneath
9	D_HAOE 19	11/04/2022	68°38.325‘ S	31°16.267 , W	Sea ice	Very little life obvious (but diatoms)
10	D_HAOE 25	17/04/2022	64°50.629‘ S	44°15.222 , W	Far iceberg	Abyssal sea depth underneath
11	D_HAOE 36	22/04/2022	63°32.439‘ S	51°23.225‘ W	Far iceberg	Scoured seabed at some point?
12	D_HAOE 37	22/04/2022	63°32.439‘ S	51°23.225‘ W	Sea ice	Very little life obvious (but diatoms)

The measurement wire (30 cm) was added from dive 3 onwards. On dive 4 the ROV leaked and the lights flooded, leading to the forced haul-in by cable. The lack of success with the 'slurp gun' lead us to remove it to improve near ice under-surface manoeuvring for measurements. Finally, the pump and water capture bags were also removed during iceberg deployments because of mixed success and added strain on batteries. The ROV, cable and all control equipment were all loaded into a Pulka sledge for helicopter remote ice-station deployments. Corresponding environmental information (temperature, salinity, oxygen and fluorescence) were recorded from the nearest CTD deployment from main cruise operations.

Approximately an hour of video was collected from each dive and battery life was strong enough after some iceberg dives to allow additional exploration of adjacent seasonal sea ice. Each video had corresponding information of depth, cable out and ROV depth. The keel depths varied from 60-170 m and along the sides, shoulder, outer and inner zones of these we will measure ice scallop morphological characteristics. We will identify biota present as far as possible including the density of each type. Under ice-shelf, iceberg and sea-ice biota will be compared and results analysed to examine what these exploratory dives can tell us about the nature and fate of under-shelf life.

Fig. 7.17: Deployment of ROV from a helicopter-supported 'ice station'

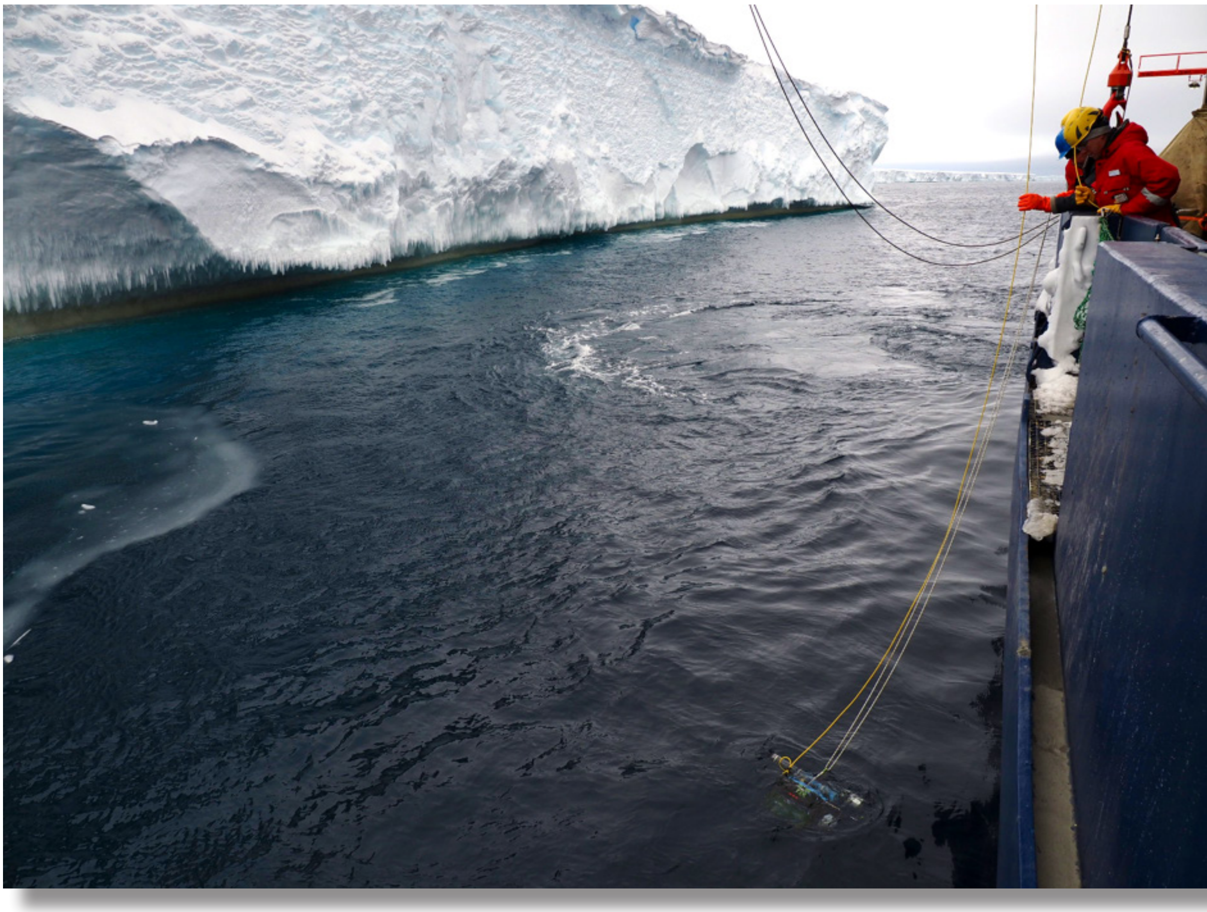

Fig. 7.18: Deployment of the ROV over the side of Polarstern

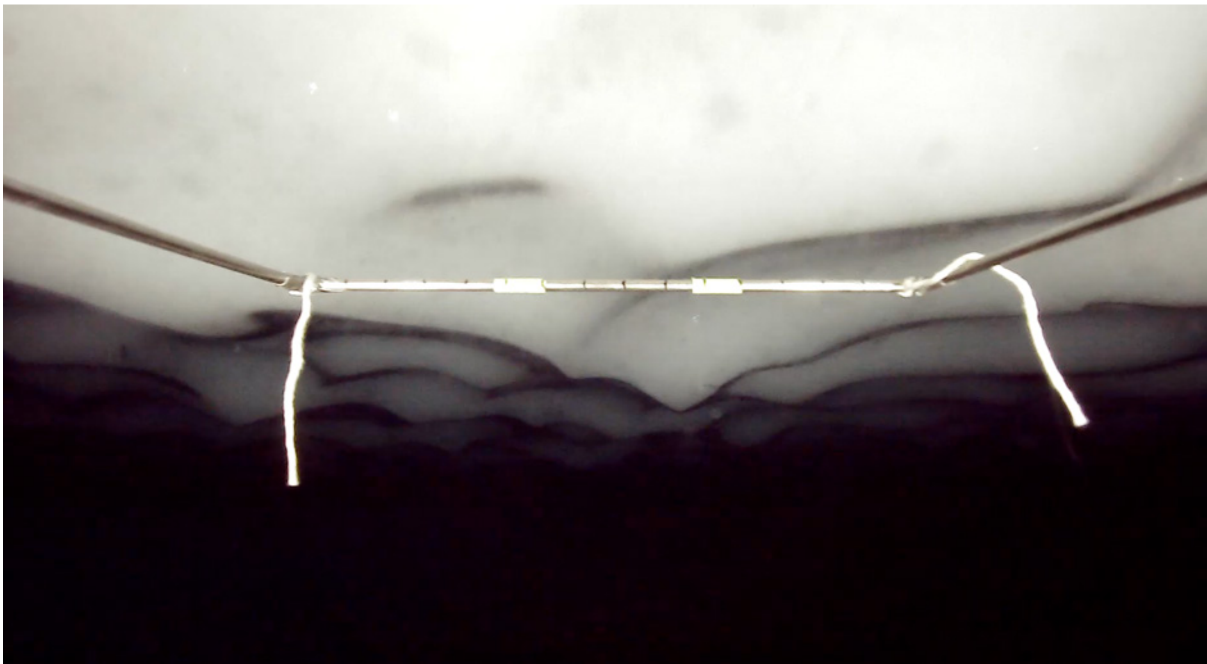

Fig. 7.19: The underside of the ice shelf near the EWOS box (station 51-1)

Conclusions

The aim of this first EWOS expedition was to assess the suitability of various interdisciplinary measurements to monitor key ecosystem processes in the Weddell Sea and their potential change in the future. In this sub-section, we focused on pelagic, sea-ice and shelf-ice associated ecosystem components and showed that it is feasible to sample these habitats with a suite of well-established methods, such as water sampling from the CTD/rosette, sea-ice coring, zooplankton nets and visual surveys. These different methods are necessary to cover the entire size range of organisms shaping the pelagic and cryo-pelagic part of the Weddell Sea ecosystem, from microbes to whales. Looking at the very first raw data, new insights emerge which might be used to guide the further development of the EWOS monitoring: (1) stratified sampling with the M-RMT has shown to be useful to assess the vertical segregation of different taxa (e.g., salps) and the presence of Antarctic krill below 200 m, which is essential information for the best possible estimates of biomass and taxonomic composition of the zooplankton community based on hydroacoustics, (2) the region of the EWOS box may constitute an important nursery area for the ecologically important forage fish *Pleuragramma antarctica* and other Antarctic fishes, including those breeding in nests (see next Section 7.3), (3) the autumn bloom in the young ice of the Weddell Sea may lead to the incorporation of large amounts of biomass in the sea ice, which may further sustain the ecosystem during winter and into the next spring, indicating that autumn might be a critical season for monitoring, (4) the underside of ice shelves and icebergs constitutes a potentially important but hitherto neglected habitat which should be considered in future long-term monitoring.

The time constraints of this expedition have severely impacted on the pelagic, under-ice fauna and sea-ice biota sampling. The low sample size of M-RMT, Multinet and SUIT deployments (only one successful deployment under ice) will make it virtually impossible to assess the zooplankton and under-ice fauna community present in the research area of PS129 in a quantitative manner. The lack of zooplankton samples from the inner Weddell Sea constitutes a painful gap in the EWOS dataset. Realizing that shiptime is limited and harsh conditions will always impact our ability to sample at an appropriate resolution in this area, sampling with sensors and autonomous observatories will need to become an important backbone of future EWOS initiatives. In this respect, the quasi-continuous data collection of the EK80 echosounder and the Autofim sampler provided highly valuable datasets coming out of PS129.

Acknowledgements

We would like to thank Olaf Hüttebräuker, Ilias Nasis, Sarah Kempf, Christopher Jones, Kerstin Beyer, Martin Graeve, Kai-Uwe Ludwichowski, Malte Pallentin, Povl Abrahamsen, Robbie Mallett and Jeremy Wilkinson for their support.

Tab. 7.9: Parameters of pelagic fauna sampling stations and numbers of samples per taxonomic group for each device operation

Station parameters							Number of samples per taxonomic group																	
Device operation	**EWOS site**	**Device**	**Date (UTC)**	**Time (UTC)**	**Latitude (N)**	**Longitude (E)**	**Coel-enterata**	**Cnidaria**	**Hydro-medusae**	**Siphono-phora**	**Scypho-medusae**	**Cteno-phora**	**Poly-chaeta**	**Gastro-poda**	**Cephalo-poda**	**Copepoda**	**Amphi-poda**	**Euphau-siidae**	**Mysida-cea**	**Decapoda**	**Tunicata**	**Actino-pterygii**	**Chaeto-gnatha**	**Zoo-plankton**	**Grand Total**
PS129_20-1	GM_03	SUIT	2022-03-13	08:20	-59.378	0.019						1					3	1			1			1	**7**
PS129_20-4	GM_03	MRMT	2022-03-13	14:41	-59.309	0.032	1			2		1	3	1	3		3	3		2	9	1		6	**35**
PS129_20-5	GM_03	MN	2022-03-13	17:16	-59.299	0.041																		5	**5**
PS129_25-4	GM_05	MRMT	2022-03-15	17:20	-64.092	0.073	1		2				9	6	3	1	9	16			4	12	4	11	**78**
PS129_25-6	GM_05	SUIT	2022-03-15	21:25	-64.075	0.069						1	1	4			5	14			1		2	2	**30**
PS129_25-7	GM_05	MN	2022-03-15	00:42	-64.071	0.103																		5	**5**
PS129_27-1	GM_06	SUIT	2022-03-16	20:02	-66.487	-0.065							7	6			3	14		2	2		3	3	**40**
PS129_27-3	GM_06	MN	2022-03-17	02:09	-66.482	-0.094																		5	**5**
PS129_27-8	GM_06	MRMT	2022-03-17	16:53	-66.557	-0.097			3	1	3	2		3	3		9	17		2	24	18	6	9	**100**
PS129_40-11	EWOS_01	MRMT	2022-03-22	20:53	-70.722	-10.878			4	1		1	5	3	2		3	41			21	31	2	9	**123**
PS129_40-6	EWOS_01	MN	2022-03-21	23:55	-70.725	-10.956																		5	**5**
PS129_45-1	EWOS_08	MRMT	2022-03-25	02:45	-70.788	-10.704			2	2		1	3	10	1		16	43			4	14	3	10	**109**
PS129_47-2	EWOS_08	MN	2022-03-25	18:01	-70.787	-10.757																		5	**5**
PS129_49-7	EWOS_06	MN	2022-03-26	21:56	-70.943	-10.526																		5	**5**
PS129_49-8	EWOS_06	MRMT	2022-03-26	22:55	-70.954	-10.531	1			1		4	2	8			8	8	1		27	7		8	**75**
PS129_52-5	EWOS_05	SUIT	2022-03-27	18:00	-70.942	-10.648						1						2				4		2	**15**
PS129_54-4	EWOS_10	MRMT	2022-03-29	04:06	-70.643	-10.987		1	1	1		2	3	3	2		7	35			22	11	3	12	**103**
PS129_54-5	EWOS_10	MN	2022-03-29	06:12	-70.651	-10.977																		5	**5**
PS129_72-5	WS_10	MRMT	2022-04-07	20:47	-68.977	-27.066		2	1	2	5	3		5	3		9	8		1	41	15	4	10	**109**
PS129_74-8	WS_11	SUIT	2022-04-09	20:00	-70.636	-29.397			1	1		1	1	6			17	30		2			1	5	**65**
Grand Total							**3**	**3**	**14**	**11**	**8**	**18**	**34**	**55**	**17**	**1**	**92**	**232**	**1**	**9**	**156**	**113**	**28**	**123**	**924**

7.3. Seafloor habitats and benthic fauna of the eastern Weddell Sea in Ewos (EWOS III)

Heike Link, Kerstin Beyer, Christopher Gebhardt, Marie Kaufmann, Malte Pallentin, Martin Powilleit, Autun Purser, Henning Schröder
not on board: Jürgen Laudien, Dieter Piepenburg, Claudio Richter, Judith Piontek

Grant-No. AWI_PS129_06

Outline

The Weddell Sea features complex sea-ice dynamics and rich and diverse ecosystems. Its role for global ocean ecosystems and carbon sequestration can only be determined by integrating ecosystem components from the upper ocean (EWOS I and II) and the seafloor ecosystem (EWOS III). Existing time series, spanning approximately 30 years, indicate that benthic community shifts in response to climate change are already underway in Southern Ocean regions of intense environmental change, such as within the waters off the western Antarctic Peninsula (Montes-Hugo et al., 2009; Sahade et al., 2015), but also in the Weddell Sea. In most of the Southern Ocean, sea ice increased between the 1970s and 2014 before it rapidly decreased. A 1988–2014 record of macro- and megafauna from the north-eastern Weddell Sea shelf indicated that benthic biomass decreased by two thirds and composition shifted from suspension feeders to deposit feeders (Pineda-Metz et al., 2020). At the same time, organic matter mineralization, reflected by the intensity of interfacial solute exchange and particle reworking, and therefore carbon sequestration, is related to the benthic infauna community (Link et al., 2013; Renz and Forster, 2013; Morys et al., 2017; Powilleit and Forster, 2018).

EWOS III aims at coordinated and systematic observations of the benthic realm on the shelf of the Weddell Sea ecosystem in order to describe changes in the past and in the future. This will provide the baseline for a mechanistic understanding of effects of climate change on the seafloor system. This study will act as a driver for the international research and monitoring activities to be carried out under the proposed Weddell Sea Marine Protected Area (WSMPA). Specifically, the EWOS III activities aim to complement HAFOS (Chapter 2) with biological analyses of carbon and nutrient fluxes to and from the sea floor, and the respective biota. Two work areas were foreseen: i) the shelf and inflow region off Kapp Norvegia, and ii) stations off the Antarctic Peninsula. The expected results will provide valuable quantitative information on benthic communities from microbes to megabenthos and ecosystem functions, such as carbon export and secondary production. They will constitute an important baseline for the decision about the need for a long-term EWOS observatory. During the PS129 cruise, the EWOS III field studies comprised three interrelated components and gears (Fig. 7.20).

Seafloor habitats and their associated epibenthic megafauna were investigated with the Ocean Floor Observation and Bathymetry System (OFOBS). OFOBS is a towed device capable of deployment in moderately ice-covered regions and capable of concurrently collecting acoustic as well as video and still image data from the seafloor (Purser et al., 2018). The device is the latest iteration of the camera sleds used in Antarctica for several decades. In order to reveal how climatic change affects macro-infauna, historical stations were re-sampled using the Multiboxcorer (MG). For this purpose, the methodology used in previous *Polarstern* expeditions (i.e., PS12, 48, 56, 84, 96) and the same sampling device (MG) was used in order to achieve comparability (Pineda-Metz et al., 2020). Benthic processes are a missing component to estimate the overall role of benthos in potential carbon sequestration. They will be assessed through experimental and observational sampling of sediments from the TV-MUC. Fluxes of oxygen and solutes from incubation chambers together with microbial to macrofaunal assemblages are sampled. Experiments and sampling of particle and solute flux tracers will provide the mechanistic link of benthic biota activity and organic matter remineralization.

Fig. 7.20: Sampling gear deployed for EWOS III
Photos: C. Gebhardt, Uni Rostock

Objectives

The general objective of EWOS III is to provide coordinated and systematic observations of the benthic realm including its processes and its relation to the other ecosystem components (EWOS I and II, HAFOS) in order to describe changes in the past and in the future. Guided by the three components, EWOS III will address the following specific objectives:

- map the habitats using OFOBS data streams that are integrated to produce high-resolution 3D spatial models (topographic maps) of the seafloor. These models allow subsequent high-resolution analysis on a finer scale than has previously been possible of terrain variables, such as slope, aspect and rugosity, and their relationship to ice-berg scour marks and the distribution of benthic fauna in the PS129 research area
- describe the composition, biodiversity, abundance and biomass of microorganismic, endobenthic meio- and macrofauna (with TV-MUC), macro- to megabenthic (with MG) and epibenthic megafauna (with OFOBS) communities by integrating results from all three field survey components
- ground-truthing of non-invasive benthic assessment methods (OFOBS) with the potential of higher spatial and temporal monitoring with direct sampling of benthic assemblages, including the infaunal component hidden beneath the sediment surface
- assess temporal changes in habitats and communities through comparison with surveys dating back to the 1980s

- quantify the benthic processes (functions) relevant for the ecosystem's carbon caused by macro- and meiobenthic communities in relation to environmental variability.

Benthic processes are quantified as the short-term oxygen consumption, nutrient- and solute tracer fluxes, as well as particle reworking activity at and below the sediment-water interface caused by macro- and meiobenthic communities. Solute transport intensity (bio-irrigation) can be quantified by calculating the inventory of Br^- tracer transported into the sediment. Modelling is based on tracer concentration-depth profiles, with overall solute exchange expressed as exchange coefficient α (Powilleit and Forster, 2018). Bioturbation is quantified in terms of diffusion-analogous (Db) and advective (r) transport coefficients by applying the data to a bioturbation model (Hedman et al., 2011). For the first time, the diversity of microbial communities will be assessed in parallel using amplicon sequencing. The relation of fluxes and particle reworking rates to faunal and microbial diversity, organic carbon and detritus availability, and seafloor substrate will thus be determined.

Taxonomic and functional biodiversity and composition of benthic biota will be linked to environmental data, compared with historical ones in order to reveal shifts in function, energy flow, production and species interactions to also allow for forecasts.

Work at sea

Overall, nine EWOS sites could be sampled for the seafloor system, whereas the full set of objectives was met by retrieving samples for three sites (Tab. 7.15; Fig. 7.21).

Tab. 7.15: Overview of sampling gear used and onboard experiments performed by EWOS III

For further information see the end of Chapter 7.3

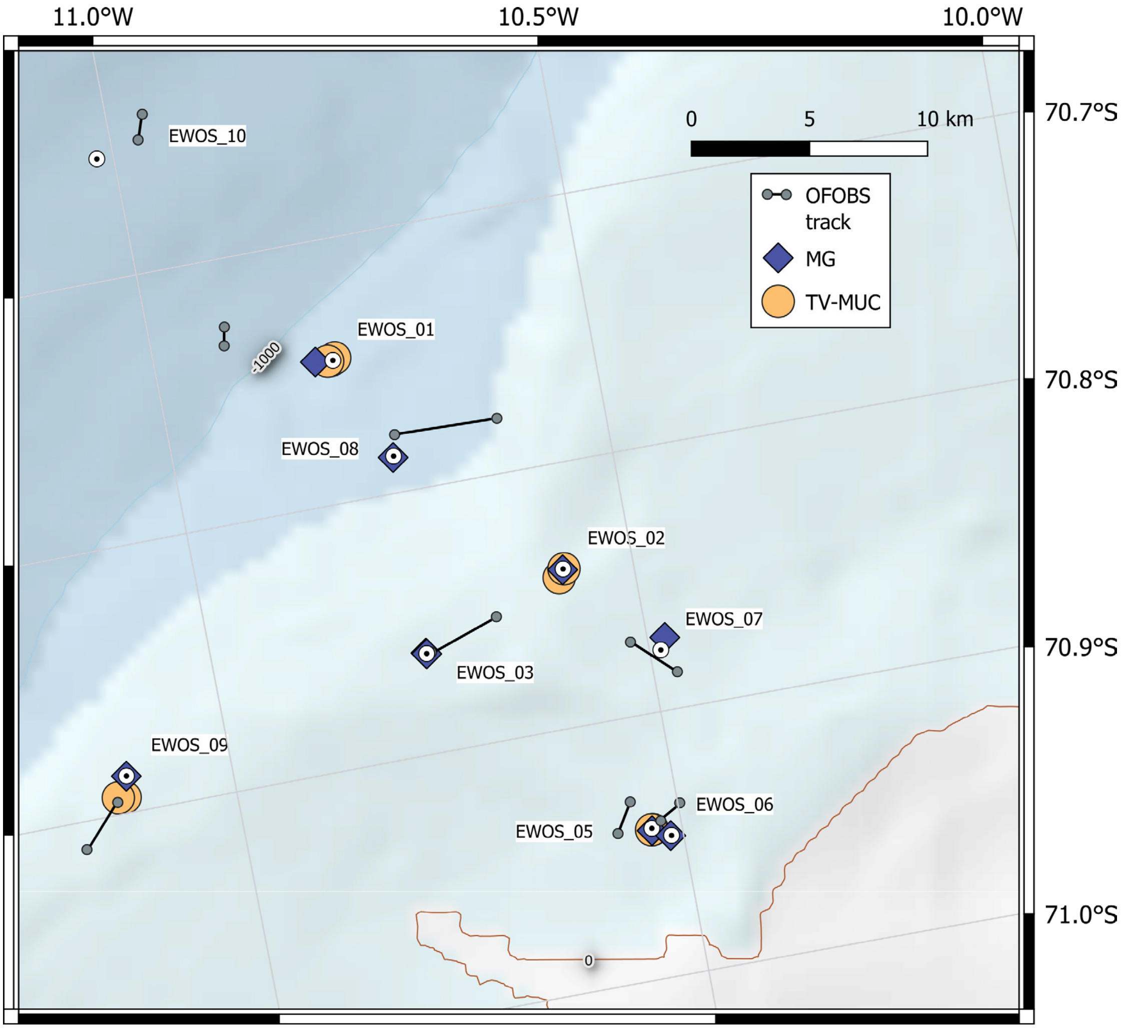

Fig. 7.21: Map showing the exact deployment stations to demonstrate proximity of EWOS III sampling stations in the EWOS area

Seafloor habitat mapping and epibenthic megafauna

The Ocean Floor Observation and Bathymetry (OFOBS) system (Purser et al., 2019) was deployed 9 times in the EWOS box (see Tab. 7.15). Two deployments were made during daylight hours, with appropriate marine mammal watches maintained throughout deployments to ensure compliance with UBA requirements on POSIDONIA use. In all cases deployments were straightforward from the ship, despite adverse weather conditions at some times. Cold temperatures caused some startup problems with equipment during the descent to seafloor, but high-quality image and video surveys were collected across all deployments.

The Ultra Short Base Line (USBL) POSIDONIA system allowed georeferencing of collected images to be carried out throughout all deployments. For the majority of dives, increased positioning accuracy was achived with the onboard Inertial Navigation System (INS) and Dynamic Velocity Logger (DVL) further refining the USBL position.

Throughout 7 deployments, the forward-facing acoustic camera recorded seafloor and water column data. During all 9 deployments, sidescan data was recorded. During three dives, an *ad-hoc* water sampler collected 12 litres of bottom water (about 30-40 cm from seafloor) for onboard colleagues (C. Held and D. Barnes). This water was used for eDNA analysis in conjunction with concurrently collected seafloor image data (see below *Preliminary results*) and for chemical analysis. During 8 dives (OFOBS 2 to 9) a MicroCAT CTD profiler was additionally mounted on the OFOBS frame to record conductivity, temperature and pressure data from throughout each deployment.

Three of the OFOBS dives closely followed historically conducted OFOBS or ROV transects (OFOBS 9 repeating sections of the PS960001-4 OFOS deployment made in 2016 (Schröder et al., 2016), OFOBS 6 covering the BENDEX (Arntz et al., 2005) ROV transect made during PS77 in 2010/2011 (Fahrbach et al., 2011) and OFOBS 7 covering directly a deployment made in 1999 by another ROV during PS48 (Wolf and Gutt, 1999). With the exception of OFOBS 1 and OFOBS 8, the PS129 OFOBS deployments were made in close proximity to previous OFOS, MUC or ROV imaging deployments (Fig. 7.21). Unfortunately, poor weather conditions prevented a closer adherence to the historically conducted transects.

Macrobenthic communities and biodiversity

In total seven of the proposed EWOS sites were sampled using a Multiboxcorer (MG). Six of these stations are historical stations that have been resampled (PS48, PS96, ANTXXVII/3, BENDEX). The MG was equipped with a camera system to observe the seafloor before sampling. Nine replicated boxes (samples) can be taken in one deployment. On some stations, sample number is lower due to the composition of the seafloor and stones hindering the boxes to close (Tab. 7.15, Fig. 7.21). Subsamples for grain size determination and eDNA analysis (surface sediments) as well as a sediment core for eDNA depth profile measurements were taken from one of the boxes at each station. These subsamples were stored at -20° C for later analysis. The remaining boxes were sieved for macroinfaunal samples with a mesh size of 500 µm. For genetic analysis, one of the subsamples was fixed in 96 % ethanol, the remaining subsamples were preserved in buffered 4 % formaldehyde solution.

Assessment of the benthic processes' oxygen consumption, solute fluxes and particle reworking in relation to the benthic community

Replicated sediment cores were successfully retrieved from TV-MUC deployments at EWOS sites EWOS_01, EWOS_02 and EWOS_05 (Tab. 7.15, Fig. 7.21). Deployment at EWOS_09 (PS129_57) was not successful. In general, we strongly recommend the addition of the live camera-system with telemetry to the MUC. Particularly in patchy and sometimes gravelly terrain, the live images from the seafloor were crucial and time-efficient for successful sample retrieval.

Two cores per site were immediately sampled for molecular analyses of microbial and meiobenthic communities. For microbial community assessment samples, cores were sliced into 0-0.5, 0.5-1.0, 1.0-1.5, 1.5-2.0 and 1 cm slices down to 12 cm. For meiofauna, half slices of the cores were sampled in 1 cm intervals down to 5 cm, 5-7 cm, 7-10 cm and 10-12 cm. All subsamples were frozen at -20°C for later analyses in the home laboratories at the IOW (Rostock, Germany) and Senckenberg am Meer (Wilhemshaven, Germany).

We assessed short-term oxygen consumption as well as nutrient fluxes at the sediment-water interface through *ex situ* incubations on the remaining cores: we measured oxygen concentrations in the water phase overlying the sediments over time using a non-invasive fiberoptic probe in (dark) 96 h incubations conducted in a temperature-controlled laboratory container. Nutrient fluxes were computed as changes in nutrient concentration in the overlying water in samples taken at the start and end of the incubations (Link et al., 2013, 2016). To quantify the transport of dissolved substances into the sediment (bioirrigation) induced by organisms, the depth distribution of the tracer bromide (Br^-) in the pore water of 7 sediment cores at the three sites (PS129_40, PS129_44 and PS129_52) in the EWOS area was investigated in the same incubation experiments. After the inert NaBr was added to the near-bottom water above the sediment at a concentration of about 10 mmol/L, the 3-day incubation phase started. After the end of the incubation period, pore water samples were taken at centimetre intervals down to a sediment depth of 12 cm from pre-drilled sampling points using rhizones. These consist of fine-pored, rod-shaped frits inserted horizontally into the sediment, and through these at least 2 ml pore water could be obtained from each layer by means of negative pressure. The samples were stored at -20 °C, the actual measurement of the Br concentrations in the depth profile will be done by ion chromatography in the laboratory of the University of Rostock. Subsequently, the bioirrigation activity will be quantified by modelling the measured Br^- inputs into the sediment. Where additional pore water was available by use of rhizons (as described above), it was frozen for analyses at the University of Rostock.

After incubations, cores were cut according to two schemes: (1) sediment cores used for bioirrigation incubations were cut into 0-0.5, 0.5-1.0, 1.0-1.5, 1.5-2.0 and 1 cm slices down to 12 cm. The first half was used to subsample for chlorophyll a content, which will be later used to quantify particle reworking coefficients for this naturally occurring particle tracer, and for microbial communities. The second half was preserved in 4 % buffered formaldehyde-seawater solution for later analyses of biodiversity patterns in macro- and meiofauna (1 cm intervals down to 5 cm, 5-7 cm, 7-10 cm and 10-12 cm). (2) The remaining cores were cut into 0-2 cm and 2-5 cm slices for biodiversity patterns in macro- and meiofauna and sieved over 500 µm sieve for macrofauna biodiversity patterns for the rest of the cores. Here, sediment subsamples for chlorophyll a and grain size were taken (0-5 cm) from each core using 10 ml coring syringes and frozen at -20°C for later analyses at the University of Rostock (Link et al., 2016).

At stations PS129_48 and PS129_52, cores from additional TV-MUCs were obtained for experimental work to quantify macrofauna-induced particle reworking through addition of luminophores (Queiros et al., 2015; Fig. 7.22). 15 Cores of each station were divided into three experimental treatments with five replicates each: azoic controls, particle reworking of the natural occurring assemblage, and a single species addition. Prior to the start of each experiment, all sediment cores were stored in the dark under an ambient temperature of 1.5° C for 3-4 days. All fauna was exterminated in control treatment cores by the addition of concentrated Na_2SO_3 solution. For the species addition treatment, one brittle star was added to each core and allowed to acclimatize for two days. Dead or disintegrating specimens were replaced by new individuals of the same species. Luminophores – inert, fluorescently labeled sediment particles within the size range of 63-125 µm – were incubated in bottom seawater for 9-15 days prior to the experiment to ease suspension and were added in quantities of 2 g to each sediment core. Cores were incubated for 12 days with a daily 12h:12h aeration cycle for oxygen supply. Upon experiment termination, sediment cores were sliced into layers of 1 cm thickness down to a sediment depth of 15 cm. Sediment layers were divided into two equal-sized subsamples for luminophore quantification and fauna identification, respectively. Luminophore samples are stored at -20° C for further analysis. All fauna samples were sieved through a 500 µm mesh (except sediment samples from 0-5 cm sediment depth which will be used for macro- and meiofauna analysis) and fixed in buffered 4% formaldehyde-seawater solution for later analysis at the University of Rostock.

The time-series sampling of historical stations PS81_190 and PS96_115 with the TV-MUC off the Antarctic Peninsula and PS96_01 in the EWOS area could not be achieved due to time constraints.

Fig. 7.22: Sediment core after luminophore treatment retrieved from TV-MUC at station EWOS_06. Luminophores are clearly distinguished by the pink color compared to the original sediment core. Photo: C. Gebhardt, Uni Rostock

Preliminary results

While seafloor habitat mapping provides preliminary results (see below), laboratory analyses are required for obtaining results for macro- and meiobenthic communities and benthic processes. The expected results will provide a quantitative assessment of the benthic fauna (from meio to mega) and microbial communities in relation to environmental drivers, and their habitats in the EWOS area. For three sites, the complete assessment of seafloor communities and their processes will be available, while seven EWOS sites can be characterized based on habitat mapping and macro- to mega(epi)benthic communities. From these data, ecological indices will be derived, the community structure be described and changes to archived community data assessed. The species composition and diversity of the benthic communities will be related to environmental parameters and compared with data from previous ROV transects, underwater photographs and biological sampling to identify changes in communities, their function and species interactions and to be able to make predictions for future environmental scenarios. Process studies from three sites will reveal the oxygen consumption and nutrient fluxes at the sediment-water interface caused by macro- and meiobenthic communities in relation to organic carbon availability, seafloor substrate and microbial diversity. Furthermore, solute (Br^-) and particulate tracer (chlorophyll a, luminophores) distributions in the sediment will be used for modelling bioirrigation and bioturbation processes, which are at present scarcely or not at all available in the Weddell Sea. Overall, results will provide a valuable quantitative baseline for the decision about the need for a long-term EWOS observatory and contribute to decide on potential LTER programme sites.

Seafloor habitat mapping and epibenthic megafauna

The image, video and acoustic data collected during the 9 OFOBS transects were subject to a brief evaluation during the cruise and some statements on the key habitats and fauna imaged throughout these different deployments are introduced below. Two OFOBS deployments were made in the BENDEX area (OFOBS 5 and 6) and the here collected extensive sidescan, image and video data sets will be used to produce an accurate map for the future monitoring of recolonization over time of this 19-years-old physical disturbance experimental site.

More detailed analyses will be conducted and seafloor acoustic and image-based maps will be produced at the home institute, prior to upload to permanent data repositories. These analyses will be considered in the context of the data produced by the other EWOS scientists and will ideally be used to support integrated assessments of the surveyed regions. Below, preliminary results from the 9 OFOBS transects are shown:

OFOBS 1 at station EWOS 1 – PS129_40-5

During PS129, OFOBS was deployed to collect image, sidescan, forward sonar and video data from depths deeper than historically surveyed by previous AWI surveys in the area. OFOBS 1 was one such dive (Fig. 7.23). Collected were 337 images, showing a soft bottomed seafloor. Most abundant fauna were cup corals and shrimp, with occasional octopi, fish and echinoids also observed.

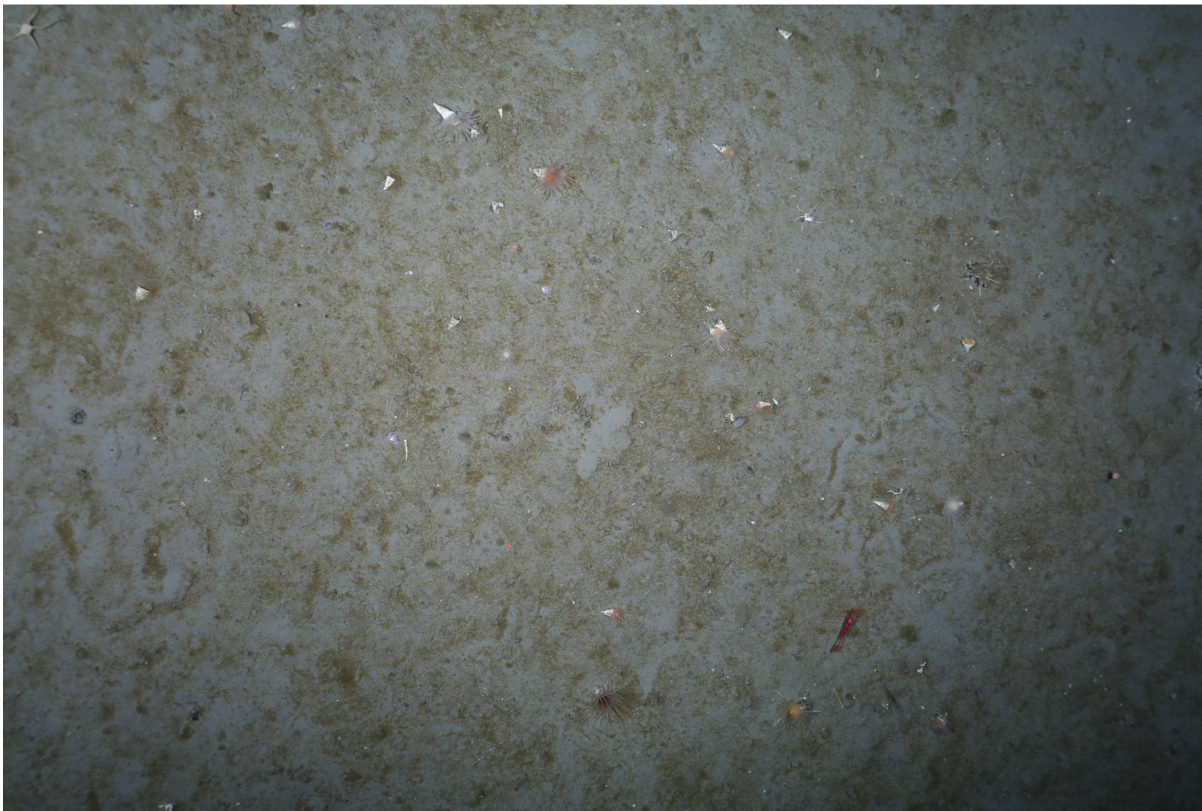

Fig. 7.23: Typical OFOBS seafloor image (TIMER_2022_03_21 at 21_15_42.jpg) from PS129_40-5. A soft and muddy detritus covered seafloor was typically recorded across the deployment. Individual cup corals and surface deposit feeders were much in evidence.

OFOBS 2 at station EWOS 3 – PS129_43-3 pt 1

OFOBS 2 recorded video, sidescan, forward acoustic camera and 505 images of a shallow (~300 m depth) area of seafloor (Fig. 7.24). A bryzoa- and sponge-rich seafloor community was primarily observed, though several areas of seafloor which had been scoured by icebergs were also imaged.

Fig. 7.24: Typical OFOBS seafloor image (TIMER_2022_03_24 at 10_48_45.jpg) from station PS129_43-3, pt 1

OFOBS 3 at station EWOS 2 – PS129_43-3 pt 2

OFOBS 3 recorded video, sidescan, forward acoustic camera and 95 images of a shallow (~300 m depth) area of seafloor. The seafloor community and condition observed were similar to recorded during the OFOBS 2 deployment.

Fig. 7.25: Typical OFOBS seafloor image (TIMER_2022_03_24 at 12_49_49.jpg) from station PS129_43-3, pt 2

OFOBS 4 at station EWOS 8 – PS129_47-4

OFOBS 4 recorded video, sidescan, forward acoustic camera and 478 images across a transect from 770 to 470 m depth. The seafloor was generally rather rugose with numerous small stones and dropstones of up to 1 m diameter reasonably abundant (Fig. 7.26). Occasional fish nest forms were observed behind dropstones, as were various fish.

Fig. 7.26: Typical OFOBS seafloor image (TIMER_2022_03_26 at 01_16_43.jpg) from station PS129_47-4

OFOBS 5 at stations EWOS 5 and EWOS 6 (BENDEX N-S mapping) – PS129_49-3

During OFOBS 5, a-figure-of-eight deployment was made over the historical BENDEX disturbance site. The purpose for this deployment plan was to ensure a complete coverage of the area with the OFOBS sidescan system, to ideally allow an accurate map of the site to be generated post-cruise from these acoustic data. Also collected were 409 images from the BENDEX trawled area and adjacent undisturbed sites. The areas trawled 19 years ago were still very much evident in the majority of image data (Fig. 7.27), though the trawls were not very deep, rendering them less distinct in the acoustic data than was predicted.

Fig. 7.27: Typical OFOBS seafloor image (TIMER_2022_03_26 at 14_56_55.jpg) from station PS129_49-3

OFOBS 6 at stations EWOS 5 and EWOS 6 (BENDEX E-W mapping) – PS129_50-1

During OFOBS 6, the sidescan mapping of the BENDEX site was continued and a historical ROV transect repeated. OFOBS 6 concentrated on east-west transects of the trawled area and cross-cutting the extreme north and south extents of the trawled areas. As with OFOBS 5, the seafloor imaged was a mix of trawl scoured seafloor and occasional islands of fauna undisturbed by the nets (Fig. 7.28). No extensive recolonization of trawled areas by megafauna were observed.

Fig. 7.28: Typical OFOBS seafloor image (TIMER_2022_03_27 at 02_25_02.jpg) from station PS129_50-1

OFOBS 7 at station EWOS 7 – PS129_53-2

OFOBS 7 directly surveyed an area of seafloor initially surveyed with ROV by Julian Gutt and his team in 1999 (Wolf and Gutt, 1999). Their initial survey plan was incorporated into the OFOBS 7 dive plan with 500 m to the west and 1 km to the east of the initial survey also imaged with OFOBS. OFOBS 7 recorded video, sidescan, forward acoustic camera and 466 images across a transect of approximately 233 m depth (Fig. 7.29). On initial examination of the collected data, it seems a decrease in local filter feeder abundance has taken place during the years since the initial survey. OFOBS 7 was locally particularly rich in starfish abundances.

Fig. 7.29: Typical OFOBS seafloor image (TIMER_2022_03_28 at 03_38_34.jpg) from station PS129_53-2

OFOBS 8 at station EWOS 10 – PS129_54-2

OFOBS 8 surveyed an area of seafloor at about 1340 m depth. A soft sedimented area abundant with shrimp, starfish, fish and anenomes, though wholly absent of dropstones or hard ground was imaged in 265 images (Fig. 7.30). Video, sidescan and forward acoustic camera images were also collected.

Fig. 7.30: Typical OFOBS seafloor image (HOTKEY_2022_03_28 at 23_51_20.jpg) from station PS129_54-2

OFOBS 9 at station EWOS 9 – PS129_57-4

During OFOBS 9, the intention of the deployment was to re-cover an OFOS deployment carried out in 2015/2016 during PS96 (Schröder et al., 2016). Unfortunately, tough ice and weather conditions meant only the most westerly 200 m of the historical track could be resurveyed, with an extended area to the further west being additionally surveyed. During OFOBS 9, 466 seafloor images, video, sidescan and forward sonar data were collected. The average depth of the surveyewd area was about 295 m and an abundant and diverse, rugose and iceberg scoured seafloor ecosystem was imaged (Fig. 7.31), reminiscent of that surveyed during PS96. The acoustic systems of OFOBS, coupled with the western extended survey region, revealed that the individual fish nests reported in Schröder et al. (2016) were abundant across the full survey region and that in areas scoured by glaciers, nest arrays reminiscent of those reported in Purser et al. (2022) from further south in the Weddell Sea were present. In Figure 7.32, these arrays can clearly be seen in the raw sidescan 'waterfall' data recorded from the device. Whilst on the cruise, 'Structure from Motion' (SfM) modelling using video frames extracted from the raw OFOBS data were used to generate 3D mosaics of the contrasting sub-habitats utilized by nesting fish in this area. An example of the nests occupying an iceberg scour area surveyed during PS129, is given in Figure 7.33.

Fig. 7.31: Typical OFOBS seafloor image (TIMER_2022_03_30 at 04_09_57.jpg) from station PS129_57-4

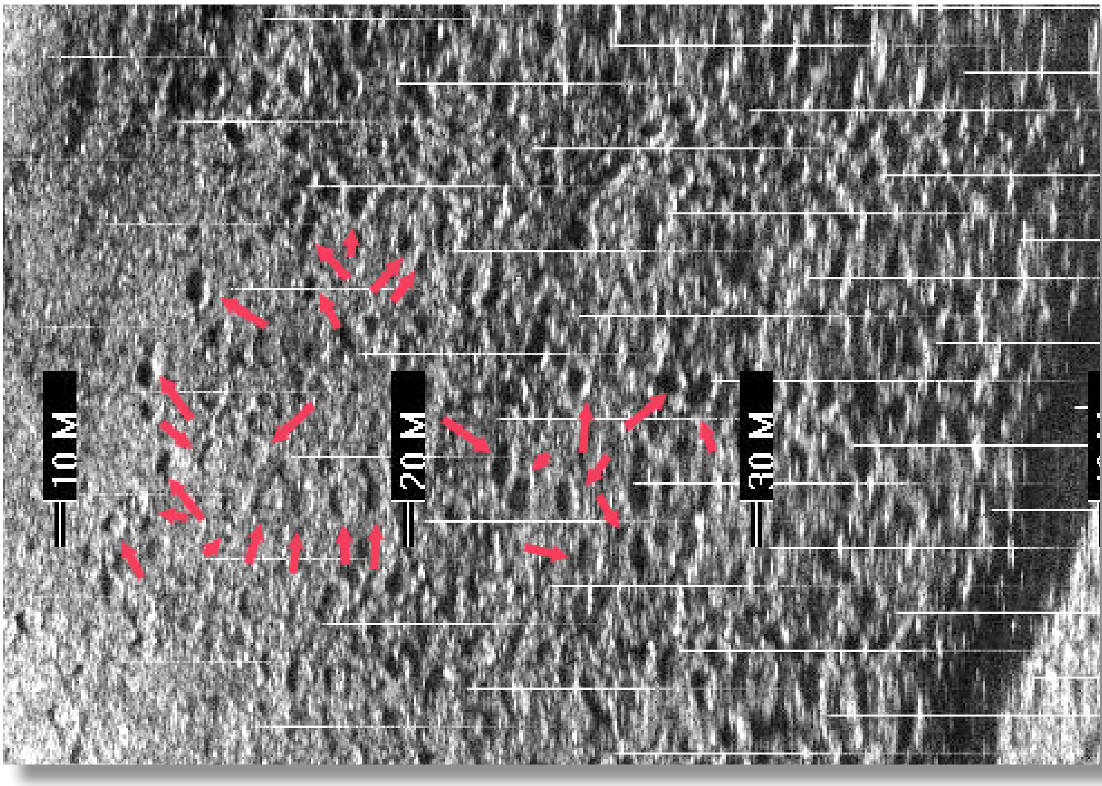

Fig. 7.32: Typical 'waterfall' sidescan data extract showing a 40 m seafloor swath from the starboard side of OFOBS collected during OFOBS 9 (PS129). As can be seen in the data, which have not yet been vertically corrected for distance, there are numerous circular fish nest forms, reflective in the acoustic beams. The pink arrows indicate a number of individual nests. Figure prepared by Autun Purser

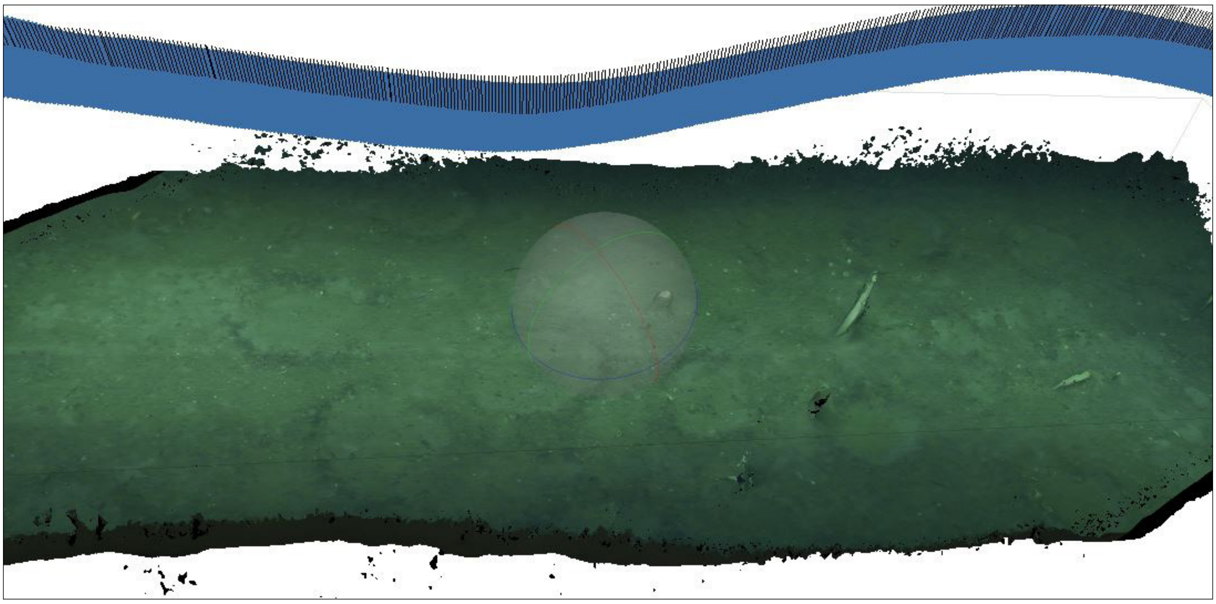

Fig. 7.33: A 'SfM' mosaic model constructed from 509 video frames extracted from the OFOBS 9 video data recorded above an iceberg scoured area of seafloor. The model covers an area of approximately 10 m x 3 m. The nests seem to be of several different sizes. Model prepared by Autun Purser

Data management

Environmental data will be archived, published and disseminated according to international standards by the World Data Center PANGAEA Data Publisher for Earth & Environmental Science (https://www.pangaea.de) within two years after the end of the cruise at the latest. By default, the CC-BY license will be applied.

Molecular data (DNA and RNA data) will be archived, published and disseminated within one of the repositories of the International Nucleotide Sequence Data Collaboration (INSDC, www.insdc.org) comprising of EMBL-EBI/ENA, GenBank and DDBJ).

Any other data will be submitted to an appropriate long-term archive that provides unique and stable identifiers for the datasets and allows open online access to the data.

This expedition was supported by the Helmholtz Research Programme "Changing Earth – Sustaining our Future" Topic 6, Subtopics 1, 2 and 4.

In all publications based on this expedition, the **Grant No. AWI_PS129_04, AWI_PS129_05,** or **AWI_PS129_06** will be quoted and the following publication will be cited:

Alfred-Wegener-Institut Helmholtz-Zentrum für Polar- und Meeresforschung (2017) Polar Research and Supply Vessel POLARSTERN Operated by the Alfred-Wegener-Institute. Journal of large-scale research facilities, 3, A119. http://dx.doi.org/10.17815/jlsrf-3-163.

References

Arntz WE, Brey T et al. (2005) The Expedition ANTARKTIS XXI/2 (BENDEX) of RV "Polarstern" in 2003 & 2004. Ber. Polarforsch. Meeresforsch., 503, ISSN 1618-3193.

Bosshart S, Erni-Cassola G, Burkhardt-Holm P (2020) Independence of microplastic ingestion from environmental load in the round goby (*Neogobius melanostomus*) from the Rhine River using high quality standards. Environmental Pollution, 267, 115664.

Daly M, Rack F, Zook R (2013). *Edwardsiella andrillae*, a new species of sea anemone from Antarctic ice. PLoS One, 8(12), e83476.

Erni-Cassola G, Wright RJ, Gibson MI, Christie-Oleza JA (2020) Early colonization of weathered polyethylene by distinct bacteria in marine coastal seawater. Microbial Ecology, 79, 517–526.

Fahrbach E et al. (2011) The Expedition of the Research Vessel "Polarstern" to the Antarctic in 2010/2011 (ANT-XXVII/2). Ber. Polarforsch. Meeresforsch., 634, ISSN 1866-3192.

Gutt J, Arndt S, Barnes DKA, Bornemann H, Brey T, Eisen O, Flores H, Griffiths H, Haas C, Hain S, Hattermann T, Held C, Hoppema M, Isla E, Janout M, Le Bohec C, Link H, Mark FC, Moreau S, Trimborn S, van Opzeeland I, Pörtner HO, Schaafsma F, Teschke K, Tippenhauer S, Van de Putte A, Wege M, Zitterbart D, Piepenburg D (2022) Reviews and syntheses: A framework to observe, understand, and project ecosystem response to environmental change in the East Antarctic Southern Ocean. Biogeosciences, 19, 5313-5342.

Hedman JE, Gunnarsson J S, Samuelsson G, Gilbert F (2011) Particle reworking and solute transport by the sediment-living polychaetes *Marenzelleria neglecta* and *Hediste diversicolor.* Journal of Experimental Marine Biology and Ecology, 407, 294-301. http://dx.doi.org/10.1016/ j.jembe.2011.06.026

Leistenschneider C, Burkhardt-Holm P, Mani T, Primpke S, Taubner H, Gerdts G (2021) Microplastics in the Weddell Sea (Antarctica): A forensic approach for discrimination between environmental and vessel-induced microplastics. Environmental Science and Technology, 55, 15900–15911.

Link H, Piepenburg D, Archambault P (2013) Are hotspots always hotspots? The relationship between diversity, resource and ecosystem functions in the Arctic. PLoS ONE 8(9), e74077. https://doi.org/10.1371/journal.pone.0074077

Link H, Veit-Köhler G, Seifert DM, Bodur Y (2016) Tracing the effect of changing ice cover on benthic ecosystem functioning - from meio to macro. In: Schröder M (ed) The expedition PS96 of the Research Vessel POLARSTERN to the southern Weddell Sea in 2015/2016. Alfred Wegener Institute for Polar and Marine Research, Bremerhaven, p 105-112.

Montes-Hugo M, Doney SC, Ducklow HW, Fraser W, Martinson D, Stammerjohn SE, Schofield O (2009) Recent changes in phytoplankton communities associated with rapid regional climate change along the western Antarctic Peninsula. Science, 323, 1470-1473.

Morys C, Powilleit M, Forster S (2017) Bioturbation in relation to the depth distribution of macro-zoobenthos in the southwestern Baltic Sea. Marine Ecology Progress Series, 579, 19-36. https://doi.org/10.3354/meps12236

Pineda-Metz SE, Gerdes D, Richter C (2020) Benthic fauna declined on a whitening Antarctic continental shelf. Nature Communications, 11(1), 2226.

Powilleit M, Forster S (2018) Continuous and high transport of particles and solutes by benthos in coastal eutrophic sediments of the Pomeranian Bay. Frontiers in Marine Science, 5, 472. https://doi.org/10.3389/fmars.2018.00472

Purser A, Hehemann L, Boehringer L, Tippenhauer S, Wege M, Bornemann H, Pineda-Metz SEA, Flintrop CM, Koch F, Hellmer HH, Burkhardt-Holm P, Janout M, Werner E, Glemser B, Balaguer J, Rogge A, Holtappels M, Wenzhoefer F (2022) A vast icefish breeding colony discovered in the Antarctic. Current Biology 32, 842-850.

Purser A, Marcon Y, Dreutter S, Hoge U, Sablotny B, Nottin S, Hehemann L. Lemburg J, Dorschel B, Biebow H, Boetius A (2019) Ocean Floor Observation and Bathymetry System (OFOBS): A towed camera/sonar system for deep-sea habitat surveys. J Ocean Eng, 44, 87-99.

Renz JR, Forster S (2013) Are similar worms different? A comparative tracer study on bioturbation in the three sibling species *Marenzelleria arctia*, *M. viridis* and *M. neglecta* from the Baltic Sea. Limnology and Oceanography, 58(6), 2046-2058. https://doi.org/10.4319/lo.2013.58.6.2046

Sahade R, Lagger C, Torre L, Momo F, Monien P, Schloss I, Barnes DKA, Servetto N, Tarantelli S, Tatián M, Zamboni N, Abele D (2015) Climate change and glacier retreat drive shifts in an Antarctic benthic ecosystem. Science Advances, 1(10), e1500050.

Schröder M et al. (2016) The Expedition PS96 of the research vessel POLARSTERN to the southern Weddell Sea in 2015/2016. Ber. Polarforsch. Meeresforsch. 700 ISSN 1866-3192. https://doi.org/10.2312/BzPM_0700_2016

Wolf EA, Gutt J (1999) The Expedition ANTARKTIS XV/3 (EASIZ II) of RV POLARSTERN in 1998. Ber. Polarforsch., 301, 229 pp.

Tab. 7.15: Overview of sampling gear used and onboard experiments performed by EWOS III

Station	Date/time	EWOS Site	Gear	Comment	Latitude	Longitude	Depth [m]	No Picture Frames	Cores/Water	Subsamples									
										Macrofauna	Meiofauna	Microbio	eDNA	grain size	O_2/solute exchange	Br^-tracer/PW	Chl a profiles	Luminophore Experiment	
PS129_40-5	21.03.22 21:56	EWOS_01	OFOBS	max depth/on ground	-70,732825	-10,916521		1089	337										
PS129_40-5	21.03.22 23:26	EWOS_01	OFOBS	information	-70,725818	-10,912191		1102,2											
PS129_40-8	22.03.22 06:42	EWOS_01	TV-MUC	max depth/on ground	-70,745915	-10,799049		914,1		8	5	7	4		2	5	3	3*	
PS129_40-9	22.03.22 09:14	EWOS_01	MG_PS	max depth/on ground	-70,745374	-10,81721		937,3		6	6	0	0	core +surface	1	0	0	0	
PS129_42-2	24.03.22 04:13	EWOS_02	MG_PS	max depth/on ground	-70,840277	-10,581677		254,9		9	9	0	0	surface	1	0	0	0	
PS129_43-1	24.03.22 06:37	EWOS_03	MG_PS	information	-70,862132	-10,755173		301,7		0	0	0	0	x	0	0	0	0	
PS129_43-2	24.03.22 06:52	EWOS_03	MG_PS	max depth/on ground	-70,862102	-10,754		302,4		8	8	0	0	core + surface	1	0	0	0	
PS129_43-3	24.03.22 08:39	EWOS_03	OFOBS	max depth/on ground	-70,86189	-10,74821		299,8	505										
PS129_43-3	24.03.22 08:39	EWOS_03	OFOBS	information	-70,86189	-10,748137		299,6	93										
PS129_43-3	24.03.22 11:51	EWOS_03	OFOBS	on deck	-70,853164	-10,666904		269,9											
PS129_44-1	24.03.22 12:32	EWOS_02	TV-MUC	max depth/on ground	-70,842983	-10,587264		244,3		0									
PS129_44-2	24.03.22 14:40	EWOS_02	TV-MUC	max depth/on ground	-70,839931	-10,578744		251,8		4	3	4	2		1	3	1	1	
PS129_47-4	25.03.22 23:24	EWOS_08	OFOBS	max depth/on ground	-70,778072	-10,743258		688,7	479										
PS129_47-4	26.03.22 02:31	EWOS_08	OFOBS	profile end	-70,779168	-10,624015		504,6											
PS129_47-5	26.03.22 04:06	EWOS_08	MG_PS	max depth/on ground	-70,786476	-10,74984		611,7		8	8	0	0	core + surface	1	0	0	0	
PS129_48-1	26.03.22 06:50	EWOS_01	TV-MUC	max depth/on ground	-70,746003	-10,797929		911,3											
PS129_48-2	26.03.22 08:01	EWOS_01	TV-MUC	max depth/on ground	-70,745869	-10,799005		912,9		8									8
PS129_48-3	26.03.22 09:03	EWOS_01	TV-MUC	max depth/on ground	-70,746146	-10,800111		912,8		7									7
PS129_49-3	26.03.22 14:45	EWOS_05	OFOBS	max depth/on ground	-70,940804	-10,523132		263,4	409										
PS129_49-3	26.03.22 17:39	EWOS_05	OFOBS	on deck	-70,935392	-10,497735		227,9											

Station	Date/time	EWOS Site	Gear	Comment	Latitude	Longitude	Depth [m]	No Picture Frames	Cores/Water	Subsamples: Macrofauna	Meiofauna	Microbio	eDNA	grain size	O_2/solute exchange	Br^-tracer/PW	Chl a profiles	Luminophore Experiment		
PS129_49-4	26.03.22 18:49	EWOS_05	MG_PS	max depth/on ground	-70,943883	-10,535249		296,2		9	9	0	0	core + surface	1	0		0	0	
PS129_49-6	26.03.22 21:03	EWOS_06	MG_PS	max depth/on ground	-70,947011	-10,514975		261,2		9	9	0	0	core + surface	1	0		0	0	
PS129_50-1	27.03.22 01:23	EWOS_06	OFOBS	information	-70,942587	-10,574757		320,5	726											
PS129_50-1	27.03.22 05:34	EWOS_06	OFOBS	on deck	-70,931621	-10,554057		299,4												
PS129_52-1	27.03.22 13:42	EWOS_05	TV-MUC	max depth/on ground	-70,94355	-10,534428		292,4		8	2	3	2		1		2	1	1	5
PS129_52-2	27.03.22 14:33	EWOS_05	TV-MUC	max depth/on ground	-70,943505	-10,534382		292,6		8	2	2	1		1		2	1	1	5
PS129_52-3	27.03.22 15:19	EWOS_05	TV-MUC	max depth/on ground	-70,943525	-10,535592		294,8		8	2	3	2		1		2	1	1	5
PS129_53-2	28.03.22 02:51	EWOS_07	OFOBS	profile start	-70,871975	-10,519886		232,9	445											
PS129_53-2	28.03.22 05:13	EWOS_07	OFOBS	on deck	-70,886296	-10,472756		232,8												
PS129_53-5	28.03.22 11:20	EWOS_07	MG_PS	failed	-70,871549	-10,482769		233,5		0	0	0	0	x	0	0		0	0	0
PS129_54-2	28.03.22 23:09	EWOS_10	OFOBS	max depth/on ground	-70,64989	-10,968565		1348	265											
PS129_54-2	29.03.22 00:38	EWOS_10	OFOBS	Stopp for water sampling	-70,639889	-10,956689		1343,6												
PS129_54-2	29.03.22 00:46	EWOS_10	OFOBS	profile end	-70,640635	-10,958279		1345,2												
PS129_57-1	29.03.22 22:36	EWOS_09	MG_PS	max depth/on ground	-70,886124	-11,122328		325,2		6	6	0	0	surface	1	0		0	0	0
PS129_57-2	30.03.22 00:53	EWOS_09	TV-MUC	max depth/on ground	-70,893879	-11,1283		296,8		0										
PS129_57-3	30.03.22 01:47	EWOS_09	TV-MUC	max depth/on ground	-70,893553	-11,136125		305,4		0										
PS129_57-4	30.03.22 03:44	EWOS_09	OFOBS	profile start	-70,910549	-11,183418		285,7	466											
PS129_57-4	30.03.22 06:35	EWOS_09	OFOBS	profile end	-70,895211	-11,137764		300,3												

* Surface sediments for Chla-degradation time samples were taken

APPENDIX

A.1 TEILNEHMENDE INSTITUTE / PARTICIPATING INSTITUTS

A.2 FAHRTTEILNEHMER:INNEN / CRUISE PARTICIPANTS

A.3 SCHIFFSBESATZUNG / SHIP’S CREW

A.4. STATIONSLISTE / STATION LIST

A.1 TEILNEHMENDE INSTITUTE / PARTICIPATING INSTITUTS

Affiliation	Address
BE.IRSNB	Institut Royal des Sciences Naturelles de Belgique Directorate Natural Enviroment Rue Vautier 29 1000 Brussels Belgium
BE.VLIZ	Vlaams Instituut voor de Zee (VLIZ)/Flanders Marine Institute Wandelaarkaai 7 8400 Oostende Belgium
CH.UNIBAS	Universität Basel Department Umweltwissenschaften Vesalgasse 1 4051 Basel Switzerland
DE.AWI	Alfred-Wegener-Institut Helmholtz-Zentrum für Polar- und Meeresforschung Postfach 120161 27515 Bremerhaven Germany
DE.DWD	Deutscher Wetterdienst Seewetteramt Bernhard-Nocht-Straße 76 20359 Hamburg Germany
DE.HeliService	Heli Service International GmbH Gorch-Fock-Straße 105 26721 Emden Germany
DE.HSB	Hochschule Bremerhaven An der Karlstadt 8 27568 Bremerhaven Germany
DE.IOW	Leibniz-Institut für Ostseeforschung Seestraße 15 18119 Rostock/Warnemünde Germany

Affiliation	Address
DE.UNI-Rostock	Universität Rostock Maritime Systeme Albert-Einstein-Straße 21 18059 Rostock Germany
ES.ULPGC	Universidad de Las Palmas de Gran Canaria Facultad de Ciencias del Mar Campus de Tafira 35017 Las Palmas de Gran Canaria Spain
GOV.NOAA	National Oceanic and Atmospheric Administration 8901 La Jolla Shores Dr. La Jolla, CA 92037 U.S.A.
IT.UNIPD	Universita Degli Studi Di Padova Via U. Bassi 58/b 35121 Padova Italy
NL.DORSSEN	M. van Dorssen Metaalbewerking Schilderend 113 1791 BE Den Burg The Netherlands
NL.NIOZ	Koninklijk Nederlands Instituut voor Onderzoek der Zee (NIOZ) P.O. Box 59 1790 AB Den Burg/Texel The Netherlands
NL.RUG	Rijksuniversiteit Groningen P.O. Box 11103 9700 CC Groningen The Netherlands
NL.WUR	Wageningen Marine Research Ankerpark 27 1781 AG Den Helder The Netherlands
UK.BAS	British Antarctic Survey High Cross, Madingley Rd. Cambridge CB3 0ET United Kingdom
UK.EBI	European Bioinformatics Institute (EMBL-EBI) Wellcome Genome Campus Hinxton, Cambridgeshire CB10 1SD United Kingdom

Affiliation	Address
UK.NOTTING	University of Nottingham Sutton Bonington Campus Nottingham LE12 5RD United Kingdom
UK.UCL	University College London Centre for Polar Observation and Modelling Gower Street London WC1E 6BT United Kingdom
UK.UNI-Liverpool-EOE	University of Liverpool, Dept. of Earth, Ocean and Ecological Sciences School of Environmental Sciences 4 Brownlow Street Liverpool L69 3GP United Kingdom

A.2 FAHRTTEILNEHMER:INNEN / CRUISE PARTICIPANTS

Name/ Last name	Vorname/ First name	Institut/ Institute	Beruf/ Profession	Fachrichtung/ Discipline
Abrahamsen	Einar Povl	UK.BAS	Scientist	Oceanography
Allerholt	Jacob	DE.AWI	Technician	Oceanography
Bach	Mareike Gabriele	NL.RUG	PhD candidate	Biology
Barnes	David	UK.BAS	Scientist	Biology
Beyer	Andrea Kerstin	DE.AWI	Technician	Biology
Boebel	Olaf	DE.AWI	Scientist	Oceanography
Chakrabarti	Lisa	UK.NOTTING	Scientist	Biology
Christensen	Jonas Overby	DE.HeliService	Pilot	Helicopter Service
Engicht	Carina	DE.AWI	Technician	Oceanography
Erni Cassola e Barata	Gabriel	CH.UNIBAS	Scientist	Biology
Feij	Bram	NL.NIOZ	Observer	Biology
Flores	Hauke	DE.AWI	Scientist	Biology
Gebhardt	Christopher	DE.UNI-Rostock	Scientist	Biology
González-Dávila	Melchor	ES.ULPGC	Scientist	Oceanography
Graeve	Martin	DE.AWI	Scientist	Chemistry
Hecken	Timo	DE.HeliService	Technician	Helicopter Service
Held	Christoph	DE.AWI	Scientist	Biology
Hoppema	Mario	DE.AWI	Scientist (chief scientist)	Oceanography
Jager	Harold	DE.HeliService	Pilot	Helicopter Service
Jones	Christopher	GOV.NOAA	Scientist	Biology
Kaufmann	Marie Elisabeth	DE.AWI	Student (Master)	Biology
Kempf	Sarah	DE.AWI	PhD candidate	Biology
Koch	Boris	DE.AWI	Scientist	Chemistry
Koschnick	Nils	DE.AWI	Engineer	Biology
Kühn	Susanne	NL.WUR	Scientist	Biology
Leuenberger	Kevin	CH.UNIBAS	Student (Master)	Biology
Link	Heike	DE.UNI-Rostock	Scientist	Biology
Llanillo del Rio	Pedro Jose	DE.AWI	Scientist	Oceanography
Ludwichowski	Kai-Uwe	DE.AWI	Engineer	Chemistry
Mallett	Robbie	UK.UCL	PhD candidate	Geophysics
Mark	Felix	DE.AWI	Scientist	Biology
Meijboom	André	NL.WUR	Scientist	Biology
Otte	Frank	DE.DWD	Technician	Meteorology
Pallentin	Malte	DE.AWI	Engineer	Biology

Name/ Last name	Vorname/ First name	Institut/ Institute	Beruf/ Profession	Fachrichtung/ Discipline
Papetti	Chiara	IT.UNIPD	Scientist	Biology
Parcerisas Serrahima	Clea	BE.VLIZ	PhD candidate	Engineering Sciences
Pinner	Ole	DE.AWI	PhD candidate	Oceanography
Powilleit	Martin	DE.UNI-Rostock	Scientist	Biology
Purser	Autun	DE.AWI	Scientist	Biology
Roca Torrecilla	Irene	DE.AWI	Scientist	Biology
Santana Casiano	Juana Magdalena	ES.ULPGC	Scientist	Oceanography
Schröder	Henning	DE.AWI	Engineer	Engineering Sciences
Spiesecke	Stefanie	DE.AWI	Engineer	Oceanography
Stenssen	Willem Albertus	DE.HeliService	Engineer	Helicopter Service
Suter	Patrick	DE.DWD	Scientist	Meteorology
Tebben	Jan	DE.AWI	Scientist	Chemistry
Tippenhauer	Sandra	DE.AWI	Scientist	Oceanography
Van de Putte	Anton	BE.IRSNB	Scientist	Biology
Van Dorssen	Michiel	NL.DORSSEN	Technician	Biology
Vortkamp	Martina	DE.AWI	Technician	Biology
Wilkinson	Jeremy	UK.BAS	Scientist	Oceanography

A.3 SCHIFFSBESATZUNG / SHIP'S CREW

No.	Nachname / Last Name	Vorname / First name	Position / Rank
1	Wunderlich	Thomas Wolf	Master
2	Kentges	Felix	Chiefmate
3	Grafe	Jens	Chief
4	Langhinrichs	Jacob	2nd Mate
5	Peine	Lutz Gerhard	2nd Mate
6	Lange	Felix	3nd Mate
7	Müller	Andreas	ELO
8	Goessmann-Lange	Petra	Ships Doc
9	Brose	Thomas Christian Gerhard	2nd. Eng
10	Haack	Michael Detlev	2nd. Eng
11	Krinfeld	Oleksandr	2nd. Eng
12	Redmer	Jens Dirk	ELO
13	Hüttebräucker	Olaf	ELO
14	Jäger	Vladimir	ELO
15	Kliemann	Olaf	ELO
16	Nasis	Ilias	ELO
17	Sedlak	Andreas Enrico	Bosun
18	Neisner	Winfried	Carpen.
19	Denzer	Florian	MP Rat.
20	Fölster	Michael	MP Rat.
21	Heinstein	Patricia	MP Rat.
22	Hoche	Jan	MP Rat.
23	Meier	Jan	MP Rat.
24	Mohr	Tassilo Peter	MP Rat.
25	Baecker	Andreas	AB
26	Burzan	Gerd-Ekkehard	AB
27	Wende	Uwe	AB
28	Preußner	Jörg	Storek.
30	Claasen	Thies	MP Rat.

No.	Nachname / Last Name	Vorname / First name	Position / Rank
30	Hänert	Ovee	MP Rat.
31	Rhau	Lars-Peter	MP Rat.
32	Klinger	Dana	MP Rat.
33	Schwarz	Uwe	MP Rat.
34	Marquart	Geron	Cook
35	Silinski	Frank	Cooksm.
36	Matter	Sebastian	Cooksm.
37	Pieper	Daniel	Chief Stew.
38	Ilk	Romy	Nurse
39	Silinski	Carmen Viola	2nd Stew.
40	Krause	Tomasz	2nd Stew.
41	Dibenau	Torsten	2nd Stew.
42	Arendt	René	2nd Stew.
43	Chen	Dansheng	2nd Stew.
44	Sun	Yongsheng	Laundym.

A.4 STATIONSLISTE / STATION LIST PS129

Station list of expedition PS132 from Cape Town to Punta Arenas; the list details the action log for all stations along the cruise track.

See https://www.pangaea.de/expeditions/events/PS129 to display the station (event) list for expedition PS129.
This version contains Uniform Resource Identifiers for all sensors listed under https://sensor.awi.de. See https://www.awi.de/en/about-us/service/computing-centre/data-flow-framework.html for further information about AWI's data flow framework from sensor observations to

Event label	Optional label	Date/Time	Latitude	Longitude	Depth [m]	Gear	Action	Comment
PS129-track		2022-03-03T00:00:00	-33.90680	18.43370		CT	Station start	Cape Town – Punta Arenas
PS129-track		2022-04-28T00:00:00	-53.14470	-70.90910		CT	Station end	Cape Town – Punta Arenas
PS129_0_Underway-28		2022-03-05T11:33:27	-37.30978	16.42730	4572.9	SWEAS	Station start	
PS129_0_Underway-28		2022-04-25T21:08:02	-58.05082	-60.63529	4265.3	SWEAS	Station end	
PS129_0_Underway-24		2022-03-05T11:45:08	-37.34008	16.41134	4575.7	TSG	Station start	
PS129_0_Underway-24		2022-04-25T21:11:45	-58.04367	-60.64601	4279.4	TSG	Station end	
PS129_0_Underway-23		2022-03-05T11:45:33	-37.34112	16.41080	4576.2	TSG	Station start	
PS129_0_Underway-23		2022-04-25T21:11:06	-58.04492	-60.64416	4274.3	TSG	Station end	
PS129_0_Underway-22		2022-03-05T11:45:53	-37.34198	16.41035	4576.2	SNDVELPR	Station start	
PS129_0_Underway-22		2022-04-25T21:10:47	-58.04552	-60.64325	4271.2	SNDVELPR	Station end	
PS129_0_Underway-14		2022-03-05T11:46:38	-37.34393	16.40933	4577.0	NEUMON	Station start	
PS129_0_Underway-14		2022-04-25T21:10:15	-58.04653	-60.64170	4267.5	NEUMON	Station end	
PS129_0_Underway-12		2022-03-05T11:47:05	-37.34510	16.40873	4577.3	GRAV	Station start	
PS129_0_Underway-12		2022-04-25T21:09:56	-58.04713	-60.64076	4264.6	GRAV	Station end	
PS129_0_Underway-11		2022-03-05T11:47:37	-37.34649	16.40802	4577.4	MAG	Station start	
PS129_0_Underway-11		2022-04-25T21:09:18	-58.04839	-60.63887	4262.9	MAG	Station end	

** Comments are limited to 130 characters. See https://www.pangaea.de/expeditions/events/PS129 to show full comments in conjunction with the station (event) list for expedition PS129.*

Event label	Optional label	Date/Time	Latitude	Longitude	Depth [m]	Gear	Action	Comment
PS129_0_Underway-10		2022-03-05T11:48:08	-37.34784	16.40733	4577.8	ICERAD	Station start	
PS129_0_Underway-10		2022-04-25T21:11:54	-58.04338	-60.64644	4279.4	ICERAD	Station end	
PS129_0_Underway-6		2022-03-05T11:49:07	-37.35041	16.40603	4578.8	MYON	Station start	
PS129_0_Underway-6		2022-04-25T21:09:06	-58.04875	-60.63834	4262.3	MYON	Station end	
PS129_0_Underway-1		2022-03-05T11:49:45	-37.35205	16.40515	4579.1	ADCP	Station start	
PS129_0_Underway-1		2022-04-25T21:08:33	-58.04982	-60.63676	4263.4	ADCP	Station end	
PS129_1-1		2022-03-05T12:43:02	-37.48802	16.33307	4620.5	FLOAT	max depth	deployed
PS129_2-1		2022-03-06T21:47:12	-41.93585	13.50208	4633.0	UWS	Station start	
PS129_2-1		2022-03-06T22:24:50	-42.02176	13.44554	4585.9	UWS	Station end	
PS129_3-1		2022-03-07T11:03:38	-43.62659	12.36885	5360.5	FLOAT	Station start	deployed
PS129_3-1		2022-03-07T11:09:27	-43.62902	12.36305	5303.6	FLOAT	Station end	deployed
PS129_4-1		2022-03-07T20:50:04	-45.00441	11.42296	4885.7	FLOAT	Station start	deployed
PS129_4-1		2022-03-07T20:52:00	-45.00268	11.42242	4891.0	FLOAT	Station end	deployed
PS129_5-1		2022-03-07T21:01:32	-45.01753	11.40903	4818.9	UWS	Station start	
PS129_5-1		2022-03-07T21:41:32	-45.12374	11.34806	4980.2	UWS	Station end	
PS129_6-1		2022-03-08T10:39:43	-46.94386	10.06358		UWS	Station start	
PS129_6-1		2022-03-08T11:20:15	-47.00619	10.00979	4448.1	UWS	Station end	
PS129_7-1		2022-03-08T11:02:58	-46.99454	10.02717	4588.6	FLOAT	Station start	deployed
PS129_7-1		2022-03-08T11:11:12	-46.99390	10.01937	4564.7	FLOAT	Station end	deployed
PS129_8-1		2022-03-08T20:21:24	-48.10073	9.22434	3854.1	UWS	Station start	
PS129_8-1		2022-03-08T21:35:17	-48.28113	9.09163	3882.9	UWS	Station end	
PS129_9-1		2022-03-09T07:59:40	-49.57345	8.12749	4430.3	UWS	Station start	
PS129_9-1		2022-03-09T09:01:47	-49.68274	8.04488	4425.4	UWS	Station end	
PS129_10-1		2022-03-09T12:42:40	-50.01319	7.76700	4451.2	FLOAT	max depth	deployed
PS129_0_Underway-7		2022-03-09T14:36:53	-50.05324	7.55476	4559.7	FBOX	Station start	
PS129_0_Underway-7		2022-04-25T21:08:02	-58.05082	-60.63529	4265.3	FBOX	Station end	
PS129_0_Underway-18		2022-03-09T14:38:07	-50.05578	7.55544	4557.9	pCO2	Station start	
PS129_0_Underway-18		2022-04-25T21:07:39	-58.05156	-60.63419	4267.7	pCO2	Station end	

Event label	Optional label	Date/Time	Latitude	Longitude	Depth [m]	Gear	Action	Comment
PS129_0_Underway-17		2022-03-09T14:38:28	-50.05652	7.55568	4557.9	pCO2	Station start	
PS129_0_Underway-17		2022-04-25T16:35:00	-58.56006	-59.86591	3074.6	pCO2	Station end	
PS129_11-1		2022-03-09T16:02:51	-50.16849	7.44155		UWS	Station start	
PS129_11-1		2022-03-09T16:44:52	-50.24766	7.40350	4543.8	UWS	Station end	
PS129_12-1		2022-03-10T10:26:40	-52.25540	6.09457	3718.4	UWS	Station start	
PS129_12-1		2022-03-10T10:57:09	-52.33067	6.03169	3151.0	UWS	Station end	
PS129_13-1		2022-03-11T09:08:00	-55.80289	3.06187	3144.4	UWS	Station start	
PS129_13-1		2022-03-11T09:46:07	-55.90400	2.96917	3370.8	UWS	Station end	
PS129_14-1		2022-03-11T10:26:09	-55.94311	2.93597	3493.3	CTD-RO	max depth	
PS129_15-1		2022-03-11T19:20:22	-57.22800	1.73001	4422.3	UWS	Station start	
PS129_15-1		2022-03-11T20:20:42	-57.38799	1.57715	4094.1	UWS	Station end	
PS129_16-1		2022-03-11T21:50:44	-57.62054	1.34966	4231.8	FLOAT	Station start	deployed
PS129_16-1		2022-03-11T21:55:03	-57.62416	1.34526	4226.2	FLOAT	Station end	deployed
PS129_17-1		2022-03-12T05:49:27	-58.89718	0.24346	3972.5	UWS	Station start	
PS129_17-1		2022-03-12T06:40:08	-59.02998	0.13278	4600.6	UWS	Station end	
PS129_18-1	AWI-227-15	2022-03-12T06:53:56	-59.04915	0.11597	4138.3	MOOR	Station start	
PS129_18-1	AWI-227-15	2022-03-12T10:33:16	-59.05163	0.15264	4623.9	MOOR	Station end	
PS129_18-2	AWI-227-16	2022-03-12T11:11:31	-59.04989	0.10809	4630.6	MOOR	max depth	deployment
PS129_18-3		2022-03-12T18:29:27	-59.09098	0.12138	4667.4	SOSOCAL	Station start	
PS129_18-3		2022-03-12T21:53:13	-59.09168	0.12277	4665.1	SOSOCAL	Station end	
PS129_18-4		2022-03-12T22:44:00	-59.09187	0.12225	4668.7	GLD	Station start	
PS129_18-4		2022-03-12T22:45:01	-59.09198	0.12233	4669.1	GLD	Station end	
PS129_18-5		2022-03-12T23:10:15	-59.09227	0.12426	4670.3	GLD	Station start	
PS129_18-5		2022-03-12T23:14:07	-59.09263	0.12547	4671.1	GLD	Station end	
PS129_18-6		2022-03-13T00:56:57	-59.08906	0.12021	4666.5	TEST	max depth	entered due to faulty entry
PS129_18-7		2022-03-13T03:20:08	-59.09118	0.12190	4667.3	CTD-RO	max depth	
PS129_18-8		2022-03-13T05:54:49	-59.11064	0.10501	4500.0	FLOAT	Station start	deployed

Event label	Optional label	Date/Time	Latitude	Longitude	Depth [m]	Gear	Action	Comment
PS129_18-8		2022-03-13T05:57:40	-59.11056	0.10388	4535.5	FLOAT	Station end	deployed
PS129_19-1		2022-03-13T07:01:31	-59.25497	0.05888	5199.1	UWS	Station start	
PS129_19-1		2022-03-13T08:00:00	-59.38827	0.02058	4593.1	UWS	Station end	
PS129_20-1		2022-03-13T08:25:59	-59.38701	0.02488	4930.9	SUIT	Station start	
PS129_20-1		2022-03-13T09:40:16	-59.34627	-0.00806	4982.2	SUIT	Station end	
PS129_20-2		2022-03-13T10:41:05	-59.34029	0.00202	5043.7	SOSOCAL	Station start	
PS129_20-2		2022-03-13T12:01:39	-59.33932	0.00316		SOSOCAL	Station end	
PS129_20-3		2022-03-13T12:02:33	-59.33909	0.00330	5054.0	M-RMT	Station start	
PS129_20-3		2022-03-13T14:20:20	-59.32106	0.02502	4942.9	M-RMT	Station end	
PS129_20-4		2022-03-13T14:21:00	-59.32110	0.02509	4948.3	M-RMT	Station start	
PS129_20-4		2022-03-13T16:42:56	-59.29954	0.04070	4849.5	M-RMT	Station end	
PS129_20-5		2022-03-13T16:43:58	-59.29944	0.04077	4848.2	MSN	Station start	
PS129_20-5		2022-03-13T18:40:16	-59.29894	0.04106	4838.9	MSN	Station end	
PS129_21-1		2022-03-13T20:17:14	-59.52571	-0.00635	4637.4	FLOAT	Station start	deployed
PS129_21-1		2022-03-13T20:18:53	-59.53005	-0.00771	4665.9	FLOAT	Station end	deployed
PS129_22-1		2022-03-13T20:55:16	-59.62582	0.00640	5078.8	UWS	Station start	
PS129_22-1		2022-03-13T21:50:34	-59.77085	1.49167	5364.1	UWS	Station end	
PS129_22-2		2022-03-13T22:18:26	-59.84375	-3.29167	5381.4	FLOAT	Station start	deployed
PS129_22-2		2022-03-13T22:18:43	-59.84449	1.39167	5381.7	FLOAT	Station end	deployed
PS129_23-1		2022-03-14T07:50:12	-61.00197	0.00092	5370.3	CTD-RO	max depth	
PS129_24-1		2022-03-14T12:11:59	-61.12738	0.05556	5375.2	UWS	Station start	
PS129_24-1		2022-03-14T13:05:13	-61.26575	-0.00343	5380.4	UWS	Station end	
PS129_25-1		2022-03-15T06:52:07	-64.02519	-0.08134	5184.2	FLOAT	Station start	deployed
PS129_25-1		2022-03-15T08:11:40	-64.01656	-0.09114	5185.5	FLOAT	Station end	deployed
PS129_25-2	AWI-229-14	2022-03-15T08:42:06	-64.02171	0.00899	5178.4	MOOR	Station start	recovery
PS129_25-2	AWI-229-14	2022-03-15T11:13:53	-64.02428	0.00015	5180.4	MOOR	Station end	recovery
PS129_25-3	AWI-229-15	2022-03-15T11:58:49	-64.02095	0.01161	5178.8	MOOR	Station start	deployment

Event label	Optional label	Date/Time	Latitude	Longitude	Depth [m]	Gear	Action	Comment
PS129_25-3	AWI-229-15	2022-03-15T15:44:52	-64.02128	0.01366	5179.1	MOOR	Station end	deployment
PS129_25-4		2022-03-15T16:14:16	-64.07066	0.02467	5176.9	M-RMT	Station start	
PS129_25-4		2022-03-15T19:07:14	-64.11797	0.14618	4989.7	M-RMT	Station end	
PS129_25-5		2022-03-15T19:46:02	-64.07515	0.06109	5177.4	SOSOCAL	Station start	
PS129_25-5		2022-03-15T21:22:30	-64.07556	0.06120	5177.7	SOSOCAL	Station end	
PS129_25-6		2022-03-15T21:52:58	-64.07533	0.06215	5177.9	SUIT	Station start	
PS129_25-6		2022-03-15T22:57:44	-64.07566	0.10607	5178.5	SUIT	Station end	
PS129_25-7		2022-03-15T23:30:23	-64.07121	0.10140	5178.1	MSN	Station start	
PS129_25-7		2022-03-16T00:45:02	-64.07277	0.08931		MSN	Station end	
PS129_25-8		2022-03-16T03:18:31	-64.08279	0.07703	5177.1	CTD-RO	max depth	
PS129_26-1		2022-03-16T07:27:55	-64.37603	0.00170	4839.2	UWS	Station start	
PS129_26-1		2022-03-16T08:24:22	-64.53839	-0.00404	4676.2	UWS	Station end	
PS129_27-1		2022-03-16T19:59:02	-66.48583	-0.06896	4529.5	SUIT	Station start	
PS129_27-1		2022-03-16T21:22:28	-66.48010	-0.01607	4480.5	SUIT	Station end	
PS129_27-2		2022-03-16T23:32:36	-66.48169	-0.07272	4438.8	CTD-RO	max depth	
PS129_27-3		2022-03-17T01:53:37	-66.48309	-0.09234	4398.4	MSN	Station start	
PS129_27-3		2022-03-17T03:29:19	-66.48001	-0.09363	4388.2	MSN	Station end	
PS129_27-4		2022-03-17T03:35:56	-66.48001	-0.09427	4387.3	SOSOCAL	Station start	
PS129_27-4		2022-03-17T05:30:41	-66.47875	-0.09502	4384.0	SOSOCAL	Station end	
PS129_27-5	AWI-231-13	2022-03-17T06:39:41	-66.51570	-0.07911	4602.7	MOOR	Station start	recovery
PS129_27-5	AWI-231-13	2022-03-17T10:25:50	-66.51069	-0.08943	4596.1	MOOR	Station end	recovery
PS129_27-6	AWI-231-14	2022-03-17T10:43:18	-66.51708	-0.07583	4602.9	MOOR	Station start	deployment
PS129_27-6	AWI-231-14	2022-03-17T14:17:16	-66.51739	-0.07448	4602.5	MOOR	Station end	deployment
PS129_27-7		2022-03-17T15:01:48	-66.51757	-0.18544	4523.0	FLOAT	Station start	deployed
PS129_27-7		2022-03-17T16:09:34	-66.54712	-0.13606	4678.7	FLOAT	Station end	deployed
PS129_27-8		2022-03-17T15:30:26	-66.54439	-0.14253	4676.8	M-RMT	Station start	
PS129_27-8		2022-03-17T18:28:31	-66.57582	-0.03443	4656.0	M-RMT	Station end	

Event label	Optional label	Date/Time	Latitude	Longitude	Depth [m]	Gear	Action	Comment
PS129_27-9		2022-03-17T19:04:30	-66.56448	-0.28476	4683.6	FLOAT	Station start	deployed
PS129_27-9		2022-03-17T19:10:06	-66.56466	-0.29061	4681.3	FLOAT	Station end	deployed
PS129_28-1		2022-03-17T19:10:35	-66.56477	-0.29141	4683.1	UWS	Station start	
PS129_28-1		2022-03-17T20:03:31	-66.55347	-0.68497	4618.6	UWS	Station end	
PS129_29-1		2022-03-18T14:05:07	-66.23370	-8.85313	4985.1	SOSOCAL	Station start	
PS129_29-1		2022-03-18T15:30:16	-66.23664	-8.82225		SOSOCAL	Station end	
PS129_29-2		2022-03-18T15:31:03	-66.23665	-8.82190	4985.8	SOSOCAL	Station start	
PS129_29-2		2022-03-18T17:16:29	-66.23649	-8.78882	4985.9	SOSOCAL	Station end	
PS129_29-3		2022-03-18T17:16:59	-66.23648	-8.78878	4986.0	SOSOCAL	Station start	
PS129_29-3		2022-03-18T18:51:49	-66.23356	-8.79153	4986.4	SOSOCAL	Station end	
PS129_30-1		2022-03-19T04:59:12	-65.93594	-12.19272	5038.0	CTD-RO	max depth	
PS129_30-2	AWI248-3	2022-03-19T07:40:44	-65.96661	-12.22697	5038.1	MOOR	Station start	recovery
PS129_30-2	AWI248-3	2022-03-19T10:33:58	-65.96105	-12.18782	5037.7	MOOR	Station end	recovery
PS129_30-3		2022-03-19T10:46:02	-65.96565	-12.18418	5037.3	FLOAT	Station start	deployed
PS129_30-3		2022-03-19T10:51:00	-65.96868	-12.18765	5037.2	FLOAT	Station end	deployed
PS129_31-1		2022-03-19T12:43:45	-66.27166	-11.98411	5015.7	UWS	Station start	
PS129_31-1		2022-03-19T13:31:25	-66.40300	-11.87633	5011.1	UWS	Station end	
PS129_32-1		2022-03-19T13:33:19	-66.40826	-11.87209	5010.8	UWS	Station start	
PS129_32-1		2022-03-19T14:08:10	-66.50500	-11.79228	5005.4	UWS	Station end	
PS129_33-1		2022-03-20T06:04:25	-69.16635	-9.46201	3739.7	UWS	Station start	
PS129_33-1		2022-03-20T06:55:00	-69.30772	-9.32917	3414.2	UWS	Station end	
PS129_34-1		2022-03-20T06:55:30	-69.30912	-9.32775	3413.0	UWS	Station start	
PS129_34-1		2022-03-20T07:22:01	-69.37487	-9.26570	3296.1	UWS	Station end	
PS129_35-1		2022-03-20T07:20:03	-69.37340	-9.26744	3303.7	FLOAT	Station start	deployed
PS129_35-1		2022-03-20T07:24:21	-69.37678	-9.26287	3276.8	FLOAT	Station end	deployed
PS129_36-1		2022-03-20T09:08:02	-69.65291	-8.99143	3148.9	UWS	Station start	
PS129_36-1		2022-03-20T10:00:32	-69.79716	-8.87204	2711.3	UWS	Station end	

Event label	Optional label	Date/Time	Latitude	Longitude	Depth [m]	Gear	Action	Comment
PS129_37-1		2022-03-20T12:26:43	-70.04672	-8.65792	2559.3	FLOAT	Station start	deployed
PS129_37-1		2022-03-20T12:27:40	-70.04721	-8.65992	2550.9	FLOAT	Station end	deployed
PS129_38-1		2022-03-20T13:00:32	-70.06166	-8.73636	2003.1	FLOAT	Station start	deployed
PS129_38-1		2022-03-20T13:04:05	-70.05908	-8.72698	2078.5	FLOAT	Station end	deployed
PS129_39-1		2022-03-20T19:14:55	-70.50912	-8.18154	240.8	ROVF	Station start	
PS129_39-1		2022-03-20T21:13:10	-70.50499	-8.17168	249.8	ROVF	Station end	
PS129_39-2		2022-03-20T22:36:26	-70.49956	-8.33908	239.9	ROVF	Station start	
PS129_39-2		2022-03-20T23:36:21	-70.49957	-8.33864	240.3	ROVF	Station end	
PS129_40-1		2022-03-21T09:30:37	-70.75365	-10.87137	958.0	EK60_EK80	max depth	calibration
PS129_40-2		2022-03-21T13:41:23	-70.75338	-10.84345	927.7	CTD-RO	max depth	
PS129_40-3		2022-03-21T15:16:53	-70.74960	-10.82120	923.3	B_LANDER	Station start	
PS129_40-3		2022-03-21T15:47:20	-70.74820	-10.82949	936.2	B_LANDER	Station end	
PS129_40-4	Longline	2022-03-21T15:55:46	-70.74747	-10.83366	944.2	MOOR	Station start	
PS129_40-4	Longline	2022-03-21T18:28:12	-70.74985	-10.92727	1046.7	MOOR	Station end	
PS129_40-5		2022-03-21T18:40:27	-70.74684	-10.92366	1052.3	OFOBS	Station start	
PS129_40-5		2022-03-21T23:43:01	-70.72533	-10.92291		OFOBS	Station end	
PS129_40-6		2022-03-21T23:53:45	-70.72604	-10.93322	1127.1	MSN	Station start	
PS129_40-6		2022-03-22T01:25:59	-70.72367	-10.97662	1179.2	MSN	Station end	
PS129_40-7		2022-03-22T02:00:17	-70.75100	-10.81818	914.0	M-RMT	Station start	
PS129_40-7		2022-03-22T03:32:12	-70.74690	-10.78223	893.8	M-RMT	Station end	
PS129_40-8		2022-03-22T06:42:33	-70.74591	-10.79905	914.1	TVMUC	max depth	
PS129_40-9		2022-03-22T07:48:50	-70.74640	-10.81339	929.1	MG	Station start	
PS129_40-9		2022-03-22T10:05:56	-70.74536	-10.82106	941.6	MG	Station end	
PS129_40-10	Longline	2022-03-22T16:30:31	-70.75100	-10.91900	1030.7	MOOR	Station start	recovery
PS129_40-10	Longline	2022-03-22T18:46:11	-70.75060	-10.90231	1010.5	MOOR	Station end	recovery
PS129_40-11		2022-03-22T19:22:34	-70.72168	-10.88604	1091.6	M-RMT	Station start	
PS129_40-11		2022-03-22T22:15:25	-70.72186	-10.84952	1058.4	M-RMT	Station end	

Event label	Optional label	Date/Time	Latitude	Longitude	Depth [m]	Gear	Action	Comment
PS129_40-12		2022-03-22T23:04:46	-70.75235	-10.82828	920.3	DRG	Station start	
PS129_40-12		2022-03-23T01:40:54	-70.75498	-10.76644	842.7	DRG	Station end	
PS129_40-13		2022-03-23T05:52:29	-70.74942	-10.83722	942.4	B_LANDER	Station start	
PS129_40-13		2022-03-23T07:31:25	-70.75270	-10.85028	939.1	B_LANDER	Station end	
PS129_41-1		2022-03-23T14:49:30	-70.53010	-8.20418	227.3	ROVF	Station start	
PS129_41-1		2022-03-23T16:18:41	-70.52888	-8.20273	224.8	ROVF	Station end	
PS129_41-2		2022-03-23T18:19:35	-70.52940	-8.20309	226.5	CTD-RO	max depth	
PS129_42-1		2022-03-24T01:44:13	-70.84230	-10.59121	251.5	CTD-RO	max depth	
PS129_42-2		2022-03-24T03:55:01	-70.84001	-10.58142	255.1	MG	Station start	
PS129_42-2		2022-03-24T04:30:43	-70.84071	-10.58582	254.5	MG	Station end	
PS129_43-1		2022-03-24T05:35:00	-70.86122	-10.75417	304.1	MG	Station start	
PS129_43-1		2022-03-24T06:38:31	-70.86217	-10.75515	301.5	MG	Station end	
PS129_43-2		2022-03-24T06:39:56	-70.86209	-10.75454	302.2	MG	Station start	
PS129_43-2		2022-03-24T07:06:58	-70.86236	-10.75454	301.7	MG	Station end	
PS129_43-3		2022-03-24T07:28:33	-70.86220	-10.75424	302.2	OFOBS	Station start	
PS129_43-3		2022-03-24T11:52:11	-70.85308	-10.66623		OFOBS	Station end	
PS129_44-1		2022-03-24T12:32:07	-70.84298	-10.58726	244.3	TVMUC	max depth	
PS129_44-2		2022-03-24T14:35:07	-70.84000	-10.57994	254.1	TVMUC	Station start	
PS129_44-2		2022-03-24T14:40:27	-70.83993	-10.57874	251.8	TVMUC	Station end	
PS129_45-1		2022-03-25T02:35:32	-70.78668	-10.75452	610.4	M-RMT	Station start	
PS129_45-1		2022-03-25T04:30:46	-70.79507	-10.62801	445.5	M-RMT	Station end	
PS129_46-1	Longline	2022-03-25T07:01:54	-70.75226	-10.90641	1009.6	MOOR	Station start	recovery
PS129_46-1	Longline	2022-03-25T15:45:33	-70.74407	-11.07474	1234.2	MOOR	Station end	recovery
PS129_47-1		2022-03-25T17:10:07	-70.78679	-10.75199	611.3	CTD-RO	max depth	
PS129_47-2		2022-03-25T17:51:39	-70.78606	-10.75181	619.0	MSN	Station start	
PS129_47-2		2022-03-25T18:55:22	-70.78875	-10.76098	593.7	MSN	Station end	
PS129_47-3		2022-03-25T19:10:00	-70.78740	-10.75557	603.2	DRG	Station start	

Event label	Optional label	Date/Time	Latitude	Longitude	Depth [m]	Gear	Action	Comment
PS129_47-3		2022-03-25T21:50:45	-70.76260	-10.70084	751.4	DRG	Station end	
PS129_47-4		2022-03-25T22:23:58	-70.76831	-10.76364	766.3	OFOBS	Station start	
PS129_47-4		2022-03-26T02:31:00	-70.77917	-10.62401	504.6	OFOBS	Station end	
PS129_47-5		2022-03-26T03:47:35	-70.78540	-10.74730	624.1	MG	Station start	
PS129_47-5		2022-03-26T04:51:25	-70.78708	-10.75592	604.8	MG	Station end	
PS129_48-1		2022-03-26T06:50:16	-70.74600	-10.79793	911.3	TVMUC	max depth	
PS129_48-2		2022-03-26T08:01:17	-70.74587	-10.79900	912.9	TVMUC	max depth	
PS129_48-3		2022-03-26T09:03:43	-70.74615	-10.80011	912.8	TVMUC	max depth	
PS129_49-1		2022-03-26T12:29:05	-70.94363	-10.53648	297.2	CTD-RO	max depth	
PS129_49-2		2022-03-26T13:20:00	-70.94008	-10.53362	287.8	B_LANDER	Station start	
PS129_49-2		2022-03-26T13:23:29	-70.94039	-10.53181	285.1	B_LANDER	Station end	
PS129_49-3		2022-03-26T13:41:06	-70.93994	-10.52735	272.9	OFOBS	Station start	
PS129_49-3		2022-03-26T17:40:00	-70.93539	-10.49770		OFOBS	Station end	
PS129_49-4		2022-03-26T18:13:39	-70.94380	-10.53552	296.5	MG	Station start	
PS129_49-4		2022-03-26T19:10:00	-70.94582	-10.53187	288.5	MG	Station end	
PS129_49-5		2022-03-26T19:18:00	-70.94734	-10.52797	282.0	B_LANDER	Station start	
PS129_49-5		2022-03-26T19:23:38	-70.94699	-10.52775	282.1	B_LANDER	Station end	
PS129_49-6		2022-03-26T19:53:56	-70.94376	-10.52834	276.1	MG	Station start	
PS129_49-6		2022-03-26T21:42:43	-70.94377	-10.52707	272.4	MG	Station end	
PS129_49-7		2022-03-26T21:44:49	-70.94345	-10.52644	270.6	MSN	Station start	
PS129_49-7		2022-03-26T22:34:39	-70.94288	-10.53013	280.6	MSN	Station end	
PS129_49-8		2022-03-26T22:35:29	-70.94284	-10.53021	280.8	M-RMT	Station start	
PS129_49-8		2022-03-26T23:46:56	-70.96985	-10.50302	276.2	M-RMT	Station end	
PS129_50-1		2022-03-27T01:04:30	-70.93924	-10.57250	316.6	OFOBS	Station start	
PS129_50-1		2022-03-27T05:37:50	-70.93184	-10.55401		OFOBS	Station end	
PS129_50-2		2022-03-27T06:17:32	-70.94105	-10.53996	296.3	B_LANDER	Station start	
PS129_50-2		2022-03-27T08:04:08	-70.94050	-10.52699	271.9	B_LANDER	Station end	

Event label	Optional label	Date/Time	Latitude	Longitude	Depth [m]	Gear	Action	Comment
PS129_51-1		2022-03-27T09:09:27	-70.99344	-10.62413	483.4	ROVF	Station start	
PS129_51-1		2022-03-27T10:35:03	-70.99357	-10.62368	482.7	ROVF	Station end	
PS129_52-1		2022-03-27T12:35:04	-70.94371	-10.53486	292.3	TVMUC	Station start	
PS129_52-1		2022-03-27T13:42:31	-70.94355	-10.53443	292.4	TVMUC	Station end	
PS129_52-2		2022-03-27T14:33:32	-70.94351	-10.53438	292.6	TVMUC	max depth	
PS129_52-3		2022-03-27T15:19:10	-70.94352	-10.53559	294.8	TVMUC	max depth	
PS129_52-4		2022-03-27T15:56:51	-70.94730	-10.52943	283.9	B_LANDER	Station start	
PS129_52-4		2022-03-27T17:14:29	-70.95657	-10.55291	329.6	B_LANDER	Station end	
PS129_52-5		2022-03-27T18:00:00	-70.93714	-10.60425	339.2	SUIT	Station start	
PS129_52-5		2022-03-27T21:50:21	-70.92957	-10.51369	241.8	SUIT	Station end	
PS129_52-6		2022-03-27T22:10:28	-70.92051	-10.49276	219.7	DRG	Station start	
PS129_52-6		2022-03-27T23:07:08	-70.90908	-10.47654	223.0	DRG	Station end	
PS129_53-1		2022-03-27T23:52:45	-70.87743	-10.48581	235.0	B_LANDER	Station start	
PS129_53-1		2022-03-28T00:07:41	-70.87700	-10.48820	234.1	B_LANDER	Station end	
PS129_53-2		2022-03-28T02:51:02	-70.87198	-10.51989	232.9	OFOBS	Station start	
PS129_53-2		2022-03-28T05:28:13	-70.88543	-10.47307		OFOBS	Station end	
PS129_53-3		2022-03-28T06:06:47	-70.87330	-10.48200	234.7	CTD-RO	max depth	
PS129_53-4		2022-03-28T06:56:52	-70.87375	-10.48240	234.7	ICERAD	Station start	Mummy Chair
PS129_53-4		2022-03-28T09:09:19	-70.87238	-10.48283	233.9	ICERAD	Station end	Mummy Chair
PS129_53-5		2022-03-28T09:19:06	-70.87208	-10.48213	234.0	MG	Station start	
PS129_53-5		2022-03-28T12:00:49	-70.87209	-10.48518	233.3	MG	Station end	
PS129_53-6		2022-03-28T12:30:04	-70.87226	-10.49067	233.1	DRG	Station start	
PS129_53-6		2022-03-28T14:30:56	-70.87577	-10.48618	233.2	DRG	Station end	
PS129_53-7		2022-03-28T14:56:03	-70.87663	-10.49305	232.6	B_LANDER	Station start	
PS129_53-7		2022-03-28T15:37:20	-70.87389	-10.49360	233.3	B_LANDER	Station end	
PS129_54-1	Longline	2022-03-28T17:36:08	-70.65348	-11.00301	1375.2	MOOR	Station start	

Event label	Optional label	Date/Time	Latitude	Longitude	Depth [m]	Gear	Action	Comment
PS129_54-1	Longline	2022-03-28T21:10:13	-70.64957	-11.10980	1470.9	MOOR	Station end	
PS129_54-2		2022-03-28T22:16:54	-70.65571	-10.98280	1350.2	OFOBS	Station start	
PS129_54-2		2022-03-29T00:46:45	-70.64064	-10.95828	1345.2	OFOBS	Station end	
PS129_54-3		2022-03-29T02:29:39	-70.66004	-11.01782	1372.5	CTD-RO	max depth	
PS129_54-4		2022-03-29T03:57:25	-70.64992	-10.99317	1374.3	M-RMT	Station start	
PS129_54-4		2022-03-29T05:45:23	-70.62840	-10.97849	1378.1	M-RMT	Station end	
PS129_54-5		2022-03-29T06:11:35	-70.64601	-10.96025	1341.7	MSN	Station start	
PS129_54-5		2022-03-29T07:51:50	-70.66076	-10.99947	1356.1	MSN	Station end	
PS129_55-1		2022-03-29T09:53:52	-70.79961	-10.61331	371.8	ICERAD	Station start	Mummy Chair
PS129_55-1		2022-03-29T10:53:10	-70.80528	-10.65203	432.6	ICERAD	Station end	Mummy Chair
PS129_55-2		2022-03-29T11:23:01	-70.80533	-10.57265	245.7	ROVF	Station start	
PS129_55-2		2022-03-29T12:12:20	-70.80531	-10.56917	247.5	ROVF	Station end	
PS129_55-3		2022-03-29T12:37:42	-70.79169	-10.56348		ROVF	Station start	
PS129_55-3		2022-03-29T13:01:44	-70.79277	-10.56860	269.2	ROVF	Station end	
PS129_55-4		2022-03-29T13:47:19	-70.79774	-10.52861	249.3	ROVF	Station start	
PS129_55-4		2022-03-29T14:19:04	-70.79742	-10.52981	249.0	ROVF	Station end	
PS129_56-1	Longline	2022-03-29T16:02:57	-70.65797	-11.10254	1447.9	MOOR	Station start	
PS129_56-1	Longline	2022-03-29T19:21:38	-70.66458	-11.11012	1441.3	MOOR	Station end	
PS129_57-1		2022-03-29T21:37:15	-70.88553	-11.12237	322.9	MG	Station start	
PS129_57-1		2022-03-29T23:38:54	-70.88943	-11.13971	318.0	MG	Station end	
PS129_57-2		2022-03-30T00:53:51	-70.89388	-11.12830	296.8	TVMUC	max depth	
PS129_57-3		2022-03-30T01:47:16	-70.89355	-11.13612	305.4	TVMUC	max depth	
PS129_57-4		2022-03-30T03:44:35	-70.91055	-11.18342	285.7	OFOBS	Station start	
PS129_57-4		2022-03-30T06:35:56	-70.89521	-11.13776	300.3	OFOBS	Station end	
PS129_58-1	EWS 01-01	2022-04-02T08:24:06	-70.87310	-11.23727	702.2	MOOR	Station start	deployment
PS129_58-1	EWS 01-01	2022-04-02T09:28:22	-70.87350	-11.24006	700.0	MOOR	Station end	deployment

Event label	Optional label	Date/Time	Latitude	Longitude	Depth [m]	Gear	Action	Comment
PS129_58-2		2022-04-02T10:41:37	-70.88627	-11.29106	696.5	CTD-RO	max depth	
PS129_59-1		2022-04-02T13:21:02	-70.84094	-11.44274	1387.6	CTD-RO	max depth	
PS129_59-2	EWS 02-01	2022-04-02T15:02:20	-70.83067	-11.33612	1368.1	MOOR	Station start	deployment
PS129_59-2	EWS 02-01	2022-04-02T17:04:59	-70.83808	-11.43777	1420.2	MOOR	Station end	deployment
PS129_60-1		2022-04-02T20:16:59	-70.60121	-12.21596	2024.1	CTD-RO	max depth	
PS129_60-2		2022-04-02T21:39:19	-70.60175	-12.21619	2023.9	FLOAT	Station start	deployed
PS129_60-2		2022-04-02T21:40:31	-70.60122	-12.21406	2023.6	FLOAT	Station end	deployed
PS129_61-1		2022-04-02T23:07:53	-70.46968	-12.79032	2348.2	FLOAT	Station start	deployed
PS129_61-1		2022-04-02T23:17:59	-70.46465	-12.81189	2359.4	FLOAT	Station end	deployed
PS129_62-1		2022-04-03T01:02:01	-70.30093	-13.45212	3317.9	SOSOCAL	Station start	
PS129_62-1		2022-04-03T03:00:39	-70.29982	-13.43315	3363.0	SOSOCAL	Station end	
PS129_62-2		2022-04-03T03:01:41	-70.29987	-13.43284	3360.5	SOSOCAL	Station start	
PS129_62-2		2022-04-03T04:50:57	-70.30127	-13.42371	3190.3	SOSOCAL	Station end	
PS129_62-3		2022-04-03T04:52:40	-70.30125	-13.42404	3190.6	SOSOCAL	Station start	
PS129_62-3		2022-04-03T06:49:30	-70.30081	-13.44205	3316.5	SOSOCAL	Station end	
PS129_62-4		2022-04-03T08:28:27	-70.29980	-13.44821	3333.6	CTD-RO	max depth	
PS129_62-5	EWS 03-01	2022-04-03T10:23:06	-70.29813	-13.44754	3352.8	MOOR	Station start	deployment
PS129_62-5	EWS 03-01	2022-04-03T12:42:29	-70.29842	-13.44624	3352.4	MOOR	Station end	deployment
PS129_62-6		2022-04-03T12:50:23	-70.29462	-13.44194	3393.0	FLOAT	Station start	deployed
PS129_62-6		2022-04-03T12:50:35	-70.29446	-13.44188	3392.5	FLOAT	Station end	deployed
PS129_63-1		2022-04-03T14:35:53	-70.09614	-14.12940	4554.2	UWS	Station start	
PS129_63-1		2022-04-03T15:15:21	-70.01652	-14.39677	4730.1	UWS	Station end	
PS129_64-1		2022-04-03T17:32:54	-69.74707	-15.29413	4752.0	FLOAT	Station start	deployed
PS129_64-1		2022-04-03T17:34:31	-69.74589	-15.29681	4752.3	FLOAT	Station end	deployed
PS129_64-2		2022-04-03T19:50:36	-69.71262	-15.40737	4757.8	CTD-RO	max depth	
PS129_65-1		2022-04-04T06:21:27	-69.08591	-17.33362	4759.4	CTD-RO	max depth	
PS129_65-2	AWI-245-5	2022-04-04T09:02:56	-69.05826	-17.38421	4762.7	MOOR	Station start	recovery
PS129_65-2	AWI-245-5	2022-04-04T12:59:47	-69.06445	-17.35740	4762.0	MOOR	Station end	recovery

Event label	Optional label	Date/Time	Latitude	Longitude	Depth [m]	Gear	Action	Comment
PS129_65-3	AWI-245-6	2022-04-04T13:33:35	-69.05915	-17.39212	4761.7	MOOR	Station start	deployment
PS129_65-3	AWI-245-6	2022-04-04T16:13:48	-69.06074	-17.39064	4761.3	MOOR	Station end	deployment
PS129_65-4		2022-04-04T16:37:12	-69.03570	-17.46215	4764.2	SOSOCAL	Station start	
PS129_65-4		2022-04-04T18:20:43	-69.03562	-17.46339	4764.8	SOSOCAL	Station end	
PS129_65-5		2022-04-04T18:21:26	-69.03560	-17.46335	4764.7	SOSOCAL	Station start	
PS129_65-5		2022-04-04T20:09:21	-69.03462	-17.46369	4765.0	SOSOCAL	Station end	
PS129_65-6		2022-04-04T20:10:32	-69.03480	-17.46358	4765.1	SOSOCAL	Station start	
PS129_65-6		2022-04-04T21:55:04	-69.03549	-17.46316	4764.9	SOSOCAL	Station end	
PS129_65-7		2022-04-04T21:56:12	-69.03556	-17.46292	4764.9	FLOAT	max depth	deployed
PS129_65-8		2022-04-04T22:06:24	-69.02976	-17.47120	4765.6	FLOAT	Station start	deployed
PS129_65-8		2022-04-04T22:07:22	-69.02878	-17.47410	4765.6	FLOAT	Station end	deployed
PS129_66-1		2022-04-04T22:39:10	-68.96913	-17.65145	4769.3	UWS	Station start	
PS129_66-1		2022-04-04T23:23:31	-68.88187	-17.89794	4781.8	UWS	Station end	
PS129_67-1		2022-04-04T23:31:28	-68.86519	-17.94656	4777.7	UWS	Station start	
PS129_67-1		2022-04-05T00:14:18	-68.76865	-18.21807	4782.3	UWS	Station end	
PS129_68-1		2022-04-05T06:10:32	-68.22057	-19.74189	4873.1	CTD-RO	max depth	
PS129_69-1		2022-04-05T10:11:16	-68.06038	-20.39831	4895.4	UWS	Station start	
PS129_69-1		2022-04-05T11:05:53	-67.96498	-20.78751	4905.1	UWS	Station end	
PS129_70-1		2022-04-05T21:02:59	-67.26669	-23.59549	4875.0	CTD-RO	max depth	
PS129_71-1		2022-04-07T09:03:46	-68.71342	-27.05018	4723.7	ICE	Station start	
PS129_71-1		2022-04-07T09:56:09	-68.71679	-27.05021	4724.1	ICE	Station end	
PS129_71-2		2022-04-07T10:28:05	-68.71819	-27.05226	4722.2	CTD-RO	max depth	
PS129_71-3		2022-04-07T11:01:16	-68.72158	-27.05117	4723.5	M-RMT	Station start	
PS129_71-3		2022-04-07T11:25:49	-68.71786	-27.06270	4723.9	M-RMT	Station end	
PS129_71-4		2022-04-07T12:00:28	-68.71363	-27.07745	4723.4	FLOAT	Station start	deployed
PS129_71-4		2022-04-07T12:02:03	-68.71344	-27.07858	4723.0	FLOAT	Station end	deployed
PS129_72-1		2022-04-07T14:12:51	-68.97160	-26.99571	4709.0	CTD-RO	max depth	

Event label	Optional label	Date/Time	Latitude	Longitude	Depth [m]	Gear	Action	Comment
PS129_72-2	BGC10	2022-04-07T14:53:57	-69.00320	-27.00177	4706.3	MOOR	Station start	recovery
PS129_72-2	BGC10	2022-04-07T19:00:04	-69.00469	-27.03937	4705.3	MOOR	Station end	recovery
PS129_72-3		2022-04-07T19:43:15	-69.00146	-27.04295	4705.3	CTD-RO	max depth	
PS129_72-4		2022-04-07T20:24:36	-69.00007	-27.04644	4706.0	M-RMT	Station start	
PS129_72-4		2022-04-07T23:55:53	-68.94041	-27.13171	4707.7	M-RMT	Station end	
PS129_73-1		2022-04-08T06:10:00	-69.95620	-27.94303	4605.9	FLOAT	Station start	deployed
PS129_73-1		2022-04-08T06:13:36	-69.95907	-27.95211	4606.7	FLOAT	Station end	deployed
PS129_74-1		2022-04-08T12:53:59	-70.84216	-28.97365	4413.5	SOSOCAL	Station start	
PS129_74-1		2022-04-08T14:31:16	-70.83560	-28.98477	4416.4	SOSOCAL	Station end	
PS129_74-2	AWI-249-3	2022-04-08T15:19:16	-70.88422	-28.95556	4401.9	MOOR	Station start	recovery
PS129_74-2	AWI-249-3	2022-04-08T16:20:02	-70.88676	-28.94853	4399.1	MOOR	Station end	recovery
PS129_74-3	AWI-249-4	2022-04-08T17:11:04	-70.82872	-29.06519	4418.9	MOOR	Station start	deployment
PS129_74-3	AWI-249-4	2022-04-08T19:56:21	-70.83255	-29.13345	4419.0	MOOR	Station end	deployment
PS129_74-4		2022-04-08T20:48:43	-70.81842	-29.24967	4425.8	CTD-RO	max depth	
PS129_74-5		2022-04-08T21:35:45	-70.81829	-29.26534	4425.1	SOSOCAL	Station start	
PS129_74-5		2022-04-08T23:02:51	-70.81881	-29.27341	4424.7	SOSOCAL	Station end	
PS129_74-6		2022-04-08T23:04:34	-70.81884	-29.27317	4424.7	SOSOCAL	Station start	
PS129_74-6		2022-04-09T00:43:25	-70.81624	-29.28260	4426.0	SOSOCAL	Station end	
PS129_74-7		2022-04-09T00:13:00	-70.81782	-29.27510	4425.1	EK60_EK80	max depth	calibration
PS129_74-8		2022-04-09T21:05:49	-70.64538	-29.39933	3909.1	SUIT	Station start	
PS129_74-8		2022-04-09T23:35:38	-70.63947	-29.34200		SUIT	Station end	
PS129_74-9		2022-04-09T23:36:18	-70.63945	-29.34188		FLOAT	Station start	deployed
PS129_74-9		2022-04-09T23:47:21	-70.63289	-29.33456		FLOAT	Station end	deployed
PS129_75-1		2022-04-10T09:51:05	-70.14564	-30.97361	2963.1	FLOAT	Station start	deployed
PS129_75-1		2022-04-10T10:02:05	-70.13151	-30.99950	4513.8	FLOAT	Station end	deployed
PS129_76-1		2022-04-10T16:35:44	-69.76708	-32.02217	4269.5	FLOAT	Station start	deployed
PS129_76-1		2022-04-10T16:36:01	-69.76688	-32.02271	4269.5	FLOAT	Station end	deployed

Event label	Optional label	Date/Time	Latitude	Longitude	Depth [m]	Gear	Action	Comment
PS129_77-1	HAFOS-CWS01-01	2022-04-10T19:39:21	-69.56225	-32.47147		MOOR	Station start	deployment
PS129_77-1	HAFOS-CWS01-01	2022-04-10T22:44:59	-69.55526	-32.47723	4476.3	MOOR	Station end	deployment
PS129_77-2		2022-04-10T22:52:22	-69.55425	-32.47359	4476.6	FLOAT	Station start	deployed
PS129_77-2		2022-04-10T22:54:06	-69.55378	-32.47015	4476.5	FLOAT	Station end	deployed
PS129_77-3		2022-04-10T23:10:03	-69.55347	-32.43990	4477.7	ICEOBS	Station start	
PS129_77-3		2022-04-11T00:34:39	-69.54578	-32.44553		ICEOBS	Station end	
PS129_78-1		2022-04-11T08:44:47	-68.99649	-31.93983	3000.9	FLOAT	Station start	deployed
PS129_78-1		2022-04-11T08:49:15	-68.99438	-31.94375	3000.6	FLOAT	Station end	deployed
PS129_79-1		2022-04-11T09:21:19	-68.99295	-31.94194	3000.6	ICEOBS	Station start	
PS129_79-1		2022-04-11T12:46:35	-68.96855	-31.92856		ICEOBS	Station end	
PS129_80-1	AWI-209-9	2022-04-12T14:48:05	-66.60566	-27.12645	4860.9	MOOR	Station start	deployment
PS129_80-1	AWI-209-9	2022-04-12T17:10:11	-66.60741	-27.12130	4861.3	MOOR	Station end	deployment
PS129_80-2		2022-04-12T19:24:19	-66.61489	-27.20598	4859.6	CTD-RO	max depth	
PS129_80-3		2022-04-12T21:56:07	-66.61638	-27.21072	4859.0	FLOAT	Station start	deployed
PS129_80-3		2022-04-12T21:59:52	-66.61664	-27.21271	4859.0	FLOAT	Station end	deployed
PS129_81-1		2022-04-12T23:19:03	-66.54597	-27.69307	4853.2	UWS	Station start	
PS129_81-1		2022-04-13T00:03:39	-66.51183	-28.00969	4842.9	UWS	Station end	
PS129_82-1		2022-04-13T07:21:41	-66.24936	-30.43571	4805.0	CTD-RO	max depth	Signalling problems, bottles not closing
PS129_83-1		2022-04-13T13:12:02	-66.10511	-31.83017	4784.6	CTD-RO	max depth	
PS129_83-2		2022-04-13T15:00:40	-66.10450	-31.83639	4785.0	CTD-RO	max depth	
PS129_84-1		2022-04-13T18:31:57	-66.10096	-32.12078	4784.5	UWS	Station start	
PS129_84-1		2022-04-13T19:16:05	-66.07340	-32.43282	4786.3	UWS	Station end	
PS129_85-1		2022-04-14T03:38:16	-65.74775	-36.10755	4764.6	UWS	Station start	

Event label	Optional label	Date/Time	Latitude	Longitude	Depth [m]	Gear	Action	Comment
PS129_85-1		2022-04-14T04:22:19	-65.71962	-36.42205	4757.7	UWS	Station end	
PS129_86-1		2022-04-14T06:45:15	-65.66800	-36.61469	4760.5	CTD-RO	max depth	
PS129_86-2	AWI-208-9	2022-04-14T09:08:14	-65.66976	-36.61600	4760.3	MOOR	Station start	recovery
PS129_86-2	AWI-208-9	2022-04-14T12:34:14	-65.70791	-36.69956	4754.5	MOOR	Station end	recovery
PS129_86-3	AWI208-10	2022-04-14T12:59:06	-65.69637	-36.68213	4755.7	MOOR	Station start	deployment
PS129_86-3	AWI208-10	2022-04-14T15:37:55	-65.69604	-36.68329	4756.0	MOOR	Station end	deployment
PS129_86-4		2022-04-14T15:43:29	-65.69525	-36.68398	4755.8	FLOAT	Station start	deployed
PS129_86-4		2022-04-14T15:50:10	-65.69082	-36.68140	4756.4	FLOAT	Station end	deployed
PS129_87-1		2022-04-14T23:07:07	-65.35605	-38.71563	4748.8	CTD-RO	max depth	
PS129_88-1		2022-04-15T10:10:33	-65.04170	-41.13704	4746.1	CTD-RO	max depth	
PS129_88-2		2022-04-15T12:27:24	-65.04378	-41.13935	4744.9	FLOAT	Station start	deployed
PS129_88-2		2022-04-15T12:33:37	-65.04425	-41.14240	4744.6	FLOAT	Station end	deployed
PS129_89-1		2022-04-15T15:41:14	-65.45447	-41.37378	4642.9	ICE	Station start	
PS129_89-1		2022-04-15T16:11:40	-65.44702	-41.35889	4641.6	ICE	Station end	
PS129_89-2		2022-04-15T16:47:37	-65.44616	-41.31480	4639.0	SOSOCAL	Station start	
PS129_89-2		2022-04-15T18:16:12	-65.44330	-41.29586	4637.9	SOSOCAL	Station end	
PS129_90-1		2022-04-16T01:50:11	-66.08079	-41.76077	4491.8	FLOAT	Station start	deployed
PS129_90-1		2022-04-16T01:53:58	-66.08127	-41.76664	4492.7	FLOAT	Station end	deployed
PS129_91-1	CWS-02-01C	2022-04-16T14:04:42	-66.40099	-41.41837	4549.5	MOOR	Station start	deployment
PS129_91-1	CWS-02-01C	2022-04-16T17:10:34	-66.37941	-41.39193	4566.1	MOOR	Station end	deployment
PS129_91-2		2022-04-16T17:17:25	-66.37960	-41.39472	4566.4	FLOAT	Station start	deployed
PS129_91-2		2022-04-16T17:20:10	-66.37974	-41.39851	4566.6	FLOAT	Station end	deployed
PS129_92-1		2022-04-17T05:01:07	-66.03719	-43.50575	4470.9	FLOAT	Station start	deployed
PS129_92-1		2022-04-17T05:03:06	-66.03685	-43.50854	4471.5	FLOAT	Station end	deployed
PS129_93-1		2022-04-17T07:59:04	-65.93949	-43.86110	4460.4	SOSOCAL	Station start	
PS129_93-1		2022-04-17T09:35:29	-65.92591	-43.84901	4449.4	SOSOCAL	Station end	

Event label	Optional label	Date/Time	Latitude	Longitude	Depth [m]	Gear	Action	Comment
PS129_94-1	WWS-002-01	2022-04-17T17:57:08	-65.43641	-44.59468		MOOR	Station start	deployment
PS129_94-1	WWS-002-01	2022-04-17T20:55:24	-65.43264	-44.59235	4463.1	MOOR	Station end	deployment
PS129_94-2		2022-04-17T20:56:28	-65.43260	-44.59248	4463.3	FLOAT	Station start	deployed
PS129_94-2		2022-04-17T21:00:56	-65.43269	-44.60086	4469.8	FLOAT	Station end	deployed
PS129_95-1		2022-04-18T04:38:21	-65.00446	-43.91008	4618.2	FLOAT	Station start	deployed
PS129_95-1		2022-04-18T04:40:30	-65.00289	-43.90825	4617.5	FLOAT	Station end	deployed
PS129_96-1		2022-04-18T10:25:25	-64.74019	-43.50725	4637.7	CTD-RO	max depth	
PS129_96-2		2022-04-18T12:34:26	-64.73945	-43.50730	4637.4	FLOAT	Station start	deployed
PS129_96-2		2022-04-18T12:38:12	-64.73817	-43.51087	4637.7	FLOAT	Station end	deployed
PS129_97-1		2022-04-18T23:25:20	-64.48025	-45.30039	4479.4	CTD-RO	max depth	
PS129_98-1		2022-04-19T03:15:29	-64.43930	-45.66407	4416.3	UWS	Station start	
PS129_98-1		2022-04-19T03:42:40	-64.42516	-45.76442	4434.2	UWS	Station end	
PS129_99-1		2022-04-19T09:54:47	-64.30040	-46.66828	4383.2	CTD-RO	max depth	
PS129_100-1	AWI-257-2	2022-04-19T16:32:01	-64.21762	-47.48982	4203.8	MOOR	Station start	recovery
PS129_100-1	AWI-257-2	2022-04-19T17:58:48	-64.23091	-47.49979	4190.6	MOOR	Station end	recovery
PS129_100-2	AWI-257-3	2022-04-19T18:10:21	-64.23651	-47.49034	4195.9	MOOR	Station start	deployment
PS129_100-2	AWI-257-3	2022-04-19T20:49:14	-64.24056	-47.48516	4197.2	MOOR	Station end	deployment
PS129_100-3		2022-04-19T22:56:57	-64.27904	-47.46921	4192.1	CTD-RO	max depth	
PS129_101-1		2022-04-20T02:18:17	-64.19928	-47.63488	4170.2	UWS	Station start	
PS129_101-1		2022-04-20T02:46:42	-64.17530	-47.71901	4159.4	UWS	Station end	
PS129_102-1		2022-04-20T06:30:09	-64.13273	-47.95395	4091.9	CTD-RO	max depth	
PS129_103-1		2022-04-20T12:37:56	-64.07762	-48.36516	3924.6	CTD-RO	max depth	
PS129_104-1		2022-04-20T18:45:32	-63.99430	-48.81941	3709.2	CTD-RO	max depth	
PS129_105-1		2022-04-21T02:20:44	-63.87645	-49.15213	3445.3	CTD-RO	max depth	
PS129_106-1		2022-04-21T07:49:09	-63.81472	-49.54474	3206.2	CTD-RO	max depth	
PS129_HELI_20220421		2022-04-21T14:37:00	-63.71720	-51.21160	2683.4	HELI	max depth	

Event label	Optional label	Date/Time	Latitude	Longitude	Depth [m]	Gear	Action	Comment
PS129_107-1		2022-04-21T16:12:49	-63.73428	-50.35083	2641.2	CTD-RO	max depth	
PS129_108-1		2022-04-21T19:23:34	-63.66442	-50.59464	2589.1	UWS	Station start	
PS129_108-1		2022-04-21T20:06:31	-63.65927	-50.73950		UWS	Station end	
PS129_109-1	AWI207-11	2022-04-21T20:36:07	-63.65331	-50.80827	2567.5	MOOR	Station start	recovery
PS129_109-1	AWI207-11	2022-04-22T04:12:35	-63.67504	-50.76677	2556.2	MOOR	Station end	recovery
PS129_109-2	AWI-207-12	2022-04-21T21:32:26	-63.63809	-50.79066	2554.6	MOOR	Station start	deployment
PS129_109-2	AWI-207-12	2022-04-21T23:54:43	-63.62857	-50.79077	2575.7	MOOR	Station end	deployment
PS129_109-3		2022-04-22T05:16:26	-63.67445	-50.75388	2379.1	CTD-RO	max depth	
PS129_110-1		2022-04-22T10:14:50	-63.61617	-51.07381	2225.4	CTD-RO	max depth	
PS129_111-1		2022-04-22T13:51:06	-63.57192	-51.30138	2013.3	CTD-RO	max depth	
PS129_112-1		2022-04-22T16:55:41	-63.53202	-51.45575	1942.4	CTD-RO	max depth	
PS129_113-1		2022-04-22T18:19:46	-63.51764	-51.48870	1891.9	UWS	Station start	
PS129_113-1		2022-04-22T18:54:19	-63.51120	-51.59317	1700.1	UWS	Station end	
PS129_114-1	AWI261-02	2022-04-22T19:32:21	-63.50608	-51.63053	1657.1	MOOR	Station start	deployment
PS129_114-1	AWI261-02	2022-04-22T21:17:11	-63.49856	-51.63743	1823.3	MOOR	Station end	deployment
PS129_114-2		2022-04-22T23:02:22	-63.47778	-51.61399	1225.7	CTD-RO	max depth	
PS129_115-1		2022-04-23T02:54:00	-63.47856	-51.84233	1231.3	CTD-RO	max depth	Due to technical problems the station is repeated
PS129_116-1		2022-04-23T03:25:03	-63.48077	-51.84001	940.2	CTD-RO	max depth	
PS129_117-1		2022-04-23T06:28:59	-63.46597	-52.09650	934.6	CTD-RO	max depth	
PS129_118-1		2022-04-23T07:21:55	-63.46916	-52.10637	801.0	UWS	Station start	
PS129_118-1		2022-04-23T07:59:43	-63.43239	-52.19101	687.2	UWS	Station end	
PS129_119-1		2022-04-23T09:00:58	-63.40989	-52.27290	459.1	CTD-RO	max depth	
PS129_120-1		2022-04-23T12:30:37	-63.35101	-52.72767	394.9	CTD-RO	max depth	
PS129_121-1		2022-04-23T17:32:43	-63.26064	-53.34989	236.9	CTD-RO	max depth	

Event label	Optional label	Date/Time	Latitude	Longitude	Depth [m]	Gear	Action	Comment
PS129_122-1		2022-04-23T21:38:26	-63.16861	-53.95431	479.0	CTD-RO	max depth	
PS129_123-1		2022-04-24T00:35:50	-63.09118	-54.52360	181.9	CTD-RO	max depth	
PS129_124-1		2022-04-24T03:23:46	-62.79945	-54.82329	201.8	UWS	Station start	
PS129_124-1		2022-04-24T03:52:11	-62.71579	-54.90981	326.3	UWS	Station end	
PS129_125-1		2022-04-24T11:16:30	-61.49088	-56.10593	349.9	UWS	Station start	
PS129_125-1		2022-04-24T11:59:27	-61.34988	-56.06718	150.0	UWS	Station end	
PS129_126-1		2022-04-24T12:47:34	-61.19415	-56.02455	186.2	UWS	Station start	
PS129_126-1		2022-04-24T13:21:06	-61.08636	-55.99542	323.9	UWS	Station end	
PS129_127-1	AWI-251-3	2022-04-24T13:45:54	-61.02462	-55.98568	313.5	MOOR	Station start	recovery
PS129_127-1	AWI-251-3	2022-04-24T14:56:02	-61.01875	-55.98757	324.6	MOOR	Station end	recovery
PS129_127-2	AWI-251-4	2022-04-24T15:31:56	-61.02342	-55.97944	324.0	MOOR	Station start	deployment
PS129_127-2	AWI-251-4	2022-04-24T16:25:04	-61.02311	-55.97813	380.5	MOOR	Station end	deployment
PS129_127-3		2022-04-24T17:10:27	-61.00111	-55.99551	366.2	CTD-RO	max depth	
PS129_128-1		2022-04-24T18:19:16	-61.00266	-55.99441		UWS	Station start	
PS129_128-1		2022-04-24T19:06:41	-60.96285	-56.05316	3896.4	UWS	Station end	
PS129_129-1		2022-04-25T00:45:43	-60.36461	-57.04599	4114.9	UWS	Station start	
PS129_129-1		2022-04-25T01:28:13	-60.28560	-57.17271	3630.4	UWS	Station end	
PS129_130-1		2022-04-25T09:41:04	-59.34074	-58.66446	3683.4	UWS	Station start	
PS129_130-1		2022-04-25T10:23:03	-59.26101	-58.78860		UWS	Station end	
PS129_131-1		2022-04-25T19:22:10	-58.25490	-60.32828	3658.0	UWS	Station start	
PS129_131-1		2022-04-25T19:44:52	-58.21180	-60.39316	3658.0	UWS	Station end	

** Comments are limited to 130 characters. See https://www.pangaea.de/expeditions/events/PS129 to show full comments in conjunction with the station (event) list for expedition PS129*

Abbreviation	Method/Device
ADCP	Acoustic Doppler Current Profiler
B_LANDER	Bottom lander
CT	Underway cruise track measurements
CTD-RO	CTD/Rosette
DRG	Dredge
EK60_EK80	Fish finder echolot, EK60 / EK80
FBOX	FerryBox
FLOAT	Floater
GLD	Glider
GRAV	Gravimetry
ICE	Ice station
ICEOBS	Ice observation
ICERAD	Ice radar
M-RMT	Multiple rectangular midwater trawl
MAG	Magnetometer
MG	Multiboxcorer
MOOR	Mooring
MSN	Multiple opening/closing net
MYON	DESY Myon Detector
NEUMON	Neutron monitor
OFOBS	Ocean Floor Observation and Bathymetry System
ROVF	Remote operated vehicle FIONA (mini)
SNDVELPR	Sound velocity probe
SOSOCAL	Sound Source Calibration
SUIT	Surface and under ice trawl
SWEAS	Ship Weather Station
TEST	Test
TSG	Thermosalinograph
TVMUC	Multicorer with television
UWS	Underway water sampling
pCO2	pCO2 sensor

Die **Berichte zur Polar- und Meeresforschung** (ISSN 1866-3192) werden beginnend mit dem Band 569 (2008) als Open-Access-Publikation herausgegeben. Ein Verzeichnis aller Bände einschließlich der Druckausgaben (ISSN 1618-3193, Band 377-568, von 2000 bis 2008) sowie der früheren **Berichte zur Polarforschung** (ISSN 0176-5027, Band 1–376, von 1981 bis 2000) befindet sich im electronic Publication Information Center **(ePIC)** des Alfred-Wegener-Instituts, Helmholtz-Zentrum für Polar- und Meeresforschung (AWI); see https://epic.awi.de. Durch Auswahl "Reports on Polar- and Marine Research" (via "browse"/"type") wird eine Liste der Publikationen, sortiert nach Bandnummer, innerhalb der absteigenden chronologischen Reihenfolge der Jahrgänge mit Verweis auf das jeweilige pdf-Symbol zum Herunterladen angezeigt.

The **Reports on Polar and Marine Research** (ISSN 1866-3192) are available as open access publications since 2008. A table of all volumes including the printed issues (ISSN 1618-3193, Vol. 377-568, from 2000 until 2008), as well as the earlier **Reports on Polar Research** (ISSN 0176-5027, Vol. 1–376, from 1981 until 2000) is provided by the electronic Publication Information Center **(ePIC)** of the Alfred Wegener Institute, Helmholtz Centre for Polar and Marine Research (AWI); see URL https://epic.awi.de. To generate a list of all Reports, use the URL http://epic.awi.de and select "browse"/"type" to browse "Reports on Polar and Marine Research". A chronological list in declining order will be presented, and pdf-icons displayed for downloading.

Zuletzt erschienene Ausgaben:

Recently published issues:

776 (2023) The Expedition PS129 of the Research Vessel POLARSTERN to the Weddell Sea in 2022, edited by Mario Hoppema with contributions of the participants

775 (2023) The Expedition PS133/2 of the Research Vessel POLARSTERN to the Scotia Sea in 2022, edited by Sabine Kasten with contributions of the participants

774 (2023) The Expedition PS133/1 of the Research Vessel POLARSTERN to the Atlantic Ocean in 2022, edited by Christine Klaas with contributions of the participants

773 (2023) A computational approach of locomotion, energy demand and dispersal of the common comatulid crinoid *Promachocrinus kerguelensis* (Echinodermata) and its circum-Antarctic success, by Nils Owsianowski

772 (2023) Russian-German Cooperation: Expeditions to Siberia in 2021, edited by Anne Morgenstern, Birgit Heim, Luidmila A. Pestryakova, Dmitry Yu. Bolshiyanov, Mikhail N. Grigoriev, Dmitry Ayunov, Antonia Dill, and Iuliia Jünger

771 (2023) The Expedition PS132 of the Research Vessel POLARSTERN to the Atlantic Ocean in 2022, edited by Karen H. Wiltshire and Angelika Dummermuth with contributions of the participants

770 (2023) The Expedition PS131 of the Research Vessel POLARSTERN to the Fram Strait in 2022, edited by Torsten Kanzow with contributions of the participants

769 (2023) The Expedition TRITON2021 of the Hendes Dansk Majestæt Skib TRITON to the Atlantic Ocean in 2021, edited by Rebecca McPherson, Carina Engicht and Torsten Kanzow

768 (2022) Mit Erich von Drygalski in die Ostantarktis – Paul Björvigs Tagebuch von der ersten deutschen Südpolarexpedition 1901-1903. Aus dem Norwegischen übersetzt von Volkert Gazert und herausgegeben von Cornelia Lüdecke

767 (2022) Expeditions to Antarctica: ANT-Land 2021/22 Neumayer Station III, Kohnen Station, Flight Operations and Field Campaigns, edited by Christine Wesche and Julia Regnery with contributions of the participants

ALFRED-WEGENER-INSTITUT
HELMHOLTZ-ZENTRUM FÜR POLAR-
UND MEERESFORSCHUNG

BREMERHAVEN

Am Handelshafen 12
27570 Bremerhaven
Telefon 0471 4831-0
Telefax 0471 4831-1149
www.awi.de

HELMHOLTZ